BIOCONCENTRATION AND BIOMAGNIFICATION OF ORGANOCHLORINE PESTICIDES BY AQUATIC MACROINVERTEBRATES AND FISH IN ESTUARINE ECOSYSTEMS, SOUTH COAST, KENYA

KOBINGI NYAKEYA
MSc. Fisheries And Aquatic Science – Aquatic Science Option
(University of Eldoret)
(BSc. Fisheries and Aquatic Science
(Moi University)

Thesis Submitted to The Board of Post-Graduate Studies in Partial Fulfilment of The Requirements for The Award of Doctor of Philosophy Degree in Limnology of The School of Agriculture and Natural Resource Management, Department of Environment, Natural Resources and Aquatic Sciences Kisii University

2026

DECLARATION AND RECOMMENDATION

DECLARATION BY THE CANDIDATE

This thesis is my original work and has not been presented for a degree in any other university.

Kobingi Nyakeya Signature _____ Date 1ST APRIL 2026

Reg. No. DAN19/00005/18

RECOMMENDATION BY SUPERVISORS

This proposal has been submitted for examination with our approval as university supervisors:

Prof. Getabu Albert Signature _____ Date 7-4-26

Associate Professor, Department of Environment Natural Resource and Aquatic Science, Kisii University

Dr. James Onchieku Signature _____ Date 7/04/26

Senior Lecturer, Department of Environment Natural Resource and Aquatic Science, Kisii University

Prof. Masese F. Onderi Signature _____ Date 04/04/2026

Associate Professor, Department of Fisheries and Aquatic Science, University of Eldoret

DECLARATION OF NUMBER OF WORDS

DECLARATION OF NUMBER OF WORDS FOR MASTERS/PROJECT/PhD THESIS

This form should be signed by the candidate and the candidate's supervisors and returned to Director of Postgraduate Studies at the same time as your copies of your thesis/project.

Please note at Kisii University Masters and PhD thesis shall comprise a piece of scholarly writing of not less than 20,000 words for Master's degree and 50,000 words for the PhD degree. In both cases this length includes references, but excludes the bibliography and any appendices.

Where a candidate wishes to exceed or reduce the word limit for a thesis specified in the regulations, the candidate must enquire with the Director of Postgraduate about the procedures to be followed. Any such enquiries must be made at least 2 months before the submission of the thesis.

Please note in cases where students exceed or reduce the prescribed word limit set out, the Director of Postgraduate may refer the thesis for resubmission requiring it to be shortened or lengthened.

Name of Candidate KOBINGI NYAKOYA ADM NO DAK19/00005/18
Faculty SANREM Department BONRAS

Thesis Title: BIOCONCENTRATION AND BIOMAGNIFICATION OF ORGANOCHLORINE PESTICIDES BY AQUATIC MACROINVERTEBRATES AND FISH IN ESTUARINE ECOSYSTEMS ALONG THE SOUTH COAST, KENYA.

I confirm the word length of:
1) the thesis including footnotes, is 60,222, 2) the bibliography is 7,590 and if applicable, 3) the appendices are 5,287

I also declare the electronic version is identical to the final hard bound copy of the thesis and corresponds with those on which the examiners based their recommendation for the award of the degree.

Signed: ..... Date: 1ST APRIL 2026
(Candidate)

I confirm that the thesis submitted by the above-named candidate complies with the relevant word length specified in the School of Postgraduate and Commission of University Education regulations for the Masters and PhD Degrees.

Signed: ..... Email: ..... Date: 7-4-26
(Supervisor)
Signed: ..... Email: ..... Date: 03/04/2026
(Supervisor)
Signed: ..... Email: ..... Date: 07/04/26
(Supervisor)

PLAGIARISM DECLARATION

Definition of plagiarism
Is academic dishonesty which involves; taking and using the thoughts, writings, and inventions of another person as one's own.

DECLARATION BY THE STUDENT

i. I declare I have read and understood Kisii University Postgraduate Examination Rules and Regulations, and other documents concerning academic dishonesty.
ii. I do understand that ignorance of these rules and regulations is not an excuse for a violation of the said rules
iii. If I have any questions or doubts, I realize that it is my responsibility to keep seeking an answer until I understand.
iv. I understand I must do my own work.
v. I also understand that if I commit any act of academic dishonesty like plagiarism, my thesis/project can be assigned a fail grade ("F").
vi. I further understand I may be suspended or expelled from the university for academic dishonesty.

Name KOBINCI NYAKEYA Signature
Reg. No. DAN19/0005/13 Date 1ST APRIL 2026

DECLARATION BY SUPERVISORS

i. I/We declare that this thesis/project has been submitted to plagiarism detection service.
ii. The thesis/project contains less than 20% of plagiarized work.
iii. I/We hereby give consent for marking:

Name PROF. ALBERT GETABU Signature
Affiliation KISII UNIVERSITY Date 7-4-26
Name PROF. FRANK MASESE Signature
Affiliation UNIVERSITY OF ELDORET Date 03/04/2026
Name DR. JAMES ONCHIEKU Signature
Affiliation KISII UNIVERSITY Date 7/04/26

COPYRIGHT

DEDICATION

This work is dedicated to my family.

ACKNOWLEDGEMENTS

This thesis marks the culmination of an academic journey that has been made possible through the support, encouragement, and contributions of many individuals and institutions. I am sincerely grateful to all who, in various ways, have walked this journey with me and contributed to the successful completion of this work. First and foremost, I wish to express my profound gratitude to my supervisors Prof. Albert M. Getabu, Prof. Franklin O. Masese and Dr. James Onchieku for their outstanding academic guidance and mentorship throughout this process. Their intellectual input, critical feedback, and unwavering commitment to academic excellence were instrumental in shaping this thesis. Their support has not only refined the quality of my work but also deepened my understanding of scientific research and academic inquiry.

I am equally indebted to the faculty members of the Graduate School of Agriculture at Kisii University, whose valuable insights and constructive criticisms significantly enriched the content and structure of this thesis. The academic forums and seminars provided a platform for rigorous peer review, and I deeply appreciate the collegial spirit and willingness of staff and fellow students to share their knowledge and perspectives. To my family, I extend heartfelt thanks for their enduring support and encouragement. Their patience and understanding during the long periods I spent away from home, immersed in fieldwork and writing, gave me the emotional strength to persevere. Their prayers and unwavering belief in my abilities have been a constant source of motivation.

Above all, I thank Almighty God for granting me good health, mental strength, and resilience throughout the research and writing process. His grace has been sufficient at every stage, and I remain forever grateful for His divine guidance and sustenance. To all others friends, colleagues, and contributors whose names may not appear here but whose support has in one way or another made a difference, I sincerely appreciate you. May God bless you abundantly and reward you richly.

ABSTRACT

The persistence of organochlorine pesticides (OCPs) in estuarine ecosystems remains a major ecological and public health concern, particularly in tropical regions with intense agricultural activity and weak regulatory enforcement. This study investigated the bioconcentration and biomagnification dynamics of legacy OCPs in estuarine systems along Kenya's South Coast. Sampling was conducted across multiple stations varying in land use and hydrology, and analyses were performed on water, sediments, and biota including benthic macroinvertebrate trophic guilds and fish (*Penaeus monodon*) to assess trophic transfer and ecological risk. Sixteen OCPs were detected across matrices, with significantly higher concentrations in biota than in sediments or water. *P. monodon* consistently exhibited the highest burdens (mean > 200 ng/g), approximately four times higher than in macroinvertebrates: *Saccostrea cucullata* and *Nerita undata*. Compounds such as alpha-HCH, o,p′-DDD, Mirex, and p,p′-DDE displayed high biomagnification factors (2.8–3.1), indicative of strong lipophilicity and persistence. Site-specific differences revealed elevated OCP levels in estuaries, suggesting ongoing anthropogenic inputs. Principal Component Analysis (PCA) showed that water parameters such as salinity, conductivity, and total dissolved solids (TDS) were negatively correlated with OCPs, while pH and dissolved oxygen were positively associated with p,p′-DDE and Mirex. These relationships highlight how physico-chemical properties influence pesticide transport and bioavailability. Bioconcentration Factor (BCF) analysis confirmed higher accumulation in *P. monodon*, with moderate BCFs in *N. undata* and *S. cucullata*, likely due to sediment-particle interactions. *Rhagovelia* species acted as intermediate vectors, facilitating contaminant trophic transfer up the food web. Sediment-based ecotoxicological indices further confirmed substantial risk. All OCPs recorded Hazard Quotients (HQs) > 1.0, and compounds like HCB, Heptachlor, and p,p′-DDE exceeded HQ = 1.75, indicating high probability of toxic effects. The Contamination Factor (Cf) and Geo-accumulation Index (Igeo) classified most sediments as extremely polluted, particularly with p,p′-DDD, Mirex, and Cis-chlordane. The Pollution Load Index (PLI) was 2.57, while the Nemerow Pollution Index (PN) reached 420.03; both indicative of widespread non-point and point pollution from sewerage facilities. Hakanson's Potential Ecological Risk Index (RI) was exceptionally high (31,352.42), far above the critical threshold (RI > 600), with gamma-HCH and p,p′-DDD posing the greatest threat. The Mean Effect Range-Median Quotient (ERM-Q) of 0.119 suggested a 21% probability of adverse effects on benthic fauna. Notably, sediment-bound pesticide levels consistently exceeded ecotoxicological thresholds, reinforcing their potential to drive chronic toxicity in estuarine habitats and disrupt benthic food webs. These results show that legacy OCPs to pose serious ecological threats despite regulatory bans. Elevated residues in *P. monodon* raise concerns for food safety among coastal human populations reliant on estuarine fisheries and international communities. The study recommends strengthened environmental monitoring, enforcement of pesticide bans, public education, and integrated pesticide and watershed management. Future research should focus on trophic markers, broader contaminant profiling, and ecological restoration to support remediation efforts.

TABLE OF CONTENT

LIST OF TABLES

LIST OF FIGURES

LIST OF APPENDICES

LIST OF ABBREVIATIONS AND ACRONYMS

ANOVA	Analysis of Variance
ATSDR	Agency for Toxic Substances and Disease Registry
BCF	Bioconcentration Factor
BMF	Biomagnification Factor
DDD	Dichlorodiphenyldichloroethane
DDE	Dichlorodiphenyltrichloroethylene
DDT	Dichlorodiphenyltrichloroethane
DO	Dissolved oxygen
EEA	European Environment Agency
EMCA	Environmental Management and Coordination Act
Eps	Emerging pollutants
EU	European Union
FAO	Food and Agricultural Organization
GC	Gas Chromatography
HCBs	Hexachlorobenzenes
HCHs	Hexachlorocyclohexanes
HSD	Honestly Significant Difference
IPBES	Intergovernmental Science-Policy Platform on Biodiversity and Ecosystem Services
IPCC	Inter-governmental Panel on Climate Change
KISCOL	Kwale International Sugar Company Ltd.
KNBS	Kenya National Bureau of Statistics
KMFRI	Kenya Marine and Fisheries Research Institute (KMFRI)
MANOVA	Multi-variate Analysis of Variance

MECs	Measured Environmental Concentrations
MECCF	Ministry of Environment, Climate Change and Forestry
NEMA	National Environment Management Authority
NGOs	Non-governmental Organizations
NOAA	National Oceanic and Atmospheric Administration
OCPs	Organochloride pesticides
PAMACC	Pan African Media Alliance for Climate Change
PANA	Pesticide Action Network Africa
PNECs	Predicted No Effect Concentrations
PSU	Practical Salinity Units
RO	Risk Quotient
SPM	Solid Particulate Matter
SSA	Sub-Saharan Africa
TDS	Total dissolved solids
US	United States
USEPA	United States Environmental Protection Agency
WHO	World Health Organization
WIO	Western Indian Ocean
WRA	Water Resources Authority
UNEP	United Nations Environment Programme
UNDP	United Nations Development Programme

CHAPTER ONE

INTRODUCTION

1.1 Background to the study

Aquatic ecosystems globally are increasingly degraded by pollutants, with persistent organic pollutants (POPs) among the most hazardous (UNEPa, b, 2023; WHO, 2023). POPs are synthetic chemicals that resist degradation, persist in the environment, bioaccumulate, and travel long distances via air and water. These include industrial chemicals, by-products, and organochlorine pesticides (OCPs) that continue to threaten aquatic ecosystems despite regulatory efforts like the Stockholm Convention (Quinn *et al*., 2023; Barbosa *et al*., 2023). They enter water systems through agricultural runoff, atmospheric deposition, and industrial discharge, harming biodiversity, water quality, and human health. Although some regions have reduced OCPs usage, substitution with other hazardous pesticides continues to stress aquatic ecosystems (Nkya *et al*., 2022; Gbaguidi *et al*., 2021).

Pesticides, widely used to boost crop yields, are key chemical stressors in aquatic environments (FAO, 2023; IPBES, 2022). They reach water bodies through runoff, leaching, spray drift, or direct application near aquatic zones (Wang *et al*., 2025, 2023; Musonge et al., 2023). Once present, they persist in water, bind to sediments, or bioaccumulate in organisms. Their presence is linked to reduced biodiversity, species shifts, endocrine disruption, and impaired ecosystem functioning (Owino *et al*., 2022; Akinrotimi & Abu, 2021). Chronic exposure, even at low levels, significantly harms non-target aquatic species, especially at lower food web levels, and increases human health risks through seafood consumption, including neurotoxicity, hormonal disruption, and cancer (Zhou *et al*., 2024; Mburu *et al*., 2021, 2022).

The situation is particularly acute in Sub-Saharan Africa (SSA), where increasing agricultural demands driven by food insecurity and economic growth have led to the intensified use of chemical pesticides (NEMA, 2023, 2018; PANA, 2021). In many African countries, the lack of stringent regulations, weak enforcement mechanisms, and limited public awareness contribute to indiscriminate pesticide use. Inappropriate pesticide application, including excessive doses, use of banned OCPs, and poor disposal practices, further exacerbate the risks to aquatic ecosystems (Midega *et al*., 2023; Ndebele *et al*., 2022). Streams, rivers, and estuaries adjacent to farmlands become conduits for OCPs-laden runoff, especially during rainy seasons. In these regions, OCPs pollution is emerging as a key factor threatening aquatic biodiversity, ecosystem services, and public health (Kibwage *et al*., 2022; Tongo *et al*., 2022, 2021).

Estuarine ecosystems, which represent transitional zones where freshwater from rivers mixes with saltwater from the ocean, are particularly vulnerable to OCPs contamination (Viana *et al*., 2023). These systems are ecologically and economically vital, supporting diverse biological communities, acting as nurseries for juvenile fish, and providing critical ecosystem services such as nutrient cycling, carbon sequestration, and shoreline protection (Ahmed *et al*., 2024; Ndiaye *et al*., 2023). However, due to their proximity to both agricultural hinterlands and human settlements, estuaries often serve as the final sink for a wide range of pollutants, including OCPs (Maggi *et al*., 2023). The semi-enclosed nature of estuaries tends to trap pollutants, leading to elevated and prolonged exposure for resident organisms. Moreover, the fluctuating salinity, temperature, and sediment dynamics in estuarine environments can influence the behavior, bioavailability, and toxicity of OCPs, complicating the assessment and management of risks (Mutie *et al*., 2022; Dalu & Froneman, 2021).

Kenya's coastal region, particularly the South Coast, features several important estuarine systems such as the Sabaki River Estuary, Gazi Bay, and the Ramisi Estuaries (MECCF, 2023). These areas serve as key habitats for a variety of aquatic species and are closely linked to the livelihoods of local communities engaged in fishing, tourism, and agriculture. However, increasing agricultural activities in the upstream catchments and along the coastal strip have led to concerns about OCPs contamination (Mwashote *et al*., 2003; Ngugi & Mugo, 2022; Odour *et al*., 2023). Horticulture, sugarcane farming, and subsistence agriculture in these regions commonly rely on chemical pest control methods. With limited infrastructure for wastewater treatment and weak OCPs monitoring programs, estuarine ecosystems in Kenya are exposed to a cocktail of OCP residues that may accumulate in sediments and aquatic organisms over time (Mwangi *et al*., 2018, 2017).

Despite the ecological importance of estuaries and their evident vulnerability to OCPs pollution, these environments are often underrepresented in national water quality monitoring efforts (WRA, 2023; NEMA, 2023). Conventional monitoring methods primarily focus on physicochemical analysis of water samples, which provide only a snapshot of contamination levels and may fail to capture episodic or chronic exposure events (Mwangi *et al*., 2025). Physico-chemical factors such as temperature, salinity, pH, and sediment characteristics play a critical role in determining the concentration, distribution, and persistence of OCPs in aquatic ecosystems (Alegria *et al*., 2016; Jiang *et al*., 2021; Yang *et al*., 2020). Sediments, in particular, serve as long-term reservoirs for OCPs, retaining these contaminants for extended periods and influencing their bioavailability to aquatic organisms (Yang *et al*., 2020). Consequently, spatial and temporal assessments of OCPs occurrence, alongside evaluations of their

bioconcentration and biomagnification within food webs, are essential for accurate environmental and ecological risk assessment (Gobas *et al*., 1999). In contrast, biological monitoring using aquatic organisms offers a more integrated and temporally relevant assessment of ecosystem health.

Organisms that inhabit estuarine sediments or occupy various positions within the aquatic food web have the capacity to accumulate OCPs and other contaminants in their tissues over time (Mburu *et al*., 2021; Onyango *et al*., 2020, 2019). Because these organisms are in direct contact with sediments where OCPs tend to bind and persist or consume prey that has already bioaccumulated these chemicals, they effectively act as biological indicators or sentinels of environmental contamination (Kamau et al., 2022, 2019; Ochanda et al., 2020). By monitoring these species, researchers can obtain integrative and time-relevant information on the presence and bioavailability of OCPs residues in the ecosystem, beyond what is possible through water chemistry alone (Njiru et al., 2023). This bio-monitoring approach is particularly valuable because it reflects the cumulative exposure to pollutants and reveals potential sub-lethal and ecological effects that may not be immediately evident from chemical analysis of water or sediment samples (Ekanem & Obot, 2022).

Among the biological indicators available for such studies, benthic macroinvertebrates and fish are particularly useful (Miller *et al*., 2021), although rarely done at the Kenyan coast. Benthic macroinvertebrates, including mollusks, annelids, and crustaceans, live in close contact with sediments where OCPs often accumulate. Their limited mobility, sensitivity to pollution, and diverse feeding strategies make them ideal for detecting localized contamination (Amadi *et al*., 2024; Bwire *et al*., 2023). Fish, on the other

hand, occupy higher trophic levels, and integrate exposure through both dietary intake and water contact. Their ability to bioaccumulate and biomagnify OCPs allows researchers to assess the transfer of contaminants through food webs and evaluate the risks to predators, including humans who consume fish. Together, these organisms may provide a comprehensive picture of pesticide dynamics in estuarine ecosystems.

Additionally, benthic macroinvertebrates serve as a principal food source for fish and other organisms at higher trophic levels, making them critical conduits for the transfer of OCPs residues through the aquatic food web (Nguyen *et al*., 2024). Their role as prey not only facilitates the trophic transfer of pollutants but also provides a clear and measurable pathway of exposure for resident biota (Mwangi *et al*., 2025). This ecological linkage enhances their value as bioindicators, since changes in their contaminant loads can signal broader ecosystem-level risks and help predict potential impacts on fish populations and top predators (Akinyemi & Zhang, 2023). Therefore, understanding the contamination dynamics within benthic macroinvertebrate communities is essential for evaluating the overall health and resilience of estuarine ecosystems (Lee *et al*., 2022; Otieno *et al*., 2021, 2020, 2018).

While biomonitoring using macroinvertebrates and fish has been employed in freshwater and temperate marine environments, there is limited application in tropical estuarine ecosystems, particularly in SSA. Existing studies in Kenya have primarily focused on heavy metals or microbial pollution, with very few addressing pesticide contamination in estuarine fauna. This gap in knowledge hinders the development of effective management strategies and risk assessment frameworks tailored to local environmental and socio-economic conditions (Anyango et al., 2024). Moreover, data

on species-specific OCPs uptake, metabolism, and trophic transfer in tropical estuarine food webs are scarce, limiting the understanding of ecological and human health risks (Munyao *et al*., 2022; Abong'o & Nyamai, 2021).

In SSA, research has predominantly documented the presence of OCPs in inland water bodies (Kiyuka, 2022) without linking these findings to aquatic food web dynamics. Studies on coastal waters have primarily focused on the distribution, fate, and occurrence of pesticides (Wanjeri *et al*., 2022; Okuku *et al*., 2022, 2013; Wandiga, 2005). Research on emerging pollutants has often concentrated on metal contamination, with limited information on their ecological effects on organisms (Nyamora *et al*., 2023; Okuku *et al*., 2013). Investigations measuring OCPs concentrations in fish from the Tana and Sabaki rivers and estuaries exist (Munga *et al*., 2016; Lalah *et al*., 2003), but these studies have typically analyzed fish as individual organisms without assessing trophic interactions. There is insufficient data on OCPs bioconcentration and biomagnification in SSA aquatic ecosystems, which limits comprehensive toxicological risk assessments for both wildlife and humans.

The key processes governing OCPs accumulation in aquatic organisms are bioconcentration and biomagnification (Tulcan *et al*., 2021; Tongo *et al*., 2022). Bioconcentration is the direct uptake of OCPs from surrounding water through gills, skin, or membranes, while biomagnification is the increase in OCPs concentration as it moves up the food chain. Biomagnification occurs when OCPs levels rise at successive trophic levels, causing higher organisms to contain contaminant levels exceeding those of their prey, often surpassing chemical equilibrium via dietary absorption (Tulcan *et al*., 2021). These processes depend on pesticide physicochemical properties

(hydrophobicity, persistence), environmental conditions (temperature, salinity, pH), and organism traits (lipid content, metabolic capacity, trophic position) (Ngige *et al*., 2024; Onyango *et al*., 2023, 2021). In estuarine systems, where environmental gradients and species interactions are complex, understanding these pathways is essential to evaluate ecological consequences of OCPs contamination (Kamau *et al*., 2022; Ochieng *et al*., 2020).

Although many studies have documented the responses of benthic macroinvertebrates and fish to various aquatic pollutants, especially nutrients and metals, a significant gap remains regarding pesticide behavior in these organisms. To current knowledge, no study has systematically investigated OCPs bioconcentration and bioaccumulation across different feeding guilds of benthic macroinvertebrates and fish in estuarine systems along the Kenyan coast. This gap is critical given the ecological and economic importance of these habitats. While interest in OCPs bioaccumulation has increased since the 1970s (Li, 2023a; Li *et al*., 2020), empirical data on biological interactions of OCPs with estuarine and freshwater organisms remain scarce (Li, 2023a, b; Li *et al*., 2014; Zhou *et al*., 2008), including their physiological and ecological effects (Li *et al*., 2023, 2020). This underscores the need for localized studies exploring pesticide contamination across trophic groups in estuarine environments, particularly in developing regions like coastal Kenya. This study thus aims to investigate OCPs bioconcentration and biomagnification in estuarine ecosystems along Kenya's South Coast, focusing on benthic macroinvertebrates and fish. Such an integrated approach provides valuable insights into OCPs fate and effects in tropical estuaries, supports evidence-based policy, and promotes sustainable coastal resource use in Kenya.

1.2 Problem statement

Estuaries are transitional ecosystems with highly productive habitats that support diverse biological communities and provide essential ecosystem services such as nutrient cycling, carbon sequestration and fisheries that sustain local livelihoods. However, these ecosystems are increasingly threatened by contamination from OCPs from upstream agriculture, coastal farming and historical sources, whose residues enter water and sediments through runoff, leaching, and atmospheric deposition, with some exceeding safe limits for aquatic life. Because OCPs are hydrophobic and persistent, they readily bind to sediments that act as long-term reservoirs, prolonging their bioavailability to aquatic organisms. Due to constant interactions with contaminated water and sediments, macroinvertebrates and fish bio-accumulate and biomagnify OCPs, which disrupt their physiological processes, reproduction and survival. This threatens biodiversity and ecosystem functioning, and raises concerns about food safety for communities that depend on these resources for nutrition and livelihoods. In Kenya, insufficient environmental monitoring and weak regulatory frameworks in estuaries have led to poor pesticide management. Existing studies largely focus on physico-chemical water quality in inland freshwater ecosystems resulting to limited understanding of OCP contamination, bioaccumulation and trophic transfer in estuarine ecosystems. This study investigated the bioconcentration and biomagnification of OCPs in aquatic macroinvertebrates and fish within the south coast Kenyan estuarine ecosystems to support integrated contamination assessment, risk evaluation and effective policy mitigation that protect aquatic ecosystems and human health.

1.3 Justification

Physico-chemical parameters such as temperature, pH, dissolved oxygen, salinity, turbidity, and nutrient levels directly influence the fate, transport, and bioavailability of pesticides in estuarine environments (Obiero *et al*., 2020). Estuaries are dynamic ecosystems where freshwater and seawater mix, causing fluctuations in these parameters that can alter chemical degradation rates, solubility, and the partitioning of pesticides between water, sediments, and biota (Mwangi *et al*., 2018). Understanding baseline water quality is crucial because pesticide toxicity and bioaccumulation potential are modulated by these environmental factors (Ochanda *et al*., 2020). Therefore, assessing physico-chemical conditions provides essential context for interpreting pesticide contamination patterns and predicting their ecological impacts in South Coast estuaries.

OCPs tend to adsorb to sediments due to their hydrophobic properties, making sediments a long-term reservoir and source of contamination for benthic organisms (Kamau *et al*., 2019). Sediments influence exposure levels for macroinvertebrates and fish that forage or reside in or near sediment beds (Mburu *et al*., 2021). Quantifying OCPs concentrations across different environmental compartments including water, sediment, and biota from various trophic levels is essential to comprehensively assess contamination levels and exposure risks. Additionally, trophic guild–specific OCPs burdens reveal differential exposure and accumulation patterns, reflecting dietary habits and habitat preferences, thus providing critical insights into the pathways of OCPs transfer in estuarine food webs (Wanjala *et al*., 2022).

The interaction between water quality parameters and pesticide concentrations is complex and influences OCPs behavior such as degradation, dilution, and bioavailability (Onyango *et al*., 2019). For example, pH and temperature affect OCPs hydrolysis and volatilization rates, while salinity can influence the partitioning of OCPs between dissolved and particulate phases (Ngugi *et al*., 2018). Establishing correlations between water quality attributes and OCPs levels helps identify environmental drivers that regulate OCPs persistence and transport in estuarine waters. This understanding is important for predicting contamination hotspots and temporal trends, thereby improving risk assessments and informing management strategies that consider changing environmental conditions in Kenyan estuaries.

Bioconcentration and biomagnification are critical processes that influence the distribution and toxicity of these chemicals in aquatic ecosystems (Mburu *et al*., 2021). Benthic macroinvertebrates serve as important bioindicators and prey for fish, making them key species for tracing OCPs movement through trophic levels (Kamau *et al*., 2018). By mapping the pathways and magnitude of OCPs transfer from abiotic compartments to biota across trophic levels, this study will reveal how contaminants accumulate and pose risks to higher trophic organisms, including commercially important fish species. This knowledge is essential for protecting biodiversity, ensuring fisheries sustainability, and safeguarding human health in coastal communities reliant on these ecosystems.

Beyond quantifying OCPs residues, assessing the ecotoxicological risks associated with detected levels is vital to understanding potential adverse effects on aquatic life and ecosystem functioning (Otieno *et al*., 2020). Risk assessments integrate OCPs

concentrations with toxicity thresholds to evaluate the likelihood of harmful biological impacts, including mortality, reproductive impairment, and behavioral changes (Munga *et al*., 2016). Estuarine species may be exposed to complex mixtures of pesticides, necessitating assessment of cumulative and synergistic effects (Ochanda *et al*., 2020). By identifying ecotoxicological risks, this study will provide evidence-based guidance for regulatory agencies and stakeholders to implement targeted interventions that mitigate OCPs pollution and conserve the ecological integrity of Kenyan estuarine ecosystems.

1.4 Objectives of the study

1.4.1 General objective of the study

The general objective of this study was to assess the bioconcentration and biomagnification of OCPs by aquatic macroinvertebrates and fish in estuarine ecosystems along the South Coast of Kenya.

1.4.2 Specific objectives of the study

The specific objectives of this study are to:

1. Determine the selected physico-chemical water quality parameters (temperature, dissolved oxygen, pH, conductivity, salinity, total dissolved solids, ammonia, phosphates and nitrates) in estuarine ecosystems of South Coast, Kenya.
2. Characterize the concentration of OCPs in sediments, waters, trophic guilds of benthic macroinvertebrates and fish in estuarine ecosystems of South Coast, Kenya.
3. Analyze the relationship between physico-chemical water quality parameters and OCPs concentrations in water in estuarine ecosystems of South Coast,

Kenya.

4. Investigate the bioconcentration and biomagnification of OCPs in water, sediments, the trophic levels of benthic macroinvertebrates and fish in estuarine ecosystems of South Coast, Kenya.
5. Assess the potential ecotoxicological risk posed by OCPs in sediments, water, trophic guilds of benthic macroinvertebrates and fish in estuarine ecosystems of South Coast, Kenya.

1.5 Hypotheses of the study

H_{01}: There are no significant variations in the selected physico-chemical water quality parameters across the estuarine ecosystems of the South Coast, Kenya.

H_{02}: OCPs concentrations in sediments, waters, and aquatic organisms do not differ significantly among different matrices (sediments, water, macroinvertebrates, and fish) in the estuarine ecosystems, South Coast, Kenya.

H_{03}: There is no significant correlation between physico-chemical water quality parameters and pesticide concentrations in estuarine waters, South Coast, Kenya.

H_{04}: OCPs do not bioconcentrate or biomagnify through trophic levels in the estuarine ecosystem, South Coast, Kenya.

H_{05}: OCPs levels in sediments, water, and aquatic organisms do not pose significant ecotoxicological risks to the estuarine ecosystem, South Coast, Kenya.

1.6 Assumptions of the Study

The assumptions of this study included:

i. The legacy OCPs could be found in all the study matrices.
ii. That the OCPs could bioaccumulate and biomagnify along the food chain/web.
iii. That the OCPs could occur in the trophic transfer across food chain/webs.
iv. Environmental factors could influence pesticide bioavailability and uptake rates.
v. Decline in sensitive taxa could occur with increasing pesticide toxicity.
vi. Macroinvertebrates in estuaries absorb pesticide residues from sediments and water, functioning as vectors for transfer to fish.
vii. Fish species, higher up the food web, accumulate pesticides through both direct exposure (contaminated water/sediments) and prey ingestion, with biomagnification depending on the compound's biochemical properties.

1.7 Scope of the Study

This study assessed the bioconcentration and biomagnification of OCPs by aquatic macroinvertebrates of functional feeding groups (FFGs) and fish in estuarine ecosystems of South Coast of Kenya. It sought to analyze OCPs residues in both abiotic and biotic compartments of the estuarine ecosystem of South Coast, Kenya and assess potential ecological and human health risks. The study covered both spatial and temporal variations in OCPs concentrations, while in cognizant of different anthropogenic activities (industrialization, urbanization, agriculture, and hydrodynamics) and ecological characteristics across discharging rivers' catchments to respective estuaries.

The study was limited to South Coast estuary of Kenya, consisting of such sub-estuaries as Umba near the Kenya-Tanzania border at the far-south, Mkurumdzi,

Ramisi, Mwanje and Mapu with 12 sampling stations selected purposively and spread across the respective sub-estuaries. It also targeted five main FFGs of macroinvertebrates namely: predators (*Rhagovelia* species), collector-gatherers (Atyidae), Filterers (*Saccostrea cucullata),* Shredder-grazers (*Nerita undata),* shredders *(Terebrallia palustris),* and fish (*Penaeus monodon*). Two more compartments were also included: water and sediments whereas selected environmental variables or water quality parameters were included in the study to establish their influence on OCPs. Sampling covered both wet/rainy and dry seasons to evaluate seasonal variation of all the measured parameters or variables. To assess the pollution and ecological effects of the OCPs in the estuarine ecosystem of South Coast Kenya, different indices were applied: Contamination Factor (Cf), Geo-accumulation Index (Igeo), Pollution Load Index (PLI), Potential Ecological Risk Index (RI), Nemerow Pollution Index (PN), and Mean Effect Range-Median Quotient (ERM-Q).

1.8 Limitations of the Study

The present study was affected by several limitations including methodological, ecological and logistical. Inconsistent long-term strategy became a hindrance due to lack of sufficient funding. Challenges in sampling strategies and approaches, and chemical detection were experienced. Estuarine ecosystems are quite dynamic and complex unlike freshwater systems. Species level differences and the trophic dynamics made the study challenging in sampling and analysis of OCPs. Lastly, data paucity on OCP studies along the Kenyan estuarine system making it difficult to generalize findings from inland water systems to estuaries characterized by dynamic coastal environment.

1.9 Delimitations of the Study

To overcome the stated limitations, the following strategies were incorporated into the study:

i. A concise choice of study sites (12 stations) was undertaken while considering proximity from the station/laboratory. The study period was minimized to 12 months.

ii. Sensitive analytical tools for a broader range of compounds, which improved limit of detection issues were used.

iii. Environmental variability that involved rigorous contextual data collection was applied where a number of community attributes were collected and the resident taxa that was readily found in all the sampling areas were used.

iv. The present study was zeroed along the south coast estuarine ecosystem of Kenya where data for OCPs by the benthic macroinvertebrate FFGs and fish was undertaken. However, to back up the data collected and make generalized/meaningful interpretation, the sporadic data was supplemented by literature from other estuarine ecosystems globally.

1.10 Definition of Terms

The following list provides the definition of terms specifically operationalized to suit the current study:

Bioconcentration — Process by which OCPs are absorbed by aquatic macroinvertebrates and fish directly from the surrounding water in the south coast estuarine system of Kenya, resulting in a higher concentration of the OCPs in the organism than in the water and is measured as bioconcentration factor (BCF).

Biomagnification — This is the increase in concentration of OCPs in aquatic macro-invertebrates and fish at successively higher trophic levels of a food chain along the south coast estuary, Kenya.

Bioaccumulation — Is the general process by which aquatic macroinvertebrates and fish accumulate OCPs from both water and food over time along the south coast estuarine system, Kenya.

Persistent Organic Pollutants (POPs) — Refers to OCPs that persist in the environment (south coast estuarine system, Kenya), bioaccumulate in macroinvertebrates and fish, and pose ecological risks to human health and the environment.

Aquatic Macroinvertebrates — Are invertebrate animals (no backbone) that are large enough to be seen without an aid of a microscope and live in the estuarine ecosystem of south coast, Kenya and are used as indicators of OCPs pollution.

Fish — It refers to any aquatic organism that is exploited or harvested by the fishermen in south coast Kenya for food and economic use. In this context, the fish in refernce is *P. monodon*.

Estuarine Ecosystems	Are Kenyan south coastal water bodies where freshwater from rivers Umba, Ramisi, Mkurumdzi, Mwena and Mapu mixes with saltwater from the Indian Ocean in the West Indian Ocean region (WIO), creating brackish conditions.
Lipophilicity	Refers to the chemical affinity of OCPs for fat (lipid) tissues from macroinvertebrates and fish over water sampled along the south coast estuarine system of Kenya.
Trophic Level	Refers to the position an aquatic macroinvertebrate and fish occupies in the food chain along the south coast estuarine system of Kenya.
Trophic Transfer	Is the movement of OCPs through a food chain/web as predators (fish and predatory macroinvertebrate guild) consume prey (shredders, scrapers/grazers, filterers and collector-gatherers) along the south coast estuarine system of Kenya.
Bioindicator Species	These are aquatic macroinvertebrate and fish species used to assess the health of the south coast estuarine system of Kenya on the presence of OCPs based on their sensitivity or ability to accumulate toxins.
Ecotoxicology	Is the study of the toxic effects of OCPs along the south coast estuarine ecosystems of Kenya, particularly on how OCPs affect aquatic macroinvertebrate and fish species interactions, populations, and food webs.

Exposure Pathways	Refers to the routes by which aquatic macroinvertebrate and fish species come into contact with OCPs along the south coast estuarine ecosystems of Kenya. They include: direct uptake from water (bioconcentration), Ingestion of contaminated food (biomagnification and contact with contaminated sediments.

CHAPTER TWO

LITERATURE REVIEW

2.1. Introduction

This chapter begins by examining the general overview of OCPs in aquatic ecosystems before reviewing literature on: physico-chemical water quality parameters in estuarine ecosystems; occurrence and concentration of OCPs in estuarine sediments, water, and biota; relationship between physico-chemical water quality parameters and OCPs concentrations; bioconcentration and biomagnification of OCPs in aquatic food webs; and ecotoxicological risk assessment of OCPs in estuarine ecosystems.

2.2. General overview of OCPs in aquatic ecosystems

Estuarine ecosystems are ecologically and economically significant transitional zones that provide habitat for a wide variety of aquatic organisms and act as natural buffers between terrestrial and marine environments. They play a crucial role in nutrient cycling, shoreline protection, and supporting fisheries that sustain local livelihoods. However, these systems are increasingly under pressure from anthropogenic pollution, particularly pesticides originating from agricultural runoff, industrial discharge, and urban stormwater (Amankwaa et al., 2021; Beger et al., 2019). The persistence, hydrophobicity, and bioactive properties of many pesticides such as OCPs remain in estuarine systems for extended periods, posing significant risks to aquatic organisms and food web integrity through processes such as bioconcentration and biomagnification (Li *et al*., 2020; Zhou *et al*., 2020).

Understanding OCPs dynamics in estuarine environments is critical for biodiversity conservation and the protection of ecosystem services. The transport, fate, and

ecological effects of OCPs in estuaries are influenced by a range of environmental factors, including salinity gradients, hydrodynamics, sediment composition, and trophic interactions (Belaidi et al., 2023). This literature review synthesizes current knowledge on water quality parameters, OCPs occurrence, and bioaccumulation processes in estuarine environments, with a focus on African and Kenyan coastal contexts. It also examines the ecotoxicological risks associated with OCPs in aquatic food webs, thereby framing the research objectives and highlighting key knowledge gaps.

2.3. Physico-Chemical Water Quality Parameters in Estuarine Ecosystems

Estuaries are among the most productive and dynamic aquatic ecosystems globally, characterized by the mixing of freshwater and marine influences that create highly variable and complex environments (van Niekerk *et al*., 2022). These transitional zones serve as critical habitats for diverse species, including fish, crustaceans, and migratory birds, while also providing essential ecosystem services such as nutrient cycling, sediment trapping, nursery grounds for fisheries, and water filtration (van Niekerk *et al*., 2022; Amankwaa *et al*., 2021). The ecological health and function of estuaries depend heavily on physico-chemical water quality parameters, which dictate the suitability of habitat and influence biological productivity and biodiversity (Costa & Mouri, 2018).

Key physico-chemical parameters commonly monitored in estuarine systems include temperature, salinity, pH, dissolved oxygen (DO), turbidity, and nutrient concentrations (e.g., nitrogen and phosphorus compounds) (Chilton *et al*., 2021; Costa & Mouri, 2018). These parameters interact dynamically, governing the chemical and biological processes within estuaries. For instance, temperature regulates metabolic rates of

aquatic organisms, influencing respiration, growth, and reproduction, and also affects the solubility and reaction kinetics of various dissolved substances (Belaidi *et al*., 2023). Salinity, a defining characteristic of estuarine waters, varies spatially and temporally due to freshwater inputs, mainly from influent rivers, and tidal mixing, influencing osmoregulation in aquatic fauna, nutrient availability, and sediment dynamics (van Niekerk *et al*., 2022). The pH levels affect chemical speciation and solubility of nutrients and metals, impacting their bioavailability and toxicity (Chilton *et al*., 2021). Dissolved oxygen is critical for sustaining aquatic life. Fluctuations in DO can lead to hypoxic or anoxic conditions detrimental to sensitive species (Costa & Mouri, 2018). Turbidity, caused by suspended particles and organic matter in the water column, influences light penetration, affecting photosynthesis and habitat quality for submerged aquatic vegetation (Amankwaa *et al*., 2021). Nutrients, especially nitrogen and phosphorus, control primary productivity but when elevated, can trigger eutrophication leading to harmful algal blooms and oxygen depletion (Costa & Mouri, 2018). Despite their individual importance, these parameters rarely act in isolation. Their interactive and sometimes nonlinear effects are critical to understanding estuarine ecosystem dynamics.

For example, temperature-driven increases in metabolic activity may amplify oxygen demand at the same time that eutrophication-related turbidity reduces photosynthetic oxygen production. Additionally, natural factors such as tidal cycles, seasonal rainfall, and freshwater inflow combine with anthropogenic influences, resulting in complex spatial and temporal variability (van Niekerk *et al*., 2022). Emerging environmental stressors related to climate change, such as sea-level rise, altered precipitation patterns, and rising temperatures, are expected to exacerbate fluctuations and introduce new

challenges to estuarine water quality management (van Niekerk *et al*., 2022; Chilton *et al*., 2021).

In the African context, estuarine systems are vital to coastal biodiversity and local economies but are increasingly impacted by human activities and climate variability (van Niekerk *et al*., 2022). Studies from estuaries along West, East, and Southern African coasts show wide seasonal and regional variability in physico-chemical parameters influenced by land use, urbanization, and hydrological changes (van Niekerk *et al*., 2022; Adewumi *et al*., 2020). However, many of these studies generalize findings across diverse estuaries without adequately considering localized socio-economic and ecological factors. Furthermore, the lack of long-term and high-resolution datasets limits the ability to discern trends or forecast responses to ongoing environmental changes (van Niekerk *et al*., 2022). For example, in the Niger Delta estuaries, oil exploration activities and agricultural runoff contribute to elevated nutrient loads, altered pH, and increased turbidity, resulting in episodic hypoxia and degradation of aquatic habitats. Similarly, urban stormwater inputs in South African estuaries increase nutrient concentrations and conductivity, fostering eutrophication and shifts in species assemblages. The Senegal River estuary experiences significant salinity fluctuations due to upstream damming and water withdrawals, profoundly influencing water quality and biological communities (Costa & Mouri, 2018). These case studies highlight how estuarine water quality is shaped by a complex interplay of natural and anthropogenic drivers. However, comprehensive, integrated assessments that capture the cumulative effects of these factors across multiple scales are still limited in African estuaries.

Along the Kenyan coast, estuarine systems such as the Sabaki, Ramisi, and Vanga provide critical ecosystem services supporting fisheries, biodiversity, and livelihoods for coastal communities (Kairo *et al*., 2009). The physico-chemical water quality in these estuaries is primarily governed by seasonal rainfall, tidal mixing, and freshwater inflows, resulting in strong gradients of salinity (ranging from about 5 to 35 Practical Salinity Units - PSU) and temperature fluctuations between 25 °C and 32 °C (Otwoma *et al*., 2021; Lu *et al*., 2019). Dissolved oxygen levels in these estuaries vary widely, sometimes dropping to hypoxic levels (~2 mg/L) especially in areas with high organic matter loads and limited tidal flushing, but generally ranging up to well-oxygenated conditions (~7 mg/L). These values show significant spatial and temporal variability driven by natural factors but are also influenced by increasing anthropogenic pressures and climate change. For instance, altered rainfall patterns and changes in tidal regimes may exacerbate fluctuations in salinity, DO, and turbidity beyond natural variability, with potential consequences for estuarine biodiversity and fisheries productivity (Otwoma *et al*., 2021).

Human activities in the South Coast region such as agriculture, urban development, and industry contribute to changes in nutrient levels, pH alterations, and increased sediment loading in estuarine waters (Oduor *et al*., 2023). Land use changes in watersheds upstream of these estuaries can lead to increased runoff carrying sediments and nutrients, thus influencing estuarine water quality and ecosystem functioning. Climate change impacts, including rising temperatures and shifting precipitation patterns, compound these effects by altering freshwater inflow, sediment transport, and nutrient cycling (van Niekerk *et al*., 2022). For example, elevated nutrient inputs near urban centers have been associated with increased turbidity and higher risks of eutrophication,

which can impair aquatic habitats and fisheries productivity (Adewumi *et al.*, 2020). However, much of the research to date has been fragmented, focusing on individual parameters rather than on their combined or synergistic effects, limiting understanding of the holistic estuarine water quality status.

Alterations in physico-chemical water quality parameters have direct and indirect ecological consequences in estuarine environments. Elevated nutrient levels can stimulate eutrophication processes, resulting in oxygen depletion (hypoxia or anoxia) which negatively affects fish, benthic fauna, and overall biodiversity (Howarth & Marino, 2006). Changes in pH and salinity regimes may shift species assemblages by favoring tolerant species and disadvantaging sensitive taxa, thus altering community structure and trophic interactions (Onyango *et al.*, 2019). Despite the well-documented ecological impacts, there is limited critical discussion in the literature about the effectiveness of restoration measures such as wetland rehabilitation, nutrient load management, and riparian buffer zones in African estuaries. Additionally, the potential lag effects in ecosystem recovery following interventions where ecological improvements may take years or decades to manifest are often overlooked, complicating the assessment of management success.

Temperature increases influence not only the solubility of dissolved oxygen but also microbial activity and biogeochemical cycling in estuarine waters, potentially accelerating nutrient turnover and organic matter decomposition (Szewczyk *et al.*, 2023; Chen *et al.*, 2025). High turbidity levels limit light penetration, reducing photosynthetic activity of submerged aquatic vegetation and affecting primary productivity and habitat quality (Lunt *et al.*, 2020). However, these impacts are

complex and may include compensatory mechanisms such as shifts in species composition toward more tolerant or opportunistic species, and increased heterotrophic microbial productivity. The interplay between temperature, turbidity, and biotic responses remains an important area for further research.

While baseline physico-chemical water quality data exist for some Kenyan estuaries (NEMA, 2018; Otwoma *et al.*, 2021), most studies focus on snapshots of individual parameters rather than comprehensive, integrated assessments. The fragmented nature of existing research is often driven by funding constraints and disciplinary silos, which hinders holistic understanding of estuarine ecosystem dynamics. There is a pressing need for collaborative, multidisciplinary research approaches that combine in situ measurements, long-term monitoring, remote sensing, and modeling to capture the spatial and temporal complexity of estuarine water quality (Teshome, 2020).

The estuaries along the South Coast of Kenya remain under-studied with respect to detailed, seasonally resolved physico-chemical water quality parameters. Addressing these gaps is essential to provide robust scientific knowledge that supports sustainable estuarine resource management and effective conservation planning. Moreover, integrating traditional ecological knowledge with scientific data can yield more context-specific and culturally appropriate management strategies that bolster the resilience of estuarine ecosystems in the face of increasing anthropogenic and climatic pressures.

2.4. Occurrence and Concentration of OCPs in Estuarine Sediments, Water, and Biota

Pesticides, including OCPs, organophosphates, carbamates, and pyrethroids, are widely used in agricultural and vector control activities worldwide, leading to their frequent detection in aquatic ecosystems (Datta, 2025). The rapid increase in OCPs application over the years is largely driven by the surge in human population demanding greater food production (Alexandratos & Bruinsma, 2012). This trend, which has been evident since the last century, is projected to continue as population growth persists, compounded by global conflicts and climate change impacts that disrupt agricultural productivity and food security (UN, 2015). Consequently, intensive farming practices increasingly rely on pesticides to maximize yields, often compromising environmental integrity.

Estuarine ecosystems, as transitional zones between freshwater and marine environments, are particularly vulnerable to pesticide contamination due to their proximity to agricultural lands and urban centers (Onyango et al., 2023). Sediments in estuaries act as sinks and reservoirs for hydrophobic pesticides, whereas dissolved pesticides in water represent the bioavailable fraction accessible to aquatic organisms (Wang *et al*., 2025). The presence of OCPs residues in aquatic environments, especially in developing countries, poses serious deleterious effects on terrestrial and aquatic ecosystems, contaminating aquatic food resources and threatening fisheries and aquaculture (EEA, 2013). Understanding the occurrence and concentration of OCPs in sediments, water, and biota is thus essential for assessing ecological impacts and food safety risks.

Sediments in estuarine systems serve as repositories for OCPs through sedimentation and adsorption. The hydrophobic nature of many OCPs, such as dichlorodiphenyltrichloroethane (DDT) and its metabolites, favors their partitioning into sediment particles rich in organic carbon and fine-grained material (Wang *et al*., 2025). The occurrence of OCPs in aquatic environments depends on different matrices water, sediments, interstitial water and functional feeding groups of organisms as well as degradation processes affecting each partition (Rajan, 2025). Globally, pesticide residues in sediments range from trace levels to highly contaminated zones near agricultural runoff points, particularly for OCPs and organophosphorus compounds (López-Benítez *et al*., 2024). For example, sediment analyses in the Chesapeake Bay estuary, USA, have detected persistent OCPs decades after their ban, indicating their long-term persistence and ecological risk (Yuan *et al*., 2015). Despite the insights provided by sediment analyses, many studies rely on surface sediment samples that may not reflect vertical contaminant profiles, potentially underestimating total pesticide burdens (Rajan, 2025). Analytical methodologies also vary in sensitivity, complicating inter-study comparisons (López-Benítez *et al*., 2024).

In East Africa, data on OCPs residues in estuarine sediments, particularly along the Kenyan coast, remain limited. Ngugi *et al*. (2020) reported trace organophosphate pesticides in Tudor Creek estuary sediments, though with limited spatial and temporal coverage. Such gaps restrict understanding of pesticide dynamics amid varying hydrological and anthropogenic influences. Comprehensive spatial and temporal sediment sampling is therefore essential for effective characterization of OCPs contamination patterns. The aqueous phase in estuaries represents the immediate medium for OCPs bioavailability to aquatic organisms. Factors such as temperature,

pH, salinity, and microbial activity influence pesticide solubility, stability, and degradation in water (Mellor & Turner, 2017).

Although OCPs concentrations in estuarine waters are typically low due to dilution, episodic runoff or point source inputs can cause acute toxicity risks (Islam *et al*., 2016). Pesticide concentrations vary seasonally and geographically, as documented in the Yangtze River estuary, China, where organophosphates like chlorpyrifos and diazinon were detected in nanogram to microgram per liter ranges (Zhang *et al*., 2018). Similar seasonal trends have been observed in European estuaries linked to agricultural application periods (Brack *et al*., 2016). However, few studies simultaneously assess OCPs concentrations in water, sediments, and biota, limiting comprehensive risk assessments. Water sampling often involves grab samples, which may miss temporal variability and episodic contamination, while rapid OCPs degradation in water can lead to underestimation of exposure if sampling is infrequent (Mellor & Turner, 2017; Islam et al., 2016). These limitations underscore the need for continuous or high-frequency sampling.

Along the Kenyan coast, pesticide data in estuarine waters are sparse. Otieno et al. (2018) detected low but measurable synthetic pyrethroids in the Sabaki River estuary; however, lack of concurrent sediment or biota data limits understanding of ecological risks. The presence of pesticide residues in estuarine waters and sediments primarily stems from agricultural runoff, urban wastewater, and atmospheric deposition (Jiang *et al*., 2021). Persistent OCPs (such as DDT, endosulfan) alongside newer organophosphates and pyrethroids are commonly detected worldwide (Khan *et al*., 2018). In Kenya's coastal regions, Omondi *et al*. (2020) reported chlorpyrifos and

cypermethrin concentrations in Mtwapa estuary sediments exceeding sediment quality guidelines, while Wanyama *et al*. (2022) detected OCPs in edible coastal fish species, raising food safety concerns.

Benthic macroinvertebrates are key trophic players in estuarine food webs and valuable bioindicators of aquatic pollution due to their sedentary nature and sediment contact (Sánchez-Avila *et al*., 2011). Pesticide bioaccumulation in macroinvertebrates depends on pesticide properties, organism physiology, feeding habits, and sediment contamination (Fisher *et al*., 2014). Organophosphates and pyrethroids bioaccumulate in invertebrates, impairing survival, reproduction, and community structure (Mackay *et al*., 2015). Studies in North America and Europe reveal OCPs residues in amphipods, polychaetes, and mollusks, often at higher levels than in water due to sediment interactions (Franklin *et al*., 2013). For instance, the Scheldt estuary in Belgium showed high OCPs burdens in sediment-dwelling amphipods aligned with sediment contamination hotspots (Mehler *et al*., 2018). Many biomonitoring studies focus on limited taxa, risking oversight of species-specific pesticide uptake and metabolism differences (Fisher *et al*., 2014). Laboratory exposures may not mimic field fluctuations such as salinity changes or pesticide mixtures, limiting ecological relevance (Mackay *et al*., 2015). In Kenyan estuaries, OCPs accumulation in benthic macroinvertebrates is understudied, presenting a crucial research gap given their ecological importance and role as prey. Priorities include assessing diverse taxa and integrating field and lab studies to clarify bioaccumulation and effects.

Fish, integral to estuarine food webs, are often ultimate OCPs recipients via bioconcentration from water and biomagnification through trophic transfer (Borgå *et al*., 2012). Lipophilic pesticides such as OCPs biomagnify extensively, posing risks to

fish health and human consumers (López-Antia *et al*., 2015). Global studies document OCPs residues in fish tissues with species-specific accumulation patterns linked to feeding and habitat (Sánchez-Avila *et al*., 2011). Predators generally show higher OCPs loads due to trophic magnification (Lohmann *et al*., 2016). Legacy pesticides persist in fish decades post-ban, as seen in the Gulf of Mexico (Morrison *et al*., 2015). Many studies quantify total pesticides without distinguishing parent compounds from metabolites, which differ in toxicity and environmental fate (Borgå *et al*., 2012). Fish sampling often targets commercially important species, potentially biasing ecological risk assessments (López-Antia *et al*., 2015). Kenyan coastal fish contamination by pesticides remains poorly documented. Early findings by Mwamburi *et al*. (2017) reveal detectable residues but lack trophic-level or sediment-water contextualization, limiting understanding of OCPs transfer in food webs and human health risk via fish consumption.

The extent of pesticide bioaccumulation in estuarine organisms is influenced by physicochemical properties of pesticides such as octanol-water partition coefficient (K_ow), persistence, and degradation rates (Mackay *et al*., 2015). Highly hydrophobic OCPs with high K_ow accumulate in lipid-rich tissues and biomagnify through food chains (Zhou *et al*., 2017). Environmental factors like salinity, temperature, and organic matter modulate pesticide availability and uptake (Mellor & Turner, 2017). Most bioconcentration and biomagnification models derive from freshwater or marine systems, often overlooking estuarine salinity gradients and dynamics (Islam *et al*., 2016). These gradients affect OCPs sorption, organism physiology, and metabolism, complicating extrapolations (Kennish, 2002). Lack of estuary-specific bioaccumulation models hinders accurate OCPs fate predictions in these transitional systems (Mellor & Turner, 2017). Moreover, OCPs mixtures common in estuaries pose complex

interactive effects rarely addressed, influencing bioaccumulation outcomes (Fisher *et al*., 2014).

The reviewed literature underscores that OCPs persist in estuarine sediments and water, bioaccumulate in benthic macroinvertebrates, and biomagnify in fish with spatial and temporal variability governed by their characteristics and environmental conditions. However, significant knowledge gaps remain for Kenyan coastal estuaries regarding integrated sediment, water, and biota analyses across trophic levels. Most studies suffer from limited sampling, narrow species focus, and insufficient consideration of estuarine-specific dynamics. Therefore, multidisciplinary research is urgently needed to characterize OCPs concentrations in sediments.

2.5. Relationship between Physico-Chemical Water Quality Parameters and OCPs Concentrations

Estuarine ecosystems are dynamic interfaces between freshwater and marine environments, characterized by high biological productivity and complex physico-chemical gradients. These ecosystems along the Kenyan coast are particularly vulnerable to OCPs contamination due to agricultural runoff and urbanization (Tongo *et al*., 2021). OCPs entering estuarine waters pose significant risks to aquatic organisms through bioaccumulation, bioconcentration, and biomagnification (Katagi, 2010a, b). Understanding the relationship between physico-chemical water quality parameters and OCPs concentrations is critical for assessing ecological health and risks to fisheries and human consumers. While current studies emphasize OCPs presence, there is limited focus on the integration of water quality dynamics influencing their bioavailability in Kenyan estuaries, which could lead to underestimations of ecological risk (Onyango *et al*., 2019). Most research focuses on pollutant concentrations rather than their

interactions with changing physico-chemical parameters such as pH, salinity, and dissolved oxygen, which directly affect pesticide toxicity and bioaccumulation potential (Li, 2023b).

Water quality parameters such as pH, temperature, dissolved oxygen (DO), salinity, turbidity, light intensity, and nutrients strongly influence OCPs solubility, degradation, and partitioning in estuarine waters (Liu *et al*., 2025; Katagi, 2010a). For instance, OCPs degradation rates often increase with temperature and sunlight exposure but can vary with pH and salinity, which affect chemical stability and bioavailability (Oloo *et al*., 2023). Salinity gradients in estuaries can cause OCPs to partition differently between dissolved and particulate phases, altering their uptake by macroinvertebrates and fish (Khouni *et al*., 2023). Elevated turbidity often correlates with higher OCPs adsorption to suspended particles, facilitating their accumulation in benthic organisms (Commelin *et al*., 2022). Although many studies report correlations between salinity and OCPs distribution, the causal mechanisms remain poorly understood, particularly under the fluctuating conditions typical of Kenyan estuaries (Njiru *et al*., 2023). There is a lack of experimental studies assessing the combined effects of multiple physico-chemical parameters on OCPs fate, which could help develop predictive models for contamination hotspots (Mugambi *et al*., 2023).

Pesticides entering Kenyan estuarine systems mainly originate from agricultural runoff, especially from smallholder farms using organophosphates, pyrethroids, and carbamates (Tongo *et al*., 2021). These chemicals vary in hydrophobicity, persistence, and toxicity, influencing their bioaccumulation patterns (Katagi, 2010b). Organophosphates, such as chlorpyrifos, tend to be less persistent but highly toxic to

aquatic fauna, while pyrethroids like cypermethrin are more hydrophobic and highly bioaccumulative (Li, 2023a, b). The persistence of these pesticides in sediments further enhances exposure risks to benthic macroinvertebrates and bottom-feeding fish (Cuevas *et al*., 2018). Most pesticide monitoring in Kenya is sporadic and lacks continuous data, which limits understanding of seasonal and long-term contamination trends (Brander & Mehinto, 2021). The diversity of pesticides used and their metabolites is often underestimated in biomonitoring studies, leading to incomplete risk assessments for aquatic biota (DeLorenzo *et al*., 2001).

Aquatic macroinvertebrates are vital bioindicators due to their varied habitat preferences and trophic roles in estuarine food webs (Brander & Mehinto, 2021). Pesticide uptake in these organisms occurs primarily via water exposure and ingestion of contaminated sediments or food particles (DeLorenzo *et al*., 2001). Bioconcentration factors (BCFs) vary widely depending on pesticide properties and organism physiology, including lipid content and metabolic capacity (Li, 2023b). For example, highly hydrophobic pesticides like pyrethroids show strong accumulation in lipid-rich macroinvertebrates such as crustaceans (Cuevas *et al*., 2018). There is insufficient species-specific data on pesticide bioconcentration in Kenyan estuarine macroinvertebrates, which hinders the development of accurate bioindicator frameworks (Brander & Mehinto, 2021). The interaction between pesticide exposure and other stressors like salinity and hypoxia on bioaccumulation is poorly characterized, limiting ecological relevance of laboratory-based BCF estimates (Cuevas *et al*., 2018).

Fish, especially those higher in the food chain, can biomagnify OCPs through dietary intake, leading to increased tissue concentrations relative to their prey (Katagi, 2010). Estuarine fish along the Kenyan coast such as tilapia and mullet exhibit variable OCPs burdens linked to feeding habits and habitat use (Tongo *et al*., 2021). Studies show that lipophilic pesticides, including pyrethroids, accumulate in fish muscle and liver tissues, posing risks to fish health and consumers (Li, 2023a). Seasonal changes in water quality also affect OCPs uptake rates and elimination, influencing biomagnification dynamics (Brander & Mehinto, 2021). Existing biomagnification studies often overlook sub-lethal effects of OCPs on fish physiology and reproduction, which could have population-level consequences (Cuevas *et al*., 2018). There is a paucity of research on how estuarine fish migration patterns modulate OCPs exposure and biomagnification, particularly in the context of changing water quality parameters (DeLorenzo *et al*., 2001).

Water quality parameters modulate pesticide toxicity to aquatic organisms by influencing bioavailability and organism stress responses (Merga *et al*., 2021). For example, low dissolved oxygen levels can exacerbate OCPs toxicity by impairing organism detoxification pathways (Bashir *et al*., 2020). Moreover, pH variations affect OCPs ionization states and membrane permeability, altering uptake and toxicity profiles (Pinheiro *et al*., 2021). Salinity-induced physiological stress may increase susceptibility to OCPs, compounding adverse effects on aquatic fauna (NOAA Coastal Science, n.d.). Most toxicity assessments do not replicate the complex physico-chemical conditions of estuaries, leading to potential underestimation of pesticide impacts (Merga *et al*., 2021). There is a need for integrated ecotoxicological studies

combining multiple stressors and realistic exposure scenarios to better inform management strategies (Onyango *et al*., 2023).

The accumulation of OCPs in estuarine biota has far-reaching ecological impacts, including reduced biodiversity, altered food web dynamics, and impaired fisheries productivity (Olisah *et al*., 2021, 2020a,b). Human communities relying on estuarine fish for food face potential health risks from OCPs residues, necessitating ongoing monitoring and regulation. Additionally, sediment-bound OCPs can act as long-term contamination reservoirs, complicating remediation efforts (Olisah *et al*., 2021, 2020a). The complexity of OCPs mixtures and their interactions with water quality further challenge risk management frameworks along the Kenyan coast (Agricultural Pollution, 2025). Risk communication to local communities is often inadequate, leading to underappreciation of OCPs exposure risks from fish consumption (Agricultural Pollution, 2025). Regulatory standards may not fully account for the combined effects of multiple OCPs and variable estuarine conditions, risking gaps in environmental protection (Merga *et al*., 2021).

The relationship between physico-chemical water quality parameters and OCPs concentrations in Kenyan estuarine ecosystems critically influences bioconcentration and biomagnification in aquatic macroinvertebrates and fish. While significant progress has been made in characterizing OCPs presence, important gaps remain in understanding the mechanistic links between water quality dynamics and OCPs bioaccumulation processes. Future research should prioritize multi-parameter experimental studies, long-term monitoring, and species-specific bioaccumulation data to improve risk assessments. Addressing these gaps will enhance conservation and sustainable management of Kenya’s coastal estuarine resources.

2.6. Bioconcentration and Biomagnification of OCPs in Aquatic Food Webs

Estuarine ecosystems along the Kenyan coast function as vital transitional zones between freshwater and marine environments. These ecologically rich and highly productive habitats sustain diverse communities of aquatic macroinvertebrates and fish, underpinning both ecosystem health and local livelihoods. However, intensifying agricultural practices and urban growth have resulted in rising pesticide inputs into these systems. Two processes are key to the study of the effects of OCPs in aquatic ecosystems: bioconcentration and biomagnification. Bioconcentration occurs when organisms absorb contaminants directly from water while biomagnification is the process through which contaminants increase in concentration at successive trophic levels along the food chain (Arnot & Gobas, 2006). These contaminants include legacy OCPs like DDT and aldrin, organophosphates such as chlorpyrifos, and synthetic pyrethroids like cypermethrin, all commonly detected in Kenyan aquatic systems such as Lake Naivasha, where DDT, aldrin, lindane, and endosulfan have been found in fish and crustaceans (Gitahi *et al*., 2021, 2002). The ecological and human health implications are profound, yet the interplay between water quality parameters and contaminant dynamics in Kenyan estuaries remains under-studied. While national trends in OCPs usage are recognized, this introduction lacks localized, fine-scale data on OCPs loading specific to the coastal counties most affected. In addition, the current emphasis on broad contaminant classes omits emerging pesticide categories such as neonicotinoids which may also be accumulating in these waters.

Pesticide contamination within Kenya's coastal estuaries arises primarily from agricultural runoff, urban wastewater, and atmospheric deposition. For instance, in Lake Naivasha's catchment, 56 different pesticides including fungicides, herbicides, and insecticides like chlorpyrifos and diazinon were detected, with several surpassing toxicity thresholds for crustaceans (Cacciatori *et al*., 2025). These compounds are hydrophobic and persistent, characteristics that favor long-term environmental accumulation and entry into food webs. Although many detection studies provide valuable spatial data, they typically offer static snapshots rather than capturing temporal variation in contaminant influx.

Physicochemical water quality parameters such as pH, temperature, dissolved oxygen, salinity, turbidity, and dissolved organic matter influence OCPs behavior in aquatic systems. Chemical characteristics like the octanol-water partition coefficient (log K_ow), persistence, and water solubility further govern bioaccumulation potential (Arnot & Gobas, 2006). Estuarine salinity gradients can cause OCPs to shift between dissolved and particulate phases, affecting their environmental fate and toxicological pathways. For instance, increasing turbidity can enhance adsorption of OCPs to sediment particles, making them available to benthic filter feeders and detritivores. However, research connecting these physico-chemical variables to pesticide uptake in Kenyan estuarine organisms remains limited, underscoring the need for coupled environmental-toxicological studies.

Macroinvertebrates constitute key links within estuarine food webs and are highly sensitive to contaminant exposure due to their benthic and particulate feeding behaviors. Although studies in Kenyan estuaries specifically documenting

organochlorine uptake by mollusks or amphipods are rare, findings from Lake Naivasha demonstrate significant bioconcentration in both crayfish and fish, linked to lipid content differences (Gitahi *et al*., 2021). Yet, mechanistic studies into physiological detoxification pathways such as cytochrome P450 activity or multidrug resistance systems remain sparse; expanding taxonomic breadth beyond mollusks and crustaceans is a priority.

Biomagnification within estuarine fish species is a pressing concern. For example, DDT and its metabolites, known to biomagnify across trophic levels, have been widely documented (Bwire *et al*., 2023). Techniques such as lipid-normalized trophic magnification factors (TMFs) based on stable isotope analysis are increasingly used to refine trophic position assessments and reflect ecosystem-level biomagnification, but remain rare in Kenyan coastal systems.

Interaction between water quality parameters and contaminant toxicity affects organismal responses. For instance, low dissolved oxygen may impair metabolic detoxification, increasing OCPs bioavailability (Gitahi *et al*., 2002). Similarly, pH and salinity shifts can alter OCPs speciation and cell permeability. However, most ecotoxicology studies rely on static exposure scenarios, failing to capture the fluctuating physico-chemical environments characteristic of Kenyan estuaries a gap that needs addressing.

The ecological and human health implications of OCPs bioaccumulation in estuarine food webs are profound. OCPs can disrupt endocrine systems, impair reproduction, and reduce survival in sensitive species, leading to altered community structure and

biodiversity loss (Cuevas *et al*., 2018). For communities relying on estuarine fish and shellfish, chronic exposure may pose developmental and neurological risks (Dalu & Froneman, 2021). While risk assessments are beginning to incorporate pesticide data, most frameworks fail to account for cumulative exposure to multiple pesticide classes and existing stressors. There is a lack of epidemiological studies directly linking fish consumption to adverse health outcomes; neglecting mixture exposures might underestimate public health risks.

Mitigation strategies include promoting integrated pest management (IPM), establishing vegetative buffer zones, improving wastewater treatment, and enforcing regulations on pesticide use. Kenya's Pest Control Products Board banned 77 highly hazardous pesticides and restricted use of 202 others in May 2025, signaling progress in environmental health policy (PAMACC, 2025). Yet, implementation is constrained by limited monitoring capacity and coordination. Community-based surveillance and social-ecological approaches incorporating fisher knowledge and governance could bolster stewardship.

In a nutshell, while bioconcentration and biomagnification are well-established processes in aquatic ecosystems, critical gaps persist for Kenyan coastal estuaries. Addressing them requires a systems-based research agenda: long-term, high-resolution monitoring across water quality gradients; mechanistic studies on biotransformation; application of isotope ecology; and integrated risk assessments encompassing trophic levels and human health. Without such comprehensive efforts, local communities may remain exposed to a silently accumulating chemical legacy.

2.6.1 Biomagnification Along Trophic Levels

Estuarine ecosystems along Kenya's coast, such as the Sabaki, Vanga, and Ramisi estuaries, are vital interfaces between land and the marine environment. They support diverse aquatic life and sustain local fisheries and coastal communities (Wanjeri *et al*., 2022). However, widespread agricultural and urban OCPs use, combined with seasonal runoff, has led to their accumulation in estuarine waters and sediments. Studies conducted in other coastal regions of Africa, such as Nigeria and DRC, reveal detectable levels of OCPs, organophosphates, and related pesticides; yet comparable data for Kenya's estuaries remain limited (Olisah *et al*., 2020b). This paucity undermines our ability to understand bioconcentration and biomagnification patterns specific to Kenyan macroinvertebrates and fish. First, several studies extrapolate findings from inland or riverine systems, which may not reflect complex salinity dynamics and species interactions in estuaries. Second, varying analytical methods ranging from simple GC-FID to advanced LC-MS/MS make direct comparisons unreliable.

OCPs partitioning between water and sediments strongly influences their availability for benthic organisms. Sediments often harbor higher concentrations due to adsorption and settling of hydrophobic compounds, creating a persistent contaminant reservoir (Wanjeri *et al*., 2022). Sediment characteristics in Kenyan estuaries, high organic matter and fine texture facilitate OCPs binding, potentially elevating exposure risks for burrowing macroinvertebrates. Limited studies using biota–sediment accumulation factors (BSAFs) have shown elevated uptake in Chironomidae and oligochaetes in tropical estuarine settings, though no equivalent assessments currently exist for Kenya's coast. One, dependencies on laboratory-based BSAF models may not translate

well to field conditions where multiple chemicals co-occur. Two, sediment sampling often lacks fine spatial resolution, failing to account for toxicity hotspots.

Macroinvertebrates, particularly benthic taxa like snails and insect larvae, are key indicators of pesticide bioaccumulation. In estuarine food webs, they serve as primary consumers and prey for higher trophic levels (Tulcan *et al*., 2021). Globally, studies have documented substantial bioconcentration of pesticides in macroinvertebrate tissue, correlated with lipid content and exposure duration (Khan *et al*., 2018; Kidd *et al*., 2001). In Kenyan estuaries, available data suggest modest OCPs residues in these organisms, but sample sizes and temporal coverage are insufficient for robust conclusions. First, identifying species-level accumulation variability is neglected, yet essential for ecological risk profiling. Second, combining metrics across taxa (e.g., amphipods and bivalves) may mask meaningful species-specific trends.

Fish represent a critical trophic level where biomagnification of OCPs becomes especially relevant. In systems like Lake Ziway, organochlorine methyl-metabolites (for example, DDT derivatives) have shown biomagnification factors exceeding 10 in predatory fish (Khan *et al*., 2018). Coastal estuaries with fluctuating salinities may modulate OCPs uptake and depuration, but Kenyan research is sparse. Preliminary data for *Mugil cephalus* and *Oreochromis mossambicus* in the Sabaki estuary indicate detectable OCPs residues, though trophic enrichment trends remain undocumented (Kamau *et al*., 2022). First, lake-based biomagnification models may not apply to estuarine fish due to diet shifts and osmotic regulation. Second, often fish sampling in Kenya is opportunistic, lacking trophic-structure analysis necessary for biomagnification modeling.

Understanding trophic transfer in estuarine food webs requires stable isotope analysis ($\delta^{15}N$ and $\delta^{13}C$), which anchors contaminant data in trophic context (Peris *et al*., 2024). Globally, studies show positive correlations between trophic level and OCPs residue concentration across benthic invertebrates, crustaceans, and fish (Kang *et al*., 2016). While a few Kenyan researchers have incorporated isotopic baselines, none have yet applied this method to OCPs studies in estuaries. This hinders our ability to quantify biomagnification factors accurately in local systems. Isotopic baselines may shift seasonally, but most Kenyan studies rely on static values, reducing interpretive accuracy. Additionally, budget constraints often limit sample size and site replication, affecting statistical robustness.

Analytical capacity in Kenya for OCPs monitoring remains constrained. Most laboratories are equipped for targeted analysis of legacy organochlorines, with limited capabilities for modern pesticides such as neonicotinoids or pyrethroids (PANA, 2021). Furthermore, quality assurance and inter-laboratory calibration are weak, impeding data comparability (Otieno *et al*., 2018). Adoption of high-resolution techniques like GC-HRMS and LC-MS/MS offers a way forward but is limited by cost and technical support. Heavy reliance on legacy pesticide metrics may overlook the presence and effects of newer compounds. Also, inconsistent QA procedures diminish the reliability and utility of generated data.

The public health implications of biomagnification in fish consumed locally are significant. Daily dietary surveys in coastal communities show fish constitute up to 60% of animal protein intake (Owino *et al*., 2022). Without clear residue thresholds and risk communication, communities remain vulnerable to chronic OCPs exposure (Otieno

et al., 2020). Yet, few studies integrate contaminant levels with dietary exposure and risk analysis. There's a critical disconnect between ecotoxicological data and food safety protocols in Kenya residue data seldom inform health guidelines. Additionally, socio-economic contexts (e.g., subsistence fishing dependence) are often overlooked in risk assessments.

Emerging research priorities include establishing seasonally resolved OCPs profiles across water, sediment, macroinvertebrates, and fish, coupled with trophic modeling and risk assessment. Collaborative frameworks between universities, government, and local communities are essential for sustainable monitoring. There is also a need to invest in analytical capacity, particularly for modern pesticide classes, and to standardize methodologies for long-term data comparability. Proposed solutions often fail to address systemic funding constraints and policy implementation gaps. Moreover, community engagement tends to be transactional rather than capacity-building, risking unsustainable monitoring efforts.

2.7. Ecotoxicological Risk Assessment of Pesticides in Estuarine Ecosystems

Estuarine ecosystems along the Kenyan coast are increasingly subjected to OCPs contamination from upstream agricultural runoff, aquaculture inputs, and urban effluents. These contaminants accumulate in both water and sediments, acting as persistent sources of exposure to aquatic biota (Wanjeri *et al.*, 2022). The estuarine environment characterized by fluctuating salinity, pH, and turbidity modulates the bioavailability and toxicity of these compounds. For example, organophosphate pesticides such as azinphos-methyl degrade faster in alkaline water but can persist in sediment due to strong sorption (Tongo *et al.*, 2022). Sediment-bound pesticides pose ecotoxicological risks through direct contact or ingestion by deposit-feeding organisms

like polychaetes and oligochaetes (Stark *et al*., 2023). Many studies fail to consider the dynamic interplay between abiotic factors (e.g., temperature, pH) and OCPs bioavailability. Additionally, few assessments have been conducted under field-realistic, estuarine-specific conditions in Kenya, limiting predictive accuracy.

In aquatic systems, sediments act as both sinks and secondary sources of OCPs exposure. Benthic macroinvertebrates such as chironomids, amphipods, and bivalves interact closely with sediments and are thus particularly vulnerable to sediment-associated contaminants (Shimbira *et al*., 2021). Chronic exposure can impair growth, reproduction, and survival, affecting entire trophic guilds (Maulvault *et al*., 2021). Sub-lethal effects such as altered enzyme activity and oxidative stress biomarkers have been documented in estuarine invertebrates elsewhere (Merga *et al*., 2021; Miller *et al*., 2021; Zhu *et al*., 2019), yet equivalent bioassays remain sparse for Kenyan species. This knowledge gap weakens our ability to evaluate functional responses of key ecological groups, including detritivores and filter feeders, which are crucial for estuarine nutrient cycling. Biomarker studies in Kenyan estuaries are nearly non-existent, leaving ecotoxicological pathways underexplored. Moreover, most ecotoxicity tests apply to temperate species, not locally adapted tropical taxa, creating uncertainties in risk thresholds.

The water column presents a more immediate but often transient exposure pathway for pelagic and nektonic organisms. Water-soluble pesticides, such as glyphosate and atrazine, can cause acute toxicity to fish and macroinvertebrates during pulse runoff events (Bakhtiari *et al*., 2020). In Kenya's coastal estuaries, episodic rainfall events following prolonged dry seasons lead to sharp pulses of OCPs-laden runoff,

significantly increasing acute exposure risk (Bwire *et al*., 2023). Species at higher trophic levels, such as carnivorous fish, may experience both direct toxicity and indirect effects through prey reduction (Burgess *et al*., 2025). These shifts can disrupt food web dynamics and ecosystem resilience. Most Kenyan monitoring programs focus on chronic rather than acute exposure windows, missing peak toxicity events. In addition, ecological modeling tools like Species Sensitivity Distributions (SSDs) have not been widely applied, limiting the ability to generalize risk levels across taxa.

Trophic guilds within benthic macroinvertebrates differ in their sensitivity and exposure routes to OCPs. Grazers (e.g., certain gastropods) are more affected by waterborne pesticides through dermal absorption and ingestion of contaminated periphyton, while deposit feeders (oligochaetes) primarily accumulate sediment-bound toxins (Stark *et al*., 2023). This differentiation is crucial for ecosystem-level assessments because OCPs-induced shifts in the dominance of tolerant over sensitive species can lead to biodiversity loss and reduced ecosystem function (Cacciatori *et al*., 2025). Estuarine monitoring in Kenya has largely emphasized community composition (e.g., richness, abundance), but not functional guild responses, which would offer deeper insight into long-term ecological integrity (Bwire *et al*., 2023). The lack of functional trait analysis in current biomonitoring hinders the detection of subtle yet ecologically significant impacts. Furthermore, the reliance on taxonomic indices (e.g., Shannon diversity) without linking to trophic roles obscures mechanistic understanding of OCPs effects.

Fish in estuarine ecosystems are vulnerable to both bioconcentration from water and biomagnification through dietary intake of contaminated invertebrates. Species such as *O. mossambicus*, *Liza macrolepis*, and *Sphyraena barracuda* are common in Kenyan estuaries and occupy various trophic levels (Wanjeri *et al*., 2022). Accumulation of lipophilic pesticides like DDT and endosulfan, and their metabolites, in fish liver and muscle has been reported in other tropical estuaries, leading to immunosuppression, endocrine disruption, and reproductive failure (Hladik *et al*., 2021). However, systematic studies quantifying these impacts across fish trophic guilds in Kenyan waters remain rare. Tissue residue analyses in Kenyan fish often lack trophic context, making it difficult to trace exposure pathways. Additionally, most sampling is done on commercially important species, neglecting ecologically significant or endangered species.

The cumulative ecotoxicological risk in estuarine food webs is compounded by the presence of pesticide mixtures. Studies in other estuaries have shown that mixtures of OCPs, pyrethroids, and herbicides exhibit synergistic or antagonistic effects, leading to unpredictable outcomes (Belden *et al*., 2020). Such interactions may elevate toxicity beyond what would be expected from individual compounds. In Kenya, however, OCPs risk assessments typically evaluate single compounds using standard toxicity thresholds, ignoring interactive effects that may occur under natural conditions. Risk assessments that overlook mixture toxicity may vastly underestimate ecological threats. Furthermore, limited chemical monitoring coverage (i.e., testing for only 5–10 common pesticides) means potential high-risk contaminants may go undetected.

2.8 Theoretical Framework of the Study

The theoretical framework for this study is grounded in ecotoxicological and trophic transfer theories that explain how contaminants such as pesticides move through aquatic ecosystems, accumulate in organisms, and affect ecological health. The three core theories underpinning this study are the Bioaccumulation and Bioconcentration Theory, Biomagnification and Trophic Transfer Theory, and the Ecotoxicological Risk Assessment Model. Together, these theories help conceptualize the flow of contaminants through abiotic and biotic compartments and their risks to ecosystem health.

2.8.1 Bioaccumulation and Bioconcentration Theory

The Bioaccumulation Theory provides a foundational framework for understanding how aquatic organisms absorb and retain contaminants such as OCPs from their environment over time. This theory encompasses various uptake pathways, including bioconcentration (direct uptake from water), bioaccumulation (uptake from all environmental sources), and biomagnification (increasing concentration through trophic levels). In aquatic systems, these processes are especially significant due to the persistence, solubility, and lipophilicity of many pesticides used in agriculture (Brander *et al*., 2021).

Bioconcentration refers specifically to the uptake of dissolved pesticides directly from water via the gills, skin, or other permeable membranes of aquatic organisms. This occurs when the concentration of a contaminant in an organism exceeds that in the surrounding water without accounting for dietary intake. The Bioconcentration Factor (BCF) is commonly used to quantify this relationship: BCF = Concentration in organism tissue / Concentration in ambient water. Values of BCF greater than 1,000 are

considered indicative of high bioconcentration potential (Commelin *et al*., 2022; Arnot & Gobas, 2006). For example, POPs such as DDT and lindane have been observed to accumulate in fish tissues at levels thousands of times higher than those found in ambient water (Cuevas *et al*., 2018; Weisbrod *et al*., 2007; Arnot & Gobas, 2006). This accumulation not only threatens the physiological health of aquatic species causing endocrine disruption, reproductive impairment, or mortality but also poses significant risks to human populations that consume contaminated seafood.

In Kenyan coastal estuarine ecosystems, where agriculture and urbanization are major drivers of OCPs input, this theory is particularly relevant. Studies have detected elevated levels of OCPs and organophosphates in estuarine waters and biota, attributed to upstream runoff and poor pesticide management (Wanjeri *et al*., 2022). Benthic macroinvertebrates, due to their sediment-dwelling and detritivorous habits, are especially susceptible to pesticide uptake from both pore water and contaminated sediments (Zhang *et al*., 2018). These invertebrates, in turn, serve as prey for higher trophic organisms like fish, creating a pathway for contaminant transfer and amplification through trophic transfer (Zhou *et al*., 2024). Furthermore, the sediment–water interface in estuarine zones acts as both a sink and a secondary source of OCPs re-release, influencing bioavailability and bioconcentration dynamics over time (Arnot & Gobas, 2006). Understanding these patterns is essential for risk assessment and mitigation strategies, especially in subsistence fishing communities along Kenya's coast where fish contribute significantly to dietary protein.

2.8.2 Biomagnification and Trophic Transfer Theory

While bioconcentration describes the direct uptake of contaminants from the environment, the Trophic Transfer and Biomagnification Theory addresses how contaminants, particularly OCPs, increase in concentration as they move up the food chain. This process, known as biomagnification, is driven by the repeated ingestion of contaminated prey and the limited capacity of organisms to metabolize or excrete certain compounds especially POPs that are lipophilic, bioresistant, and prone to accumulation in fatty tissues (Kidd *et al*., 2018; Wiesbrod *et al*., 2007). Over time, predators at higher trophic levels, such as fish, may contain significantly higher OCPs concentrations than primary consumers like benthic macroinvertebrates.

Two key metrics used to quantify trophic transfer are the Trophic Magnification Factor (TMF) and the Trophic Transfer Factor (TTF). The TMF represents the rate at which a contaminant's concentration increases per trophic level in a food web. A TMF value greater than 1 indicates a biomagnifying compound (Lavoie *et al*., 2013). The TTF refers to the ratio of contaminant concentration in a predator relative to its prey. These tools help to model the extent of risk that chemicals pose as they move through aquatic food webs. This phenomenon is especially concerning in estuarine ecosystems along the Kenyan coast, where runoff from agricultural lands delivers pesticides such as DDT, lindane, chlorpyrifos, and carbamates into rivers and coastal waters (Wanjeri *et al*., 2022). These pesticides enter the food web through sediments and water, with benthic macroinvertebrates acting as a critical point of entry due to their sediment-feeding and detritivorous behavior. These organisms which include worms, insect larvae, mollusks, and crustaceans play a vital role in nutrient recycling and are key prey for estuarine fish species.

Predatory fish that consume these contaminated invertebrates are at risk of accumulating higher levels of pesticide residues. This can affect fish health through endocrine disruption, altered growth and reproduction, and increased mortality (Hladik *et al.*, 2021). Additionally, such fish are often consumed by local human populations, raising concerns about food safety and long-term health risks, including carcinogenicity and neurological effects (WHO, 2021). Studies from other African estuaries have shown biomagnification of DDT and other OCPs in fish to levels exceeding WHO safety thresholds for human consumption (ATSDR, 2022; Ochanda *et al*., 2020). In this context, understanding trophic transfer and biomagnification is crucial for assessing ecological and public health risks, guiding OCPs management practices, and informing sustainable fishing and environmental conservation strategies along the Kenyan South Coast.

2.8.3 Ecotoxicological Risk Assessment Model

The Ecotoxicological Risk Assessment (ERA) Model is a scientifically robust framework used to evaluate the potential adverse effects of chemical contaminants, such as OCPs, on aquatic organisms and ecosystems. Central to this approach is the comparison of actual contaminant levels in the environment referred to as Measured Environmental Concentrations (MECs) with Predicted No Effect Concentrations (PNECs). PNECs represent threshold values below which harmful ecological effects are not expected to occur (Molnar et al., 2021; European Commission, 2003). By evaluating the ratio between MECs and PNECs, the ERA framework quantifies ecological risk using a metric known as the Risk Quotient (RQ): an $RQ < 1$ suggests a low risk to the ecosystem, while an $RQ \geq 1$ signals a potential or significant ecological risk requiring further investigation, regulatory intervention, or remediation (Manuilova, 2003).

This model is particularly valuable in estuarine environments, where complex interactions between water, sediment, and biological communities influence contaminant dynamics (Munyaka *et al*., 2017). For example, if the concentration of a pesticide in sediment exceeds the PNEC established for sensitive benthic macroinvertebrates such as *Chironomus* spp., the RQ would indicate a level of concern, potentially predicting harmful impacts on reproduction, growth, or survival of these organisms. Similarly, if fish tissues show MECs above thresholds for sub-lethal toxicity, ERA can guide regulatory and conservation action.

In the context of Kenya's South Coast estuarine ecosystems, where agricultural runoff introduces organophosphate, carbamate, and OCPs into aquatic systems (Wanjeri *et al*., 2022), the ERA model becomes a crucial tool. These ecosystems support diverse biological communities and are socioeconomically important as fishing and biodiversity hotspots. However, routine environmental monitoring is limited, and there is insufficient enforcement of pesticide regulation, thereby increasing the likelihood of ecological risks going undetected (Molnar et al., 2021; European Commission, 2003).

Moreover, this model directly links with objective 2 (characterizing pesticide concentrations in environmental matrices) and objective 5 (establishing ecotoxicological risk) of this study. By applying the ERA framework, this research not only assesses contaminant presence but also interprets their biological and ecological relevance. It allows for a science-based approach to evaluate the magnitude of OCPs threats and prioritize areas or species for protection.

Ultimately, applying the ERA model in Kenya's estuarine zones provides actionable insights for environmental management, contributing to evidence-based policy, sustainable coastal resource use, and safeguarding of public health.

2.9. Summary and Research Gaps

The literature reveals that while OCPs contamination in estuarine ecosystems is a recognized concern globally and in East Africa, significant knowledge gaps persist, particularly regarding: comprehensive, simultaneous quantification of OCPs in water, sediments, benthic macroinvertebrates, and fish; relationships between water quality parameters and OCPs bioavailability under tropical estuarine conditions; quantitative assessments of bioconcentration and biomagnification across trophic guilds in Kenyan estuaries; and integrated ecotoxicological risk assessments reflecting local OCPs use, species sensitivity, and ecosystem dynamics.

The study addressed these gaps by applying a multidisciplinary approach to evaluate OCPs dynamics and risks in South Coast Kenyan estuaries, thereby contributing crucial baseline data and informing sustainable coastal resource management.

CHAPTER THREE

MATERIALS AND METHODS

3.1 Introduction

This chapter presents the study area; study sites and their descriptions; study design; sampling design and procedures; sample extraction and chemical analysis; pollution indices and ecotoxicological risk assessment; statistical modelling approach; and hypothesis testing framework.

3.2 Study Area

3.2.1 Background

The southern region of the Kenyan coast (Figure 3.1), where this study was conducted, is particularly rich in biodiversity and ecological productivity (Kairo *et al*., 2009). It is also home to expansive estuarine systems that support both marine and freshwater species, making it a critical zone for environmental conservation and community-based livelihoods. Despite this ecological richness, scientific studies have disproportionately focused on the northern coast, thereby creating a knowledge gap in the southern region, which this study seeks to address (Kairu *et al*., 2021).

3.2.2 Climate

The region experiences a tropical climate primarily influenced by the Western Indian Ocean monsoon winds (Kairu *et al*., 2021). There are two dominant monsoon seasons: The Southeast Monsoon (SEM), lasting from April to September, brings cooler conditions. The Northeast Monsoon (NEM), from October to March, is drier and relatively warmer (Nyamora *et al*., 2023). Traditionally, the long rains begin in March, peaking around April or May, and taper off by August or September. Short rains usually occur in October and November. However, recent climatic changes have made

rainfall increasingly erratic and unpredictable (Kairu *et al*., 2021). The average annual rainfall in the southern coast is approximately 1,016 mm, with temperature ranges between 20°C and 35°C (Kairo *et al*., 2017).

Figure 3.1:
Map of the study area

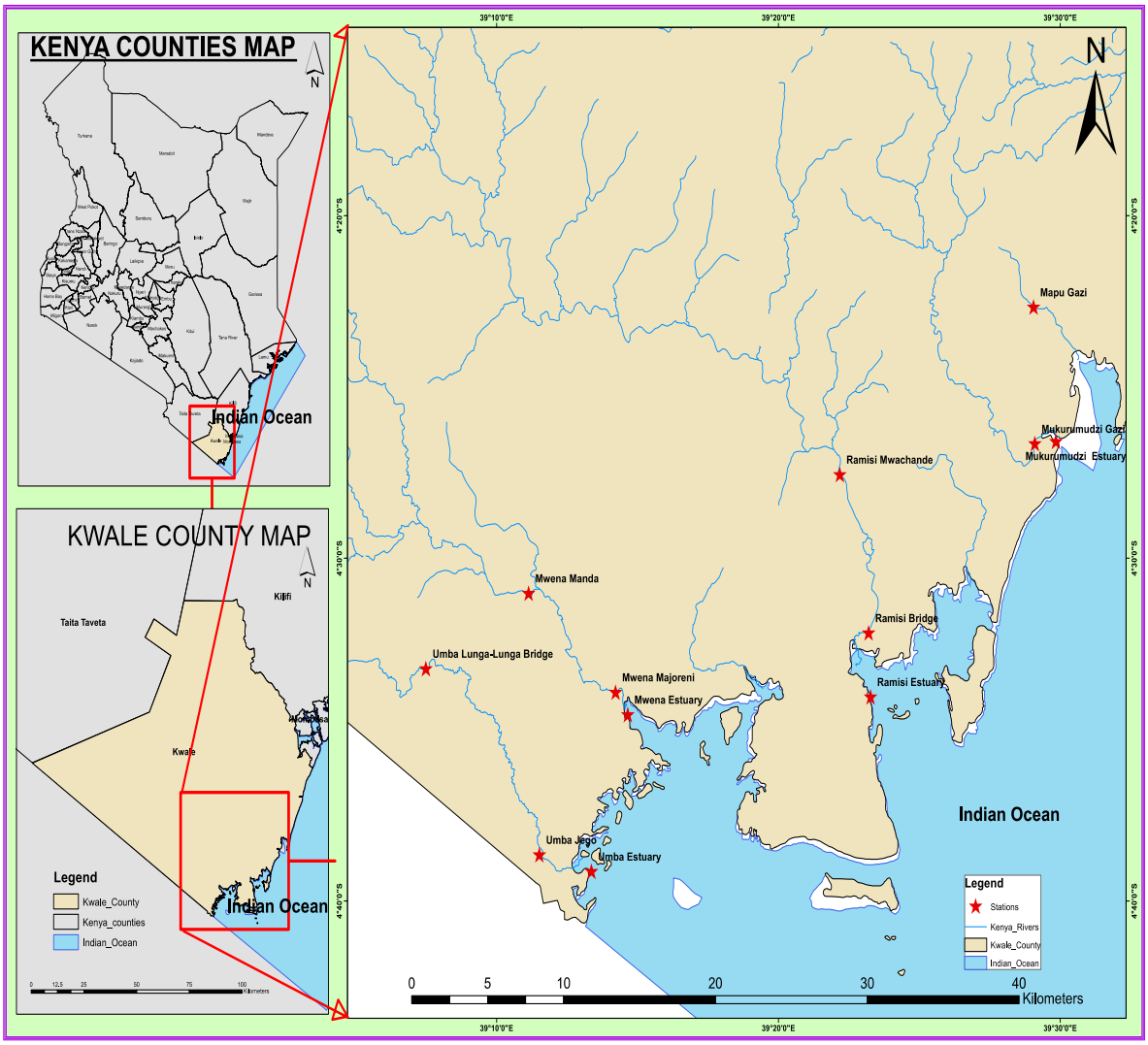

3.2.3 Hydrology

The hydrological systems in the southern Kenyan coast are dominated by rivers and estuaries that flow into the Indian Ocean (Kairo *et al*., 2017). The main rivers in this study Mkurumdzi, Mwena, Ramisi, Umba, and Mapu serve as important freshwater inputs into estuarine ecosystems. These rivers play a crucial role in sediment transport, nutrient cycling, and sustaining the brackish water environment necessary for

mangroves and estuarine biodiversity (Kairo *et al*., 2017). Notably, these rivers are fed by both surface runoff and groundwater recharge, allowing some to maintain year-round flow despite seasonal rainfall variability (Kamau, 2022). Salinity levels, especially in estuaries like Ramisi, are also influenced by geothermal infiltration, highlighting the complex hydrodynamics of the region.

3.2.4 Geology and Soils

The southern coastal region is geologically diverse, featuring both alluvial and sedimentary formations (Kairu *et al*., 2021). The river basins are characterized by a mix of fertile alluvial soils, sandy coastal deposits, and occasional lateritic soils in the upper catchments (Katuva, 2014). The soils support mangrove forests, agriculture, and other vegetation types. The geology includes limestone and coral rag formations in the coastal lowlands, while the inland hills are composed of crystalline rocks and volcanic soils (Kairo *et al*., 2017).

3.2.5 Economic Activities

The region is economically active and sustains a growing population. According to the 2019 Kenya National Census, Kwale County where the study was conducted has a population of 866,820, with an annual growth rate of 3.1%. Approximately 17% of the population is concentrated along the coast, exerting pressure on marine and estuarine systems (KNBS, 2019). The economy is driven by a mix of activities, including: agriculture (e.g., sugarcane, maize, cassava, millet), fishing (both riverine and marine), livestock rearing, commercial mining (notably Base Titanium Ltd.), tourism (linked to beaches, coral reefs, and Shimba Hills National Reserve) (Katuva, 2014).

Domestic and small-scale water abstraction. The expanding population and anthropogenic activities contribute to habitat degradation, water pollution, and increased pressure on aquatic ecosystems.

3.3 Study sites and their descriptions

This study was conducted in 5 key estuarine ecosystems along the southern coast of Kenya originating from the following rivers: Mapu, Mwena, Mkurumdzi, Ramisi, and Umba (Table 3.1). Sampling sites in each estuary were selected based on their ecological importance, variation in human disturbance levels, and accessibility for long-term monitoring. The southern coast is characterized by a mosaic of habitats including mangroves, mudflats, freshwater creeks, and mixed macrophyte beds, which support high biodiversity and serve as crucial spawning and nursery grounds for fish and invertebrates. In total, 12 sampling stations were established across the estuaries to capture spatial variability in environmental conditions and biotic assemblages (Table 3.1).

Table 3. 1:
Summary of Study Sites and Key Characteristics

Estuary	Basin Area (km^2)	No. of Sampling Stations	Key Features	Disturbance Level
Mapu	~50	1	Pristine, macrophyte-dominated, low human influence	Low (Reference Site)
Mwena	~180	3	Population pressure, reduced dry-season flow	Moderate
Mkurumudzi	~230	2	Agro-industrial impact, mining, dense mangroves	High
Ramisi	~400	3	Hot springs, estuarine crocodiles, sugarcane farming	High
Umba	~8,000	3	Transboundary, large catchment, tidal flats, siltation issues	Moderate–High

3.3.1 Mapu River

The Mapu estuary station was located near Msambweni town and represents a relatively pristine and minimally disturbed ecosystem (04.38’242” S, 039.45’644” E). It is bordered by dense vegetation, including macrophytes, mangroves (*Rhizophora* spp., *Avicennia* spp.), and freshwater shrubs, which provide excellent habitat for aquatic organisms (Kairu *et al*., 2021; Kairo *et al*., 2017). The river has a narrow channel and flows into a sheltered coastal lagoon, leading to relatively low sediment input and moderate nutrient levels. Due to limited agricultural or industrial activity in the catchment, the Mapu estuary was selected as a reference site, representing near-natural environmental conditions against which the other, more disturbed sites could be compared.

3.3.2 Mwena River

Located close to Gazi village, the Mwena River drains a basin of approximately 180 km² and flows into the northern reaches of Gazi Bay, a semi-enclosed coastal system bordered by dense mangrove forests and seagrass beds (Kairu *et al*., 2021).

3.3.2.1 Mwena Manda

This site was situated on the upper side of the estuary where salinity was low (04.52’082” S, 039.18'470" E). The river banks were characterized by erratic soil erosion with minimal natural riparian vegetation. At some points were patchy trees planted and some coconuts. Across the divide of the river channel were residential areas with small-scale farming activities for family livelihoods. Fishing activities were witnessed whereby women and their teenage children seined through the shallow waters using mosquito nets.

3.3.2.2 Mwena Majoreni

The Mwena Majoreni sampling site lies between 04º35’37” S and 039º16’28” E. It lacked natural vegetation on both sides of the channel. It was marked by intensive agricultural activities and large-scale grazing land that was bare in most part of the year. This was also a watering point for livestock. Although there were signs of significant human settlements, the population was somehow small compared to the upper station. Soil erosion was, however, evident. Small-scale irrigation was the order of the day.

3.3.2.3 Majoreni Estuary

The Mwena Estuary was situated at 04.59’554” S, 039.27’516” E. The estuary is significantly impacted by population growth, land-use change, and water abstraction, particularly for domestic use and small-scale irrigation upstream. During the dry season, flow levels decrease considerably, often resulting in reduced freshwater inflow, increased salinity, and habitat degradation. Nutrient inputs from nearby human settlements and agricultural runoff influence water quality and primary productivity (Okuku *et al*., 2022). Mwena represents a moderately disturbed system, useful for assessing the impacts of population pressure and seasonal variability on estuarine health.

3.3.3 Mkurumdzi River

The Mkurumudzi River originates from the Shimba Hills National Reserve, a protected area characterized by tropical forest ecosystems, and flows southwards into the central part of Gazi Bay. The basin covers about 230 km² and includes both natural forested catchments and heavily modified landscapes (Katuva, 2014). This estuary is influenced by a range of anthropogenic activities, including: Sugarcane irrigation and processing by KISCOL; mining operations, particularly titanium extraction by Base Titanium Ltd; and piped domestic water supply schemes (Kairo *et al*., 2017). Two sampling sites (Mkurumdzi Gazi and Mkurumdzi Estuary) were established in the upper and lower reaches, respectively, to capture the gradient of impact from relatively natural headwaters to downstream areas influenced by agro-industrial discharge. The estuary supports dense mangroves and seasonally fluctuating macrophyte beds.

3.3.3.1 Mkurumdzi Gazi

Mkurumdzi Gazi (MG) station was located at what is termed as Gazi bridge on your way from Gazi village to Msambweni sub-county of Kwale County, Kwale-Vanga Road at 04.44’513” S, 039.48’801” E (Figure 3.1). The rifles of this station were made up of logs of wood, boulders and stones of medium sizes whereas the runs were dominated by very small stones and sandy substrate. The pools comprised of mainly mud and some remains of pieces of wood. The riparian zone was well protected with a mixture of natural and planted vegetation but it was dominated by natural grass. However, some farming activities mainly dominated by sugar cane fields was well pronounced, 5 meters from the bank of the river. Soils range from dark clay to silt loam.

3.3.3.2 Mkurumdzi Estuary

ME station was situated at a point where total mixing of Mkurumdzi river and the waters of Indian Ocean occurs. The site is characterized by the heavy presence of mangroves with 100% canopy in some places and open areas. The station lied between 04.44’458” S and 039.39’910” E occurring at an elevation of 0 m asl (Figure 3). The mean depth during low tide ranges between 0.5 m and 0.65 m deep whereas during the high tide it ranged between 10 m and 15 m. The substrate is muddy especially towards the forested areas and sandy in the open waters. Part of the dropping leaves from the mangrove’s forms part of the substratum which acts as a form of particulate organic matter hence a source of nutrition for the benthic organisms including the microbes.

3.3.4 Ramisi River

The Ramisi River is one of the major river systems in Kwale County, originating from the Chenze Ranges and draining into the Ramisi Channel near Funzi Island, an ecologically rich marine area (Kairo *et al*., 2017). It has a large and complex drainage basin with multiple ephemeral tributaries, which only flow during the wet season. Three sampling stations were established to evaluate the effects of freshwater inflow variability, thermal pollution, and human encroachment.

3.3.4.1 Ramisi Mwachande

A unique feature of the Ramisi system is the presence of geothermal inflows, notably the Mwananyamala hot springs, which influence temperature and salinity dynamics in the estuary (Katuva, 2014). Ramisi Mwachande station was situated upstream at 04.53^{o} S, 039.38^{o} E. The station was influenced by agricultural activities right to its banks and human settlements. Soil erosion and some aspects of siltation were common features.

3.3.4.2 Ramisi Bridge

Ramisi Bridge was located at the bridge along the Msambweni Lunga-Liunga road at 04.53’363” S, 039.39’016” E. The station was dominated by agricultural production where sugarcane farming, growing of maize, and horticulture was common. There is a sugar processing factory located just about 1 km from the station. Livestock farming also featured prominently around this station. Therefore, the significant sugarcane farming, water abstraction, and domestic effluent discharge from nearby settlements affect the ecological balance of this site.

3.3.4.3 Ramisi Estuary

Ramisi estuary occurs at 04.58’018” S, 039.39’625” E. It is surrounded by extensive mangrove forests, tidal creeks, and intertidal mudflats, and is home to important populations of fish, birds, and estuarine crocodiles (*Crocodylus niloticus*) (Kairu *et al*., 2021). The station was also characterized by sedimentation and mudflats. Overly, the tidal cycles highly influenced the salinity gradients.

3.3.5 Umba River

The Umba River is a transboundary watercourse, originating from the Usambara Mountains in northeastern Tanzania and flowing eastward for over 200 km before draining into the Indian Ocean near Vanga town, at the Kenya–Tanzania border (Onyango *et al*., 2019). The Umba catchment spans approximately 8,000 km², making it the largest basin in the study. Given its geopolitical importance and ecological diversity, the Umba system has been identified in the proposed Transboundary Conservation Area (TBCA) encompassing both Kenyan and Tanzanian coastal ecosystems (Otieno *et al*., 2020). Three sampling sites/stations were selected to assess the transboundary influences on habitat condition, water quality, and species assemblages.

3.3.5.1 Umba Lunga-Lunga Bridge

Umba Lunga-Lunga Bridge station lied between 04.55’846” S and 039.21’494” E, just 400 m to the boundary between Kenya and Tanzania. It is mainly characterized by rapid urbanization and agricultural activities to feed the increasing human population. The riparian zone is highly human influenced with pronounced soil erosion taking place. Sedimentation and siltation are also evident.

3.3.5.2 Umba Lejo

This station lies between 04º39’48” S and 039º13’36” E. Land use in the Umba Lejo station includes agriculture, timber harvesting, and settlement development, which contribute to nutrient loading and siltation. Sedimentation influenced both by tidal cycles and land degradation is evident. At some sections of the river lies bolders, log of woods, small gravel, and to some extent thick mud flats.

3.3.5.3 Umba Estuary

This was the last station towards the ocean and lied between 04.65’439” S and 039.21’494” E. it registered the presence of rare estuarine and migratory species, including juvenile fish and crustaceans. The estuary experiences seasonal salinity shifts, strong tidal currents, and substantial sediment deposition, especially during the wet season. This estuary is ecologically significant due to its: High biodiversity, with extensive mangrove wetlands, tidal flats, and inland floodplains (Kairo et al., 2017).

3.4 Study Design

This study employed a longitudinal, cross-sectional field-based design to investigate the spatial and temporal patterns of pesticide contamination and associated ecological impacts in estuarine and riverine ecosystems along the Kenyan coast. The selected approach allowed for a systematic examination of pesticide occurrence, bioaccumulation, and ecosystem responses over time and across distinct geographical gradients. The design was intentionally integrative, combining field-based ecological monitoring, laboratory chemical analyses, and bioindicator-based assessment, providing a comprehensive framework for understanding pesticide pollution in dynamic aquatic environments.

3.4.1 Temporal and Spatial Dimensions

To account for seasonal variability, the study adopted a longitudinal approach, whereby sampling was conducted monthly over a full calendar year. This period included both wet seasons (comprising the long and short rains) and dry seasons, thus capturing fluctuations in OCPs concentrations associated with rainfall-driven runoff, agricultural cycles, and water flow dynamics. This temporal resolution enabled the identification of episodic pollution events and trends linked to seasonal land-use practices.

Spatially, the study was structured around a cross-sectional design, with sampling stations distributed along six major rivers and their associated estuarine zones along the Kenyan coastline (Figure 3.1). For each river, three longitudinal stations upstream, midstream, and downstream (including the estuary) were selected. These locations reflected varying degrees of anthropogenic influence, such as agriculture, urban development, and industrial activities, and allowed for the detection of pollution gradients from source to sink. This spatial-temporal structure made it possible to discern site-specific pollution patterns while accounting for natural hydrological and ecological variations, thus ensuring the robustness and relevance of the data.

3.4.2 Integration of Ecological and Chemical Assessments

The study combined ecological field assessments with instrumental laboratory analysis to evaluate pesticide pollution comprehensively. Sampling focused on four primary environmental matrices: water, sediment, macroinvertebrates, and fish tissues. These components were selected to represent different levels of the aquatic ecosystem and to allow for a holistic understanding of pesticide distribution, persistence, and biological uptake.

3.4.3 Stratified Sampling and Site Selection

A stratified sampling approach was employed, where each river represented a distinct stratum. Within each stratum, three sampling stations were established for Umba, Ramisi and Mwena estuaries; two for Mkurumdzi and one for Mapu based on purposive selection criteria, which included land-use patterns, pollution potential, hydrological features, and accessibility. This design allowed for both within-river (temporal) and between-river (spatial) comparisons.

Importantly, a reference site with minimal anthropogenic disturbance was included in the design to serve as a baseline for comparison. This site, located at Mapu Stream near Gazi town, was characterized by limited agricultural and urban influence and thus offered an ecologically appropriate benchmark for assessing pollution severity and anthropogenic impact at other sites.

At each sampling station, additional random sampling within microhabitats (e.g., pools, riffles, and runs) was conducted for biological samples. This helped to ensure representativeness and reduce spatial bias in ecological data, particularly in heterogeneous river-estuary systems.

3.4.4 Ecosystem-Based Approach and Indicator Metrics

The study employed an ecosystem-based approach to understand how pesticide contamination affects biological communities and ecological processes. By analyzing multiple indicators chemical, biological, and functional the design allowed for the evaluation of both structural diversity and functional integrity (e.g., trophic interactions and feeding dynamics). The FFG framework provided insight into alterations in

resource use and energy flow, while trophic levels supported the calculation of bioaccumulation and biomagnification metrics such as BCF, BMF, and TMF. These ecological assessments were carefully aligned with the study's overarching objectives and enabled the identification of early warning signals of ecological degradation due to pesticide exposure.

3.4.5 Overall Strengths and Justification of Design

This study design offered several strengths. First, it provided a high-resolution temporal dataset, capturing the seasonal dynamics of pesticide runoff and ecological responses. Second, its spatial framework allowed for meaningful comparisons between more and less impacted sites, enhancing the ability to infer causality. Third, the integration of chemical and biological data created a robust, multidimensional perspective on pollution, bridging the gap between contaminant presence and ecological consequence.

Moreover, the inclusion of a reference site added value by allowing the assessment of anthropogenic impacts relative to a natural baseline. The use of multiple matrices and trophic levels further strengthened the ecological relevance of the findings, making the results applicable to both scientific inquiry and environmental management.

The chosen study design was well-suited for the complex task of characterizing pesticide pollution in tropical aquatic ecosystems. It facilitated the collection of diverse, high-quality data necessary for understanding both the distribution and the ecological implications of pesticide residues along the Kenyan coast.

3.5 Sampling Design and Procedures

3.5.1 Site Selection

Sampling stations for this study were purposively selected based on ecological, hydrological, and anthropogenic criteria. The main objective of site selection was to capture variability in pesticide exposure due to differences in land use, pollution sources, and riverine conditions. Sites were chosen to represent a gradient of anthropogenic pressure, particularly focusing on locations with known proximity to agricultural farmlands, urban settlements, and industrial activities, which are potential sources of pesticide runoff and discharge.

Each river system included three fixed sampling stations along its longitudinal gradient upstream, midstream, and downstream/estuarine reaches (I.e. Umba, Ramisi and Mwena) and two stations for Mkurumdzi. These locations allowed for the investigation of contaminant dynamics along the flow direction, accounting for dilution, accumulation, and transformation processes within the aquatic system.

A minimally disturbed reference site was established at Mapu Stream, a small tributary originating northeast of Gazi town. This stream, which lies in a relatively pristine catchment with minimal land use interference, was used as a control site to establish natural background levels of environmental and ecological variables, and to assess deviations observed in more impacted systems.

3.5.2 Sampling Frequency and Protocol

Sampling was conducted on a monthly basis over a period of twelve consecutive months, covering both the wet seasons (long and short rains) and the dry seasons. This high-frequency temporal design allowed for the identification of seasonal patterns in

pesticide loading, particularly those associated with agricultural activities and precipitation-induced runoff events.

To ensure consistency and reduce potential for cross-contamination between samples, a standardized sampling order was maintained during each field campaign. At each site visit, sampling commenced with the measurement of *in situ* physico-chemical water parameters, followed by the collection of water samples, fish, and finally macroinvertebrates. This sequence minimized disturbances to the water column and substrate that could influence subsequent sample integrity.

Within each station, microhabitats such as pools, riffles, and runs were randomly selected to ensure spatial representativeness of both physico-chemical and biological data. For each habitat type, three replicate samples were taken for biological assessments to minimize intra-site variability and to improve the robustness of ecological interpretations, which resulted to a sample size (n) of 6,910 for OCPs and 3,886 for water quality.

3.5.3 Water Sampling

Water sampling aimed to characterize the physico-chemical quality of each aquatic system and to provide a matrix for pesticide residue analysis. Surface water samples were collected at a depth of approximately 50 cm using pre-cleaned, acid-washed polyethylene bottles to avoid contamination.

At each station, *in situ* parameters including temperature, pH, dissolved oxygen (DO), salinity, electrical conductivity (EC), and total dissolved solids (TDS) were measured using a multi-parameter YSI Professional Plus meter (USA). This ensured that real-time environmental conditions were recorded accurately and consistently across all sites and time periods.

For nutrient analysis, samples were collected in triplicate, placed in clean amber bottles, and immediately stored in dark, cooled containers to prevent degradation. Upon return to the laboratory, samples were analyzed for nitrates (NO_3^-), orthophosphates (PO_4^{3-}), and ammonia (NH_3/NH_4^+) using a SKALAR SAN++ nutrient auto-analyzer, following standard methods prescribed by APHA (2005) and Grasshoff (1999).

3.5.4 Sediment Sampling

Sediment samples were collected to assess the accumulation of persistent pesticide residues in the benthic zone. Using a stainless-steel Ekman dredge sampler, surface sediments were retrieved from the top 0–5 cm layer, which is typically most reactive and representative of recent contaminant deposition.

Approximately 100–150 grams of wet sediments were collected per replicate sample. Immediately after collection, sediments were wrapped in pre-rinsed aluminum foil (treated with HPLC-grade hexane), placed in aluminum-lined containers, and transported in cooler boxes containing dry ice to preserve chemical integrity.

In the laboratory, samples were air-dried at room temperature, sieved through a 2 mm mesh to remove coarse materials, and thoroughly homogenized. These pre-treatment steps ensured consistency in texture and composition prior to chemical extraction and instrumental analysis.

3.5.5 Macroinvertebrate Sampling

Benthic macroinvertebrates were sampled to serve as biological indicators of ecological health and pesticide exposure. Sampling was carried out using a Surber sampler with a 0.09 m^2 frame and a 250 µm mesh size, allowing for efficient capture of small-bodied organisms in shallow, wadeable sections of the river.

At each station, three replicate samples were collected from randomly selected points across different microhabitats. Samples were placed in cooler boxes and transported live to the laboratory, where they were preserved in 70% ethanol for subsequent identification and analysis.

Macroinvertebrates were sorted and identified under a dissecting microscope to the lowest taxonomic level possible, using standard keys appropriate for East African freshwater and estuarine taxa (Branch *et al.*, 2008; Richmond, 1997) and freshwater (Ramirez and Gutierrez-Fonseca, 2014; Gerber & Gabriel, 2002; Merritt & Cummins, 1996) systems. They were then sorted to five different feeding guilds, counted, weighted, and frozen at -20 °C until analyzed. The most abundant macroinvertebrate species in each feeding group was selected for pesticide contamination analysis. The five feeding guilds were based on Merrit *et al.* (2019) and Begon *et al.* (1990) categorization as elaborated below:

i. Collector Gatherer (C-G) – refers to macroinvertebrates which gathers small particles of organic material from the sediments;
ii. Scraper Grazer (S-G) – are macroinvertebrates that forage and/or graze on epiphytes, algae, micro-organisms and films attached on stones and other substrates such as pieces of wood;
iii. Predator (Pr) - macroinvertebrates which eat or predate on other organisms;
iv. Shredder (Sh) - macroinvertebrates that feeds on coarse particles of organic matter deposited in/on sediments and the particle sizes are usually >1.0 mm;
v. Filterer (Fi) - macroinvertebrates that feeds on minute particles suspended in water (suspension feeders), which are strained through mucus or a meshwork of lamellae. Food particles range between 0.01-1.0 mm.

Therefore, based on the above criteria, I settled on Atyidae, *Nerita undata*, *Rhagovelia* species, *Terebrallia palustris* and *Saccostrea cucullata* for C-G, S-G, Pr, Sh and Fi respectively.

3.5.6 Fish Sampling

Fish were selected as higher trophic-level bioindicators of pesticide biomagnification. Sampling was conducted using a generator-powered electrofisher (Honda GX240, 8HP; 400V and 10A), with voltage and amperage settings adjusted based on site-specific conductivity to optimize capture efficiency while minimizing harm to fish.

Sampling occurred during daylight hours, and stunned fish were immediately collected using dip nets. Captured individuals were placed in clean containers with site water and then euthanized humanely. Each fish was identified to species level using morphological keys and validated against FishBase and regional taxonomic literature.

The Giant tiger prawn, *Penaeus monodon* was used for this study because it was ubiquitous in all the identified sampling stations.

In the field, each specimen was dissected using sterilized instruments, and tissues including liver, gills, gonads, muscle, and stomach contents were excised and transferred to pre-cleaned amber glass jars. Tissue samples were preserved in liquid nitrogen (-196°C) during field handling and later stored at –20°C in the laboratory until pesticide residue analysis.

These tissue samples provided essential information on the bioaccumulation and trophic transfer of pesticide contaminants within fish, enabling the calculation of Bioconcentration Factors (BCF), Biomagnification Factors (BMF), and contributions to Trophic Magnification Factor (TMF) estimations across the aquatic food web.

3.6 Sample Extraction and Chemical Analysis

3.6.1 Water

Water samples were filtered and preserved under refrigeration for two days until the determination of residual levels of different pesticides were done. The extraction method that was employed for the extraction method to be used for pesticides was standardized using the Environmental Protection Agency of USA (USEPA,1987), consistent in a liquid-liquid partition of the water with dichloromethane.

3.6.2 Sediment

For sediment sample extraction, processing and analysis was done following laboratory methods/procedures proposed by Perez-Ruzafa *et al*. (2000) and Simpson *et al*. (2005). Approximately 100 g of wet sediment samples were weighed in a 0.0001 g Electronic

Analytical Balance (Model: BA-E1204). They were then be kept in well sterilized aluminum containers that were covered with perforated aluminum sheets and dried for a maximum of 48 hours in a Heto Power Dry LL 3000 Freezer Dryer (Thermo Scientific). This was followed by the weighing of samples that were sieved via a 2 mm mesh-sized sieve before they were stored in amber bottles for further analysis. Before pesticide extraction, approximately 3 g of each sample was placed in vials and spiked with 30 µL of an internal standard containing a mixture of 4,4-dib-romooctafluorobiphenyl (DBOFB), PCB 103, and PCB 198 (Dr Ehrenstorfer GmbH, Ausburg, Germany).

A 30 mL dichloromethane (Fisher Scientific, USA) was added to the samples and then processed for about 20 minutes using the START E micro-wave-assisted extraction system (Milestone, Italy). They (samples) were then filtered into 25 mL capacity amber glass vials via glass funnels stuffed with glass wool before being concentrated to about 1 mL. Samples were then cleaned-up of lipids and sulfur using a micro-column containing acidified silica (Silica gel, 0.063 ± 0.2 mm, Merck, Darmstadt, Germany) and activated copper (40 mesh, 99.5 % purity, Aldrich, Saint Quentin Fallavier, France). The PCBs were then purified on the micro-column by eluting 3 x 5 mL with a mixture of n-pentane and dichloromethane (90/10 v/v). The extracts were finally concentrated under nitrogen and transferred to 100 µL isooctane (99 % extra pure, Scharlau, ICS, St Medard en Jalles, France). Furthermore, the solution was re-concentrated to 100 µL in an injection vial, and 1 µL of the sample injected for analysis using Gas Chromatography. Sediment samples were spiked with internal standards and extracted using microwave-assisted extraction, followed by clean-up with acidified silica gel and activated copper columns.

3.6.3 Biota

Penaeus monodon (fish) and macroinvertebrate samples were extracted following the methods outlined by Environmental Monitoring Guidelines for South Africa Development Cooperation (SADC) Region (Åkerblom, 1995). Before cleaning, they were dried up by the use of anhydrous sodium sulphate (USEPA, 2007). 20 g samples (i.e. in duplicates) were measured, then added to a 10 g pre-cleaned sand and sodium sulphate weighing approximately 20 g and put in a mortar (Perez-Ruzafa *et al*., 2000).

The mixture was crushed using a pestle until a dry homogenous mixture was realized. The sample content was poured into a homogenizer already containing dichloromethane for a maximum period of 20 minutes. The organism (*P. monodon* or macroinvertebrate FFG) extracts were then sieved through a glass wool plug into an evaporating flask. This was repeated in triplicates of 20 cm^3 of dichloromethane, pooled then evaporated at a maximum temperature of 30 ^oC to give fat that was transferred to extralute-3 column where they were eluted (washed) with 4 portions of 5 cm^3 acetonitrile. These elute compartments were then combined and left to evaporate to a level of 2 cm^3 in a rotary evaporator (Buchi Rotavapor GR-200 Series) (APHA, 2005).

3.6.4 Instrumental Analysis

The OCPs detection was performed using a TSQ Vantage Triple-Stage Quadrupole Mass Spectrophotometer (Thermo Electron) equipped with a heated electrospray ionization probe (HESI-II). Separation, detection, identification and quantification of target analyses followed the same methods described by Wille *et al*. (2011).

The identification and quantification of chlorinated pesticides were performed with a Agilent Technologies 6890N gas chromatograph with an electron capture detector (GC–ECD) using a 30 m 0.25 mm i.d. capillary column coated with 5% phenyl-substituted dimethylpolysiloxane phase (0.25 lm film thickness). Automatic split less injections of 2 µL was applied and the total purge rate adjusted to 50 ml min^{1}. Hydrogen was used as the carrier gas at a constant pressure of 40 kPa at 100 °C, while nitrogen made-up gas at a rate of 60 ml min^{1}. Injector and detector temperatures were set at 280°C and 320 °C, respectively. Oven temperature was calibrated as follows: 70 °C for 1 min, raised at 40 °C min^{1} to 170 °C, then raised at 1.5 °C min^{1} to 230 °C where they were held for 1min and at 30°C min^{1} to 300°C with a final hold of 5 min. Retention times and mass spectra were compared against authentic standards and databases for compound identification.

3.6.5 Quality Assurance and Quality Control (QA/QC)

To ensure quality assurance/quality control (QA/QC) was adhered to, the analytical methods were ensured by the use of a standard reference material (SRM 1941b – organics in marine sediment) purchased from the National Institute of Standards and Technology, USA. This was done in duplicate and average recovery of analytes was obtained. The analytes recovery was achieved through spiked blanks and matrices. Analytes in procedural blanks were subtracted from the samples. Laboratory check solutions were routinely injected into GC–ECD and GC–MS to confirm instrument accuracy and precision. Calibration of the instruments was performed using a nine-level analytical curve and quantification of analytes followed the internal standard procedure and the surrogate recoveries were acceptable. The method-detection limits were 0.000 ng/L in water and 0.0014 ng/g for sediments and biota.

3.7 Pollution Indices and Ecotoxicological Risk Assessment

This study employed multiple pollution indices and ecotoxicological risk assessment models to evaluate the extent of organochlorine pesticide (OCP) contamination and its ecological implications in estuarine sediments of the South Coast, Kenya. These indices provide insight into both the intensity of sediment pollution and the potential biological threats posed to benthic macroinvertebrates and higher trophic levels, including fish. The indices used include the Contamination Factor (Cf), Geo-accumulation Index (Igeo), Pollution Load Index (PLI), Potential Ecological Risk Index (RI), Nemerow Pollution Index (PN), and Mean Effect Range-Median Quotient (ERM-Q). Each index was applied to the concentration data of sixteen OCPs detected across twelve estuarine sampling stations.

3.7.1 Contamination Factor (Cf)

The Contamination Factor (Cf) was used to quantify the enrichment of OCPs in sediments relative to their minimum recorded concentrations. The Cf offers a basic but powerful measure of contamination by comparing current concentration levels against presumed background values. It was calculated using the formula:

Cfi=CiCmin,i\text{Cf}_i=\frac{C_i}{C_{\text{min},i}}Cfi=Cmin,iCi…….1

where CiC_iCi is the mean concentration of compound *i* across all stations, and Cmin,iC_{\text{min},i}Cmin,i is the minimum observed concentration of the same compound, serving as a proxy for the natural or pre-industrial background level. The contamination factor allows categorization of pollution into four levels: low (Cf < 1), moderate (1 ≤ Cf < 3), considerable (3 ≤ Cf < 6), and very high (Cf ≥ 6), based on the framework developed by Hakanson (1980). This index was computed individually for each of the sixteen OCPs to determine compounds posing the highest contamination threats.

3.7.2 Geo-accumulation Index (Igeo)

To further interpret the extent of anthropogenic influence on sediment pollution, the Geo-accumulation Index (Igeo) was employed. This index compares the observed concentration of a pollutant to its background level, adjusted for possible natural variability. The Igeo was calculated as:

Igeoi=log2(Ci1.5×Cmin,i)\text{Igeo}_i=\log_2\left(\frac{C_i}{1.5\times C_{\text{min},i}}\right)Igeoi=log2(1.5×Cmin,iCi)……..2

In this formula, CiC_iCi denotes the mean concentration of the compound, while Cmin,iC_{\text{min},i}Cmin,i is its minimum observed concentration. The factor 1.5 accounts for natural variability in sediment composition and geochemical background. According to Müller's (1969) classification, Igeo values are interpreted in seven classes ranging from Class 0 (unpolluted), ≤ 2 (moderately polluted), ≤ 3 (heavily polluted), ≤ 4 (heavily to extremely polluted), and > 5 (extremely polluted), thereby offering a standardized pollution rating scale for comparison across compounds.

3.7.3 Pollution Load Index (PLI)

The Pollution Load Index (PLI) offers a cumulative measure of the total contamination burden across multiple compounds in sediment. It integrates the individual contamination factors of all detected OCPs to produce a single, composite pollution metric. The PLI was calculated using the geometric mean of the Cf values:

PLI=(∏i=1nCfi)1/n\text{PLI}=\left(\prod_{i=1}^{n}\text{Cf}_i\right)^{1/n}PLI=(i=1∏nCfi)1/n……3

where n represents the total number of OCPs considered (n = 16 in this study). A PLI value equal to one indicates baseline or background conditions, values less than one indicate no pollution, and values greater than one suggest progressive pollution. This index is useful for summarizing the overall contamination status of a site and was applied to generate a region-wide view of pesticide pollution in the estuarine sediment.

3.7.4 Potential Ecological Risk Index (RI)

To evaluate the ecological threat associated with the contamination, the Potential Ecological Risk Index (RI) was used. This index incorporates both the level of contamination and the ecological toxicity of individual compounds (Hakanson, 1980). First, the Ecological Risk Factor (Er) was calculated for each OCP using the formula:

Eri=Cfi×Tri\text{Er}_i = \text{Cf}_i \times \text{Tr}_iEri = Cfi×Tri

……4

where Tri\text{Tr}_iTri is the toxic response factor assigned to compound *i*, reflecting its toxicity, environmental persistence, and bioaccumulative potential. The values for Tri\text{Tr}_iTri were obtained from Hakanson (1980) and relevant literature. The overall Potential Ecological Risk Index (RI) was then calculated as the sum of the individual Er values:

RI=∑i=1nEri\text{RI}=\sum_{i=1}^{n}\text{Er}_iRI=i=1∑nEri……..5

According to Hakanson's criteria, RI values less than 150 indicate low risk, 150–300 moderate risk, 300–600 considerable risk, and greater than 600 indicate very high ecological risk. This index provides a compound-weighted perspective on ecological harm and allows prioritization of OCPs based on their combined contamination and toxicological influence.

3.7.5 Nemerow Pollution Index (PN)

The Nemerow Pollution Index (PN) was included to account for the combined effect of both average and maximum contamination levels, thereby capturing spatial extremes in pollution. It was computed using the formula:

PN= (Cfmean2+Cfmax2)2……..……6

where Cfmean is the average of all contamination factors, and Cfmax is the maximum single contamination factor among the sixteen OCPs. This index is considered more stringent than the PLI because it highlights peak contamination that could be ecologically damaging even if the average levels appear moderate. A PN value below 1 indicates no pollution, between 1 and 2 suggests slight pollution, between 2 and 3 reflects moderate pollution, and values greater than 3 indicate heavy pollution.

3.7.6 Mean Effect Range Median Quotient (ERM-Q)

The Mean Effect Range-Median Quotient (ERM-Q) was calculated to assess the potential combined toxicity of multiple sediment-associated OCPs to benthic organisms. This index compares measured concentrations of contaminants to sediment quality guideline values linked with adverse biological effects. The ERM-Q was calculated using the formula:

ERMQ=1n∑i=1n(CiERMi).....……..7

In this formula, CiC_iCi represents the mean concentration of each OCP and ERMiis the corresponding Effect Range-Median value obtained from published sediment quality benchmarks. The quotient was averaged across all compounds with available ERM values. The interpretation of ERM-Q values follows the classification by Long *et al*. (2005), where values less than 0.1 indicate a low probability (~10%) of toxicity, values between 0.1 and 0.5 suggest moderate probability (~21%), values between 0.5 and 1.5 indicate a high probability (~49%), and values above 1.5 signal a very high probability (~76%) of adverse ecological effects.

These indices were selected to provide a robust multi-metric evaluation of sediment quality, contaminant bioavailability, and ecological risk. Together, they facilitated a detailed understanding of the contamination landscape and informed the subsequent interpretation of ecological threats to estuarine food webs in the study area.

3.8 Statistical Modelling Approach

All statistical analyses in this study were carried out using R version 4.5.2. A combination of descriptive, inferential, and multivariate techniques was used to assess organochlorine pesticide (OCP) contamination patterns, ecotoxicological risk levels, and trophic transfer dynamics across sediment, benthic macroinvertebrates, and fish samples.

3.8.1 Data Screening and Normality Testing

Prior to conducting inferential analyses, raw data underwent initial screening for completeness, consistency, and outlier detection. The Shapiro–Wilk test was employed to assess the normality of each variable, particularly the OCP concentrations and pollution indices such as Cf, Igeo, RI, and ERM-Q. Visual inspection of histograms and Q-Q plots further aided in confirming distribution characteristics. For variables that failed the normality assumption ($p < 0.05$), appropriate non-parametric tests were selected. In addition, Levene's test was used to verify homogeneity of variances before applying parametric procedures like ANOVA.

3.8.2 Descriptive and Comparative Analyses

Descriptive statistics including mean, median, minimum, maximum, and standard error were used to summarize pesticide concentrations in each environmental matrix and station. These summaries were also used in computing pollution indices such as the Contamination Factor (Cf), Geo-accumulation Index (Igeo), Pollution Load Index (PLI), and Potential Ecological Risk Index (RI).

To identify spatial and temporal differences in pesticide levels, the study applied One-Way Analysis of Variance (ANOVA) for normally distributed data while 2-Way ANOVA was used to test for spatio-temporal variations. These tests were used independently for each matrix (sediment, invertebrates, and fish) to detect significant differences among stations and sampling months. Tukey's Honest Significant Difference (HSD) test followed significant ANOVA results for pairwise comparisons.

3.8.3 Multivariate Analyses: Principal Component Analysis (PCA)

To uncover patterns in pesticide distribution across stations and to explore similarities in compound behavior, Principal Component Analysis (PCA) was performed. The analysis was conducted on log-transformed and standardized OCP concentration data to normalize variance across different compounds. PCA allowed for the identification of major axes of variation, highlighting station-specific OCP profiles and revealing clusters of chemically similar pesticides. Biplots were generated to visualize associations among stations and OCPs in reduced dimensions.

3.8.4 Trophic Transfer Analysis

To assess biomagnification potential, Trophic Magnification Factor (TMF) analysis was calculated using the formula:

TMF=10slope…… ……8

A TMF greater than 1 indicated that the compound biomagnified through the food web, while a value below 1 suggested trophic dilution. The statistical significance of the regression slopes was assessed to support conclusions on the trophic behavior of individual OCPs.

3.8.5 Software, Packages, and Significance Criteria

All data analyses were performed within the R statistical environment. Key packages included *ggplot2* for visualizations, *vegan* for PCA, *car* for regression diagnostics, and FSA and PMCMRplus for *post hoc* non-parametric comparisons. Data wrangling and reshaping were facilitated by the *dplyr* and *tidyverse* packages. All hypothesis tests were two-tailed, and a significance threshold of $p < 0.05$ was used throughout the study. This combination of rigorous statistical testing and multivariate modeling provided a strong foundation for identifying spatial and trophic contamination patterns and for estimating ecological risks associated with sediment-bound organochlorine pesticides.

3.9 Hypothesis Testing Framework

Table 3.2 provides a summarized hypothesis testing framework for this study:

Table 3. 2:
Summarized hypothesis testing framework

Objective	Hypothesis (H_0)	Statistical Test	Decision Rule
Assess spatial variability in water quality	No significant site differences	ANOVA	Reject H_0 if $p < 0.05$
Compare pesticide concentrations across matrices	No difference between water, sediment, biota	ANOVA	Reject H_0 if $p < 0.05$
Test water quality–pesticide relationship	No correlation between parameters	Correlation (r)	Reject H_0 if $r \neq 0$ ($p < 0.05$)
Examine trophic transfer	No biomagnification occurs	TMF > 1 or regression slope	Reject H_0 if TMF > 1
Evaluate ecological risk	Pesticide levels are safe	Risk Quotient (RQ)	Reject H_0 if $RQ \geq 1$

3.10 Ethical Considerations

All field and laboratory procedures adhered to ethical and regulatory standards for environmental and biological research in Kenya. The study obtained an ethical approval (Ref. No. KSU ISERC PROTOCOL No. 0011/7/24, Appendix II) from the Institutional Scientific and Ethics Review Committee (ISERC), Kisii University. The study also obtained official research authorization (Ref No. 515470, appendix III) through a National Commission for Science, Technology and Innovation (NACOSTI) permit.

Ethical considerations included:

i. Minimizing ecological disturbance during sampling, particularly in reference and sensitive habitats
ii. Humane treatment of fish, with electrofishing settings adjusted to minimize stress and mortality
iii. Proper disposal of chemical reagents and contaminated materials in compliance with KMFRI safety protocols
iv. Data confidentiality and appropriate reporting of results, ensuring transparency and scientific integrity
v. Informed consent and communication with local stakeholders, including communities near sampling locations, to ensure mutual understanding and benefit-sharing

Research activities were reviewed and approved by the Kenya Marine and Fisheries Research Institute (KMFRI) Research Ethics Committee, which confirmed that the study complied with institutional guidelines and national legislation on environmental research.

CHAPTER FOUR

RESULTS

4.1 Introduction

This chapter presents results on: spatial and temporal variation in water quality parameters in estuarine ecosystems of South Coast; levels of pesticides in sediments, waters, trophic guilds of benthic macroinvertebrates and fish in estuarine ecosystems of South Coast, Kenya; relationship between physico-chemical water quality parameters and pesticide concentrations in water in estuarine ecosystems; bioconcentration and biomagnification of OCPs in water, sediments, the trophic levels of benthic macroinvertebrates and P. monodon in estuarine ecosystems of South Coast, Kenya; and ecotoxicological risk posed by OCPs in sediments, water, FFGs of benthic macroinvertebrates and P. monodon in estuarine ecosystems of South Coast, Kenya.

4.2 Spatial and temporal variation in water quality parameters in estuarine ecosystems of South Coast, Kenya

4.2.1 Spatial variation in water quality parameters

The spatial distribution of water quality parameters across 12 stations in the study area are presented in Figure 4.1. These parameters include temperature, dissolved oxygen (DO), conductivity, total dissolved solids (TDS), salinity, pH, phosphate, nitrate, and ammonia. Each box plot captures the variability and range of values per parameter at each site, providing a visual overview of spatial heterogeneity.

Figure 4.1:
Spatial distribution of water quality parameters across the 12 sampling stations in the study area.

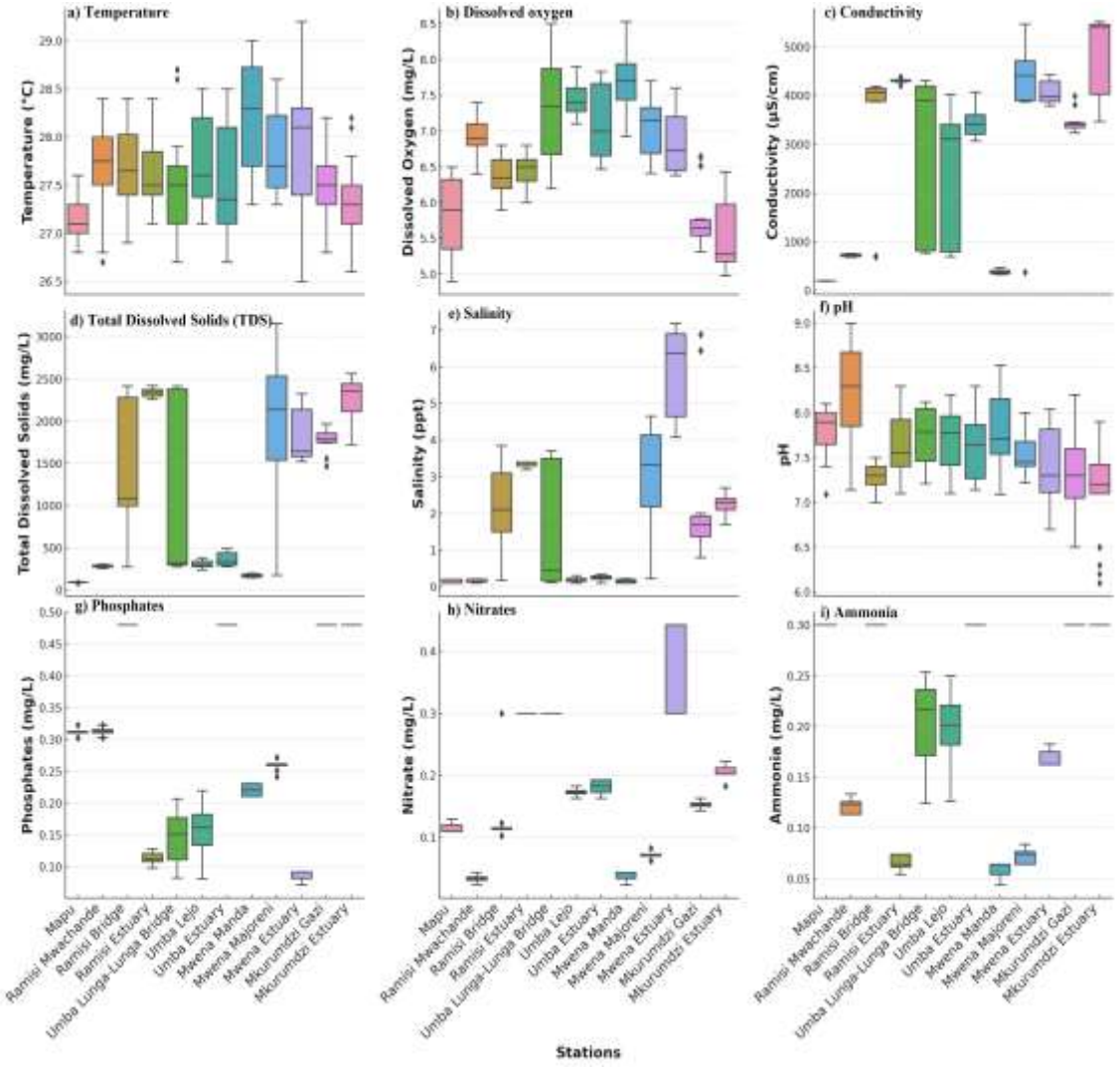

The highest mean temperatures were recorded at downstream estuarine locations such as Mwena Estuary (28.3 ± 0.6°C), Mwena Majoreni (28.2 ± 0.7°C), Umba Estuary (28.1 ± 0.4°C), Umba Lejo (28.2 ± 0.3°C) and Ramisi Estuary (28.3 ± 0.5°C) except Mwena Manda (28.7 ± 0.6°C) at the upper part of the river. In contrast, the upper part stations such as Mapu (27.0 ± 0.4°C), Umba Lunga-Lunga Bridge (27.1 ± 0.6°C), and Mkurumdzi Gazi (27.3 ± 0.5°C) registered lower temperatures (Figure 4.1). Mid-range values were observed at Ramisi Bridge (28.0 ± 0.4°C), Ramisi Mwachande (28.0 ± 0.5°C) and Mkurumdzi Estuary (27.4 ± 0.7°C). Tukey's post hoc test (Appendix

II, Table A1) confirmed statistically significant differences between Ramisi Estuary (28.3 ± 0.5°C) and upstream stations such as Mapu (27.0 ± 0.4°C), Ramisi Mwachande (28.0 ± 0.5°C), Umba Lejo (28.2 ± 0.3°C), Mwena Manda (28.7 ± 0.6°C), Ramisi Bridge (28.0 ± 0.4°C) underscoring the heterogeneity in thermal profiles between inland and estuarine water bodies. Stations Ramisi Mwachande, Umba Lunga-Lunga Bridge, Mwena Majoreni and Mkurumdzi Estuary did not differ significantly.

To statistically support the above observations (spatial heterogeneity), a one-way ANOVA was conducted for each parameter (Table 4.1), followed by Tukey HSD *post-hoc* tests to identify significant pairwise differences between stations. The ANOVA results revealed that all parameters varied significantly across stations ($p < 0.001$). Notably, parameters such as conductivity, TDS, salinity, phosphates, nitrate, and ammonia showed exceptionally high F-values, signifying large disparities between upstream freshwater stations and estuarine or lowland sites.

Table 4.1:
One-Way ANOVA Results for spatial variation in water quality parameters across the 12 Sampling Stations

Parameter	Source	df	$F_{(11, 420)}$	*p* value
Temperature (°C)	Station	11	11.173	<0.001
	Residual	420		
DO (mg/L)	Station	11	84.764	<0.001
	Residual	420		
Conductivity (µS/cm)	Station	11	114.893	<0.001
	Residual	420		
TDS (mg/L)	Station	11	118.312	<0.001
	Residual	420		
Salinity (ppt)	Station	11	107.393	<0.001
	Residual	420		
pH	Station	11	17.933	<0.001
	Residual	420		
Phosphates (mg/L)	Station	11	679.356	<0.001
	Residual	420		
Nitrate (mg/L)	Station	11	909.534	<0.001
	Residual	420		
Ammonia (mg/L)	Station	11	1068.343	<0.001
	Residual	420		

DO (mg/L) displayed significant spatial variation ($F_{(11, 420)} = 84.76$, $p < 0.001$). Stations such as Mkurumdzi Gazi (5.5 ± 0.40 mg/L), Mkurumdzi Estuary (5.6 ± 0.24 mg/L) and Mapu (5.9 ± 0.41 mg/L) had markedly lower DO, while higher levels were observed at Mwena Manda (7.7 ± 0.26 mg/L), Umba Lunga-Lunga Bridge (7.3 ± 0.37 mg/L), and Umba Estuary (7.2 ± 0.44 mg/L). Tukey tests (Appendix II, Table A1) generally confirmed that DO at estuarine stations differed significantly ($p < 0.001$) from those at upstream freshwater sites i.e. Umba Estuary (7.2 ± 0.44 mg/L) was different from Mwena Manda (7.7 ± 0.26 mg/L), Mwena Majoreni (7.0 ± 0.35 mg/L) and Mkurumdzi

Gazi (5.5 ± 0.40 mg/L). However, such stations as Umba Lunga-Lunga, Umba Lejo, Ramisi Mwachande, Ramisi Estuary, Mkurumdzi Estuary and Ramisi Bridge were statistically similar.

Conductivity (µS/cm) showed among the highest F-values ($F_{(11, 420)}$ = 114.89, p < 0.001), indicating sharp spatial contrasts. Conductivity was lowest at Mapu (214.82 ± 13.66 µS/cm), Mwena Manda (220.43 ± 15.23 µS/cm), and Ramisi Mwachande (235.66 ± 11.49 µS/cm), and highest at Mwena Majoreni (≈5500.37 ± 51.77 µS/cm), Mkurumdzi Gazi (4200.02 ± 49.02 µS/cm) Mwena Estuary (4000.26 ± 47.16 µS/cm), and Ramisi Estuary (4100.51 ± 43.71 µS/cm), reflecting saline water intrusion and ion accumulation. Post-hoc tests (Appendix II, Table A1) confirmed significant differences between stations Umba Lunga-Lunga Bridge (3900 ± 37.2 µS/cm), Umba Lejo (3070 ± 32.4 µS/cm), Umba Estuary and Mapu. Stations Mkurumdzi Estuary, Mkurumdzi Gazi and Mwena Estuary; Ramisi Bridge, Ramisi Mwachande and Umba Estuary did not differ statistically.

TDS, (mg/L) like conductivity levels were significantly higher among stations $F_{(11, 420)}$ = 118.31, p < 0.001). Elevated TDS were observed at Ramisi Estuary (2400 ± 42.57 mg/L), Mkurumdzi Estuary (2400± 42.56 mg/L), Mwena Estuary (1600.25 ± 29.68 mg/L) and Mwena Majoreni (2100.51 ± 25.93 mg/L), suggesting strong estuarine influence or mineral loading. Tukey results supported these differences (Appendix II, Table A1), with significant contrasts between upstream stations such as Mapu (145.03 ± 11.61 mg/L), Mkurumdzi Gazi (1700 ± 30.2 mg/L) and Ramisi Mwachande (350 ± 13.54 mg/L) and estuarine locations like Ramisi Estuary (2400 ± 42.57 mg/L)

and Mkurumdzi Estuary (2400 ± 42.56 mg/L). However, stations Umba Lejo, Ramisi Bridge and Mkurumdzi Gazi did not differ significantly.

Salinity (ppt) exhibited a clear spatial gradient, increasing downstream $F_{(11,\ 420)}$ = 107.39, $p < 0.001$). Near-zero salinity values were recorded at Mapu (0.10 ± 0.04 ppt), Mwena Manda (0.14 ± 0.04 ppt), and Umba Lunga-Lunga Bridge (0.16 ± 0.05 ppt), while elevated values occurred at Mwena Estuary (6.5 ± 0.11 ppt), Ramisi Estuary (3.1 ± 0.13 ppt) and Mkurumdzi Estuary (2.2 ± 0.12 ppt). This supports the presence of marine water intrusion. Tukey post-hoc tests (Appendix II, Table A1) confirmed statistically significant differences between freshwater and estuarine locations where such stations as Umba Estuary (0.2 ± 0.1 ppt), Ramisi Mwachande (0.17 ± 0.06 ppt), Ramisi Bridge (2.03 ± 0.21 ppt) and Mwena Majoreni (3.2 ± 0.13 ppt) were statistically different while Umba Lunga-Lunga Bridge (0.16 ± 0.05 ppt), Umba Lejo (0.17 ± 0.06 ppt) and Mwena Manda (0.14 ± 0.04 ppt) did not differ statistically.

Spatial differences in pH were modest but statistically significant $F_{(11, 420)} = 17.93$, $p < 0.001$). Higher pH levels were observed at Ramisi Mwachande (8.3 ± 0.09) and Mwena Manda (7.67 ± 0.07). Lower pH values were recorded at Mkurumdzi Estuary (7.15 ± 0.05) and Mwena Estuary (7.3 ± 0.06), suggesting higher organic content or localized acidity. Tukey comparisons (Appendix II, Table A1) revealed significant contrasts between such sites as Mapu (7.8 ± 0.04), Mkurumdzi Gazi (7.3 ± 0.06) and Mwena Majoreni (7.5 ± 0.07). Stations Umba Lejo, Umba Lunga-Lunga Bridge, Mwena Manda and Mkurumdzi Gazi were statistically similar.

Phosphate concentrations (mg/L) were highly variable across sites $F_{(11, 420)} = 679{,}356.1$, $p < 0.001$). Elevated levels were detected at Mwena Majoreni (0.26 ± 0.10 mg/L), Ramisi Mwachande (0.32 ± 0.09 mg/L), and Mwena Manda (0.21 ± 0.11 mg/L), likely influenced by agricultural runoff, livestock pens, or domestic wastewater. Lower levels were observed at Ramisi Estuary (0.11 ± 0.09 mg/L) and Mwena Estuary (0.09 ± 0.02 mg/L). Tukey HSD tests confirmed significantly different stations between Ramisi Mwachande (0.32 ± 0.09 mg/L) and Mwena Majoreni (0.26 ± 0.10 mg/L) whereas Ramisi Estuary, Umba Lejo, Umba Lunga-Lunga Bridge and Ramisi Mwachande were not significantly different at $p < 0.05$.

Nitrate (mg/L) displayed significant spatial variation $F_{(11, 420)} = 909.53$, $p < 0.001$). High concentrations were observed at Mwena Estuary (0.35 ± 0.11 mg/L), Umba Lejo (0.18 ± 0.02 mg/L), and Umba Estuary (0.19 ± 0.10 mg/L). Lower levels were recorded at Ramisi Mwachande (0.01 ± 0.00 mg/L) and Mwena Manda (0.02 ± 0.00 mg/L). Tukey post-hoc tests confirmed significant differences between Umba Estuary (0.19 ± 0.10 mg/L), Umba Lejo (0.18 ± 0.02 mg/L) and Ramisi Mwachande (0.01 ± 0.00 mg/L) while Mkurumdzi Estuary, Mwena Majoreni and Umba Estuary were statistically not different (Appendix II, Table A1).

Ammonia levels (mg/L) showed the highest variation $F_{(11, 420)} = 1{,}068{,}765$, $p < 0.001$), indicating intense localized pollution. Peak concentrations were found at Umba Lunga-Lunga Bridge (0.22 ± 0.11 mg/L), Umba Lejo (0.2 ± 0.07 mg/L), and Mwena Estuary (0.16 ± 0.12 mg/L). Lower ammonia values were recorded at Ramisi Estuary (0.06 ± 0.01 mg/L) and Mwena Manda (0.06 ± 0.02 mg/L). Tukey analysis confirmed significant differences between these extremes (Appendix II, Table A1).

4.2.2 Temporal Variation in Water Quality Parameters

The monthly (temporal) variation in physical, chemical, and nutrient water quality parameters across the study period (September 2018–August 2019) are as shown in Figure 4.2. One-way ANOVA results (Table 4.2) showed that temperature, dissolved oxygen (DO), electrical conductivity, total dissolved solids (TDS), and pH varied significantly across months ($p < 0.05$), while salinity, phosphates, nitrate, and ammonia did not show statistically significant monthly differences ($p > 0.05$). Although some nutrients did not show significant month effects, their dispersion across months (Figure 4.2).

Temperature (°C) varied significantly across months $F_{(11, 420)} = 2.624$, $p < 0.05$), with notably higher values observed between February and April 2019 (mean: 27.7 ± 0.6°C). The lowest mean temperatures were recorded in November (27.4 ± 0.5°C) and December (27.41 ± 0.4°C), aligning with the short rains. Tukey post-hoc comparisons (Appendix II, able A2) confirmed that March 2019 (27.7 ± 0.6°C), April (27.7 ± 0.6°C), July (27.2 ± 0.3°C) and November (27.4 ± 0.5°C) were significantly different, highlighting the expected seasonal thermal fluctuations. The months of September, October, January and March were statistically the same.

Figure 4.2:
Monthly trends (± SE) in water quality parameters measured across 12 stations from September 2018 to August 2019

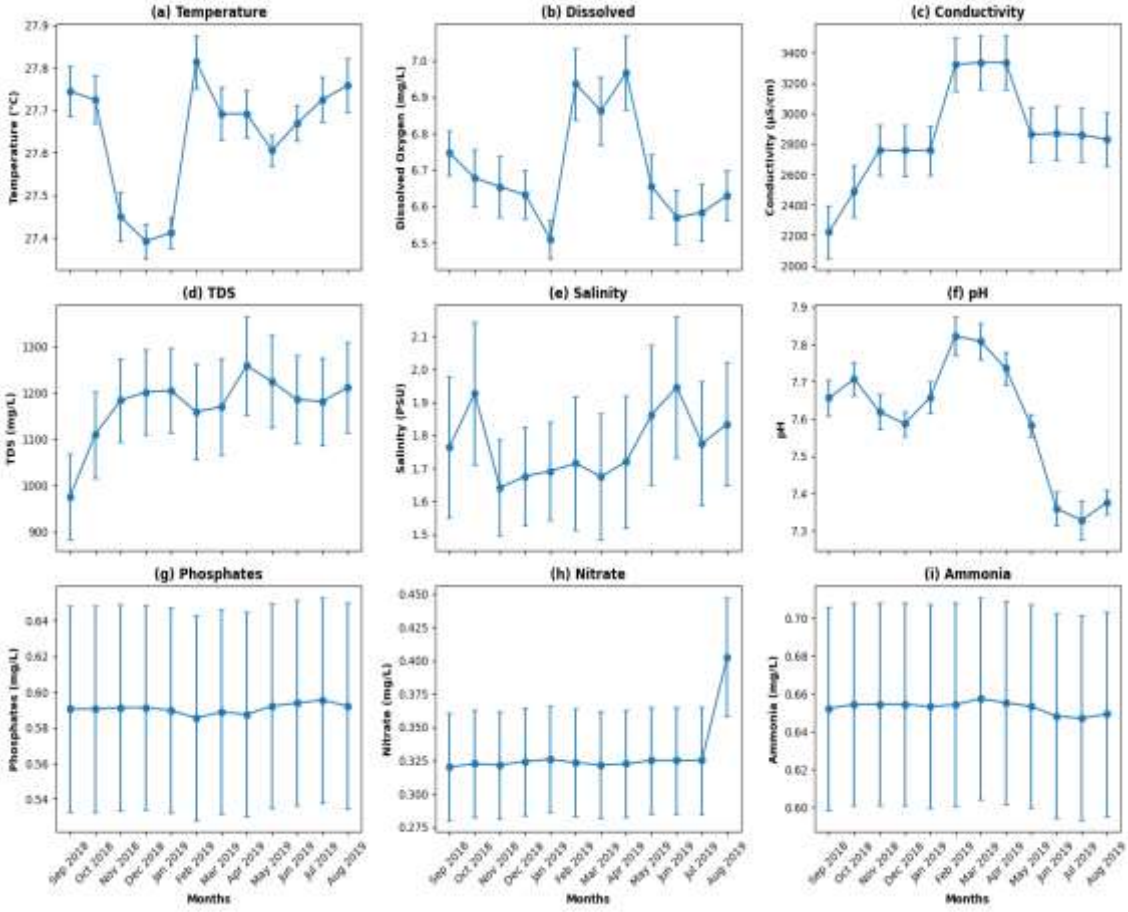

DO displayed significant variation across months $F_{(11,\ 420)} = 2.505$, $p < 0.05$). The highest monthly mean DO values were recorded in April (6.95 ± 0.3 mg/L) and February (6.9 ± 0.2 mg/L). The lowest DO concentrations occurred in the month of January (6.5 ± 0.4 mg/L). While overall variation was limited, Tukey tests indicated that January (6.5 ± 0.4 mg/L), February (6.9 ± 0.2 mg/L), May (6.65 ± 0.3 mg/L) and July (6.6 ± 0.2 mg/L) DO levels were significantly different at $p < 0.05$ while September, October, November, March, April and May were not significantly different (Appendix II, Table A2).

Table 4. 2:
One-way ANOVA results for temporal (monthly) variation in water quality parameters across the 12 sampling months (September 2018–August 2019)

Parameter	Source	df	F value	*p* value
Temperature (°C)	Month	11	2.624	0.003
	Residual	420		
DO (mg/L)	Month	11	2.505	0.028
	Residual	420		
Conductivity (µS/cm)	Month	11	6.065	<0.001
	Residual	420		
TDS (mg/L)	Month	11	6.783	<0.001
	Residual	420		
Salinity (ppt)	Month	11	0.105	0.994
	Residual	420		
pH	Month	11	2.933	0.027
	Residual	420		
Phosphates (mg/L)	Month	11	0.002	0.8234
	Residual	420		
Nitrate (mg/L)	Month	11	0.125	0.9994
	Residual	420		
Ammonia (mg/L)	Month	11	0.04	0.9345
	Residual	420		

Electrical conductivity (µS/cm) also exhibited significant monthly variation $F_{(11, 420)} = 6.065$, $p < 0.001$). The highest conductivity was observed in February, March and April (each recording 3075.74 ± 303.49 µS/cm). The lowest values were observed in September 2018 (2250.83 ± 361.52 µS/cm), coinciding with higher freshwater input. Post hoc tests confirmed that January (2750 ± 207.4 µS/cm), October (2500 ± 187.30 µS/cm), December (2750 ± 207.4 µS/cm) and May (2800 ± 211.52 µS/cm) differed significantly unlike October, November, February and April which statistically were similar (Appendix II, Table A2).

TDS showed a similar trend to conductivity, with a significant difference across months $F_{(11, 420)} = 6.783$, $p < 0.001$). TDS levels peaked in April (1250.04 ± 830.73 mg/L), while lower values were recorded in September 2018 (990.25 ± 266.25 mg/L). Tukey comparisons (Appendix II, Table A2) confirmed significant contrasts between December (1200 ± 801.27 mg/L), November (1190 ± 782.41 mg/L), September (990.25 ± 266.25 mg/L) and April (1250.04 ± 830.73 mg/L). September, January, February, July and August were statistically not different.

Although salinity did not show a statistically significant overall month effect ($F_{(11, 420)} = 0.105$, $p > 0.05$), substantial fluctuations were observed across individual months. Elevated salinity values occurred during selected dry-season periods, particularly at estuarine stations experiencing marine intrusion, while markedly lower values were recorded during high freshwater discharge months. These pronounced but spatially uneven fluctuations increased within-group variability in the ANOVA model, thereby reducing the ability to detect a consistent month-level effect across the entire system. In effect, salinity changes were episodic and station-specific rather than uniformly seasonal across all 12 stations. The high dispersion across stations likely masked clear statistical differences at the system-wide monthly scale.

pH varied modestly but significantly across months ($F_{(11, 420)} = 2.933$, $p < 0.05$). The highest monthly means were recorded in February and March 2019 (≈7.8), while lower values were observed in July (≈7.31), consistent with shifts in biological activity and catchment inputs. Tukey tests (Appendix II, Table A2) confirmed significant contrasts among selected months.

Phosphate concentrations did not exhibit significant monthly variation ($F_{(11,\ 420)}$ = 0.002, $p > 0.05$), yet marked fluctuations were evident in the raw monthly values. Sharp peaks occurred in certain months, likely linked to localized runoff events, agricultural inputs, and nutrient enrichment episodes. However, these spikes were not consistently distributed across all stations, resulting in high intra-month variance. The large dispersion within months increased the residual mean square in the ANOVA, thereby reducing the F-ratio and obscuring statistically significant overall temporal patterns. Thus, phosphate dynamics appear to be episodic and spatially heterogeneous rather than uniformly seasonal across the system

Nitrate levels also remained statistically unchanged across months ($F_{(11,\ 420)}$ = 0.125, $p > 0.05$), despite visible fluctuations ranging from very low to elevated concentrations during specific periods. Elevated nitrate values were recorded during selected wet-season months, likely reflecting nutrient runoff and catchment inflows. Nevertheless, these increases were confined to particular stations and did not occur consistently across the entire estuarine network. The resulting high within-month variability increased the error term in the ANOVA model, thereby masking clear temporal differences at the system level.

Ammonia concentrations also exhibited no significant temporal variation $F_{(11,\ 420)}$ = 0.0054, $p > 0.05$). The most elevated values were observed in March 2019, but overall trends remained steady, with data showing relatively stable mean levels and reduced spread across months. Like nitrates, Tukey test did not show any significant differences during the months for ammonia (Appendix II, Table A2).

4.2.3 Spatio-temporal variation in water quality parameters

The spatio-temporal interaction plots for water quality parameters across the 12 stations and twelve sampling periods (September 2018–August 2019) are displayed in Figure 4.3. Table 4.3 summarizes results of the two-way ANOVA, which confirmed statistically significant variations ($p < 0.001$) in most parameters due to station, month, and their interaction.

Temperature consistently increased across months and stations, peaking in July 2019, when Mwena Estuary recorded 29.2°C, the highest during the study. Conversely, the lowest value (26.5°C) was also recorded at the same station in November 2018. The significant station × month interaction ($F_{(121,288)} = 275.786$, $p < 0.001$) indicates that the magnitude of temperature increase varied spatially across sites.

Figure 4. 3:
Spatio-temporal interaction plots for water quality parameters across 12 sampling stations and 12 sampling months (September 2018 – August 2019). Data are shown as mean ± SE per station per month

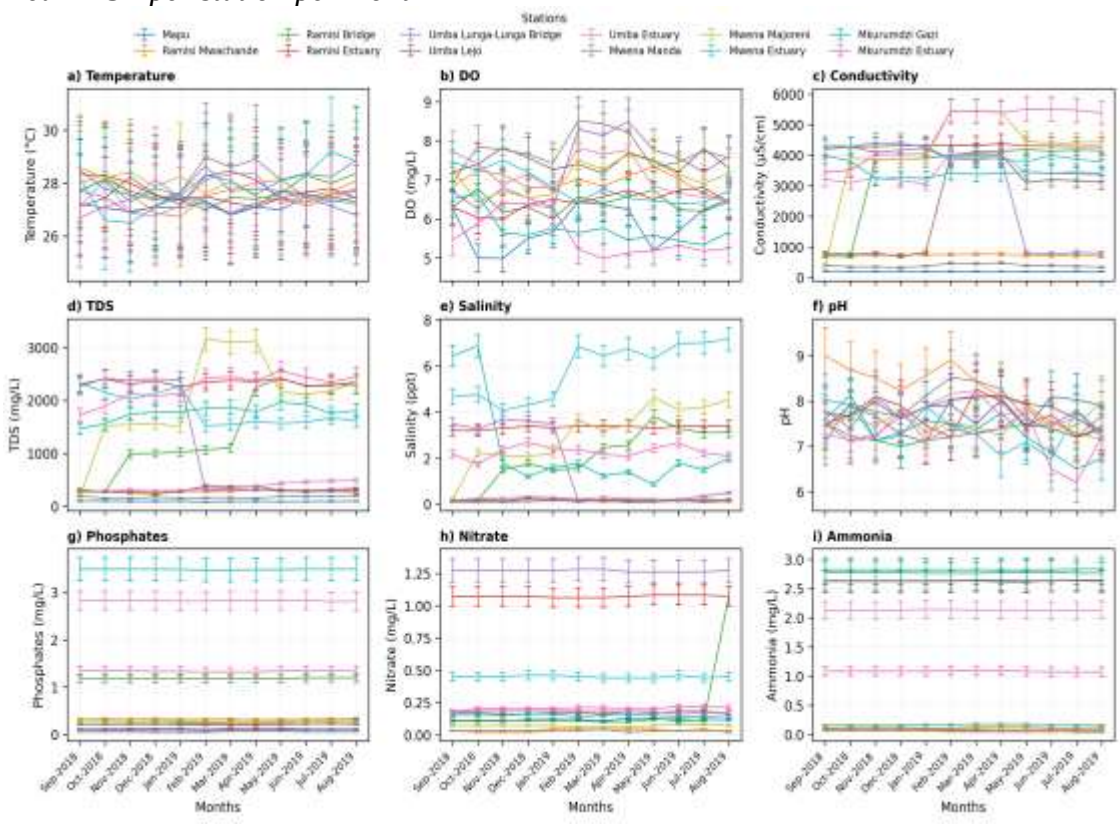

Table 4.3:
Two-Way ANOVA results for physico-chemical water quality parameters across stations and months.

Parameter	Source	df	*F* value	*p* value
Temperature (°C)	Station	11	11.173	<0.001
	Month	11	2.623	0.003
	Station × month	121	275.794	<0.001
	Residual	288		
DO (mg/L)	Station	11	84.76	<0.001
	Month	11	1.20	0.028
	Station × month	121	220.22	<0.001
	Residual	288		
Conductivity (µS/cm)	Station	11	114.894	<0.001
	Month	11	1.3423	0.197
	Station × month	121	1026.297	<0.001
	Residual	288		
TDS (mg/L)	Station	11	118.314	<0.001
	Month	11	0.203	0.997
	Station × month	121	18.377	<0.001
	Residual	288		
Salinity (ppt)	Station	11	107.394	<0.001
	Month	11	0.103	0.994
	Station × month	121	582.344	<0.001
	Residual	288		
pH	Station	11	17.934	<0.001
	Month	11	5.286	<0.001
	Station × month	121	88.355	<0.001
	Residual	288		
Phosphates (mg/L)	Station	11	679.356	<0.001
	Month	11	0.0045	0.8234
	Station × month	121	2095.403	<0.001
	Residual	288		
Nitrates (mg/L)	Station	11	909.533	<0.001
	Month	11	0.122	0.9998
	Station × month	121	909.526	<0.001
	Residual	288		
Ammonia (mg/L)	Station	11	106.876	<0.001
	Month	11	0.007	0.9345
	Station × month	121	11.223	<0.001
	Residual	288		

Water temperature exhibited significant spatial, temporal, and spatio-temporal variation across the 12 sampling stations and 12 months. Although temperature changes were generally moderate compared to salinity and nutrient parameters, distinct patterns were observed across stations, reflecting differences in shading, flow conditions, tidal influence, and downstream warming effects. Two-way ANOVA confirmed that temperature differed significantly across stations ($F_{(11, 288)} = 11.17$, $p < 0.001$) and also varied significantly across months ($F_{(11, 288)} = 2.62$, $p = 0.003$), indicating seasonal influence likely associated with rainfall cycles and ambient climatic conditions. Importantly, the station × month interaction was also highly significant ($F_{(121, 288)} = 275.79$, $p < 0.001$), demonstrating that monthly temperature fluctuations were not uniform across all stations. This interaction suggests that temperature dynamics were site-specific, with estuarine and lowland stations responding differently to seasonal climatic variability than upstream freshwater stations.

Dissolved oxygen (DO) exhibited clear seasonal changes, with elevated values observed during some months and declines during others. For instance, the highest DO (8.52 ± 0.45 mg/L) was recorded at Mwena Manda in February 2019, while the lowest DO (4.95 ± 0.52 mg/L) occurred at Mapu in October 2018. Statistically, DO varied significantly across stations ($F_{(11, 420)} = 84.76$, $p < 0.001$) and across months ($F_{(121, 420)} = 1.20$, $p = 0.028$). The significant interaction term ($F_{(121, 288)} = 220.22$, $p < 0.001$) confirms that temporal patterns were not uniform across stations, indicating strong spatio-temporal dependence in oxygen dynamics.

Conductivity and TDS showed pronounced spatial differentiation consistent with estuarine mixing and ion accumulation. Conductivity ranged from a low of 190.57 µS/cm at Mapu (May 2019) to 5513.30 µS/cm at Mkurumdzi Estuary (May 2019), while TDS ranged from 84.83 mg/L at Mapu (February 2019) to 3158.27 mg/L at Mwena Majoreni (February 2019). Two-way ANOVA showed strong spatial effects for conductivity ($F_{(121, 288)} = 114.89$, $p < 0.001$) and TDS ($F_{(121, 288)} = 118.31$, $p < 0.001$). However, the month main effect was not significant for conductivity ($F_{(11, 420)} = 1.34$, $p = 0.197$) or TDS ($F_{(11, 420)} = 0.20$, $p = 0.997$), suggesting that temporal changes were inconsistent at the overall system level. Importantly, both parameters had highly significant station × month interactions (conductivity: $F_{(121, 288)} = 10{,}262{,}977.00$, $p < 0.001$; TDS: $F_{(121, 288)} = 1{,}837{,}736.00$, $p < 0.001$), confirming that station-specific temporal fluctuations drive the observed variability.

Salinity remained near-zero at most upstream freshwater stations but increased sharply at estuarine sites during specific months, reflecting episodic marine intrusion. For example, Mwena Estuary recorded the highest salinity (6.99 ± 0.35 ppt in June 2019), while Mapu recorded the lowest (0.096 ± 0.002 ppt in October 2018). Statistically, salinity differed significantly by station ($F_{(11, 420)} = 107.39$, $p < 0.001$), whereas the month main effect was not significant ($F_{(11, 420)} = 0.10$, $p > 0.05$). The significant interaction ($F_{(121, 288)} = 582.34$, $p < 0.001$) indicates that salinity peaks were confined to particular stations during specific months, consistent with seasonal marine water intrusion under reduced freshwater discharge.

pH ranged from 6.20 ± 0.30 at Mkurumdzi Estuary (July 2019) to 9.00 ± 0.20 at Ramisi Mwachande (September 2018). Two-way ANOVA showed statistically significant spatial ($F_{(11, 288)} = 17.93$, $p < 0.001$) and temporal ($F_{(11, 288)} = 5.28$, $p < 0.001$) variation, together with a significant station × month interaction ($F_{(121, 288)} = 88.35$, $p < 0.001$). Although pH differences were smaller compared to conductivity, salinity and nutrients, the interaction indicates that pH responses over time differed between stations, likely reflecting localized processes such as organic matter decomposition, CO_2 accumulation, and photosynthetic activity.

Phosphates exhibited extreme station-specific peaks. The highest concentration (3.492 mg/L) occurred at Mkurumdzi Gazi (September 2018), while the lowest (0.046 mg/L) was recorded at Umba Lunga-Lunga Bridge (December 2018). The station main effect was highly significant ($F_{(11, 420)} = 679{,}356.10$, $p < 0.001$), while the month main effect was not significant ($F_{(11, 420)} = 0.00$, $p = 0.8234$). However, the significant station x month interaction ($F_{(121, 288)} = 20{,}095.40$, $p < 0.001$) indicates that phosphate dynamics depended strongly on station and month jointly, with localized episodic peaks obscuring a consistent overall temporal trend.

Nitrate concentrations ranged from 0.024 mg/L at Ramisi Mwachande (November 2018) to 1.283 mg/L at Umba Lunga-Lunga Bridge (March 2019). The station effect was significant ($F_{(11, 420)} = 909.53$, $p < 0.001$), while the month effect was not ($F_{(11, 420)} = 0.12$, $p = 0.9998$). The strong interaction ($F_{(121, 288)} = 909.5260$, $p < 0.001$) confirms that nitrate patterns were highly site-specific and temporally episodic, consistent with localized nutrient loading and hydrological pulses rather than uniform seasonal shifts.

Ammonia showed sharp localized spikes, with the maximum value (2.833 mg/L) recorded at Mkurumdzi Gazi (August 2019) and the minimum (0.044 mg/L) at Mwena Manda (July 2019). The spatial effect was highly significant ($F_{(11, 420)}$ = 1,068,765.00, $p < 0.001$), while the month main effect was not significant ($F_{(11, 420)}$ = 0.00, $p = 0.9345$). Nonetheless, the significant interaction ($F_{(121, 288)}$ = 11.22, $p < 0.001$) confirms spatio-temporal irregularities, suggesting that ammonia peaks occurred only at certain stations and months, most likely driven by localized pollution inputs and biological transformation processes.

4.3 Levels of pesticides in sediments, waters, trophic guilds of benthic macroinvertebrates and fish in estuarine ecosystems of South Coast, Kenya

4.3.1 Levels of pesticides in sediments

4.3.1.1 Spatial variation in OCPs in sediments

The spatial variation in organochlorine pesticide (OCP) concentrations in sediment samples across the sampling stations is summarised in Figure 4.4, with descriptive statistics (mean ± SD) indicating broadly comparable concentration levels across sites for most compounds. Overall, the distributions of OCP residues showed substantial overlap among stations, suggesting limited site-specific enrichment. The concentration of pesticides is shown in Figure 4.4.

Figure 4.4:
Spatial distribution of OCPs concentrations in sediments across sampling stations

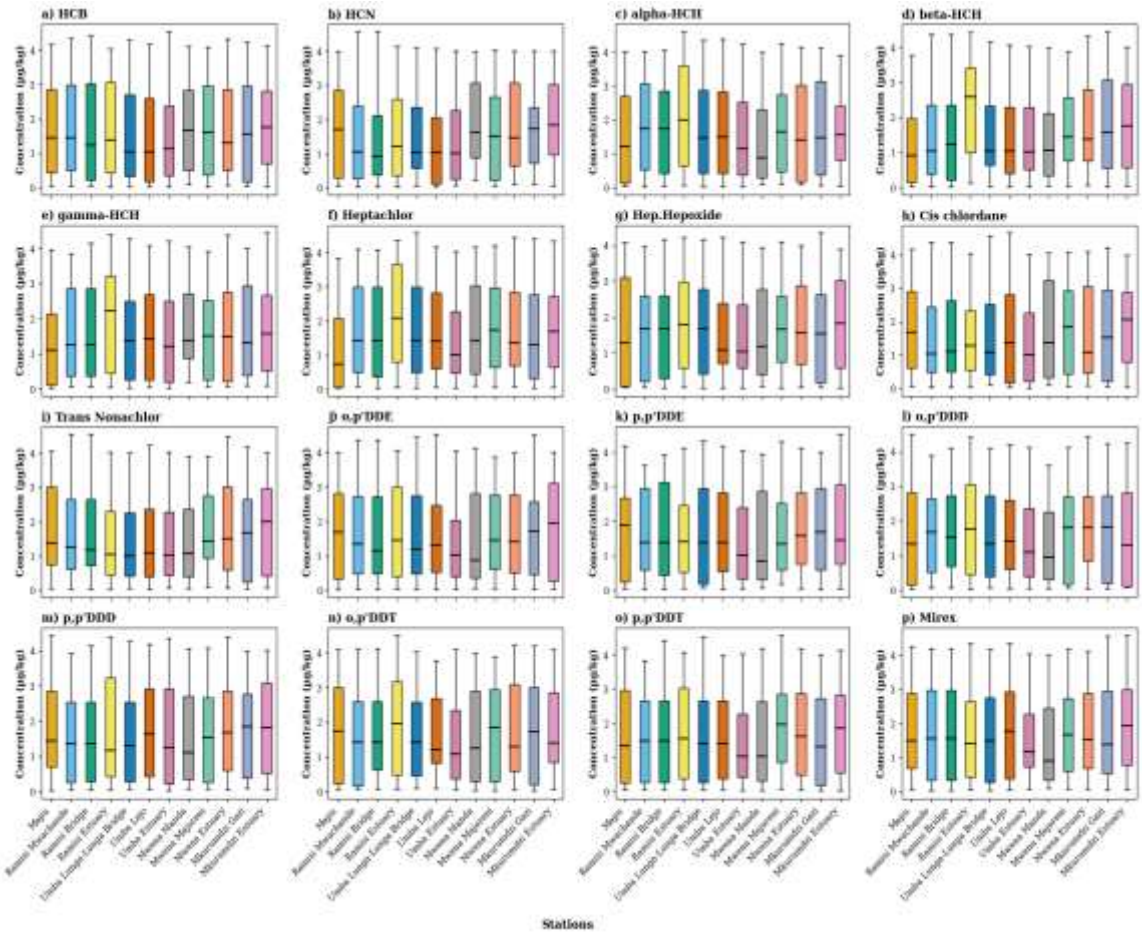

To statistically evaluate these spatial patterns, one-way ANOVA was performed for each of the 16 OCP compounds, with station as the independent factor. As presented in Table 4.4, F-statistics were consistently low and associated *p*-values were > 0.05 for all compounds, confirming no statistically significant spatial variation in sediment OCP concentrations across the study sites. For example, hexachlorobenzene showed no significant differences among stations (HCB: $F_{(11, 420)} = 0.12$, $p > 0.05$), and similarly non-significant results were observed for γ-HCH ($F_{(11, 420)} = 0.59$, $p > 0.05$) and p,p′-DDT ($F_{(11, 420)} = 0.30$, $p > 0.05$). Consistent with these outcomes, none of the DDT and HCH isomers, chlordane-related compounds, or heptachlor metabolites demonstrated evidence of site-specific accumulation.

Table 4.4:
One-way ANOVA results for spatial variation in organochlorine pesticide (OCP) concentrations in sediments across sampling stations

OCPs	***F* value**	***p* value**
HCB	$F_{(11, 420)} = 0.12$	1.00
HCN	$F_{(11, 420)} = 0.65$	0.79
alpha-HCH	$F_{(11, 420)} = 0.66$	0.78
beta-HCH	$F_{(11, 420)} = 1.43$	0.15
gamma-HCH	$F_{(11, 420)} = 0.59$	0.84
Heptachlor	$F_{(11, 420)} = 0.99$	0.45
Hep.Hepoxide	$F_{(11, 420)} = 0.19$	1.00
Cis chlordane	$F_{(11, 420)} = 0.25$	0.99
Trans Nonachlor	$F_{(11, 420)} = 0.35$	0.97
o,p'DDE	$F_{(11, 420)} = 0.22$	1.00
p,p'DDE	$F_{(11, 420)} = 0.27$	0.99
o,p'DDD	$F_{(11, 420)} = 0.40$	0.96
p,p'DDD	$F_{(11, 420)} = 0.15$	1.00
o,p'DDT	$F_{(11, 420)} = 0.22$	1.00
p,p'DDT	$F_{(11, 420)} = 0.30$	0.99

4.3.1.3 Temporal Variation in OCP in sediments

The monthly trends (Figure 4.5) in sediment concentrations of OCPs from September 2018 to August 2019. The solid trend lines (mean ± SE) illustrate distinct variation over time across all measured compounds. Across most OCPs including HCB, HCN, α-HCH, β-HCH, and γ-HCH a rise in concentrations is visually apparent between February and April 2019, followed by a decline toward mid-2019.

Figure 4. 5:
Temporal distribution of OCPs in sediments across sampling stations Boxplots show median, interquartile range, and spread for each compound

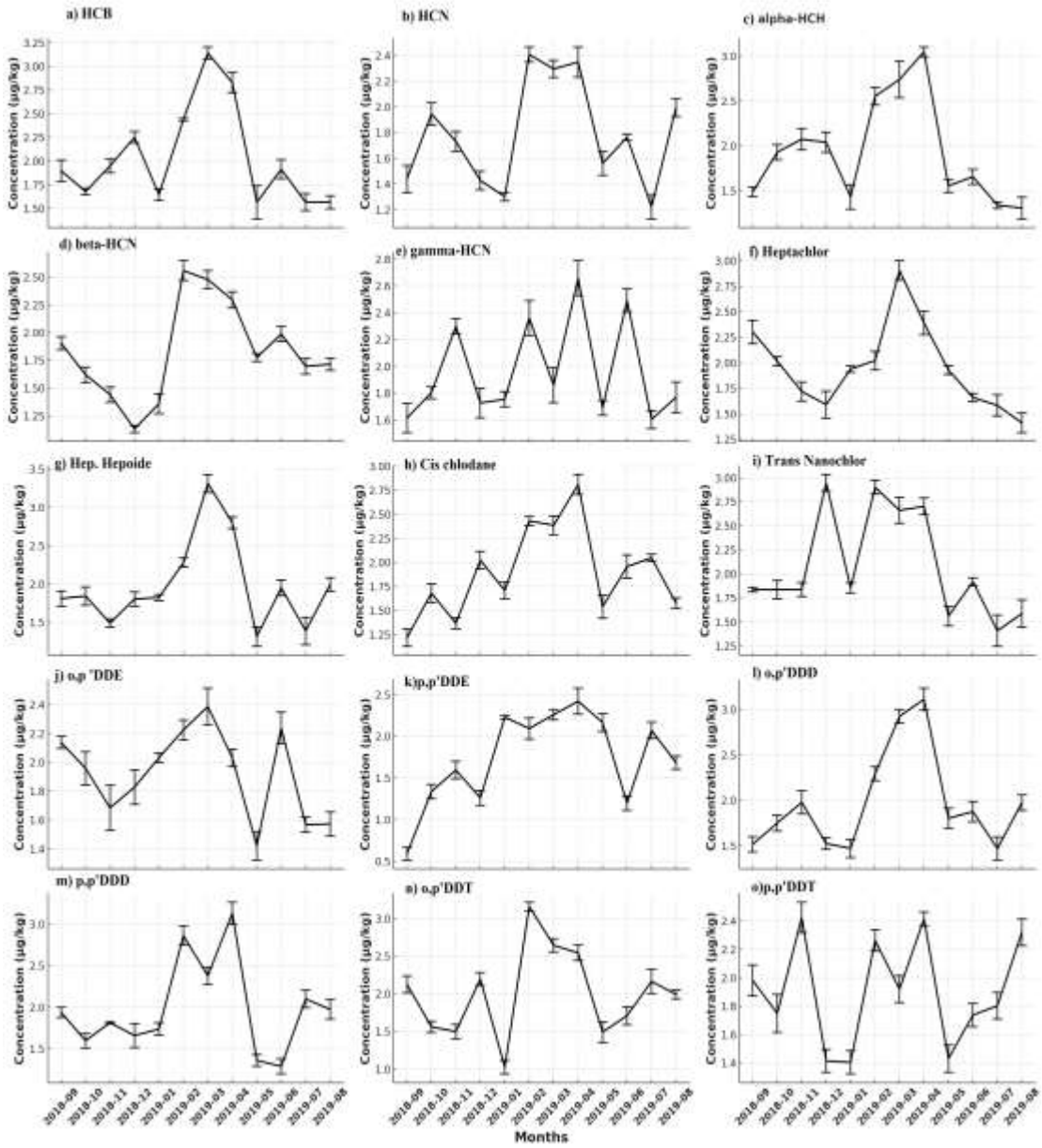

To statistically verify these patterns, one-way ANOVA was conducted for each OCP compound with month as the independent factor. Results showed statistically significant temporal variation across all compounds analyzed, with F-statistics ranging from 403.50 to 1281.33 and *p*-values consistently below 0.001 (Table 4.5). Further pairwise comparisons using Tukey's post hoc test indicated that for all compounds, the

concentrations recorded were significantly different during the months. For instance, γ-HCH and α-HCH exhibited significantly elevated concentrations in April 2019 (3.0 ± 0.11 µg/kg) compared to September (1.5 ± 0.06 µg/kg) and October (1.59 ± 0.08 µg/kg) 2018 (Appendix II, Table A4). The same trend was observed for β-HCH and p,p'-DDT derivatives.

Table 4. 5:
One-way ANOVA results showing temporal variation in sediment concentrations of OCPs across sampling months from September 2018 to July 2019

OCPs	***F* value**	***p* value**
HCB	$F_{(11, 420)} = 1281.33$	< 0.001
HCN	$F_{(11, 420)} = 403.50$	< 0.001
alpha-HCH	$F_{(11, 420)} = 736.56$	< 0.001
beta-HCH	$F_{(11, 420)} = 538.26$	< 0.001
gamma-HCH	$F_{(11, 420)} = 800.97$	< 0.001
Heptachlor	$F_{(11, 420)} = 674.02$	< 0.001
Hep.Hepoxide	$F_{(11, 420)} = 994.36$	< 0.001
Cis chlordane	$F_{(11, 420)} = 759.04$	< 0.001
Trans Nonachlor	$F_{(11, 420)} = 778.95$	< 0.001
o,p'DDE	$F_{(11, 420)} = 654.83$	< 0.001
p,p'DDE	$F_{(11, 420)} = 632.99$	< 0.001
o,p'DDD	$F_{(11, 420)} = 842.95$	< 0.001
p,p'DDD	$F_{(11, 420)} = 1097.00$	< 0.001
o,p'DDT	$F_{(11, 420)} = 1008.61$	< 0.001
p,p'DDT	$F_{(11, 420)} = 1222.53$	< 0.001

4.3.1.3 Spatio-temporal Variation in OCPs in sediments

The monthly variations in the concentrations of sixteen OCPs across different sampling stations between September 2018 and August 2019 are as illustrated in Figure 4.6. The plots show distinctive spatial and temporal trends in OCPs residues, with clear fluctuations across stations and sampling periods. Notably, compounds such as γ-HCH,

β-HCH, and p,p'-DDT exhibited pronounced peaks in early 2019 (February–April), whereas others like HCB, HCN, and Cis chlordane remained relatively low and stable throughout the study period. Several compounds, including o,p'-DDT, Heptachlor, and Trans Nonachlor, also demonstrated elevated concentrations during the dry months of May to July 2019. Meanwhile, fluctuations in Mirex which was simulated using Heptachlor data showed a more flattened pattern, indicating spatial consistency across the sampling sites.

One-way ANOVA results (Table 4.6) revealed statistically significant differences ($p < 0.001$) in the mean concentrations of all the OCPs across the sampling stations. The F-values ranged from $F_{(11, 420)} = 11.45$ for HCN to $F_{(11, 420)} = 25.34$ for γ-HCH, indicating varying degrees of spatial heterogeneity in OCP distribution. Specifically, γ-HCH ($F_{(11, 420)} = 25.34$), p,p'-DDT ($F_{(11, 420)} = 15.03$), and α-HCH ($F_{(11, 420)} = 20.51$) recorded the highest F-statistics, reflecting their strong spatial discrimination across stations.

Figure 4.6:
Spatio-temporal trends in the concentrations of OCPs in sediments across sampling stations from September 2018 to August 2019

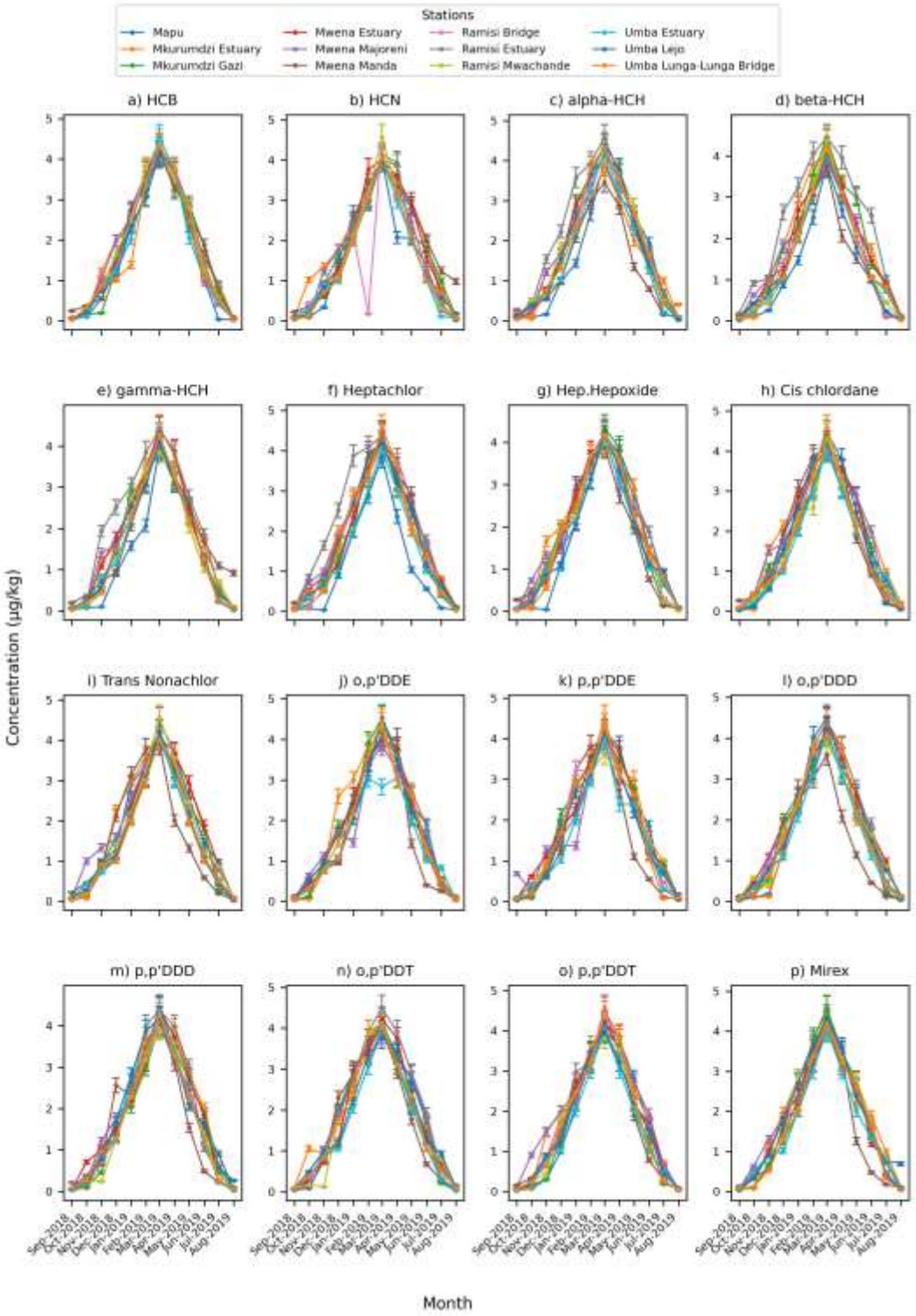

Table 4.6:
One-way ANOVA results showing statistically significant spatial variation ($p < 0.001$) in sediment concentrations of OCPs across sampling stations

OCPs	*F* value	*p* value
HCB	$F_{(11, 420)} = 14.05$	<0.001
HCN	$F_{(11, 420)} = 11.45$	<0.001
alpha-HCH	$F_{(11, 420)} = 20.51$	<0.001
beta-HCH	$F_{(11, 420)} = 20.09$	<0.001
gamma-HCH	$F_{(11, 420)} = 25.34$	<0.001
Heptachlor	$F_{(11, 420)} = 17.69$	<0.001
Hep.Hepoxide	$F_{(11, 420)} = 32.08$	<0.001
Cis chlordane	$F_{(11, 420)} = 45.18$	<0.001
Trans Nonachlor	$F_{(11, 420)} = 19.48$	<0.001
o,p'DDE	$F_{(11, 420)} = 24.27$	<0.001
p,p'DDE	$F_{(11, 420)} = 13.16$	<0.001
o,p'DDD	$F_{(11, 420)} = 29.72$	<0.001
p,p'DDD	$F_{(11, 420)} = 16.66$	<0.001
o,p'DDT	$F_{(11, 420)} = 25.03$	<0.001
p,p'DDT	$F_{(11, 420)} = 15.03$	<0.001
Mirex	$F_{(11, 420)} = 22.82$	<0.001

4.3.2 Levels of OCPs in water

4.3.2.1 Spatial variation in the Levels of OCPs in water

The concentrations of sixteen organochlorine pesticide (OCP) compounds were analyzed across twelve sampling stations in water to determine spatial variation. Figure 4.7 shows the distribution of values using boxplots, with each compound displayed across all stations. One-way ANOVA was conducted for each compound, and the results are presented in Table 4.7.

The ANOVA results indicated that fifteen of the sixteen compounds exhibited statistically significant differences in concentration across stations in water ($p < 0.05$). Among the compounds, HCB ($F_{(11, 420)} = 5.65$, $p < 0.001$), HCN ($F_{(11, 420)} = 4.87$, $p < 0.001$), and α-HCH ($F_{(11, 420)} = 4.40$, $p < 0.001$) had particularly high F-values. β-HCH ($F_{(11, 420)} = 1.74$, $p = 0.057$) was not statistically significant at the 5% level. γ-HCH ($F_{(11, 420)} = 2.15$, $p = 0.013$) showed moderate variation across stations.

Figure 4.7:
Boxplots showing spatial variation in OCP concentrations in water across 12 sampling stations. Each subplot represents a different compound with median, interquartile range, and outliers indicated

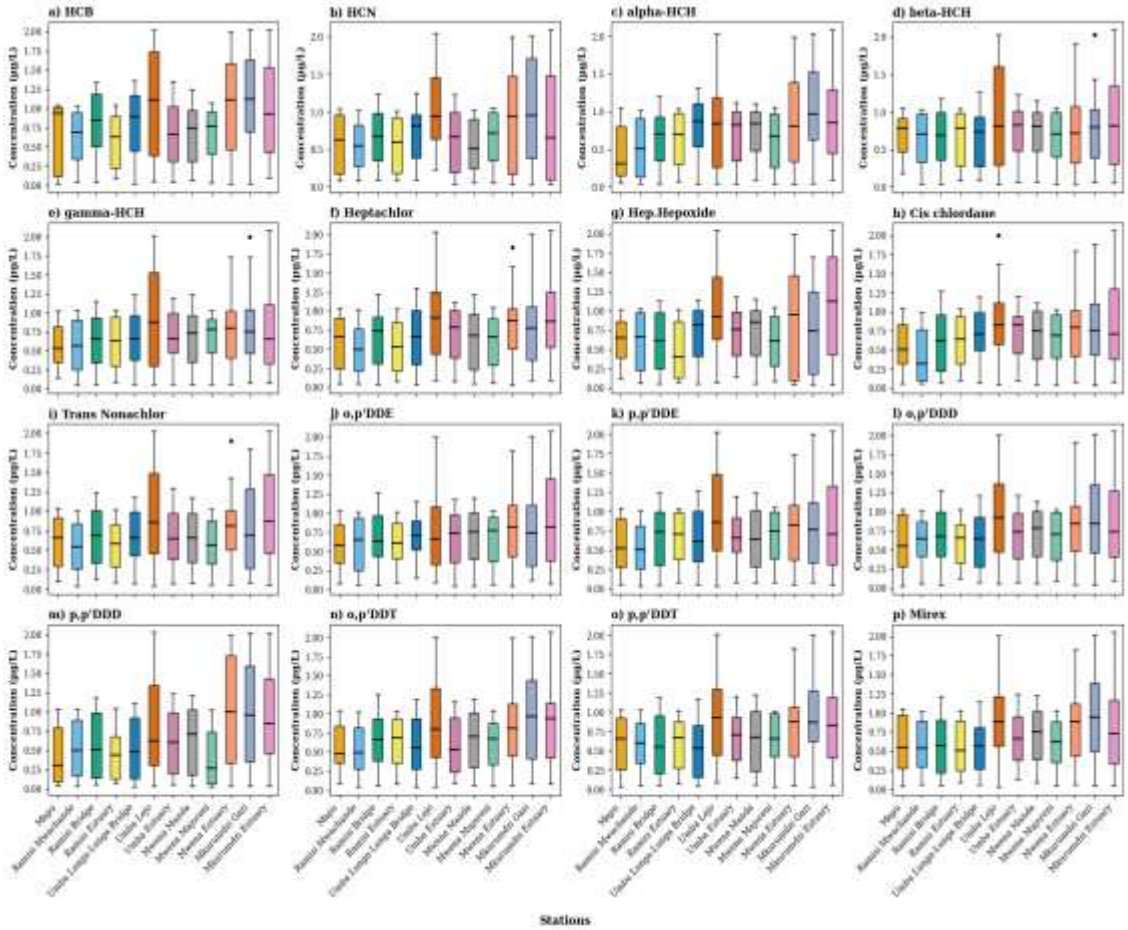

Tukey HSD post hoc tests further confirmed statistically significant pairwise differences between stations for the majority of the compounds. For example, HCB differed significantly between Mapu (1.0 ± 0.01 µg/kg), Mkurumdzi Estuary (0.59 ±

0.05 µg/kg), Mwena Estuary (1.2 ± 0.07 µg/kg) and Mwena Manda (0.58 ± 0.02 µg/kg), while γ-HCH was significantly different between Mapu (0.5 ± 0.01 µg/kg), Mkurumdzi Estuary (0.51 ± 0.01 µg/kg), Mwena Estuary (0.56 ± 0.02 µg/kg), Mwena Majoreni (0.55 ± 0.01 µg/kg) and Mwena Manda (0.53 ± 0.01 µg/kg). Stations such as Mwena Manda, Ramisi Estuary, and Ramisi Mwachande were not significantly different for HCB (Appendix II, Table A5).

Table 4. 7:
One-Way ANOVA results for OCP concentrations across stations. Statistically significant F-values ($p < 0.05$) indicate spatial variation in compound levels

OCPs	F value	*p* value
HCB	$F_{(11, 420)} = 5.653$	<0.001
HCN	$F_{(11, 420)} = 4.874$	<0.001
alpha_HCH	$F_{(11, 420)} = 4.402$	<0.001
beta_HCH	$F_{(11, 420)} = 1.743$	0.057
gamma_HCH	$F_{(11, 420)} = 2.154$	0.0131
Heptachlor	$F_{(11, 420)} = 3.986$	<0.001
Hep_Hepoxide	$F_{(11, 420)} = 4.604$	<0.001
Cis_chlordane	$F_{(11, 420)} = 3.332$	<0.001
Trans_Nonachlor	$F_{(11, 420)} = 4.063$	<0.001
o,p'-DDE	$F_{(11, 420)} = 2.082$	0.0171
p,p'-DDE	$F_{(11, 420)} = 2.994$	<0.001
o,p'-DDD	$F_{(11, 420)} = 3.845$	<0.001
p,p'-DDD	$F_{(11, 420)} = 6.623$	<0.001
o,p'-DDT	$F_{(11, 420)} = 4.17$	<0.001
p,p'-DDT	$F_{(11, 420)} = 3.934$	<0.001
Mirex	$F_{(11, 420)} = 4.425$	<0.001

4.3.2.2 Temporal variation in the levels of OCPs in water

Figure 4.8 presents the monthly distribution patterns of sixteen OCP compounds across sampling stations along the southern coast of Kenya from September 2018 to August 2019. The line plots with standard error bars reveal compound-specific and seasonal fluctuations in concentration trends.

One-way ANOVA results (Table 4.8) showed that all sixteen OCPs exhibited statistically significant temporal variation ($p < 0.001$). For example, γ-HCH recorded $F_{(11, 420)} = 166.34$, $p < 0.001$, p,p′-DDE recorded $F_{(11, 420)} = 171.02$, $p < 0.001$, and Heptachlor recorded $F_{(11, 420)} = 160.12$, $p < 0.001$. Cis-chlordane recorded $F_{(11, 420)} = 147.07$, $p < 0.001$. Tukey's HSD tests revealed statistically significant differences between specific months for several compounds (Appendix II).

Figure 4. 8:
Temporal distribution of OCPs in water across sampling stations

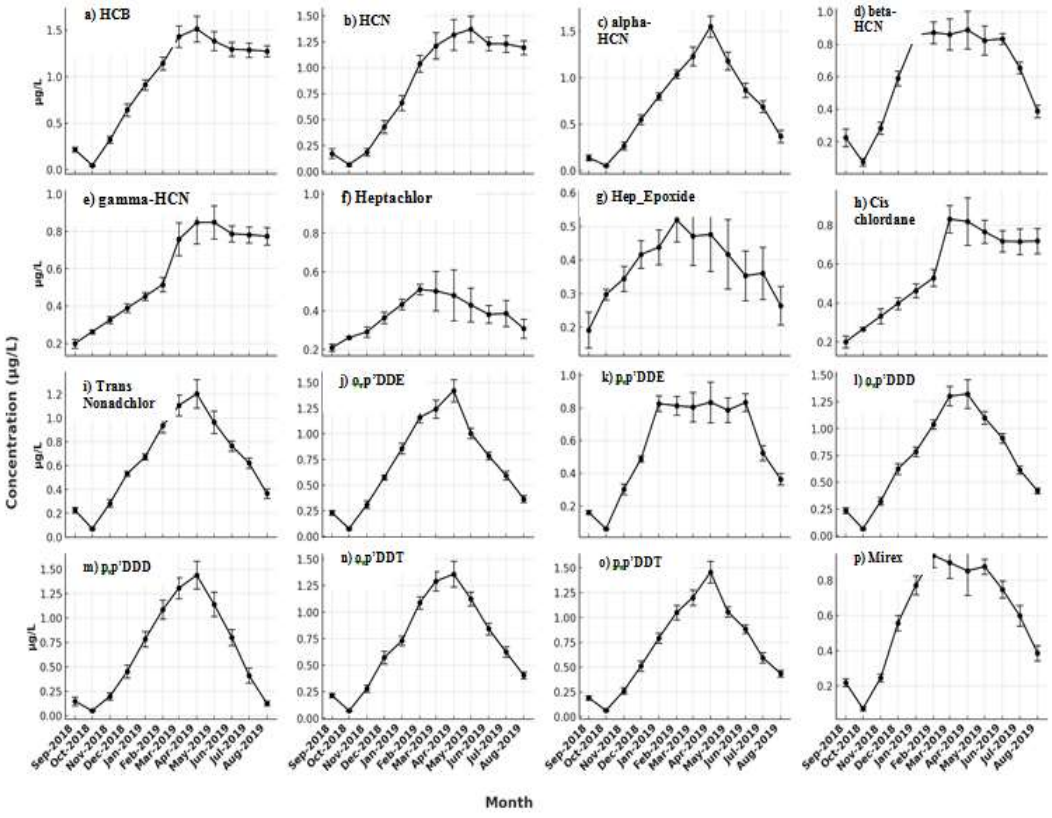

One-way ANOVA results (Table 4.8) demonstrated statistically significant temporal variation in the concentrations of all sixteen OCPs compounds across the twelve-month sampling period (September 2018–August 2019). For each compound, the calculated F-statistics were associated with $p < 0.001$, indicating that monthly concentrations differed significantly during the study period.

The magnitude of temporal variability differed among compounds, as reflected by the range of F-values. The highest month-to-month variation was observed for p,p′-DDE ($F(11, 420) = 171.02$, $p < 0.001$), followed closely by γ-HCH ($F_{(11, 420)} = 166.34$, $p < 0.001$) and o,p′-DDD ($F(11, 420) = 165.45$, $p < 0.001$). Similarly elevated temporal variation was recorded for trans-nonachlor ($F_{(11, 420)} = 160.28$, $p < 0.001$) and heptachlor ($F_{(11, 420)} = 160.13$, $p < 0.001$), indicating pronounced fluctuations in concentrations across sampling months.

Moderately high temporal variability was observed for cis-chlordane ($F_{(11, 420)} = 147.07$, $p < 0.001$), p,p′-DDT ($F_{(11, 420)} = 152.32$, $p < 0.001$), o,p′-DDT ($F_{(11, 420)} = 149.04$, $p < 0.001$), Mirex ($F_{(11, 420)} = 145.50$, $p < 0.001$), and β-HCH ($F_{(11, 420)} = 138.06$, $p < 0.001$). Although still statistically significant, comparatively lower F-values were recorded for HCN ($F_{(11, 420)} = 103.91$, $p < 0.001$) and p,p′-DDD ($F_{(11, 420)} = 105.93$, $p < 0.001$), suggesting relatively smaller, though significant, monthly fluctuations.

Post hoc Tukey's HSD tests further confirmed that significant pairwise differences existed between specific months for each compound ($p < 0.05$), indicating that the temporal variation was not driven by a single outlying month but reflected multiple month-to-month contrasts across the annual cycle.

Table 4.8:
Results of one-way ANOVA for monthly variation in OCPs concentrations (September 2018 – August 2019) in water

OCPs	F value	*p* value
HCB	$F_{(11, 420)} = 128.772$	< 0.001
HCN	$F_{(11, 420)} = 103.913$	< 0.001
alpha_HCH	$F_{(11, 420)} = 125.394$	< 0.001
beta_HCH	$F_{(11, 420)} = 138.062$	< 0.001
gamma_HCH	$F_{(11, 420)} = 166.344$	< 0.001
Heptachlor	$F_{(11, 420)} = 160.126$	< 0.001
Hep_Hepoxide	$F_{(11, 420)} = 111.794$	< 0.001
Cis_chlordane	$F_{(11, 420)} = 147.073$	< 0.001
Trans_Nonachlor	$F_{(11, 420)} = 160.284$	< 0.001
o,p'DDE	$F_{(11, 420)} = 160.482$	< 0.001
p,p'DDE	$F_{(11, 420)} = 171.023$	< 0.001
o,p'DDD	$F_{(11, 420)} = 165.445$	< 0.001
p,p'DDD	$F_{(11, 420)} = 105.934$	< 0.001
o,p'DDT	$F_{(11, 420)} = 149.035$	< 0.001
p,p'DDT	$F_{(11, 420)} = 152.322$	< 0.001
Mirex	$F_{(11, 420)} = 145.495$	< 0.001

4.3.2.3 Spatio-temporal variations in the levels of pesticides in water

Figure 4.9 illustrates the monthly variation in concentrations of sixteen organochlorine pesticide (OCP) compounds in water across sampling stations from September 2018 to August 2019. The concentration profiles demonstrate clear month-by-station variability, with compound-specific fluctuations observed across the monitoring period. Several compounds exhibited distinct concentration peaks between March and May 2019. For example, concentrations of γ-HCH, β-HCH, heptachlor, and p,p′-DDE

increased from late 2018 and reached higher values during the March–May period before declining in subsequent months.

Figure 4.9:
Spatio-temporal variation in concentrations (mean ± SE) of 16 OCPs in water samples collected monthly from twelve stations between September 2018 and August 2019

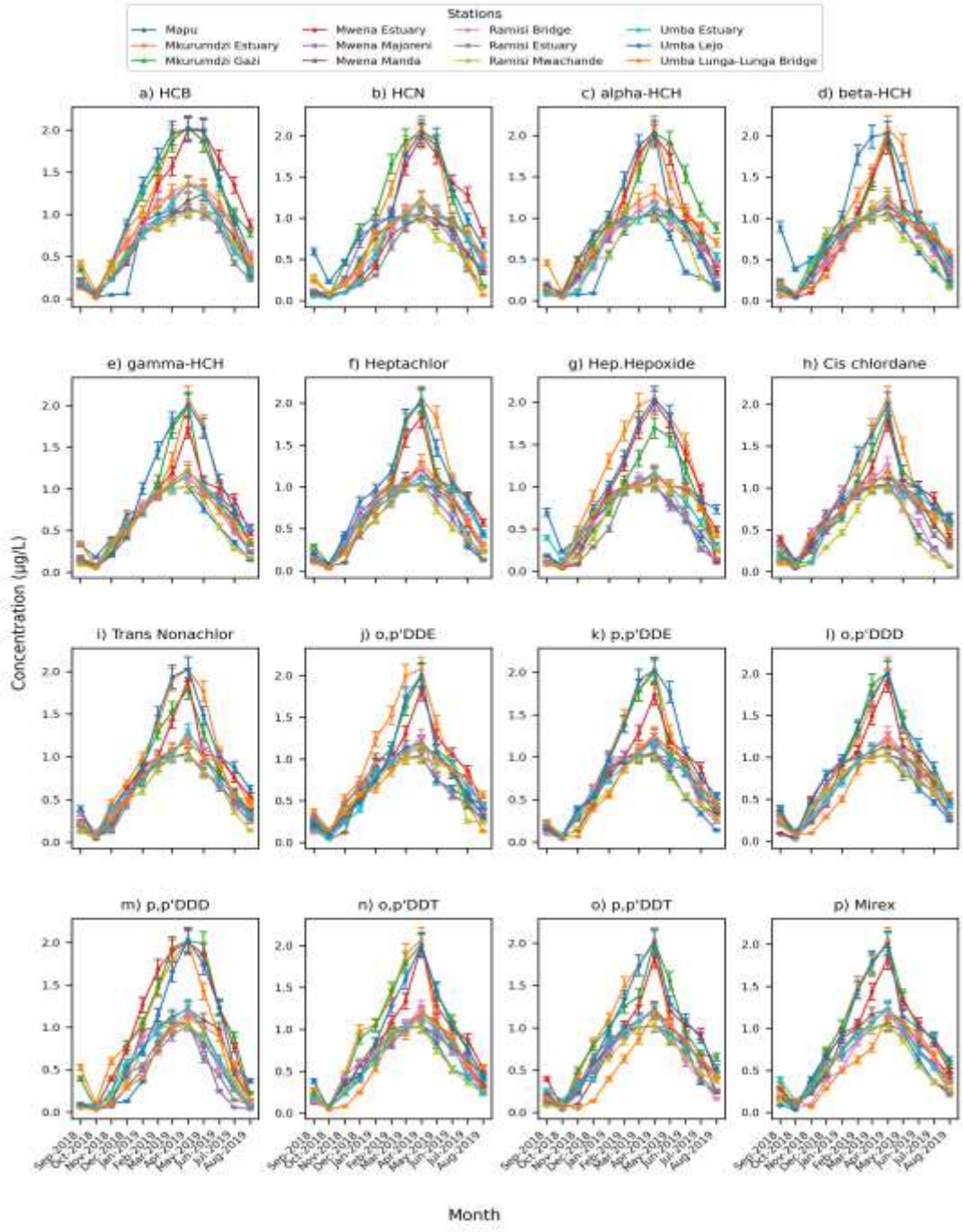

Two-way ANOVA results (Table 4.9) showed statistically significant station x month interaction effects for all sixteen OCPs (all $p < 0.001$), indicating that temporal variation was not uniform across sampling stations. The highest interaction effects were recorded for p,p′-DDE ($F_{(121, 288)} = 88.15$, $p < 0.001$), β-HCH ($F_{(121, 288)} = 78.23$, $p < 0.001$), γ-HCH ($F_{(121, 288)} = 70.96$, $p < 0.001$), and trans-nonachlor ($F_{(121, 288)} = 72.37$, $p < 0.001$). Moderate interaction effects were observed for o,p′-DDD ($F_{(121, 288)} = 68.96$, $p < 0.001$), o,p′-DDE ($F_{(121, 288)} = 56.29$, $p < 0.001$), p,p′-DDT ($F_{(121, 288)} = 87.93$, $p < 0.001$), and HCB ($F_{(121, 288)} = 36.50$, $p < 0.001$). Comparatively lower, though statistically significant, interaction effects were recorded for heptachlor ($F_{(121, 288)} = 9.26$, $p < 0.001$), Mirex ($F_{(121, 288)} = 11.08$, $p < 0.001$), p,p′-DDD ($F_{(121, 288)} = 12.32$, $p < 0.001$), and α-HCH ($F_{(121, 288)} = 13.36$, $p < 0.001$).

Tukey's HSD *post hoc* comparisons further revealed statistically significant differences between specific month–station combinations for several compounds ($p < 0.05$). For instance, γ-HCH and p,p′-DDE concentrations differed significantly between March–May and September–November across selected stations. Similarly, cis-chlordane, o,p′-DDE, and trans-nonachlor exhibited significant pairwise contrasts across multiple months depending on station. Overall, the significant interaction terms indicate that the magnitude of monthly concentration changes differed among stations for all compounds.

Table 4.9:
Two-way ANOVA results showing interaction (station x month) variation in OCPs concentrations

OCPs	*F* value	*p* value
HCB	$F_{(121, 288)} = 36.501$	<0.001
HCN	$F_{(121, 288)} = 21.514$	<0.001
alpha_HCH	$F_{(121, 288)} = 13.365$	<0.001
beta_HCH	$F_{(121, 288)} = 78.233$	<0.001
gamma_HCH	$F_{(121, 288)} = 70.962$	<0.001
Heptachlor	$F_{(121, 288)} = 9.263$	<0.001
Hep_Hepoxide	$F_{(121, 288)} = 41.691$	<0.001
Cis_chlordane	$F_{(121, 288)} = 21.153$	<0.001
Trans_Nonachlor	$F_{(121, 288)} = 72.373$	<0.001
o_pDDE	$F_{(121, 288)} = 56.294$	<0.001
p_pDDE	$F_{(121, 288)} = 88.153$	<0.001
o_pDDD	$F_{(121, 288)} = 68.963$	<0.001
p_pDDD	$F_{(121, 288)} = 12.322$	<0.001
o_pDDT	$F_{(121, 288)} = 59.224$	<0.001
p_pDDT	$F_{(121, 288)} = 87.932$	<0.001
Mirex	$F_{(121, 288)} = 11.082$	<0.001

4.3.3 Levels of pesticides in trophic guilds of benthic macroinvertebrates

4.3.3.1 Concentration of OCPs in shredders, *Terebrallia palustris*

The spatial distribution of OCPs concentrations in *T. palustris* across the 12 sampled stations is illustrated in Figure 4.10. Each subplot displays the spread of concentration values for one of the 16 compounds, with median lines, interquartile ranges (IQR), and outliers clearly marked. The visual layout enables comparisons of distribution patterns across stations, highlighting variation in central tendency and dispersion.

Several compounds exhibited variable concentration ranges among stations. For instance, o,p′-DDD, γ-HCH, and HCB showed wide interquartile ranges and frequent outliers at stations including Umba Estuary, Mwena Majoreni, and Mkurumdzi Estuary. In contrast, upstream stations such as Mapu and Ramisi Mwachande displayed narrower interquartile ranges and comparatively lower medians for compounds such as HCB, p,p′-DDT, and trans-nonachlor. Compounds including o,p′-DDT and p,p′-DDE exhibited skewed distributions at selected stations. Mirex, α-HCH, and β-HCH also showed elevated values at specific stations, indicating spatial differences in concentration levels.

Figure 4.10:
Boxplots showing spatial variation in organochlorine pesticide concentrations in T. palustris across 12 sampling stations.

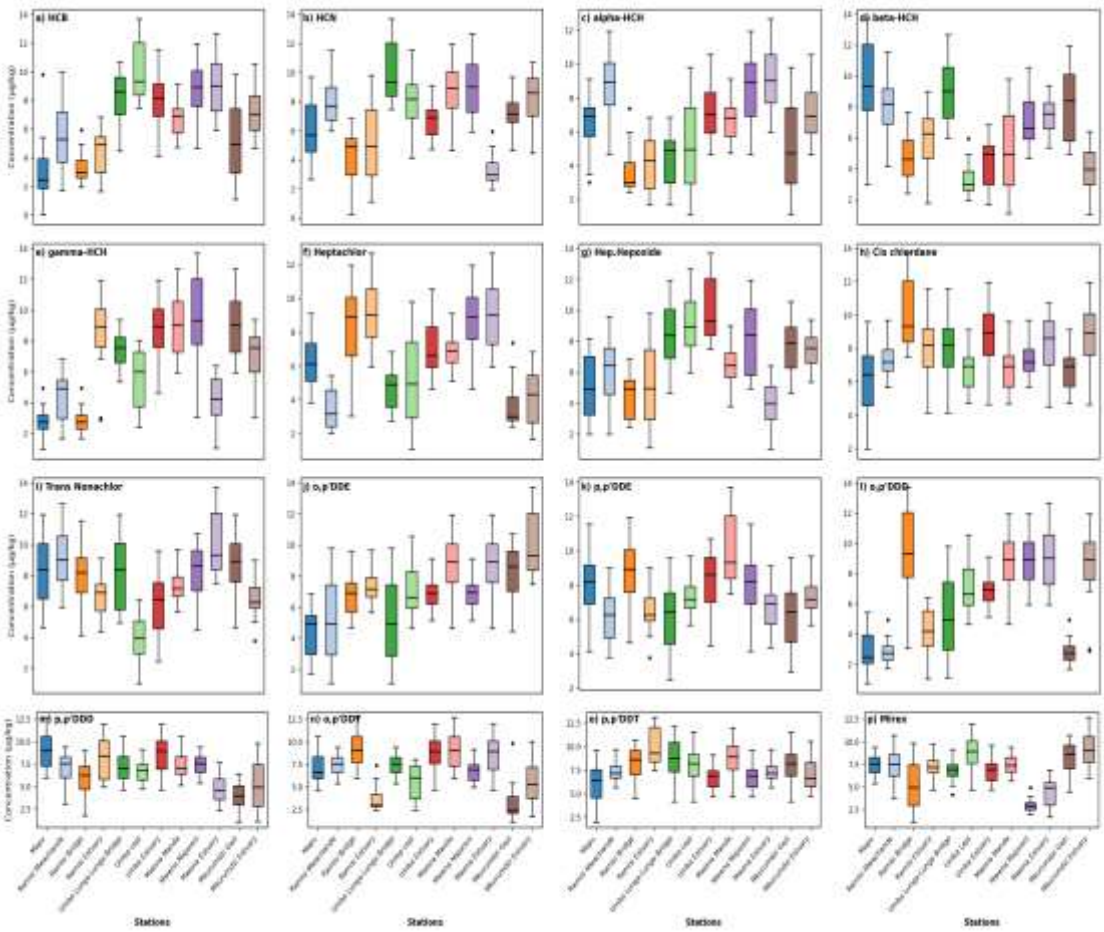

The results of the one-way ANOVA, summarized in Table 4.10, confirmed statistically significant spatial variation for all sixteen pesticides (all $p < 0.001$). The highest F-values were recorded for o,p′-DDD ($F_{(11, 420)} = 64.024$, $p < 0.001$), γ-HCH ($F_{(11, 420)} = 59.744$, $p < 0.001$), and HCB ($F_{(11, 420)} = 46.673$, $p < 0.001$). Heptachlor ($F_{(11, 420)} = 46.155$, $p < 0.001$), HCN ($F_{(11, 420)} = 41.503$, $p < 0.001$), and o,p′-DDT ($F_{(11, 420)} = 39.153$, $p < 0.001$) also showed substantial spatial variability. Additional compounds exhibiting significant spatial variation included Mirex ($F_{(11, 420)} = 38.172$, $p < 0.001$), β-HCH ($F_{(11, 420)} = 37.003$, $p < 0.001$), heptachlor epoxide ($F_{(11, 420)} = 35.56{,}5$ $p < 0.001$), α-HCH ($F_{(11, 420)} = 31.885$, $p < 0.001$), o,p′-DDE ($F_{(11, 420)} = 26.944$, $p < 0.001$), trans-nonachlor ($F_{(11, 420)} = 26.703$, $p < 0.001$), p,p′-DDD ($F_{(11, 420)} = 24.813$, $p < 0.001$), p,p′-DDE ($F_{(11, 420)} = 17.042$, $p < 0.001$), cis-chlordane ($F_{(11, 420)} = 14.773$, $p < 0.001$), and p,p′-DDT ($F_{(11, 420)} = 13.092$, $p < 0.001$). All compounds exhibited statistically significant spatial variation across stations.

Tukey HSD post hoc comparisons (Appendix II, Table A7) identified significant pairwise differences among stations for multiple compounds ($p < 0.05$). For example, o,p′-DDD concentrations differed significantly between Mwena and Mkurumdzi estuaries and upstream stations such as Ramisi Bridge and Mapu. Similar significant contrasts were observed for γ-HCH and HCB across multiple station pairs. For cis-chlordane and p,p′-DDE, significant differences were detected between Mkurumdzi, Mwena, and Umba estuaries ($p < 0.01$). These pairwise comparisons confirm the spatial heterogeneity indicated by the ANOVA results.

Table 4.10:
One-way ANOVA results for OCPs concentrations in T. palustris *across 12 sampling stations*

OCPs (µg/kg)	***F* value**	***p* value**
o,p'-DDD	$F_{(11, 420)} = 64.024$	<0.001
gamma-HCH	$F_{(11, 420)} = 59.744$	<0.001
HCB	$F_{(11, 420)} = 46.673$	<0.001
Heptachlor	$F_{(11, 420)} = 46.155$	<0.001
HCN	$F_{(11, 420)} = 41.503$	<0.001
o,p'DDT	$F_{(11, 420)} = 39.153$	<0.001
Mirex	$F_{(11, 420)} = 38.172$	<0.001
beta-HCH	$F_{(11, 420)} = 37.003$	<0.001
Hep.Hepoxide	$F_{(11, 420)} = 35.565$	<0.001
alpha-HCH	$F_{(11, 420)} = 31.885$	<0.001
o,p'-DDE	$F_{(11, 420)} = 26.944$	<0.001
Trans Nonachlor	$F_{(11, 420)} = 26.703$	<0.001
p,p'-DDD	$F_{(11, 420)} = 24.813$	<0.001
p,p'-DDE	$F_{(11, 420)} = 17.042$	<0.001
Cis chlordane	$F_{(11, 420)} = 14.773$	<0.001
p,p'-DDT	$F_{(11, 420)} = 13.092$	<0.001

The monthly distribution of OCPs concentrations in *T. palustris* across all sampling stations is presented in Figure 4.11. Each subplot displays mean monthly concentrations with standard error bars. Visual inspection indicates monthly fluctuations in concentration levels for several compounds. For example, p,p′-DDT (10.2 ± 0.27 µg/kg), cis-chlordane (9.0 ± 0.23 µg/kg), and p,p′-DDE (9.4 ± 0.27 µg/kg) exhibited elevated values during selected months.

Figure 4.11:
Temporal distribution of OCPs in T. palustris during the study period

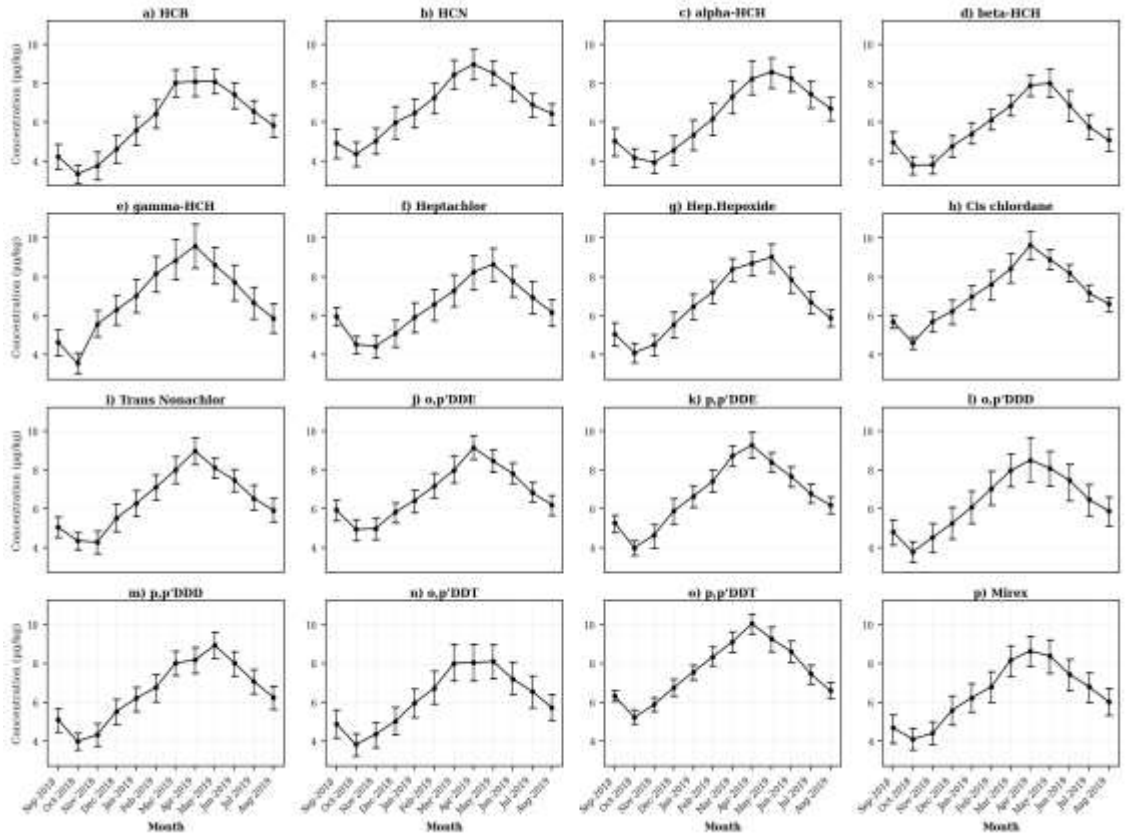

The one-way ANOVA results (Table 4.11) confirmed statistically significant temporal variation for all sixteen compounds (all $p < 0.001$). The highest temporal variability was recorded for p,p′-DDT ($F_{(11, 420)} = 59.433$, $p < 0.001$), followed by cis-chlordane ($F_{(11, 420)} = 57.772$, $p < 0.001$), p,p′-DDE ($F_{(11, 420)} = 50.215$, $p < 0.001$), and p,p′-DDD ($F_{(11, 420)} = 31.425$, $p < 0.001$). Additional compounds showing significant temporal variation included trans-nonachlor ($F_{(11, 420)} = 28.643$, $p < 0.001$), o,p′-DDE ($F_{(11, 420)} = 27.342$, $p < 0.001$), heptachlor epoxide ($F_{(11, 420)} = 22.911$, $p < 0.001$), Mirex ($F_{(11, 420)} = 21.951$, $p < 0.001$), α-HCH ($F_{(11, 420)} = 20.683$, $p < 0.001$), HCN ($F_{(11, 420)} = 20.276$, $p < 0.001$), β-HCH ($F_{(11, 420)} = 20.233$, $p < 0.001$), HCB ($F_{(11, 420)} = 17.062$, $p < 0.001$), o,p′-

DDT ($F_{(11, 420)}$ = 16.533, $p < 0.001$), heptachlor ($F_{(11, 420)}$ = 14.985, $p < 0.001$), γ-HCH ($F_{(11, 420)}$ = 13.956, $p < 0.001$), and o,p′-DDD ($F_{(11, 420)}$ = 11.232, $p < 0.001$).

Table 4.11:
One-Way ANOVA results for temporal variation in OCPs concentrations in T. palustris.

OCPs (µg/kg)	**F value**	***p*-**
p,p'DDT	$F_{(11, 420)}$ = 59.433	<0.001
Cis chlordane	$F_{(11, 420)}$ = 57.772	<0.001
p,p'DDE	$F_{(11, 420)}$ = 50.215	<0.001
p,p'DDD	$F_{(11, 420)}$ = 31.425	<0.001
Trans Nonachlor	$F_{(11, 420)}$ = 28.643	<0.001
o,p'DDE	$F_{(11, 420)}$ = 27.342	<0.001
Hep.Hepoxide	$F_{(11, 420)}$ = 22.911	<0.001
Mirex	$F_{(11, 420)}$ = 21.951	<0.001
alpha-HCH	$F_{(11, 420)}$ = 20.683	<0.001
HCN	$F_{(11, 420)}$ = 20.276	<0.001
beta-HCH	$F_{(11, 420)}$ = 20.233	<0.001
HCB	$F_{(11, 420)}$ = 17.062	<0.001
o,p'DDT	$F_{(11, 420)}$ = 16.533	<0.001
Heptachlor	$F_{(11, 420)}$ = 14.985	<0.001
gamma-HCH	$F_{(11, 420)}$ = 13.956	<0.001
o,p'DDD	$F_{(11, 420)}$ = 11.232	<0.001

Nonetheless, the spatio-temporal distribution of OCPs concentrations in *T. palustris* are as depicted in Figure 4.12. Each subplot corresponds to a specific compound and illustrates mean monthly concentrations, with separate lines representing individual stations. Error bars indicate the standard error of the mean. The Figure reveals pronounced variation in concentration patterns across both months and stations. For several compounds, including γ-HCH, β-HCH, heptachlor, and o,p′-DDD, concentration peaks are observed during selected months, with different stations exhibiting varying magnitudes of increase. In many cases, the station-level trajectories

diverge substantially within the same month, indicating spatial differences in compound accumulation.

Certain downstream stations, such as Umba Estuary, Mwena Majoreni, and Mwena Estuary, display consistently higher concentration profiles for compounds such as γ-HCH, p,p′-DDE, and trans-nonachlor compared to upstream locations including Mapu and Ramisi Mwachande. For compounds such as HCB, α-HCH, and Mirex, the temporal profiles show moderate fluctuations with visible differences among stations in both peak magnitude and timing. In several subplots, station-level concentration lines intersect across months, demonstrating shifting dominance of particular stations over time. Overall, the graphical patterns illustrate compound-specific variability in accumulation across both space and time, with clear differences in concentration magnitude, timing of peaks, and dispersion among stations throughout the annual sampling period.

Figure 4.12:
Spatio-temporal variation of OCPs concentrations in T. palustris during the study period

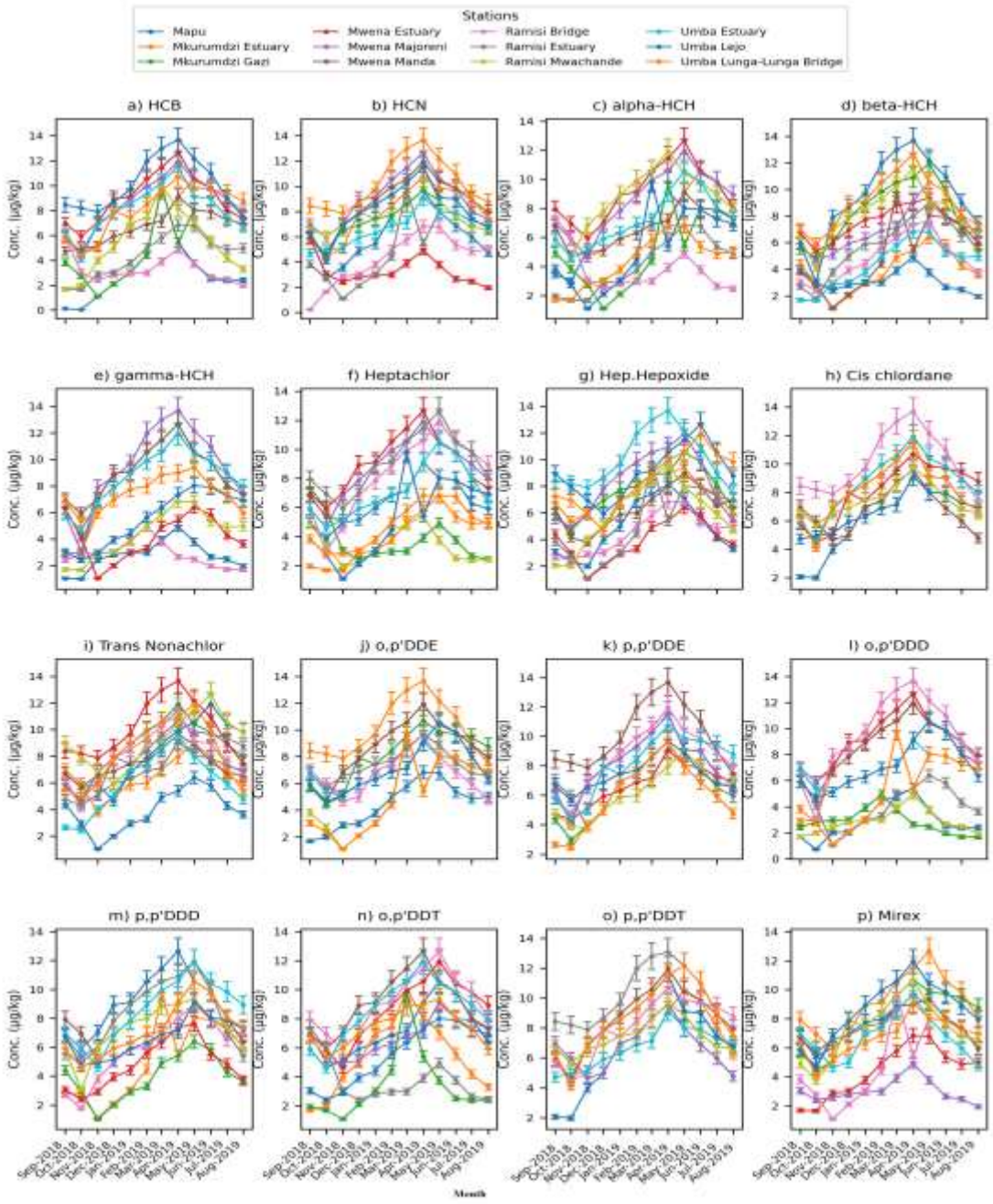

The highest station x month interaction effects were recorded for γ-HCH ($F_{(121, 288)}$ = 25,674.004, $p < 0.001$), o,p′-DDD ($F_{(121, 288)}$ = 107,176.005, $p < 0.001$), and p,p′-DDD ($F_{(121, 288)}$ = 104,274.004, $p < 0.001$). Substantial interaction effects were also observed for trans-nonachlor ($F_{(121, 288)}$ = 11,144.605, $p < 0.001$), o,p′-DDE ($F_{(121, 288)}$ =

11,280.803, $p < 0.001$), p,p′-DDT ($F(121, 288) = 7,363.202$, $p < 0.001$), heptachlor ($F_{(121, 288)} = 8,194.704$, $p < 0.001$), and α-HCH ($F_{(121, 288)} = 7,413.704$, $p < 0.001$). Moderate interaction effects were recorded for p,p′-DDE ($F_{(121, 288)} = 3,975.434$, $p < 0.001$), cis-chlordane ($F_{(121, 288)} = 3,443.363$, $p < 0.001$), o,p′-DDT ($F_{(121, 288)} = 2,030.383$, $p < 0.001$), HCB ($F_{(121, 288)} = 1,887.303$, $p < 0.001$), and heptachlor epoxide ($F_{(121, 288)} = 1,589.114$, $p < 0.001$). The lowest, though still statistically significant, interaction effects were recorded for Mirex ($F_{(121, 288)} = 978.421$, $p < 0.001$) and HCN ($F_{(121, 288)} = 262.413$, $p < 0.001$). These results indicate statistically significant compound-specific variation across both stations and months.

Table 4.12:
Two-way ANOVA Station x Month interaction effects on OCPs concentrations in T. palustris

OCPs (µg/kg)	F-value	*p*-value
HCB	$F_{(121, 288)}$ = 1887.303	< 0.001
HCN	$F_{(121, 288)}$ = 262.413	< 0.001
α-HCH	$F_{(121, 288)}$ = 7413.704	< 0.001
γ -HCH	$F_{(121, 288)}$ = 10242.004	< 0.001
gamma-HCH	$F_{(121, 288)}$ = 25674.004	< 0.001
Heptachlor	$F_{(121, 288)}$ = 8194.704	< 0.001
Hep.Hepoxide	$F_{(121, 288)}$ = 1589.114	< 0.001
Cis chlordane	$F_{(121, 288)}$ = 3443.363	< 0.001
Trans Nonachlor	$F_{(121, 288)}$ = 11144.605	< 0.001
o,p'DDE	$F_{(121, 288)}$ = 11280.803	< 0.001
p,p'DDE	$F_{(121, 288)}$ = 3975.434	< 0.001
o,p'DDD	$F_{(121, 288)}$ = 107176.005	< 0.001
p,p'DDD	$F_{(121, 288)}$ = 104274.004	< 0.001
o,p'DDT	$F_{(121, 288)}$ = 2030.383	< 0.001
p,p'DDT	$F_{(121, 288)}$ = 7363.202	< 0.001
Mirex	$F_{(121, 288)}$ = 978.421	< 0.001

4.3.3.2 Concentration of OCPs in scrapper-grazers, *Nerita undata*,

Spatial distribution of OCP concentrations in *N. undata* across 12 sampling stations is presented in Figure 4.13. Each subplot represents a distinct compound and shows the distribution of values by station, including medians, interquartile ranges (IQR), and outliers. The figure reveals substantial spatial heterogeneity across multiple compounds. Notable differences in median concentrations and spread are observed among stations, with downstream and estuarine sites showing more pronounced IQRs and higher concentration levels. For example, elevated values and wide spreads are evident in o,p′-DDD, HCN, and γ-HCH at stations such as Mwena Estuary, Mwena

Manda, Mkurumdzi Estuary, and Mwena Majoreni. Compounds like o,p′-DDT, Mirex, and cis-chlordane also show broad dispersion at selected sites, with estuarine stations consistently displaying elevated upper ranges. Outliers were particularly common at Mapu across many compounds, suggesting localized episodic exposure or high within-station variability. By contrast, some upstream/less-influenced stations (e.g., Ramisi Bridge and Mkurumdzi Gazi) showed narrower boxes and lower medians for several pesticides, including HCB, p,p′-DDE, and β-HCH. The visual differentiation between stations is most pronounced for compounds like o,p′-DDD and HCN, where outlier clustering is clearly visible and suggests site-specific contamination levels.

Figure 4.13:
Spatial variation in OCPs in N. undata during the study period

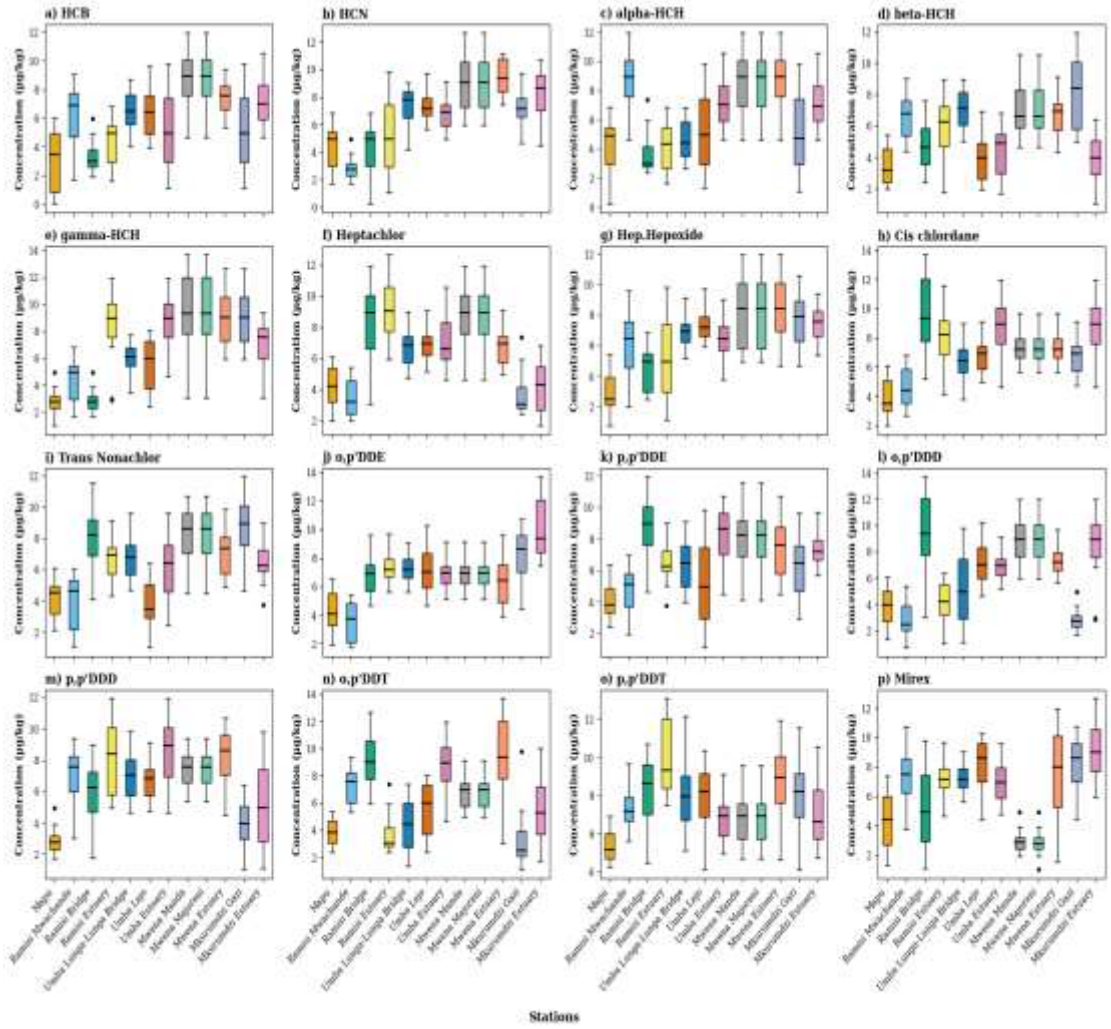

The one-way ANOVA results (Table 4.13) support the spatial differences observed in the figure. All 16 OCP compounds showed statistically significant variation across the stations ($F_{(11, 132)}$, $p < 0.001$ for all compounds). The highest F-value was recorded for o,p′-DDD [$F_{(11, 432)} = 57.526$, $p < 0.001$], followed by HCN [$F_{(11, 432)} = 55.825$, $p < 0.001$] and γ-HCH [$F_{(11, 432)} = 53.194$, $p < 0.001$]. Other compounds with similarly strong spatial variation include heptachlor [$F_{(11, 432)} = 52.463$, $p < 0.001$], o,p′-DDE [$F_{(11, 432)} = 46.385$, $p < 0.001$], o,p′-DDT [$F_{(11, 432)} = 44.073$, $p < 0.001$], and Mirex [$F_{(11, 432)} = 41.822$, $p < 0.001$]. Cis-chlordane [$F_{(11, 432)} = 36.893$, $p < 0.001$], α-HCH [$F_{(11, 432)} = 35.192$, $p < 0.001$], and p,p′-DDD [$F_{(11, 432)} = 34.183$, $p < 0.001$] also displayed strong spatial differences. Additional significant variation was noted for trans-nonachlor [$F_{(11, 432)} = 33.683$, $p < 0.001$], β-HCH [$F_{(11, 432)} = 32.264$, $p < 0.001$], HCB [$F_{(11, 432)} = 31.284$, $p < 0.001$], and heptachlor epoxide [$F_{(11, 432)} = 29.684$, $p < 0.001$]. The lowest (but still statistically significant) *F* values were recorded for p,p′-DDE [$F_{(11, 432)} = 23.402$, $p < 0.001$] and p,p′-DDT [$F_{(11, 432)} = 17.334$, $p < 0.001$].

Tukey HSD post hoc comparisons confirmed that many of the observed differences between stations were statistically significant for multiple pairwise combinations. For example, *N. undata* collected from Ramisi Estuary exhibited significantly higher concentrations of o,p′-DDD and γ-HCH compared to Mwena Manda and Mkurumdzi Gazi (Tukey HSD, $p < 0.001$). Ramisi Bridge also differed significantly from downstream stations such as Ramisi, Mwena, and Mkurumdzi estuaries for compounds including p,p′-DDT, Mirex, o,p′-DDE, and trans-nonachlor (Tukey HSD, $p < 0.01$). For heptachlor epoxide and cis-chlordane, significant pairwise differences were also observed between downstream/estuarine and upstream stations (Tukey HSD, $p < 0.05$).

Table 4.13:
One-Way ANOVA results for OCPs in N. undata across sampling stations

OCPs (µg/kg)	*F* value	*p* value
o,p'DDD	$F_{(11,432)} = 57.526$	< 0.001
HCN	$F_{(11,432)} = 55.825$	< 0.001
gamma-HCH	$F_{(11,432)} = 53.194$	< 0.001
Heptachlor	$F_{(11,432)} = 52.463$	< 0.001
o,p'DDE	$F_{(11,432)} = 46.385$	< 0.001
o,p'DDT	$F_{(11,432)} = 44.073$	< 0.001
Mirex	$F_{(11,432)} = 41.822$	< 0.001
Cis chlordane	$F_{(11,432)} = 36.893$	< 0.001
alpha-HCH	$F_{(11,432)} = 35.192$	< 0.001
p,p'DDD	$F_{(11,432)} = 34.183$	< 0.001
Trans Nonachlor	$F_{(11,432)} = 33.683$	< 0.001
beta-HCH	$F_{(11,432)} = 32.264$	< 0.001
HCB	$F_{(11,432)} = 31.284$	< 0.001
Hep.Hepoxide	$F_{(11,432)} = 29.684$	< 0.001
p,p'DDE	$F_{(11,432)} = 23.402$	< 0.001
p,p'DDT	$F_{(11,432)} = 17.334$	< 0.001

The monthly distribution of OCPs concentrations in *N. undata* across all sampling stations **is** presented in Figure 4.14. Each subplot represents a specific compound and displays monthly mean concentrations with standard error bars, providing a visual indication of variability over time. The figure reveals distinct temporal trends in pesticide concentrations, with several compounds showing elevated mean values during the months corresponding to the long rains (March to May). For instance, p,p′-DDT, p,p′-DDE, and heptachlor epoxide display clear seasonal peaks during this period, suggesting increased accumulation during wetter months. Variability in standard errors is also evident, with wider bars occurring during months of higher concentrations, indicating increased dispersion in pesticide accumulation among sampling sites.

Compounds such as cis-chlordane, β-HCH, and o,p′-DDE also follow a similar pattern, with concentrations rising during the first and second quarters of the year before declining in subsequent drier periods. Conversely, compounds like o,p′-DDD and Mirex show less abrupt changes over time but still exhibit recognizable seasonal oscillations.

Figure 4. 14:
Temporal distribution of OCPs concentrations in N. undata during the study period

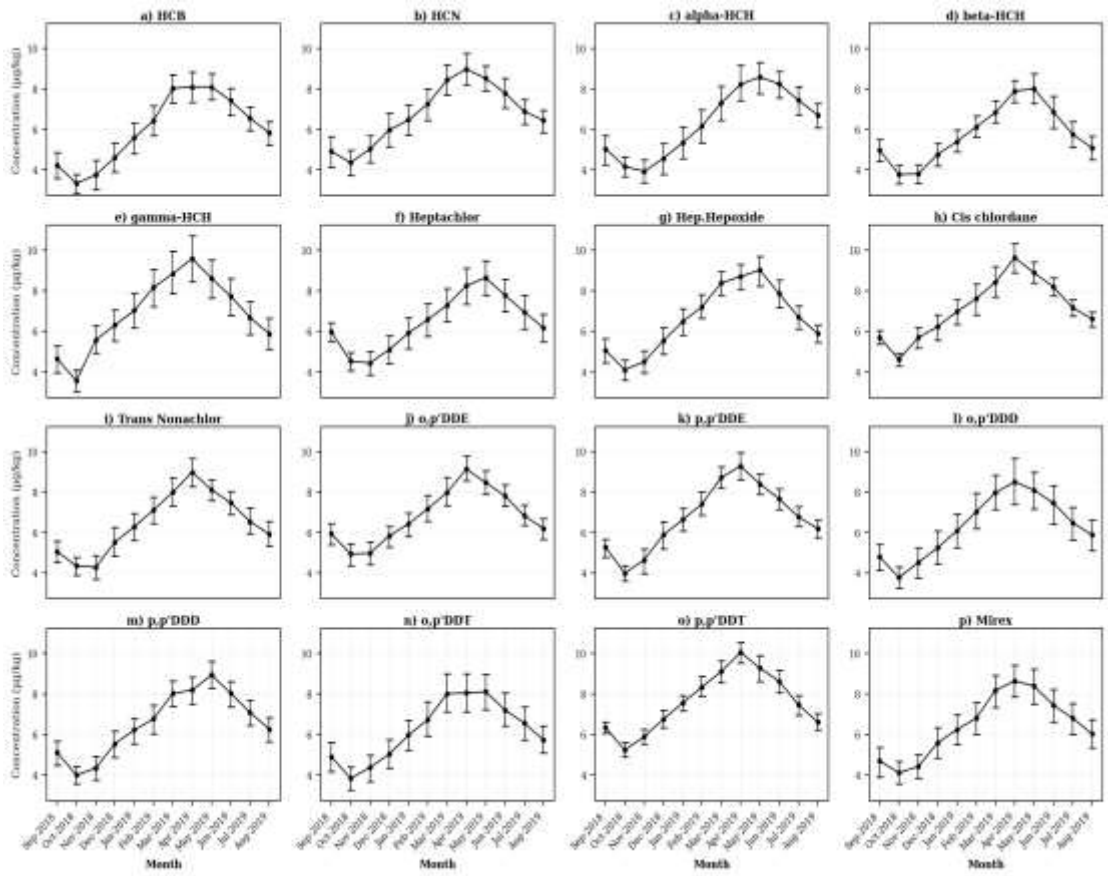

Statistical analysis using one-way ANOVA (Table 4.14) confirms that all sixteen assessed compounds varied significantly across months, with $F_{(11, 432)}$ reported for each compound and $p < 0.001$ throughout. The strongest monthly variation was observed in p,p′-DDT [$F_{(11, 432)} = 39.854$, $p < 0.001$], followed closely by p,p′-DDE [$F_{(11, 432)} = 34.633$, $p < 0.001$]. Heptachlor epoxide also demonstrated marked temporal variability

[$F_{(11, 432)} = 27.492$, $p < 0.001$], as did cis-chlordane [$F_{(11, 432)} = 25.241$, $p < 0.001$] and HCB [$F_{(11, 432)} = 24.422$, $p < 0.001$]. Moderate yet statistically significant temporal variation was observed for p,p′-DDD [$F_{(11, 432)} = 23.763$, $p < 0.001$], trans-nonachlor [$F_{(11, 432)} = 22.763$, $p < 0.001$], and β-HCH [$F_{(11, 432)} = 21.577$, $p < 0.001$]. The compounds o,p′-DDE [$F_{(11, 432)} = 20.586$, $p < 0.001$] and α-HCH [$F_{(11, 432)} = 19.525$, $p < 0.001$] also demonstrated measurable month-to-month differences.

Further, HCN [$F_{(11, 432)} = 16.564$, $p < 0.001$], Mirex [$F_{(11, 432)} = 16.553$, $p < 0.001$], and γ-HCH [$F_{(11, 432)} = 16.272$, $p < 0.001$] all showed significant variation across time. The lowest significant F-values were observed for o,p′-DDT [$F_{(11, 432)} = 13.323$, $p < 0.001$], heptachlor [$F_{(11, 432)} = 13.184$, $p < 0.001$], and o,p′-DDD [$F_{(11, 432)} = 12.408$, $p < 0.001$]. These results align with the visual patterns observed in Figure 4.14, confirming that temporal fluctuations in pesticide concentrations among *N. undata* are widespread, compound-specific, and statistically robust.

Table 4.14:
One-Way ANOVA results for monthly variation in OCPs in N. undata

OCPs (µg/kg)	*F* value	*p* value
p,p'DDT	$F_{(11,432)} = 39.854$	< 0.001
p,p'DDE	$F_{(11,432)} = 34.633$	< 0.001
Hep.Hepoxide	$F_{(11,432)} = 27.492$	< 0.001
Cis chlordane	$F_{(11,432)} = 25.241$	< 0.001
HCB	$F_{(11,432)} = 24.422$	< 0.001
p,p'DDD	$F_{(11,432)} = 23.763$	< 0.001
Trans Nonachlor	$F_{(11,432)} = 22.763$	< 0.001
beta-HCH	$F_{(11,432)} = 21.577$	< 0.001
o,p'DDE	$F_{(11,432)} = 20.586$	< 0.001
alpha-HCH	$F_{(11,432)} = 19.525$	< 0.001
HCN	$F_{(11,432)} = 16.564$	< 0.001
Mirex	$F_{(11,432)} = 16.553$	< 0.001
gamma-HCH	$F_{(11,432)} = 16.272$	< 0.001
o,p'DDT	$F_{(11,432)} = 13.323$	< 0.001
Heptachlor	$F_{(11,432)} = 13.184$	< 0.001
o,p'DDD	$F_{(11,432)} = 12.408$	< 0.001

The spatio-temporal patterns of OCP concentrations in *N. undata* are presented in Figure 4.15. Each subplot corresponds to a different compound and displays monthly mean concentrations with standard error bars. Distinct lines represent different stations, enabling visualization of site-specific temporal trajectories. The plots reveal considerable spatio-temporal variability across the compounds, with fluctuations that differ in both magnitude and timing among the stations. For several compounds, including γ-HCH, α-HCH, and heptachlor, distinct concentration peaks occur at downstream stations such as Mwena, Mkurumdzi, and Umba during the long rainy season months of March to May. These peaks are often accompanied by steep rises in station-specific lines, while upstream stations like Mapu and Ramisi Bridge show either

delayed or minimal responses during the same period. Divergence in station-level trends is also seen for compounds such as β-HCH, trans-nonachlor, and p,p′-DDD, with clear differences in the timing and amplitude of monthly increases across locations.

Other compounds, such as HCB and cis-chlordane, show mid-year shifts in some stations but not others, while fluctuations in Mirex and o,p′-DDE often occur in short pulses, particularly during the short rains around October and November. In many subplots, the non-parallel and intersecting station lines suggest substantial variation in monthly concentration trajectories between sites. The presence of staggered or asynchronous peaks further supports the notion that temporal patterns of OCP exposure and uptake were not uniform across the spatial gradient.

Figure 4. 15:
Spatio-temporal variation of OCPs concentrations in N. undata during the study period

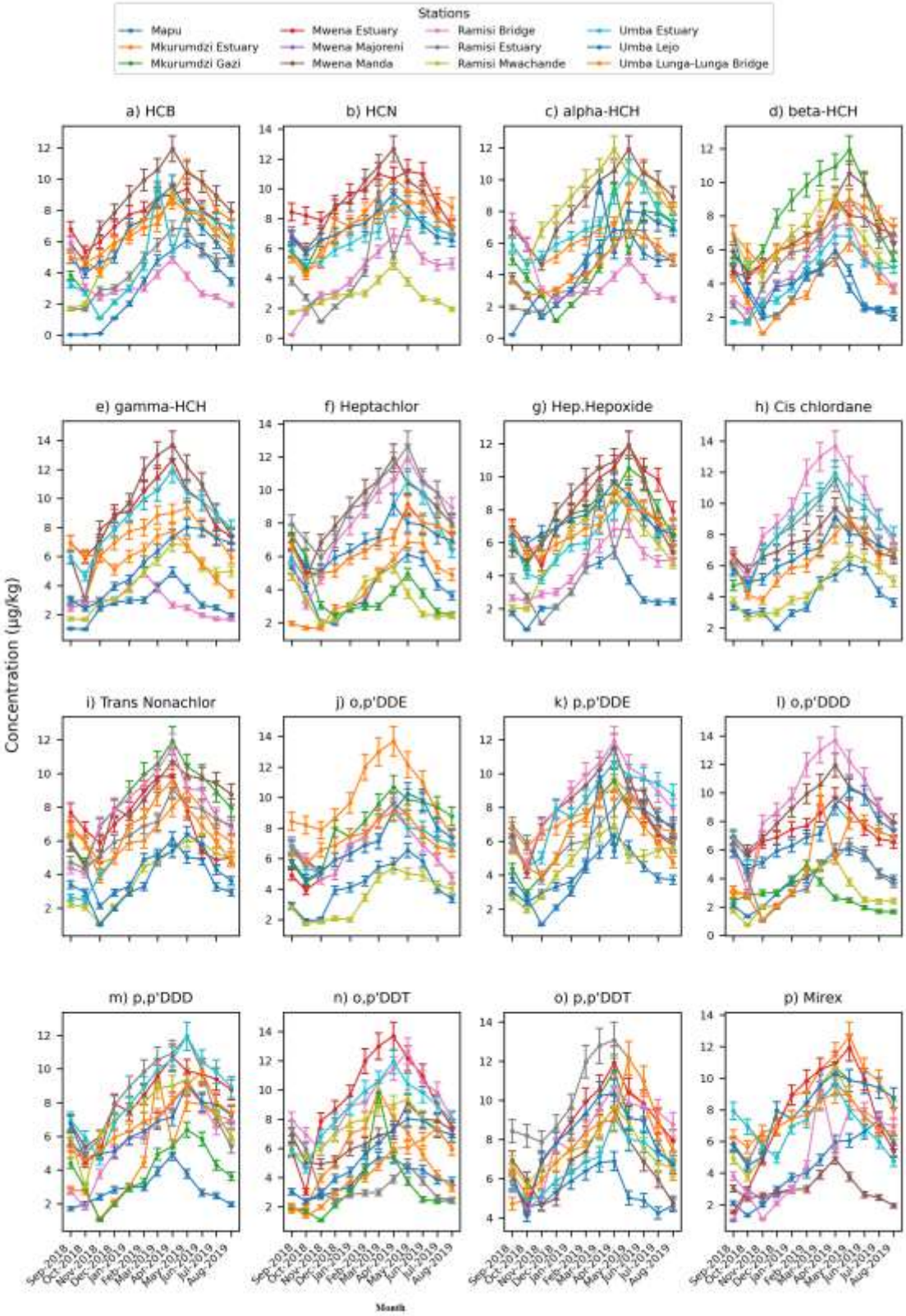

The interaction terms from the two-way ANOVA, summarized in Table 4.15, confirm significant station × month effects for all 16 compounds (all $p < 0.001$), indicating that temporal changes in concentrations differed across stations. The strongest interaction effects were recorded for γ-HCH [$F_{(121, 288)} = 13253.100$, $p < 0.001$], followed by heptachlor [$F_{(121, 288)} = 10544.930$, $p < 0.001$] and α-HCH [$F_{(121, 288)} = 10430.250$, $p < 0.001$]. o,p′-DDD and p,p′-DDD also showed strong interactions [$F_{(121, 288)} = 3031.840$ and 2987.820, respectively; $p < 0.001$]. Substantial interaction effects were further evident for trans-nonachlor [$F_{(121, 288)} = 9019.670$, $p < 0.001$], HCN [$F_{(121, 288)} = 8096.970$, $p < 0.001$], p,p′-DDT [$F_{(121, 288)} = 6804.750$, $p < 0.001$], cis-chlordane [$F_{(121, 288)} = 5664.850$, $p < 0.001$], and p,p′-DDE [$F_{(121, 288)} = 5762.790$, $p < 0.001$]. Moderate but statistically robust interaction effects were found for o,p′-DDE [$F_{(121, 288)} = 3374.640$, $p < 0.001$], HCB [$F_{(121, 288)} = 1303.090$, $p < 0.001$], and Mirex [$F_{(121, 288)} = 1532.970$, $p < 0.001$]. The smallest (yet statistically significant) interaction effects were recorded for o,p′-DDT [$F_{(121, 288)} = 245.820$, $p < 0.001$] and β-HCH [$F_{(121, 288)} = 353.830$, $p < 0.001$].

Table 4.15:
Two-way ANOVA interaction effects for OCP concentrations in N. undata across sampling stations and months

Pesticide (µg/kg)	*F* value	*p* value
HCB	$F_{(121, 288)} = 1303.090$	< 0.001
HCN	$F_{(121, 288)} = 8096.970$	< 0.001
α-HCH	$F_{(121, 288)} = 10430.250$	< 0.001
β-HCH	$F_{(121, 288)} = 353.830$	< 0.001
γ-HCH	$F_{(121, 288)} = 13253.100$	< 0.001
Heptachlor	$F_{(121, 288)} = 10544.930$	< 0.001
Heptachlor epoxide	$F_{(121, 288)} = 11415.370$	< 0.001
Cis-chlordane	$F_{(121, 288)} = 5664.850$	< 0.001
Trans-nonachlor	$F_{(121, 288)} = 9019.670$	< 0.001
o,p′-DDE	$F_{(121, 288)} = 3374.640$	< 0.001
p,p′-DDE	$F_{(121, 288)} = 5762.790$	< 0.001
o,p′-DDD	$F_{(121, 288)} = 3031.840$	< 0.001
p,p′-DDD	$F_{(121, 288)} = 2987.820$	< 0.001
o,p′-DDT	$F_{(121, 288)} = 245.820$	< 0.001
p,p′-DDT	$F_{(121, 288)} = 6804.750$	< 0.001
Mirex	$F_{(121, 288)} = 1532.970$	< 0.001

Together, the compound-specific line plots in Figure 4.15 and the interaction terms in Table 4.17 indicate strong and statistically significant spatio-temporal variation in OCPs concentrations in *N. undata*. These results confirm that pesticide accumulation dynamics were shaped by both spatial and seasonal influences, with temporal changes in concentrations varying markedly across different sampling sites and compounds.

4.3.3.3 Concentration of OCPs in collector-gatherers, Atyidae

The spatial distribution of OCP concentrations in *Atyidae* across the twelve sampling stations is presented in Figure 4.16. Clear spatial heterogeneity was evident across most compounds, with downstream and estuarine stations (Ramisi, Umba, Mkurumdzi, and Mwena) generally exhibiting higher median concentrations and broader interquartile ranges compared to upstream locations such as Mapu and Ramisi Mwachande.

Figure 4.16:
Boxplots showing spatial variation in OCPs concentrations in Atyidae

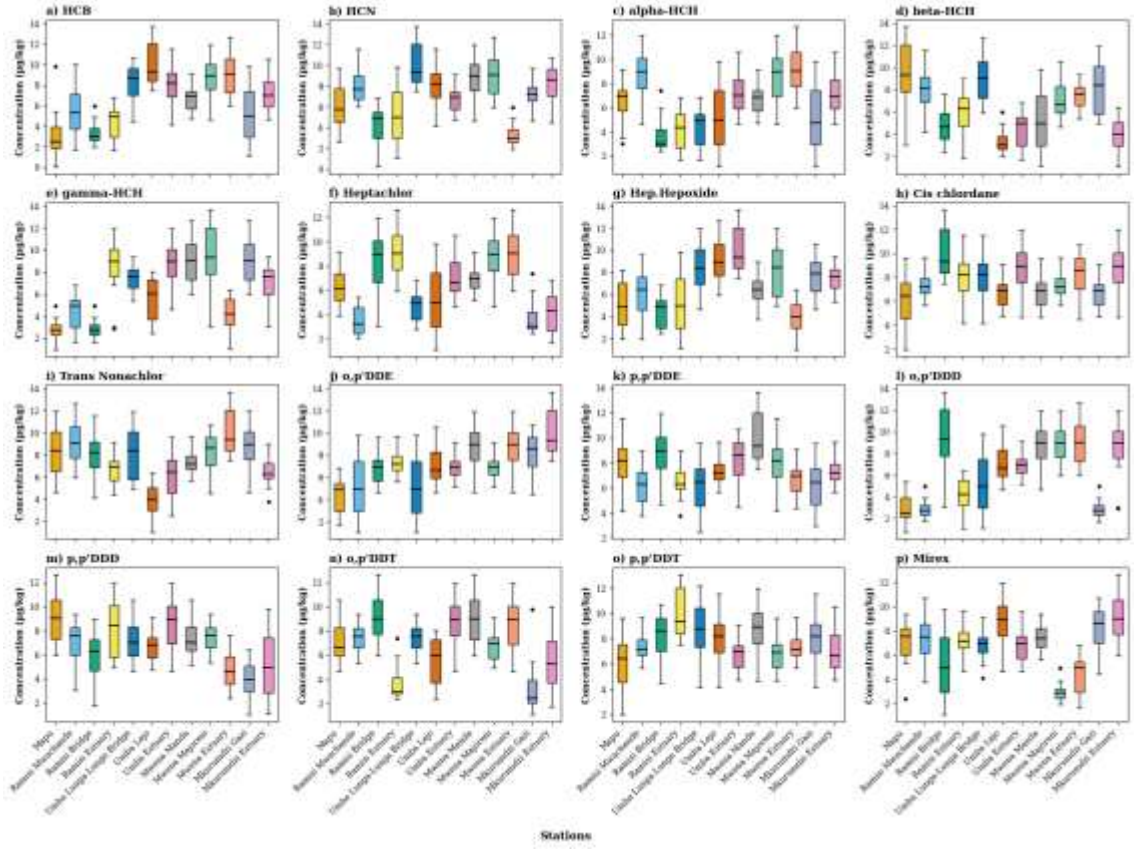

One-way ANOVA (Table 16) revealed statistically significant spatial variation for all sixteen OCP compounds (all $p < 0.001$; df = 11, 132). The highest spatial variation was observed in o,p′-DDD, which recorded $F_{(11, 432)} = 64.020$, $p < 0.001$, followed by γ-HCH ($F_{(11, 432)} = 59.740$, $p < 0.001$) and HCB ($F_{(11, 432)} = 46.680$, $p < 0.001$). Heptachlor and HCN also showed strong station effects, with $F_{(11, 432)} = 46.150$ and $F_{(11, 432)} =$

41.480, respectively (both $p < 0.001$). Similarly, o,p′-DDT displayed significant spatial variation ($F_{(11, 432)} = 39.150$, $p < 0.001$). Additional compounds demonstrating marked spatial heterogeneity included β-HCH ($F_{(11, 432)} = 37.000$, $p < 0.001$), Mirex ($F_{(11, 432)} = 35.710$, $p < 0.001$), heptachlor epoxide ($F_{(11, 432)} = 35.560$, $p < 0.001$), and α-HCH ($F_{(11, 432)} = 31.880$, $p < 0.001$). Moderate but statistically significant variation was also observed for o,p′-DDE ($F_{(11, 432)} = 26.940$, $p < 0.001$), trans-nonachlor ($F_{(11, 432)} = 26.730$, $p < 0.001$), and p,p′-DDD ($F_{(11, 432)} = 24.810$, $p < 0.001$). Although comparatively lower, spatial differences remained significant for p,p′-DDE ($F_{(11, 432)} = 17.040$, $p < 0.001$), cis-chlordane ($F_{(11, 432)} = 14.770$, $p < 0.001$), and p,p′-DDT ($F_{(11, 432)} = 13.090$, $p < 0.001$).

Table 4.16:
One-Way ANOVA results for OCPs in Atyidae across sampling stations.

Pesticide (µg/kg)	*F* value	*p* value
o,p'DDD	$F_{(11,432)} = 64.022$	< 0.001
gamma-HCH	$F_{(11,432)} = 59.743$	< 0.001
HCB	$F_{(11,432)} = 46.684$	< 0.001
Heptachlor	$F_{(11,432)} = 46.153$	< 0.001
HCN	$F_{(11,432)} = 41.484$	< 0.001
o,p'DDT	$F_{(11,432)} = 39.155$	< 0.001
beta-HCH	$F_{(11,432)} = 37.003$	< 0.001
Mirex	$F_{(11,432)} = 35.713$	< 0.001
Hep.Hepoxide	$F_{(11,432)} = 35.563$	< 0.001
alpha-HCH	$F_{(11,432)} = 31.883$	< 0.001
o,p'DDE	$F_{(11,432)} = 26.943$	< 0.001
Trans Nonachlor	$F_{(11,432)} = 26.733$	< 0.001
p,p'DDD	$F_{(11,432)} = 24.813$	< 0.001
p,p'DDE	$F_{(11,432)} = 17.044$	< 0.001
Cis chlordane	$F_{(11,432)} = 14.772$	< 0.001
p,p'DDT	$F_{(11,432)} = 13.096$	< 0.001

Monthly variation in OCP concentrations in *Atyidae* across all stations is presented in Figure 4.17.

Figure 4.17:
Temporal distribution of OCPs in Atyidae during the study period

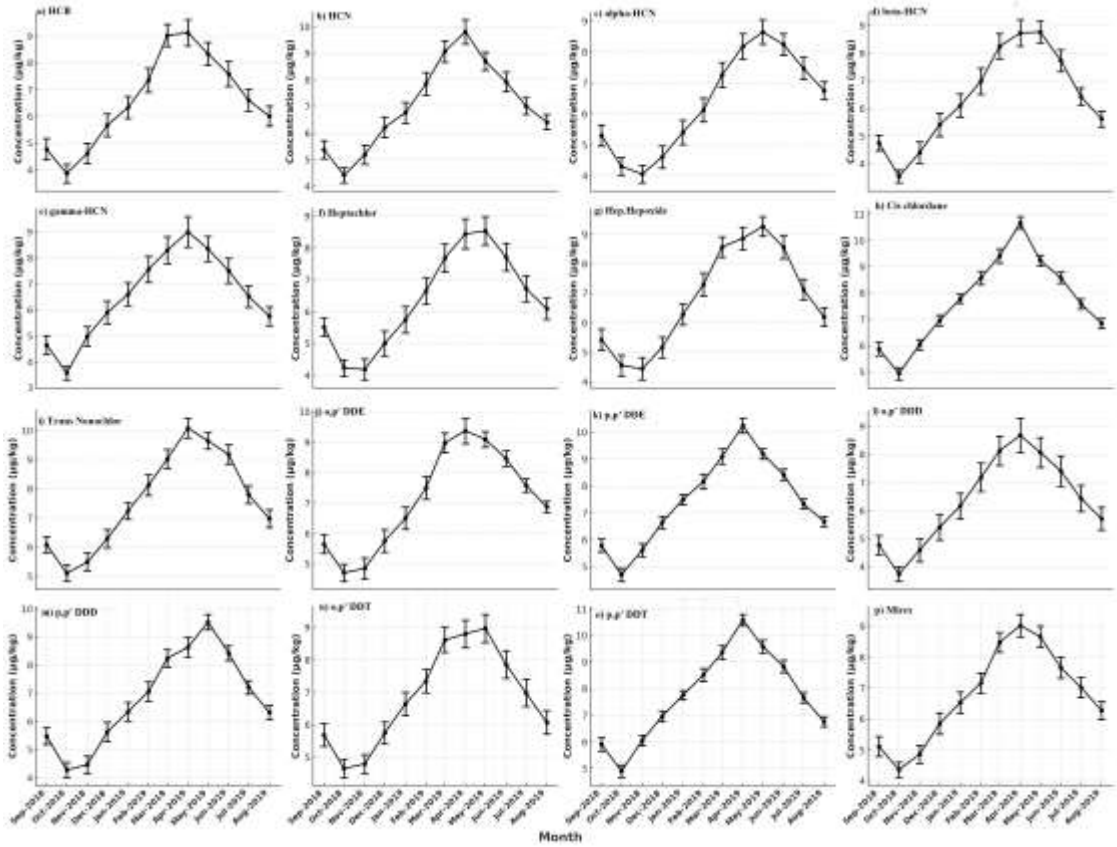

One-way ANOVA (Table 17) indicated statistically significant temporal variation for all sixteen compounds (all $p < 0.001$; df = 11, 132). The strongest temporal variation was observed for p,p′-DDT, which yielded $F_{(11, 432)} = 59.430$, $p < 0.001$, followed by cis-chlordane ($F_{(11, 432)} = 57.770$, $p < 0.001$) and p,p′-DDE ($F_{(11, 432)} = 50.210$, $p < 0.001$). Substantial monthly variation was also recorded for p,p′-DDD ($F_{(11, 432)} = 31.420$, $p < 0.001$), trans-nonachlor ($F_{(11, 432)} = 28.620$, $p < 0.001$), and o,p′-DDE ($F_{(11, 432)} = 27.340$, $p < 0.001$). Heptachlor epoxide ($F_{(11, 432)} = 22.910$, $p < 0.001$), Mirex ($F_{(11, 432)} = 22.630$, $p < 0.001$), and α-HCH ($F_{(11, 432)} = 20.680$, $p < 0.001$) also demonstrated

marked month-to-month variability. Moderate but significant temporal effects were observed for HCN ($F_{(11, 432)} = 20.260$, $p < 0.001$), β-HCH ($F_{(11, 432)} = 20.230$, $p < 0.001$), and HCB ($F_{(11, 432)} = 17.110$, $p < 0.001$). Additional significant variation was recorded for o,p′-DDT ($F_{(11, 432)} = 16.530$, $p < 0.001$), heptachlor ($F_{(11, 432)} = 14.980$, $p < 0.001$), γ-HCH ($F_{(11, 432)} = 13.950$, $p < 0.001$), and o,p′-DDD ($F_{(11, 432)} = 11.230$, $p < 0.001$).

Table 4.17:
One-Way ANOVA results for monthly variation in OCPs in Atyidae

Pesticide (μg/kg)	*F* value	*p* value
p,p'DDT	$F_{(11,432)} = 59.433$	< 0.001
Cis chlordane	$F_{(11,432)} = 57.772$	< 0.001
p,p'DDE	$F_{(11,432)} = 50.213$	< 0.001
p,p'DDD	$F_{(11,432)} = 31.424$	< 0.001
Trans Nonachlor	$F_{(11,432)} = 28.625$	< 0.001
o,p'DDE	$F_{(11,432)} = 27.343$	< 0.001
Hep.Hepoxide	$F_{(11,432)} = 22.914$	< 0.001
Mirex	$F_{(11,432)} = 22.634$	< 0.001
alpha-HCH	$F_{(11,432)} = 20.683$	< 0.001
HCN	$F_{(11,432)} = 20.262$	< 0.001
beta-HCH	$F_{(11,432)} = 20.232$	< 0.001
HCB	$F_{(11,432)} = 17.113$	< 0.001
o,p'DDT	$F_{(11,432)} = 16.534$	< 0.001
Heptachlor	$F_{(11,432)} = 14.984$	< 0.001
gamma-HCH	$F_{(11,432)} = 13.954$	< 0.001
o,p'DDD	$F_{(11,432)} = 11.234$	< 0.001

The spatio-temporal variation in OCPs concentrations in Atyidae across the 12 spatial stations were also presented (Figure 4.18). Each subplot corresponds to a single compound and illustrates mean monthly concentrations over the sampling year, with error bars representing standard errors. Each station is represented by a distinct line,

making it possible to trace both intra- and inter-station differences over time. The plotted data reveal distinct and compound-specific spatio-temporal patterns. For most compounds, monthly trends vary not only in timing but also in amplitude between stations. For instance, gamma-HCH, alpha-HCH, and heptachlor display sharp concentration peaks during March to May at downstream stations such as Umba, Mkurumdzi, and Mwena, while upstream sites like Mapu and Ramisi show flatter, delayed, or less pronounced patterns during the same months. Other compounds, including trans-nonachlor, o,p′-DDD, and Mirex, show asynchronous concentration trends between stations, with peaks occurring at different times across the spatial gradient. Temporal shifts are often accompanied by divergence in line trajectories among stations within the same compound, as observed in p,p′-DDD and o,p′-DDE, suggesting varying rates of bioaccumulation or degradation across time and location. In several subplots such as those for p,p′-DDE, HCB, and heptachlor epoxide station lines intersect or rise independently, highlighting site-specific fluctuations in pesticide exposure.

Figure 4.18:
Spatio-temporal variation of OCPs concentrations in Atyidae during the study period

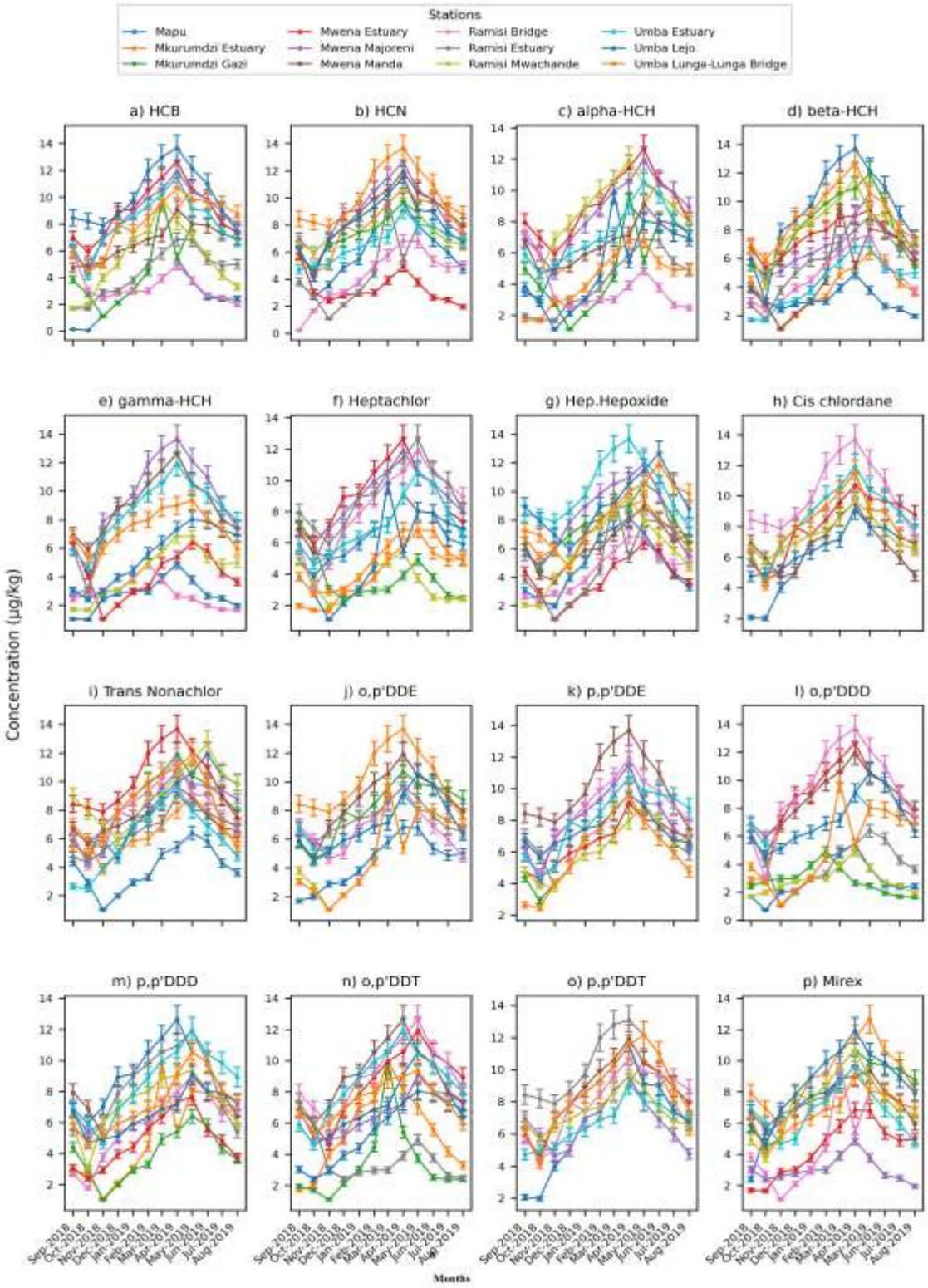

The interaction between station and month was assessed using two-way ANOVA (Table 4.18). Significant station x month interaction effects were detected for all sixteen compounds (all $p < 0.001$; df = 121, 288). The strongest interaction effect was observed for γ-HCH ($F_{(121, 288)} = 13033.099$, $p < 0.001$), followed by heptachlor ($F_{(121, 288)} = 105479.937$, $p < 0.001$) and α-HCH ($F_{(121, 288)} = 1043540.250$, $p < 0.001$). Substantial interaction effects were also recorded for o,p′-DDD ($F_{(121, 288)} = 303461.840$, $p < 0.001$) and p,p′-DDD ($F_{(121, 288)} = 298117.820$, $p < 0.001$). High-magnitude interaction terms were further observed for HCB ($F_{(121, 288)} = 130338.090$, $p < 0.001$), heptachlor epoxide ($F_{(121, 288)} = 114715.370$, $p < 0.001$), trans-nonachlor ($F_{(121, 288)} = 90192.670$, $p < 0.001$), HCN ($F_{(121, 288)} = 80969.970$, $p < 0.001$), p,p′-DDT ($F_{(121, 288)} = 68044.750$, $p < 0.001$), cis-chlordane ($F(121, 288) = 56624.850$, $p < 0.001$), and p,p′-DDE ($F_{(121, 288)} = 57620.790$, $p < 0.001$). Moderate but statistically significant interaction effects were detected for o,p′-DDE ($F_{(121, 288)} = 33764.640$, $p < 0.001$) and Mirex ($F_{(121, 288)} = 15342.970$, $p < 0.001$). The lowest interaction F-values were recorded for o,p′-DDT ($F_{(121, 288)} = 2459.820$, $p < 0.001$) and β-HCH ($F_{(121, 288)} = 353.830$, $p < 0.001$), though both remained statistically significant.

Table 4.18:
Two-way ANOVA interaction effects for OCPs concentrations in Atyidae

OCPs (µg/kg)	*F* value	*p*-value
HCB	$F_{(121,288)} = 13033.099$	< 0.001
HCN	$F_{(121,288)} = 80969.978$	< 0.001
alpha-HCH	$F_{(121,288)} = 104354.258$	< 0.001
beta-HCH	$F_{(121,288)} = 353.837$	< 0.001
gamma-HCH	$F_{(121,288)} = 132531.107$	< 0.001
Heptachlor	$F_{(121,288)} = 105479.937$	< 0.001
Hep.Hepoxide	$F_{(121,288)} = 114715.377$	< 0.001
Cis chlordane	$F_{(121,288)} = 56624.856$	< 0.001
Trans Nonachlor	$F_{(121,288)} = 90192.675$	< 0.001
o,p'DDE	$F_{(121,288)} = 33764.645$	< 0.001
p,p'DDE	$F_{(121,288)} = 57620.793$	< 0.001
o,p'DDD	$F_{(121,288)} = 303461.842$	< 0.001
p,p'DDD	$F_{(121,288)} = 298117.823$	< 0.001
o,p'DDT	$F_{(121,288)} = 2459.822$	< 0.001
p,p'DDT	$F_{(121,288)} = 68044.753$	< 0.001
Mirex	$F_{(121,288)} = 15342.972$	< 0.001

4.3.3.4 Concentration of OCPs in filterers, *Saccostrea cucullata*

The spatial distribution of OCPs concentrations in the filter-feeding oyster *Saccostrea cucullata* across the twelve sampling stations is presented in Figure 4.19. The boxplots illustrate median concentrations, interquartile ranges (IQR), and outliers for each compound, allowing comparison of spatial heterogeneity across the estuarine gradient.

Clear spatial structuring was evident across most compounds. Downstream and estuarine stations, particularly Umba, Mwena Majoreni, and Mkurumdzi, consistently exhibited elevated median concentrations and wider interquartile ranges for several OCPs, including o,p′-DDD, γ-HCH, HCN, and o,p′-DDT. These stations also displayed

frequent upper-range outliers, indicating episodic concentration spikes. In contrast, upstream stations such as Mapu, Mkurumdzi Gazi, and Ramisi Mwachande were characterized by lower medians and relatively compressed interquartile ranges for compounds such as β-HCH, p,p′-DDT, cis-chlordane, and HCB. Compound-specific dispersion patterns were also evident. For example, o,p′-DDT and Mirex displayed elevated concentrations and broader spreads at Umba and Ramisi stations. Similarly, γ-HCH and o,p′-DDD showed clustering of high-value outliers at Mwena and Mkurumdzi, whereas upstream locations generally exhibited reduced variability.

Figure 4.19:
Boxplots showing spatial variation in OCPs concentrations in S. cucullata

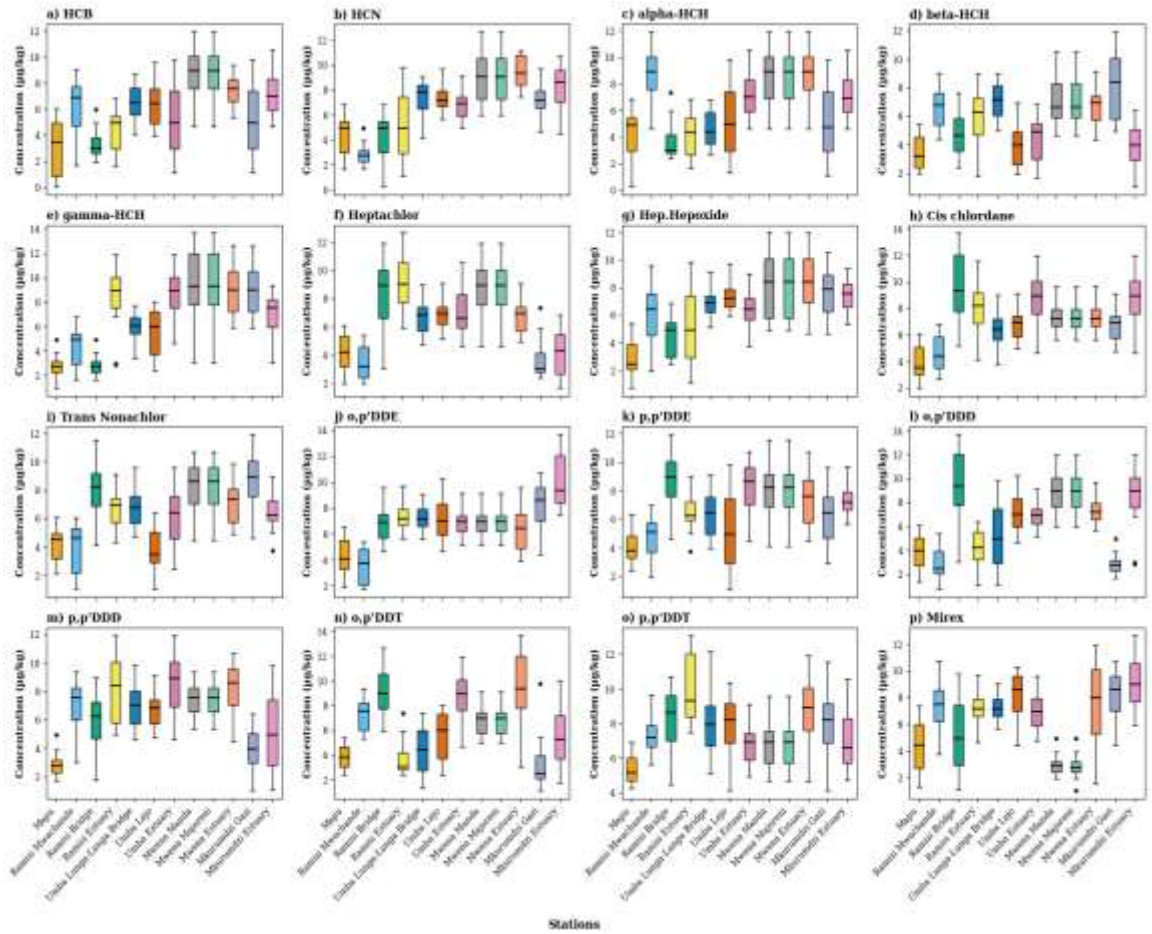

One-way ANOVA confirmed statistically significant spatial variation for all sixteen compounds (df = 11, 132; all $p < 0.001$) (Table 4.19). The strongest spatial variation was observed for o,p′-DDD ($F_{(11, 432)} = 57.526$, $p < 0.001$), followed by HCN ($F_{(11, 432)} = 55.824$, $p < 0.001$), γ-HCH ($F_{(11, 432)} = 53.195$, $p < 0.001$), and heptachlor ($F_{(11, 432)} = 52.463$, $p < 0.001$). Substantial spatial heterogeneity was also recorded for o,p′-DDE ($F_{(11, 432)} = 46.385$), o,p′-DDT ($F_{(11, 432)} = 44.074$), Mirex ($F_{(11, 432)} = 41.827$), cis-chlordane ($F_{(11, 432)} = 36.896$), α-HCH ($F_{(11, 432)} = 35.195$), and p,p′-DDD ($F_{(11, 432)} = 34.184$), all at $p < 0.001$. Even compounds with comparatively lower F-values, such as p,p′-DDE ($F_{(11, 432)} = 23.402$) and p,p′-DDT ($F_{(11, 432)} = 17.333$), remained highly significant. *Post hoc* Tukey HSD comparisons confirmed that downstream stations (e.g., Umba, Mkurumdzi, Mwena) differed significantly from upstream stations (e.g., Mapu, Ramisi) for most compounds, particularly o,p′-DDD, γ-HCH, HCN, and o,p′-DDT. These findings statistically corroborate the spatial heterogeneity observed visually.

Table 4.19:
One-Way ANOVA results for OCPs in S. cucullata across sampling stations

OCPs (µg/kg)	*F* value	p-Value
o,p'DDD	$F_{(11,432)} = 57.526$	< 0.001
HCN	$F_{(11,432)} = 55.824$	< 0.001
gamma-HCH	$F_{(11,432)} = 53.195$	< 0.001
Heptachlor	$F_{(11,432)} = 52.463$	< 0.001
o,p'DDE	$F_{(11,432)} = 46.385$	< 0.001
o,p'DDT	$F_{(11,432)} = 44.074$	< 0.001
Mirex	$F_{(11,432)} = 41.827$	< 0.001
Cis chlordane	$F_{(11,432)} = 36.896$	< 0.001
alpha-HCH	$F_{(11,432)} = 35.195$	< 0.001
p,p'DDD	$F_{(11,432)} = 34.184$	< 0.001
Trans Nonachlor	$F_{(11,432)} = 33.683$	< 0.001
beta-HCH	$F_{(11,432)} = 32.263$	< 0.001
HCB	$F_{(11,432)} = 31.284$	< 0.001
Hep.Hepoxide	$F_{(11,432)} = 29.682$	< 0.001
p,p'DDE	$F_{(11,432)} = 23.402$	< 0.001
p,p'DDT	$F_{(11,432)} = 17.333$	< 0.001

Altogether, the boxplot distributions in Figure 4.19, coupled with the ANOVA results in Table 4.21 and the supporting post hoc comparisons (appendix II, Table A13), indicate that OCP concentrations in *S. cucullata* exhibited strong spatial structuring. Distinct patterns of compound enrichment and station-specific concentration differences were evident across nearly all of the evaluated pesticides.

The monthly distribution of OCP concentrations in *S. cucullata* is shown in Figure 4.20. Each subplot presents mean monthly concentrations with standard error bars, allowing visualization of seasonal fluctuations across compounds. Temporal patterns indicate consistent seasonal shifts in OCPs levels. Concentrations for several

compounds including p,p′-DDT, p,p′-DDE, heptachlor epoxide, and cis-chlordane peaked between March and May, coinciding with the long rainy season. These peaks were often accompanied by broader standard error bars, indicating increased variability among stations during wetter months. A secondary increase in concentrations was observed during October and November (short rains) for compounds such as Mirex, β-HCH, and o,p′-DDE. Conversely, reduced concentrations were typically recorded between July and September, corresponding to the dry season. Compounds such as HCB, trans-nonachlor, and γ-HCH showed visible suppression during these months. Although the magnitude of fluctuation varied between compounds, the general temporal structure was consistent across the sampling year.

Figure 4.20:
Temporal distribution of OCPs in S. cucullata during the study period

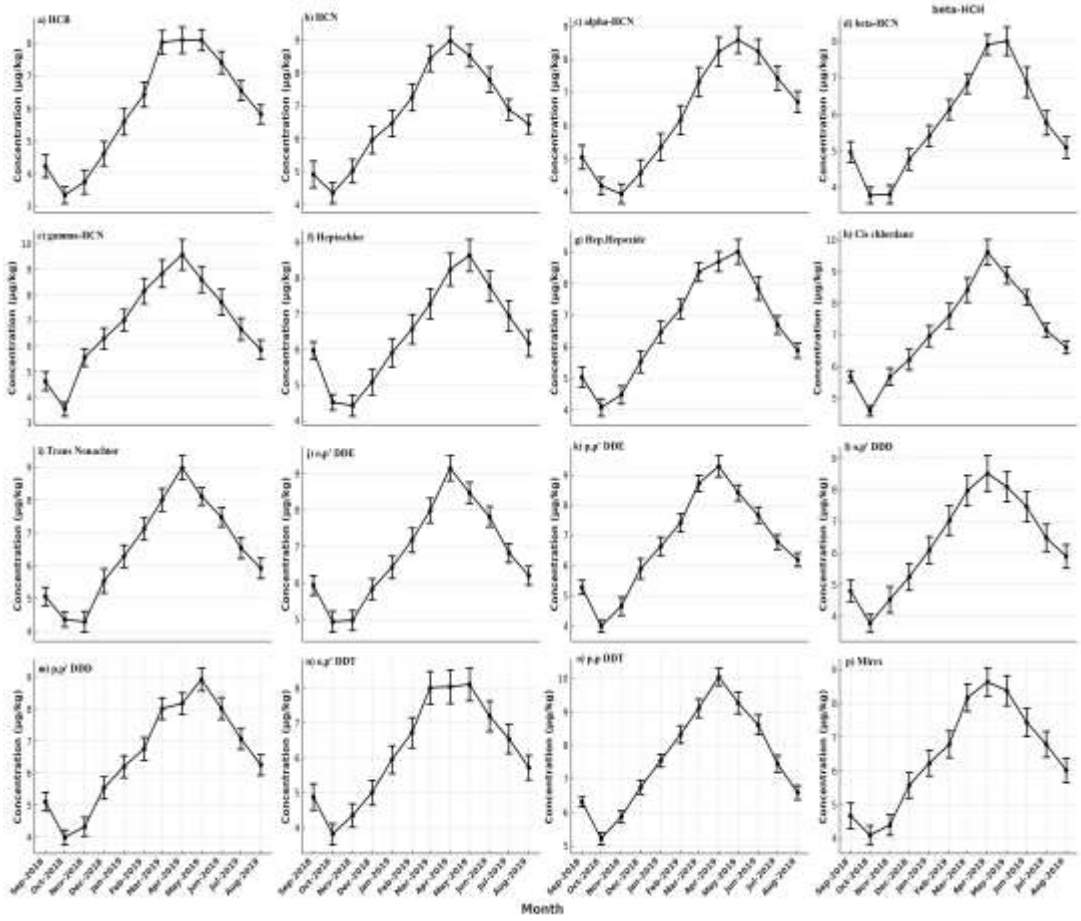

One-way ANOVA confirmed statistically significant monthly variation for all sixteen compounds (df = 11, 132; all $p < 0.001$) (Table 4.20). The highest temporal variation was recorded for p,p′-DDT ($F_{(11, 432)} = 39.852$, $p < 0.001$), followed by p,p′-DDE ($F_{(11, 432)} = 34.633$, $p < 0.001$) and heptachlor epoxide ($F_{(11, 432)} = 27.491$, $p < 0.001$). Compounds such as cis-chlordane ($F_{(11, 432)} = 25.242$), HCB ($F_{(11, 432)} = 24.422$), and p,p′-DDD ($F_{(11, 432)} = 23.764$) also showed strong temporal variability. Even compounds with lower F-values, including o,p′-DDT ($F_{(11, 432)} = 13.325$), heptachlor ($F_{(11, 432)} = 13.185$), and o,p′-DDD ($F_{(11, 432)} = 12.403$), remained statistically significant at $p < 0.001$.

Table 4.20:
One-Way ANOVA results for OCP in S. cucullata across months

OCPs (µg/kg)	*F* value	*p* value
p,p'DDT	$F_{(11,432)} = 39.852$	< 0.001
p,p'DDE	$F_{(11,432)} = 34.633$	< 0.001
Hep.Hepoxide	$F_{(11,432)} = 27.491$	< 0.001
Cis chlordane	$F_{(11,432)} = 25.242$	< 0.001
HCB	$F_{(11,432)} = 24.422$	< 0.001
p,p'DDD	$F_{(11,432)} = 23.764$	< 0.001
Trans Nonachlor	$F_{(11,432)} = 22.763$	< 0.001
beta-HCH	$F_{(11,432)} = 21.575$	< 0.001
o,p'DDE	$F_{(11,432)} = 20.586$	< 0.001
alpha-HCH	$F_{(11,432)} = 19.527$	< 0.001
HCN	$F_{(11,432)} = 16.568$	< 0.001
Mirex	$F_{(11,432)} = 16.557$	< 0.001
gamma-HCH	$F_{(11,432)} = 16.277$	< 0.001
o,p'DDT	$F_{(11,432)} = 13.325$	< 0.001
Heptachlor	$F_{(11,432)} = 13.185$	< 0.001
o,p'DDD	$F_{(11,432)} = 12.403$	< 0.001

Despite differences in the magnitude of their F-values, all compounds revealed meaningful seasonal shifts, confirming that OCPs bioavailability in *S. cucullata* is temporally dynamic and compound-specific.

The spatio-temporal distribution of OCPs concentrations in *S. cucullata* over a 12-month period across the 12 spatially distinct sampling stations are as presented in Figure 4.21. Each subplot corresponds to a specific compound and displays the mean monthly concentration per station, with standard error bars representing variability. Individual stations are represented by distinct colored lines, which enable compound-specific comparisons of concentration dynamics across time and space. Across most compounds, the figure reveals complex and non-uniform temporal patterns that vary markedly between stations.

For compounds such as gamma-HCH, beta-HCH, and heptachlor, sharp monthly peaks in concentration are observed in downstream stations like Umba and Mwena during March to May and October to November. These peaks are not mirrored at upstream stations such as Mapu and Ramisi, where concentrations remain relatively stable or low. Several compounds including o,p′-DDD, p,p′-DDD, and trans-nonachlor also demonstrate staggered monthly trends, where different stations reach peak concentrations in different months, highlighting asynchronous accumulation patterns across the catchment. In many subplots, station lines cross or diverge sharply, reflecting interactive changes in contamination over time. This is especially pronounced for o,p′-DDE, alpha-HCH, and p,p′-DDE, where trends fluctuate in direction and amplitude between sites within the same temporal window. For example, while Mkurumdzi may

show increasing concentrations of p,p′-DDE in March–April, another station like Ramisi Bridge and Mapu may show a delayed or absent peak.

Figure 4.21:
Spatio-temporal variation of OCPs in S. cucullata during the study period

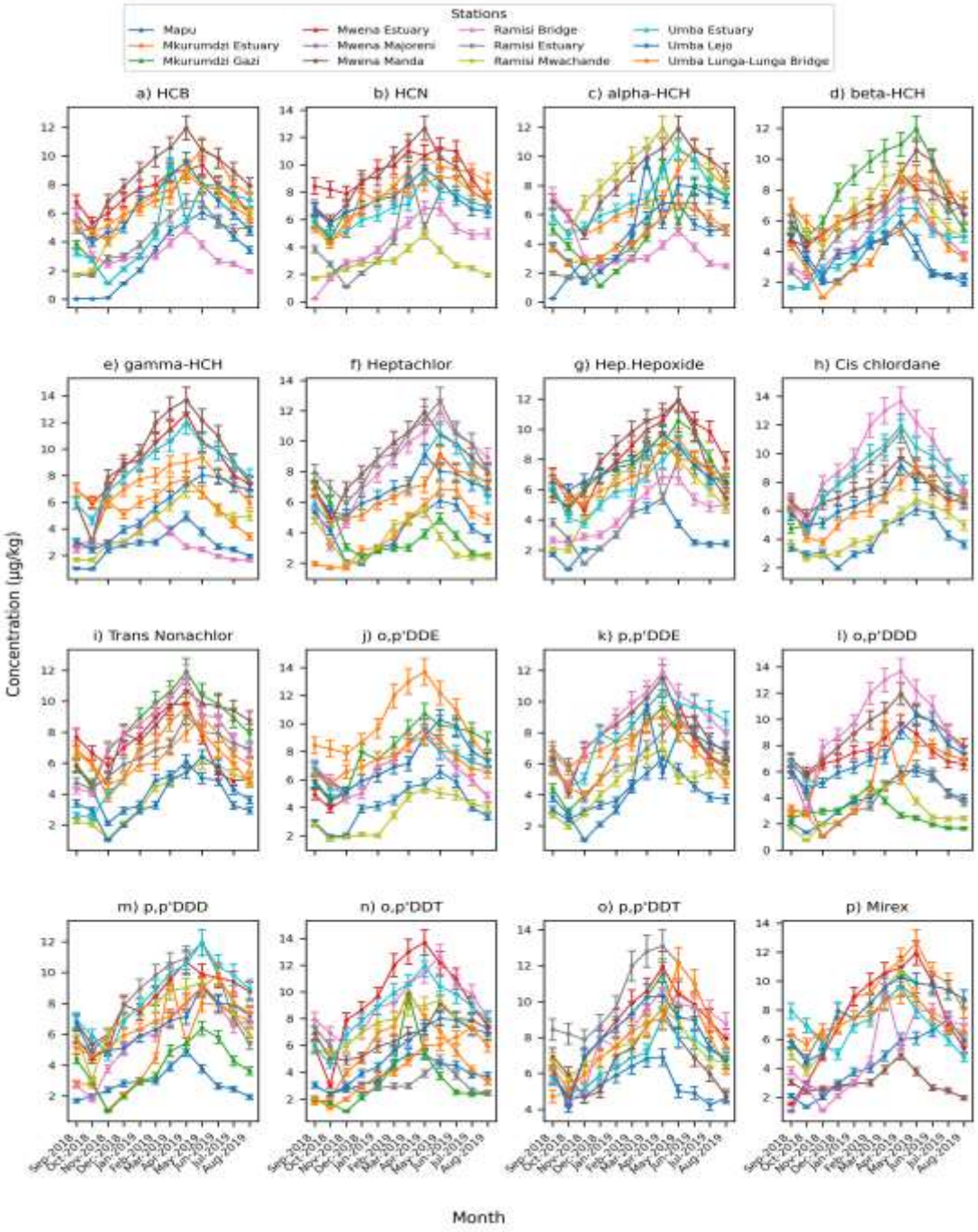

Two-way ANOVA confirmed statistically significant station × month interaction effects for all sixteen compounds (df = 121, 288; all $p < 0.001$) (Table 4.21). The strongest interaction effects were observed for γ-HCH ($F_{(121, 288)} = 1246204.620$, $p < 0.001$), β-HCH ($F_{(121, 288)} = 1022285.780$, $p < 0.001$), and o,p′-DDD ($F_{(121, 288)} = 778924.240$, $p < 0.001$). Substantial interaction effects were also recorded for heptachlor ($F_{(121, 288)} = 758035.850$), α-HCH ($F_{(121, 288)} = 716622.000$), p,p′-DDD ($F_{(121, 288)} = 469101.750$), and o,p′-DDE (F(121, 288) = 278383.240), all highly significant. Even compounds with comparatively lower interaction magnitudes such as HCB ($F_{(121, 288)} = 1557.440$), heptachlor epoxide ($F_{(121, 288)} = 1631.620$), and o,p′-DDT ($F_{(121, 288)} = 1487.110$) remained statistically significant at $p < 0.001$.

Table 4.21:
Two-way ANOVA interaction effects for OCP concentrations in S. cucullata across sampling stations and months

OCPs (µg/kg)	*F* value	*p*-value
HCB	$F_{(121,288)} = 1557.44$	< 0.001
HCN	$F_{(121,288)} = 15467.04$	< 0.001
alpha-HCH	$F_{(121,288)} = 716622.00$	< 0.001
beta-HCH	$F_{(121,288)} = 1022285.78$	< 0.001
gamma-HCH	$F_{(121,288)} = 1246204.62$	< 0.001
Heptachlor	$F_{(121,288)} = 758035.85$	< 0.001
Hep.Hepoxide	$F_{(121,288)} = 1631.62$	< 0.001
Cis chlordane	$F_{(121,288)} = 31971.66$	< 0.001
Trans Nonachlor	$F_{(121,288)} = 11463.51$	< 0.001
o,p'DDE	$F_{(121,288)} = 278383.24$	< 0.001
p,p'DDE	$F_{(121,288)} = 44538.91$	< 0.001
o,p'DDD	$F_{(121,288)} = 78924.24$	< 0.001
p,p'DDD	$F_{(121,288)} = 46901.75$	< 0.001
o,p'DDT	$F_{(121,288)} = 1487.11$	< 0.001
p,p'DDT	$F_{(121,288)} = 40904.47$	< 0.001
Mirex	$F_{(121,288)} = 7626.43$	< 0.001

Collectively, the line plots in Figure 4.21 and the two-way ANOVA results in Table 4.21 reveal that the interaction between space and time had a statistically significant and biologically meaningful effect on pesticide concentrations in *S. cucullata*. The data confirm that bioaccumulation patterns are governed not only by seasonal cycles but also by location-specific environmental processes that influence how and when contamination occurs.

4.3.3.5 Concentration of OCPs in predators, *Rhagovelia* species

The spatial distribution of OCPs concentrations in *Rhagovelia* species across the twelve sampling stations is presented in Figure 4.22. The boxplots illustrate median concentrations, interquartile ranges, and outliers for each of the sixteen compounds, thereby enabling comparison of station-level variability in pesticide bioaccumulation.

Clear spatial heterogeneity was evident across the river–estuary gradient. Downstream and estuarine stations, particularly Ramisi, Umba, Mwena, and Mkurumdzi, consistently displayed elevated median concentrations and broader interquartile ranges for multiple compounds. Compounds such as o,p′-DDD, heptachlor, γ-HCH, and Mirex showed pronounced upper-range dispersion at these locations, with frequent high-value outliers indicating substantial variability in concentration levels. In contrast, upstream stations including Mapu, Ramisi Mwachande, and Mwena Manda generally exhibited narrower interquartile ranges and comparatively lower medians for several compounds, including HCB, β-HCH, and cis-chlordane. Although some compounds such as o,p′-DDE and p,p′-DDE showed variability across all stations, elevated values were more

frequently concentrated in downstream reaches. The compound o,p′-DDT also demonstrated higher dispersion at Mkurumdzi and Umba relative to upstream locations.

Figure 4.22:
Boxplots showing spatial variation in OCPs in Rhagovelia species

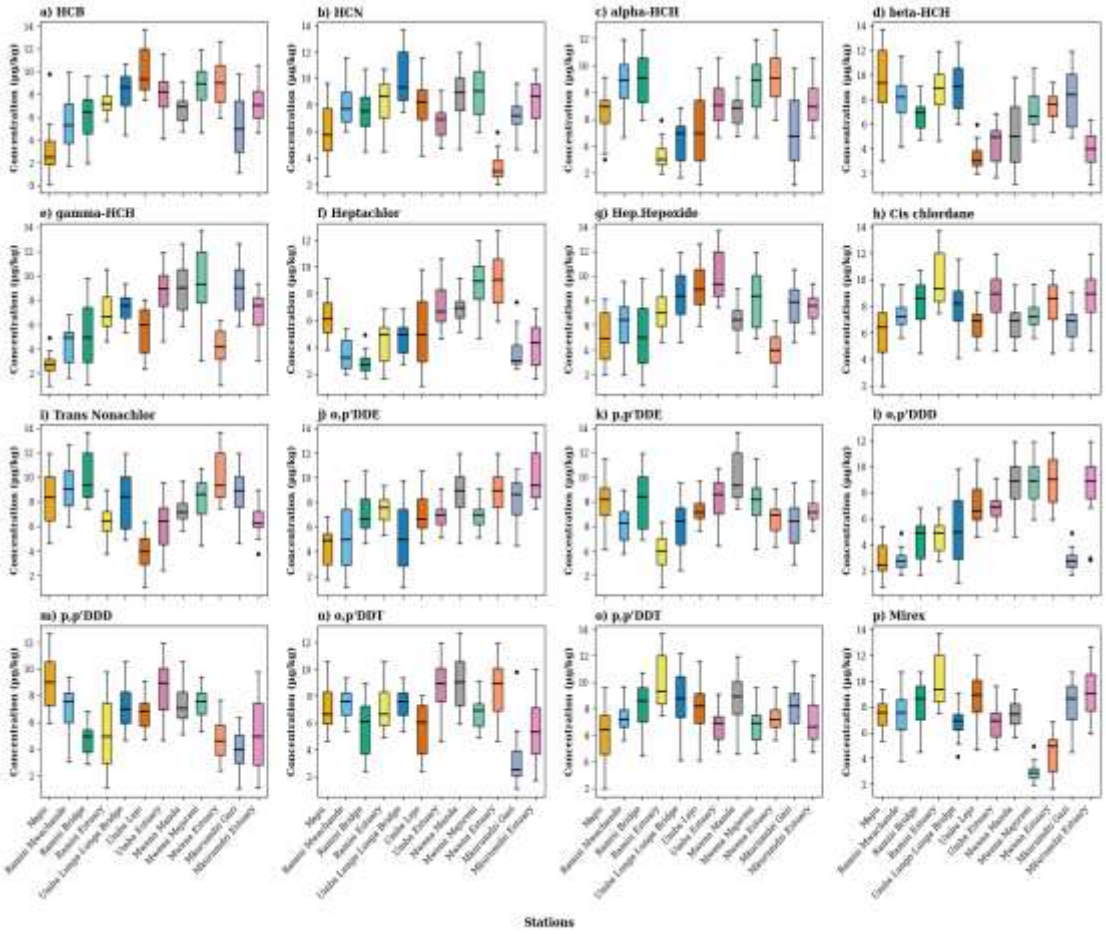

One-way ANOVA confirmed statistically significant spatial differences for all sixteen compounds (Table 4.22). All tests were significant at $p < 0.001$ with degrees of freedom F(11, 132). The strongest spatial variation was observed for o,p′-DDD ($F_{(11, 432)} = 66.200$, $p < 0.001$), followed by heptachlor ($F_{(11, 432)} = 51.700$, $p < 0.001$), Mirex ($F_{(11, 432)} = 47.110$, $p < 0.001$), and γ-HCH ($F_{(11, 432)} = 45.130$, $p < 0.001$). Substantial spatial variation was also detected for β-HCH ($F_{(11, 432)} = 38.570$, $p < 0.001$), α-HCH ($F_{(11, 432)} = 34.810$, $p < 0.001$), HCN ($F_{(11, 432)} = 32.400$, $p < 0.001$), trans-nonachlor ($F_{(11, 432)} = 31.670$, $p < 0.001$), HCB ($F_{(11, 432)} = 30.940$, $p < 0.001$), and heptachlor

epoxide ($F_{(11, 432)} = 30.170$, $p < 0.001$). Although cis-chlordane ($F_{(11, 432)} = 14.680$, $p < 0.001$) and p,p′-DDT ($F_{(11, 432)} = 13.250$, $p < 0.001$) recorded comparatively lower F-values, both remained highly significant. These results confirm marked spatial heterogeneity in OCP accumulation among *Rhagovelia* populations.

Table 4.22:
One-Way ANOVA results for OCPs concentrations in Rhagovelia species across sampling stations

OCPs (µg/kg)	F-Value	*p*-Value
o,p'DDD	$F_{(11,432)} = 66.20$	< 0.001
Heptachlor	$F_{(11,432)} = 51.70$	< 0.001
Mirex	$F_{(11,432)} = 47.11$	< 0.001
gamma-HCH	$F_{(11,432)} = 45.13$	< 0.001
beta-HCH	$F_{(11,432)} = 38.57$	< 0.001
alpha-HCH	$F_{(11,432)} = 34.81$	< 0.001
HCN	$F_{(11,432)} = 32.40$	< 0.001
Trans Nonachlor	$F_{(11,432)} = 31.67$	< 0.001
HCB	$F_{(11,432)} = 30.94$	< 0.001
Hep.Hepoxide	$F_{(11,432)} = 30.17$	< 0.001
p,p'DDD	$F_{(11,432)} = 27.75$	< 0.001
p,p'DDE	$F_{(11,432)} = 26.18$	< 0.001
o,p'DDE	$F_{(11,432)} = 26.00$	< 0.001
o,p'DDT	$F_{(11,432)} = 25.92$	< 0.001
Cis chlordane	$F_{(11,432)} = 14.68$	< 0.001
p,p'DDT	$F_{(11,432)} = 13.25$	< 0.001

Monthly variation in OCP concentrations in *Rhagovelia* species is illustrated in Figure 4.23, where each subplot presents mean monthly concentrations with associated standard error bars. Several compounds exhibited elevated mean concentrations during the March–May period. In particular, p,p′-DDT, cis-chlordane, and p,p′-DDE showed clear increases during this interval, accompanied by broader standard error margins,

indicating increased variability among stations. Additional temporal increases were observed during October–November for compounds such as o,p′-DDE, HCN, and o,p′-DDT. Other compounds, including β-HCH, Mirex, and trans-nonachlor, displayed moderate monthly fluctuations. Compounds such as γ-HCH and heptachlor showed comparatively narrower seasonal amplitude but still demonstrated identifiable temporal trends.

Figure 4.23:
Temporal distribution of OCPs concentrations in Rhagovelia species during the study period

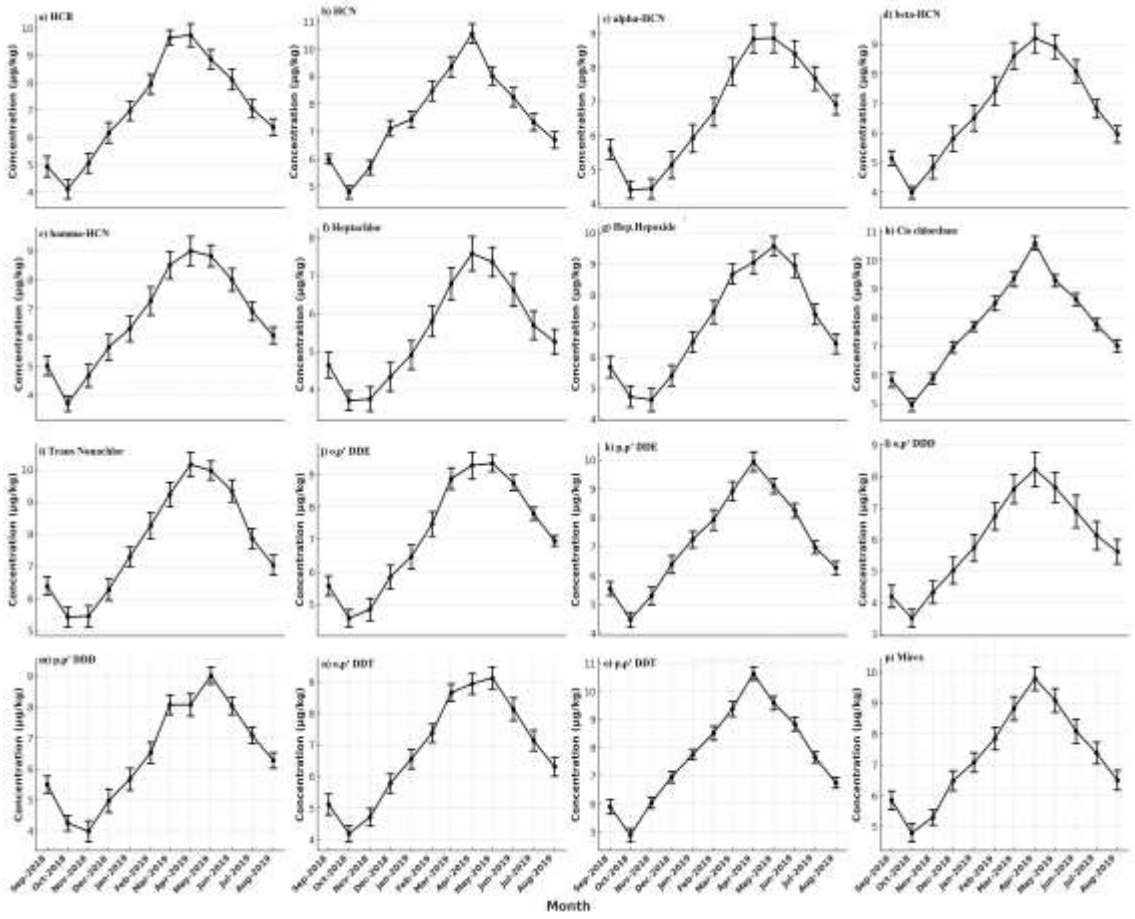

One-way ANOVA results confirmed statistically significant monthly variation for all sixteen compounds (Table 4.23). All analyses were significant at $p < 0.001$ with degrees of freedom F(11, 132). The strongest temporal variation was recorded for p,p′-DDT ($F_{(11, 432)} = 58.930$, $p < 0.001$), followed by cis-chlordane ($F_{(11, 432)} = 56.510$, $p < 0.001$) and p,p′-DDE ($F_{(11, 432)} = 35.340$, $p < 0.001$). Substantial month-to-month variation was also observed for o,p′-DDE ($F_{(11, 432)} = 29.880$, $p < 0.001$), o,p′-DDT ($F_{(11, 432)} = 29.230$, $p < 0.001$), and HCN ($F_{(11, 432)} = 29.140$, $p < 0.001$). Moderate but statistically significant temporal variation was recorded for p,p′-DDD ($F_{(11, 432)} = 27.780$, $p < 0.001$), HCB ($F_{(11, 432)} = 27.180$, $p < 0.001$), heptachlor epoxide ($F_{(11, 432)} = 25.850$, $p < 0.001$), and trans-nonachlor ($F_{(11, 432)} = 25.310$, $p < 0.001$). The remaining compounds, including γ-HCH ($F_{(11, 432)} = 18.420$, $p < 0.001$), heptachlor ($F_{(11, 432)} = 12.520$, $p < 0.001$), and o,p′-DDD ($F_{(11, 432)} = 12.210$, $p < 0.001$), also demonstrated statistically significant temporal variability.

Table 4.23:
One-Way ANOVA results for monthly variation in OCPs concentrations in Rhagovelia species

OCPs (μg/kg)	*F* value	*p* value
p,p'DDT	$F_{(11,432)} = 58.93$	< 0.001
Cis chlordane	$F_{(11,432)} = 56.51$	< 0.001
p,p'DDE	$F_{(11,432)} = 35.34$	< 0.001
o,p'DDE	$F_{(11,432)} = 29.88$	< 0.001
o,p'DDT	$F_{(11,432)} = 29.23$	< 0.001
HCN	$F_{(11,432)} = 29.14$	< 0.001
p,p'DDD	$F_{(11,432)} = 27.78$	< 0.001
HCB	$F_{(11,432)} = 27.18$	< 0.001
Hep.Hepoxide	$F_{(11,432)} = 25.85$	< 0.001
Trans Nonachlor	$F_{(11,432)} = 25.31$	< 0.001
Mirex	$F_{(11,432)} = 20.85$	< 0.001
alpha-HCH	$F_{(11,432)} = 19.78$	< 0.001
beta-HCH	$F_{(11,432)} = 19.25$	< 0.001
gamma-HCH	$F_{(11,432)} = 18.42$	< 0.001
Heptachlor	$F_{(11,432)} = 12.52$	< 0.001
o,p'DDD	$F_{(11,432)} = 12.21$	< 0.001

The spatio-temporal distribution of OCPs concentrations in *Rhagovelia* species is presented in Figure 4.24. The Figure shows compound-specific monthly trajectories across all twelve stations. Station lines frequently diverged and intersected, indicating that temporal trends differed among locations. Several compounds, including o,p′-DDD, p,p′-DDD, p,p′-DDE, and Mirex, displayed pronounced seasonal pulses that varied in magnitude and timing between stations. Downstream stations such as Umba Estuary, Mwena Majoreni, and Ramisi Estuary often exhibited higher amplitude fluctuations compared to upstream stations such as Mapu and Mwena Manda. In many subplots, station lines crossed during different months, indicating shifting relative contamination rankings across the sampling period.

Figure 4.24:
Spatio-temporal variation of OCPs concentrations in Rhagovelia species

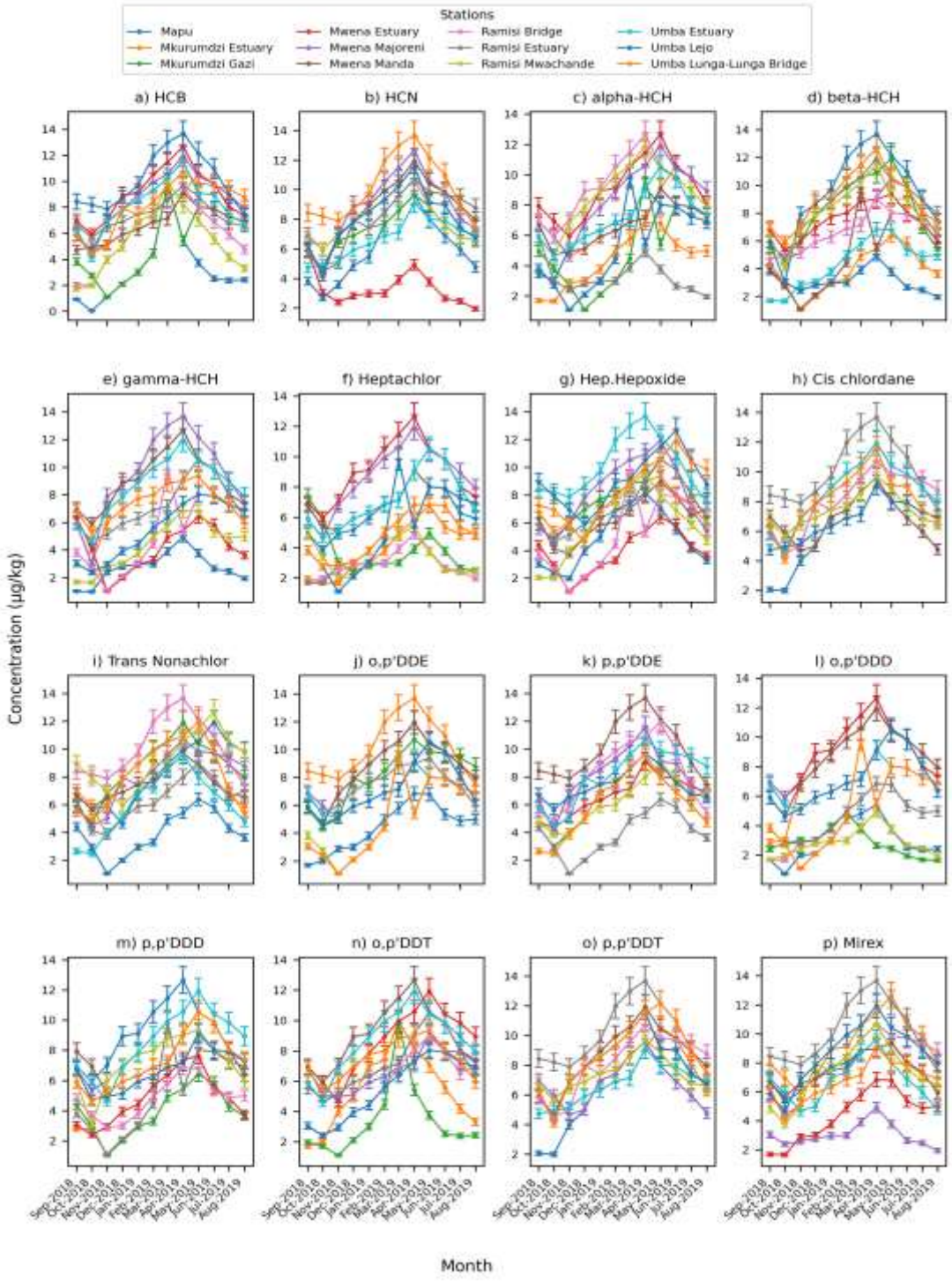

Two-way ANOVA confirmed statistically significant station x month interaction effects for all sixteen compounds (Table 4.24). All interaction terms were significant at $p < 0.001$ with degrees of freedom F(121, 288). The strongest interaction effects were recorded for o,p′-DDD (F(121, 288) = 587240.190, $p < 0.001$), p,p′-DDD (F(121, 288) = 498260.540, $p < 0.001$), o,p′-DDT (F(121, 288) = 336577.830, $p < 0.001$), Mirex (F(121, 288) = 328715.990, $p < 0.001$), and p,p′-DDT (F(121, 288) = 189530.440, $p < 0.001$). Strong interaction effects were also observed for HCN (F(121, 288) = 222121.110, $p < 0.001$) and trans-nonachlor (F(121, 288) = 102947.670, $p < 0.001$). Moderate but still highly significant interaction magnitudes were recorded for cis-chlordane (F(121, 288) = 2248.130, $p < 0.001$), heptachlor (F(121, 288) = 1618.000, $p < 0.001$), and o,p′-DDE (F(121, 288) = 1165.020, $p < 0.001$). Heptachlor epoxide exhibited the lowest interaction magnitude (F(121, 288) = 16.010, $p < 0.001$), yet remained statistically significant. These results demonstrate that OCPs accumulation in *Rhagovelia* species was governed by strong interactive effects of location and month, resulting in heterogeneous contamination dynamics across the estuarine ecosystem.

Table 4.24:
Two-way ANOVA interaction effects for OCPs concentrations in Rhagovelia species across stations and months

OCPs (µg/kg)	*F* value	*p* value
HCB	$F_{(121,288)} = 20986.00$	< 0.001
HCN	$F_{(121,288)} = 222121.11$	< 0.001
alpha-HCH	$F_{(121,288)} = 5598.23$	< 0.001
beta-HCH	$F_{(121,288)} = 1381.11$	< 0.001
gamma-HCH	$F_{(121,288)} = 1417.07$	< 0.001
Heptachlor	$F_{(121,288)} = 1618.00$	< 0.001
Hep.Hepoxide	$F_{(121,288)} = 16.01$	< 0.001
Cis chlordane	$F_{(121,288)} = 2248.13$	< 0.001
Trans Nonachlor	$F_{(121,288)} = 102947.67$	< 0.001
o,p'DDE	$F_{(121,288)} = 1165.02$	< 0.001
p,p'DDE	$F_{(121,288)} = 59141.48$	< 0.001
o,p'DDD	$F_{(121,288)} = 587240.19$	< 0.001
p,p'DDD	$F_{(121,288)} = 498260.54$	< 0.001
o,p'DDT	$F_{(121,288)} = 336577.83$	< 0.001
p,p'DDT	$F_{(121,288)} = 189530.44$	< 0.001
Mirex	$F_{(121,288)} = 328715.99$	< 0.001

4.3.4 Levels of OCPs in fish, *Penaeus monodon*

4.3.4.1 Spatial variation in the levels of OCPs in *P. monodon*

The spatial distribution of OCPs concentrations in *P. monodon* across the twelve sampling stations is presented in Figure 4.25. The boxplots illustrate median values, interquartile ranges, and outliers for each of the sixteen compounds, allowing assessment of station-level differences in pesticide accumulation.

Marked spatial heterogeneity was observed across the estuarine gradient. Estuarine stations, particularly Ramisi, Umba, and Mkurumdzi, displayed broader interquartile ranges and elevated median concentrations for several compounds, including HCN, HCB, and α-HCH. These stations also exhibited greater dispersion and more frequent outliers, especially for HCN and HCB. In contrast, upstream stations such as Mapu and Ramisi Mwachande generally showed narrower interquartile ranges and comparatively lower concentration levels across multiple compounds, including p,p′-DDT, o,p′-DDD, and trans-nonachlor. Although some compounds such as o,p′-DDE, Mirex, and γ-HCH appeared more evenly distributed along the station gradient, localized elevations were still evident at specific downstream sites. For example, o,p′-DDE concentrations were higher at Mkurumdzi and Umba relative to upstream locations. Mirex and trans-nonachlor displayed sporadic peaks across estuarine and midstream stations.

Figure 4.25:
Boxplots showing spatial variation in OCPs concentrations in P. monodon

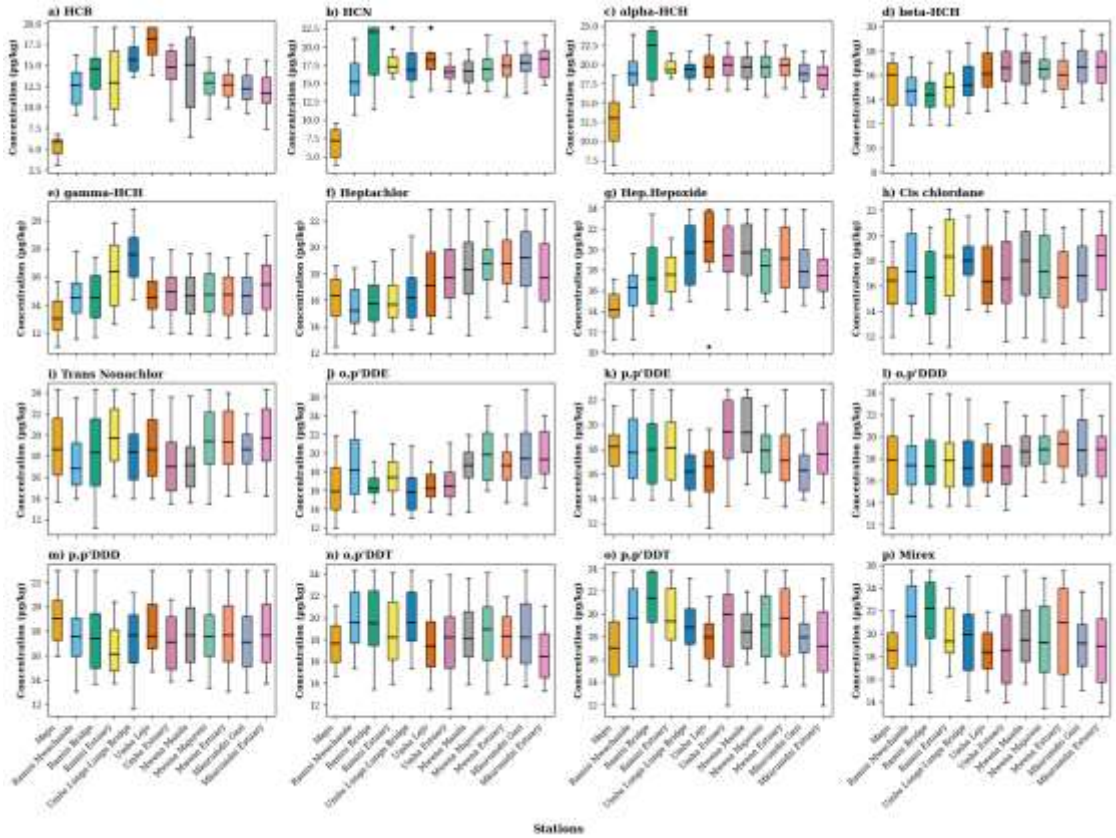

One-way ANOVA results (Table 4.25) confirmed statistically significant spatial differences for all sixteen compounds. Analyses were conducted with degrees of freedom F(11, 132). The strongest spatial variation was observed for HCN ($F_{(11, 432)}$ = 59.500, $p < 0.001$), followed by HCB ($F_{(11, 432)}$ = 45.280, $p < 0.001$) and α-HCH ($F_{(11, 432)}$ = 33.540, $p < 0.001$). Significant spatial variation was also detected for heptachlor epoxide ($F_{(11, 432)}$ = 14.030, $p < 0.001$), o,p′-DDE ($F_{(11, 432)}$ = 12.120, $p < 0.001$), and γ-HCH ($F_{(11, 432)}$ = 12.080, $p < 0.001$).

Table 4.25:
One-Way ANOVA results for OCPs in P. monodon across sampling stations

OCPs (µg/kg)	***F* value**	***p* value**
HCN	$F_{(11,432)}$ = 59.50	< 0.001
HCB	$F_{(11,432)}$ = 45.28	< 0.001
alpha-HCH	$F_{(11,432)}$ = 33.54	< 0.001
Hep.Hepoxide	$F_{(11,432)}$ = 14.03	< 0.001
o,p'DDE	$F_{(11,432)}$ = 12.12	< 0.001
gamma-HCH	$F_{(11,432)}$ = 12.08	< 0.001
Heptachlor	$F_{(11,432)}$ = 11.02	< 0.001
beta-HCH	$F_{(11,432)}$ = 8.65	< 0.001
p,p'DDE	$F_{(11,432)}$ = 6.47	< 0.001
p,p'DDT	$F_{(11,432)}$ = 4.29	< 0.001
o,p'DDT	$F_{(11,432)}$ = 4.05	< 0.001
Mirex	$F_{(11,432)}$ = 2.99	0.0007
Trans Nonachlor	$F_{(11,432)}$ = 2.77	0.0017
p,p'DDD	$F_{(11,432)}$ = 2.07	0.0213
o,p'DDD	$F_{(11,432)}$ = 2.02	0.0252
Cis chlordane	$F_{(11,432)}$ = 1.86	0.0425

Additional compounds including heptachlor ($F_{(11, 432)} = 11.020$, $p < 0.001$), β-HCH ($F_{(11, 432)} = 8.650$, $p < 0.001$), p,p′-DDE ($F_{(11, 432)} = 6.470$, $p < 0.001$), p,p′-DDT ($F_{(11, 432)} = 4.290$, $p < 0.001$), and o,p′-DDT ($F_{(11, 432)} = 4.050$, $p < 0.001$) also exhibited significant station-level differences. Mirex ($F_{(11, 432)} = 2.990$, $p = 0.0007$) and trans-nonachlor ($F_{(11, 432)} = 2.770$, $p = 0.0017$) showed comparatively lower F-values but remained highly significant. Compounds p,p′-DDD ($F_{(11, 432)} = 2.070$, $p = 0.0213$), o,p′-DDD ($F_{(11, 432)} = 2.020$, $p = 0.0252$), and cis-chlordane ($F_{(11, 432)} = 1.860$, $p = 0.0425$) exhibited statistically significant, but more moderate spatial variation. These results confirm statistically robust spatial structuring of OCPs accumulation in *P. monodon* across the estuarine system.

4.3.4.2 Temporal variation in the levels of OCPs in *P. monodon*

Monthly variation in OCPs concentrations in *P. monodon* is illustrated in Figure 4.26. Clear temporal heterogeneity was evident across most compounds. Compounds such as cis-chlordane, trans-nonachlor, and o,p′-DDD displayed pronounced peaks during March–May. Concentrations for these compounds were elevated during this period and accompanied by broader standard error margins. Additional seasonal elevations were observed during October–November for compounds such as Mirex, o,p′-DDT, and p,p′-DDE. Lower concentrations were generally recorded between June and September, with comparatively tighter standard error margins for compounds including β-HCH, HCB, and heptachlor epoxide.

Figure 4. 26:
Temporal distribution of OCPs concentrations in P. monodon

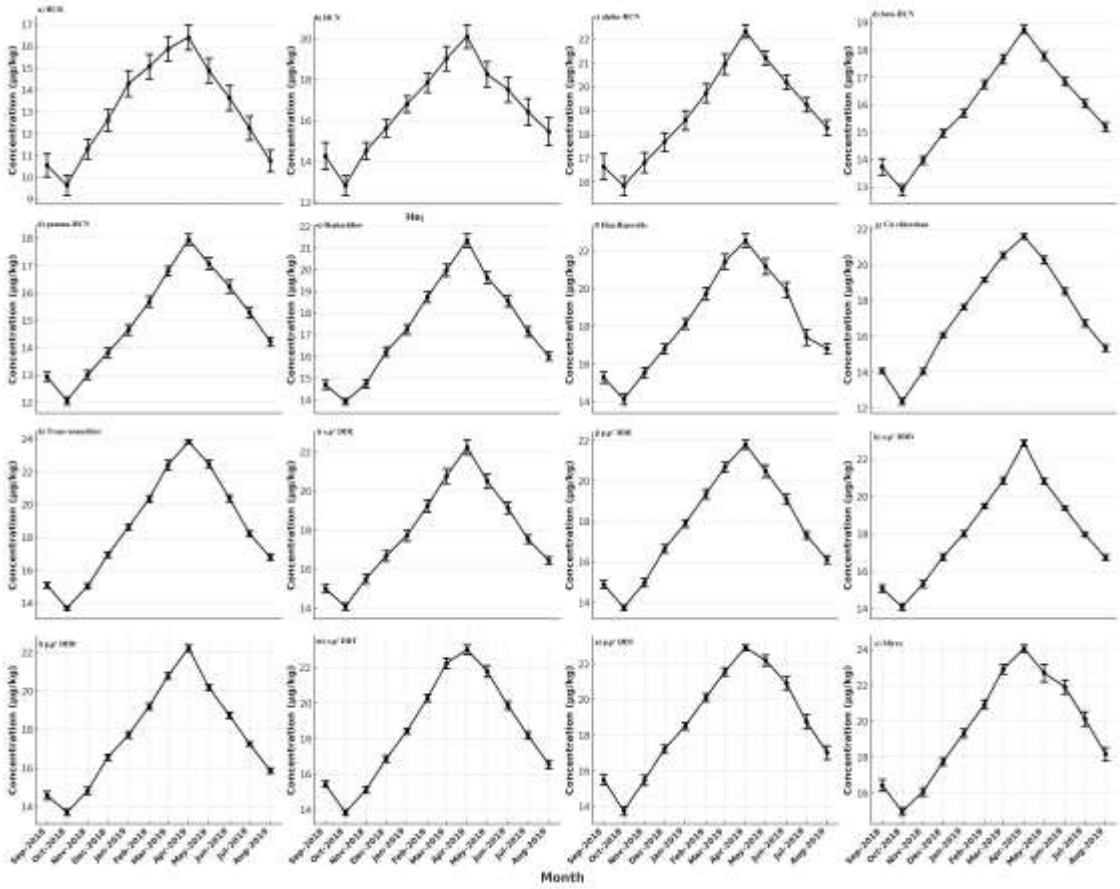

One-way ANOVA confirmed statistically significant monthly variation for all sixteen compounds (Table 4.26). Analyses were conducted with degrees of freedom F(11, 132). The highest temporal variation was recorded for cis-chlordane ($F_{(11,\ 432)}$ = 312.480, $p < 0.001$), followed by trans-nonachlor ($F_{(11,\ 432)}$ = 282.480, $p < 0.001$), o,p′-DDD ($F_{(11,\ 432)}$ = 271.730, $p < 0.001$), and p,p′-DDD ($F_{(11,\ 432)}$ = 262.760, $p < 0.001$). Substantial month-to-month variation was also observed for o,p′-DDT ($F_{(11,\ 432)}$ = 174.420, $p < 0.001$), p,p′-DDE ($F_{(11,\ 432)}$ = 139.070, $p < 0.001$), and p,p′-DDT ($F_{(11,\ 432)}$ = 107.470, $p < 0.001$).

Strong seasonal variation was further recorded for β-HCH ($F_{(11, 432)} = 105.840$, $p < 0.001$), heptachlor ($F_{(11, 432)} = 96.480$, $p < 0.001$), γ-HCH ($F_{(11, 432)} = 96.440$, $p < 0.001$), and Mirex ($F_{(11, 432)} = 91.990$, $p < 0.001$). Moderate but statistically significant variation was detected for o,p′-DDE ($F_{(11, 432)} = 77.920$, $p < 0.001$), heptachlor epoxide ($F_{(11, 432)} = 62.520$, $p < 0.001$), and α-HCH ($F_{(11, 432)} = 28.020$, $p < 0.001$). The smallest temporal differences were observed for HCB ($F_{(11, 432)} = 17.570$, $p < 0.001$) and HCN ($F_{(11, 432)} = 14.470$, $p < 0.001$), though both remained statistically significant. These findings confirm pronounced seasonal variation in pesticide accumulation in *P. monodon*.

Table 4.26:
One-Way ANOVA results for monthly variation in OCPs in P. monodon

Pesticide (μg/kg)	*F* value	*p* value
Cis chlordane	$F_{(11,432)} = 312.48$	< 0.001
Trans Nonachlor	$F_{(11,432)} = 282.48$	< 0.001
o,p'DDD	$F_{(11,432)} = 271.73$	< 0.001
p,p'DDD	$F_{(11,432)} = 262.76$	< 0.001
o,p'DDT	$F_{(11,432)} = 174.42$	< 0.001
p,p'DDE	$F_{(11,432)} = 139.07$	< 0.001
p,p'DDT	$F_{(11,432)} = 107.47$	< 0.001
beta-HCH	$F_{(11,432)} = 105.84$	< 0.001
Heptachlor	$F_{(11,432)} = 96.48$	< 0.001
gamma-HCH	$F_{(11,432)} = 96.44$	< 0.001
Mirex	$F_{(11,432)} = 91.99$	< 0.001
o,p'DDE	$F_{(11,432)} = 77.92$	< 0.001
Hep.Hepoxide	$F_{(11,432)} = 62.52$	< 0.001
alpha-HCH	$F_{(11,432)} = 28.02$	< 0.001
HCB	$F_{(11,432)} = 17.57$	< 0.001
HCN	$F_{(11,432)} = 14.47$	< 0.001

Together, the plotted monthly trends in Figure 4.26 and the statistically robust findings in Table 4.28 confirm the presence of pronounced and consistent seasonal variation in OCPs concentrations in *P. monodon*. The data show that bioaccumulation patterns are influenced by monthly environmental conditions, with peak contamination levels generally occurring during rainfall-intensive periods.

4.3.4.3 Spatio-temporal variations in the levels of pesticides in *P. monodon*

The spatio-temporal distribution of OCPs concentrations in *P. monodon* is presented in Figure 4.27. Each subplot illustrates mean monthly concentrations for individual compounds across all twelve stations. Station trajectories frequently diverged and intersected, indicating variability in temporal patterns between locations.

Several compounds, including o,p′-DDD, p,p′-DDD, and trans-nonachlor, exhibited distinct seasonal pulses that varied in magnitude among stations. Downstream stations such as Ramisi Estuary, Umba Lejo, Mkurumdzi Gazi, and Mwena Majoreni consistently showed higher amplitude fluctuations compared to upstream stations such as Mapu and Ramisi Bridge. For compounds including cis-chlordane, γ-HCH, p,p′-DDT, and Mirex, station lines diverged markedly, demonstrating that monthly concentration trajectories differed substantially among sites. In some cases, station rankings changed over time, as indicated by frequent crossovers in compounds such as β-HCH and o,p′-DDE.

Figure 4.27:
Spatio-temporal variation of OCPs concentrations in P. monodon during the study period

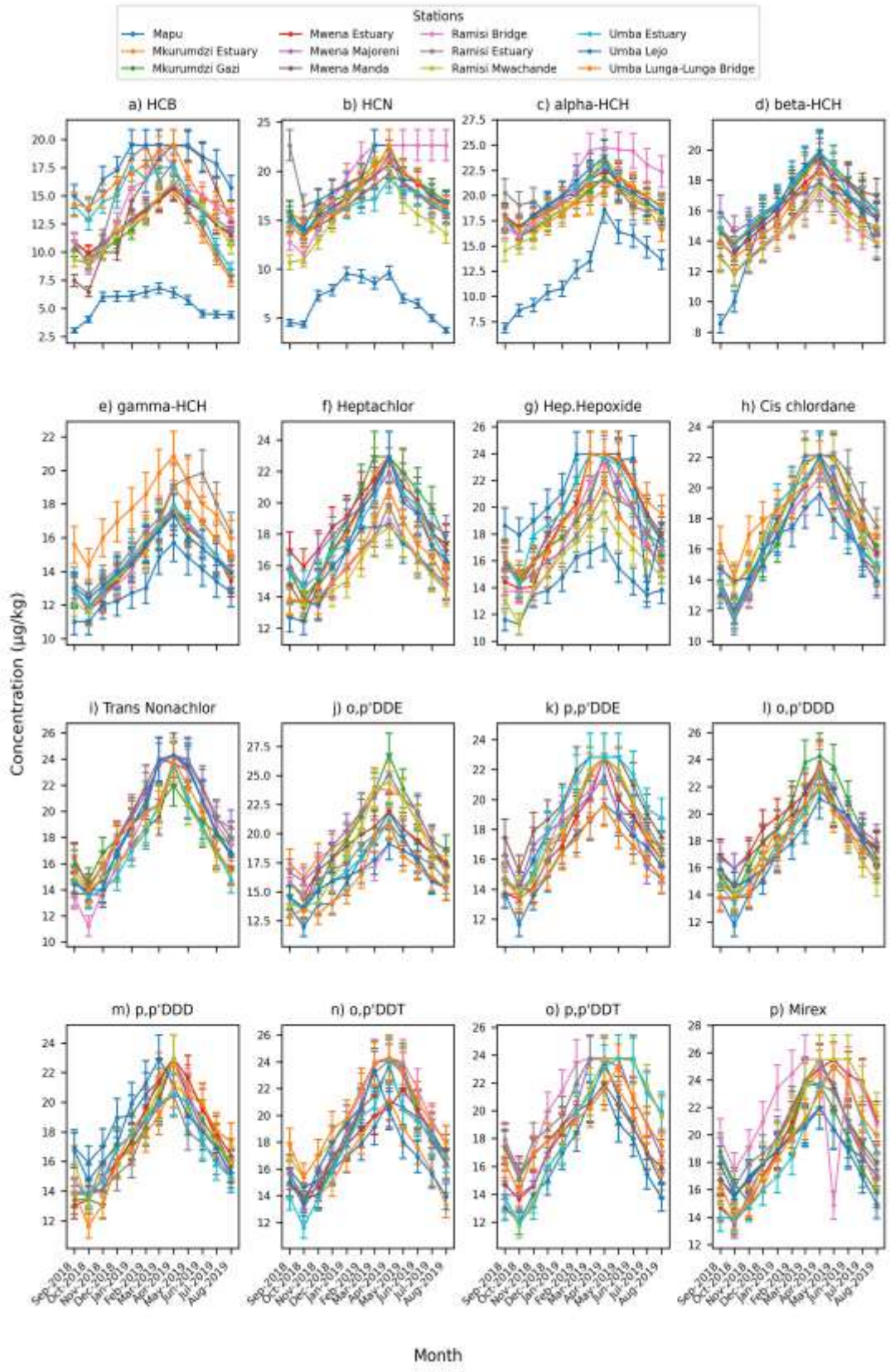

Two-way ANOVA results confirmed statistically significant station x month interaction effects for all sixteen compounds (Table 4.27). All interaction terms were significant at $p < 0.001$ with degrees of freedom F(121, 288). The strongest interaction effects were observed for γ-HCH ($F_{(121, 288)} = 1061141.370$, $p < 0.001$), heptachlor ($F_{(121, 288)} = 1019848.810$, $p < 0.001$), and o,p′-DDD ($F_{(121, 288)} = 961107.760$, $p < 0.001$). High interaction magnitudes were also recorded for p,p′-DDD ($F_{(121, 288)} = 860474.500$, $p < 0.001$), trans-nonachlor ($F_{(121, 288)} = 728313.170$, $p < 0.001$), and α-HCH ($F_{(121, 288)} = 690591.270$, $p < 0.001$). Substantial interaction effects were further observed for p,p′-DDE ($F_{(121, 288)} = 574250.880$, $p < 0.001$), o,p′-DDE ($F_{(121, 288)} = 520144.700$, $p < 0.001$), and Mirex ($F_{(121, 288)} = 519494.090$, $p < 0.001$). Moderate but significant interaction terms were recorded for β-HCH ($F_{(121, 288)} = 337066.670$, $p < 0.001$), HCN ($F_{(121, 288)} = 258103.120$, $p < 0.001$), and cis-chlordane ($F_{(121, 288)} = 227859.370$, $p < 0.001$). Although HCB ($F_{(121, 288)} = 20986.000$, $p < 0.001$) and heptachlor epoxide ($F_{(121, 288)} = 14857.380$, $p < 0.001$) exhibited comparatively lower F-values, interaction effects remained statistically significant. These findings demonstrate strong spatio-temporal structuring of pesticide accumulation in *P. monodon*, with significant interaction between sampling station and month across all assessed compounds.

Table 4.27:
Two-way ANOVA interaction effects for OCPs concentrations in P. monodon across sampling stations and months

Pesticide (μg/kg)	F-Value	*p*-Value
HCB	$F_{(121,288)} = 20986.003$	< 0.001
HCN	$F_{(121,288)} = 222121.114$	< 0.001
alpha-HCH	$F_{(121,288)} = 5598.233$	< 0.001
beta-HCH	$F_{(121,288)} = 1381.112$	< 0.001
gamma-HCH	$F_{(121,288)} = 1417.073$	< 0.001
Heptachlor	$F_{(121,288)} = 1618.005$	< 0.001
Hep.Hepoxide	$F_{(121,288)} = 16.012$	< 0.001
Cis chlordane	$F_{(121,288)} = 2248.133$	< 0.001
Trans Nonachlor	$F_{(121,288)} = 102947.672$	< 0.001
o,p'DDE	$F_{(121,288)} = 1165.023$	< 0.001
p,p'DDE	$F_{(121,288)} = 59141.482$	< 0.001
o,p'DDD	$F_{(121,288)} = 587240.193$	< 0.001
p,p'DDD	$F_{(121,288)} = 498260.542$	< 0.001
o,p'DDT	$F_{(121,288)} = 336577.832$	< 0.001
p,p'DDT	$F_{(121,288)} = 189530.442$	< 0.001
Mirex	$F_{(121,288)} = 328715.993$	< 0.001

4.4 Relationship between physico-chemical water quality parameters and OCPs concentrations in water in estuarine ecosystems

Principal Component Analysis (PCA) was conducted on nine physico-chemical water quality parameters and sixteen OCPs using standardized variables. The first two principal components accounted for 63.9% of the total variance, with PC1 explaining 41.6% and PC2 22.3%.

The loading matrix indicated that PC2 was primarily structured by salinity-related parameters. TDS exhibited the strongest negative loading on PC2 (−0.497), followed by conductivity (−0.471) and salinity (−0.418). DO showed a positive loading on PC2 (0.281), while pH also loaded positively (0.308). Temperature demonstrated a modest positive loading on PC2 (0.094) and a small negative loading on PC1 (−0.041). Ammonia, nitrate, and phosphate showed relatively small loading magnitudes on both components.

PC1 was characterized by negative loadings for all sixteen OCP compounds, indicating a common gradient of pesticide concentration. The strongest PC1 loadings among the compounds were observed for cis-chlordane (−0.278), o,p′-DDD (−0.271), trans-nonachlor (−0.270), o,p′-DDT (−0.267), γ-HCH (−0.264), heptachlor epoxide (−0.262), and p,p′-DDT (−0.260). Other compounds including β-HCH (−0.259), heptachlor (−0.257), p,p′-DDD (−0.256), p,p′-DDE (−0.250), Mirex (−0.249), α-HCH (−0.241), HCN (−0.211), HCB (−0.202), and o,p′-DDE (−0.127) also contributed negatively to PC1.

On PC2, the magnitude of OCPs loadings was generally smaller. HCN showed the strongest negative PC2 loading (−0.188), while p,p′-DDE (0.137) and p,p′-DDD (0.135) exhibited the highest positive PC2 contributions among the OCPs. Other compounds displayed modest PC2 loadings, including o,p′-DDT (0.087), cis-chlordane (0.058), Mirex (0.057), β-HCH (0.044), heptachlor epoxide (0.044), and o,p′-DDD (0.039). Several compounds, such as γ-HCH (−0.035), trans-nonachlor (−0.039), heptachlor (−0.006), and p,p′-DDT (−0.007), showed near-zero PC2 contributions.

The PCA biplot (Figure 4.28) displays water quality parameters as vectors and OCPs compounds as triangular markers positioned according to their PC1 and PC2 scores. DO and pH were positioned in the positive PC2 region, while conductivity, TDS, and salinity were located in the negative PC2 region. Temperature appeared in the positive PC2 and slightly negative PC1 domain. Most OCP compounds clustered in the negative PC1 region, with dispersion across both positive and negative PC2 quadrants.

The ordination illustrates the relative positioning of water quality variables and pesticide compounds across four quadrants defined by PC1 and PC2. All vectors were scaled within the −1.0 to +1.0 range. The x-axis represents PC1 (41.6%) and the y-axis represents PC2 (22.3%), as indicated in the figure. No mean observation markers were included in the final visual. All compound names were displayed using distinct triangle markers (▲), and clusters of compounds were distinguished by varying colors. All variables and compounds were repositioned within the range of 0.2 to 0.9 or −0.2 to −0.9 on both axes to ensure a clear and even distribution across the quadrants.

Figure 4.28:
PCA biplot showing ordination of water quality parameters (arrows) and OCPs compounds based on PC1 and PC2 scores

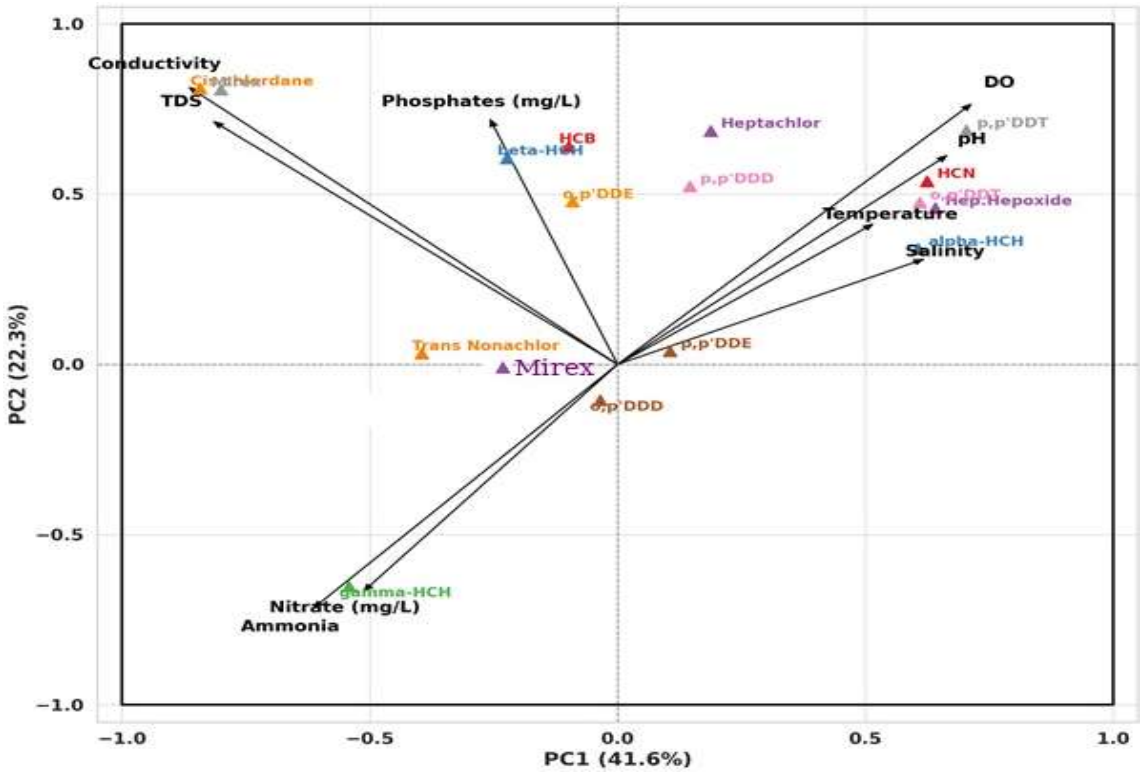

Table 4.28 presents the standardized loadings of all variables on PC1 and PC2. Loadings represent the contribution of each variable to the respective principal component.

Table 4.28:
Principal component loadings of water quality parameters and OCPs on the first two principal components (PC1 and PC2)

Variable	PC1 Loading	PC2 Loading
Ammonia (mg/L)	0.029	-0.041
pH	-0.001	0.308
Phosphates (mg/L)	-0.004	-0.184
Nitrate (mg/L)	-0.021	-0.182
Salinity (ppt)	-0.038	-0.418
Temperature (°C)	-0.041	0.094
DO (mg/L)	-0.048	0.281
TDS (mg/L)	-0.053	-0.497
Conductivity (µS/cm)	-0.09	-0.471
o,p'DDE	-0.127	-0.023
HCB	-0.202	0.017
HCN	-0.211	-0.188
alpha-HCH	-0.241	-0.097
Mirex	-0.249	0.057
p,p'DDE	-0.25	0.137
p,p'DDD	-0.256	0.135
Heptachlor	-0.257	-0.006
beta-HCH	-0.259	0.044
p,p'DDT	-0.26	-0.007
Hep.Hepoxide	-0.262	0.044
gamma-HCH	-0.264	-0.035
o,p'DDT	-0.267	0.087
Trans Nonachlor	-0.27	-0.039
o,p'DDD	-0.271	0.039
Cis chlordane	-0.278	0.058

Note: All the OCPs were measured in µg/kg

4.5 Bioconcentration and biomagnification of OCPs in water, sediments, the trophic levels of benthic macroinvertebrates and *P. monodon* in estuarine ecosystems of South Coast, Kenya

4.5.1 Biomagnification of OCPs across Aquatic Guilds

Figure 4.29 presents the biomagnification trends of sixteen OCPs across aquatic trophic guilds (Atyidae, *N. undata*, *Rhagovelia* species, *T. palustris* and *S. cucullata*, and *P. monodon*) demonstrating the increasing accumulation of contaminants from lower to higher trophic levels in the estuarine food web. The graphical representation compares mean concentrations of individual OCPs among macroinvertebrate feeding guilds and *P. monodon*, thereby enabling visual assessment of biomagnification potential.

Across the spectrum of OCPs, *P. monodon* (fish) consistently exhibited the highest concentrations for the majority of OCPs, indicating strong evidence of biomagnification. Compounds such as alpha-HCH, o,p'-DDD, p,p'-DDE, and Mirex showed notably elevated concentrations in *P. monodon* tissues compared to all macroinvertebrate guilds. For example, the concentration of alpha-HCH in *P. monodon* was more than twice the levels observed in *Rhagovelia* species (predators) and nearly three times that in *T. palustris* (shredders). Similarly, p,p'-DDE levels in *P. monodon* exceeded those in *N. undata* and Atyidae by a substantial margin, reflecting effective bioaccumulation through trophic transfer.

Among macroinvertebrates, *Rhagovelia* species and *S. cucullata* generally recorded higher contaminant burdens relative to other groups, suggesting their role as intermediate trophic accumulators. *N. undata* and Atyidae exhibited moderate concentrations, while *T. palustris* consistently displayed the lowest mean values for

most OCPs. This gradient aligns with ecological feeding strategies, where *T. palustris* occupy basal trophic positions and are less exposed to bioaccumulative transfer, while *Rhagovelia* species (predators) are more likely to ingest contaminated prey.

Certain pesticides, such as aldrin, endrin aldehyde, and endosulfan I, showed relatively uniform distribution across guilds, suggesting minimal trophic magnification. In contrast, compounds like Mirex, heptachlor epoxide, and o,p'-DDT demonstrated steep concentration increases toward fish, consistent with their lipophilicity and environmental persistence. These disparities reflect not only differences in the physico-chemical properties of the pesticides but also guild-specific uptake routes, metabolism, and habitat associations.

Overall, Figure 4.29 highlights the tendency of OCPs to biomagnify across aquatic trophic levels, with fish serving as terminal reservoirs of contamination. The data affirm the vulnerability of higher trophic consumers to long-term pesticide exposure and the ecological significance of macroinvertebrate guilds as conduits of contaminant transfer within estuarine food webs.

Figure 4.29:
Biomagnification of OCPs Across Aquatic Guilds. The macro-invertebrate FFGs shredders, scraper-grazers, filterers, collector-gatherers and predators; and fish were represented by T. palustris, N. undata, S. cucullata, Atyidae and Rhagovelia species; and P. monodon respectively

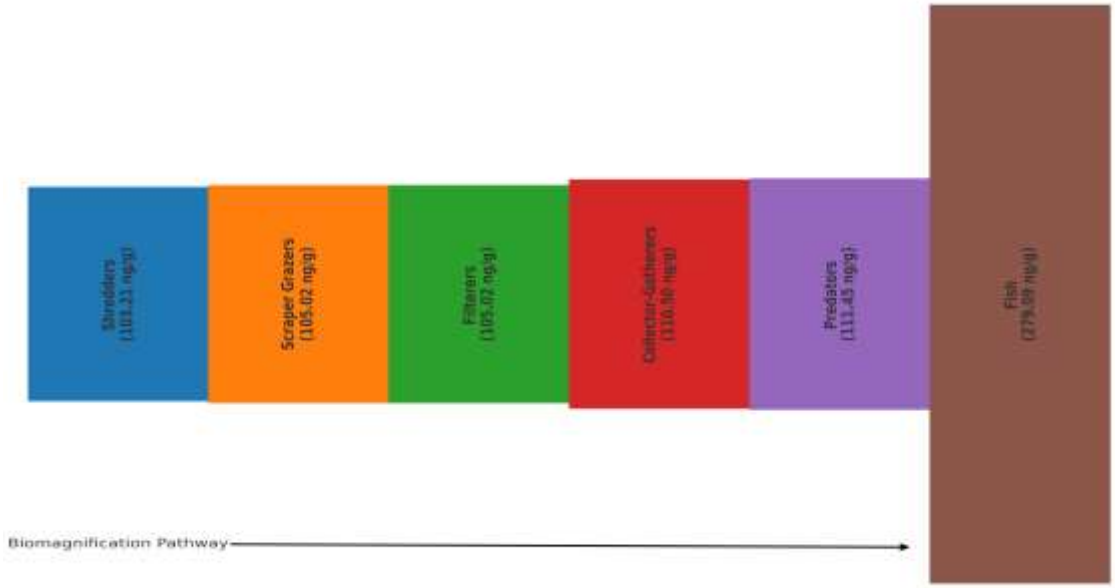

Site-specific analysis of OCPs concentrations across aquatic guilds revealed consistent patterns of trophic-level accumulation, with notable variation in magnitude across sampling locations (Figure 4.30). Across all sites, OCPs concentrations increased progressively from lower to higher trophic guilds, confirming a clear biomagnification trend. At most sites, *P. monodon* consistently exhibited the highest mean OCPs concentrations, often more than double those recorded in macroinvertebrate groups. For instance, in the Umba Estuary, *P. monodon* OCPs concentrations exceeded 280 ng/g, while concentrations in *N. undata* and *S. cucullata* typically remained below 70 ng/g. This trophic disparity was also observed in Ramisi Mwachande, where *P. monodon* accumulated substantially higher levels of OCPs compared to Atyidae, *N. undata*, and *T. palustris*.

The predator guild (*Rhagovelia* species), representing macroinvertebrate carnivores, consistently showed intermediate concentrations higher than other invertebrate guilds but lower than *P. monodon* (fish). Guilds such as *N. undata*, *S. cucullata*, and Atyidae displayed moderate levels of OCPs accumulation, with some variation depending on site conditions. Overall, the results confirm biomagnification of OCPs across aquatic food webs, with site-specific variations in concentration levels likely influenced by local contamination sources, environmental persistence, and food web dynamics. These findings emphasize the ecological risks to higher trophic organisms, particularly fish, in OCPs-impacted freshwater systems.

Figure 4.30:
Site-specific pyramids of mean OCPs across aquatic guilds. The macro-invertebrate FFGs shredders, scraper-grazers, filterers, collector-gatherers and predators; and fish were represented by T. palustris, N. undata, S. cucullata, Atyidae and Rhagovelia species; and P. monodon respectively

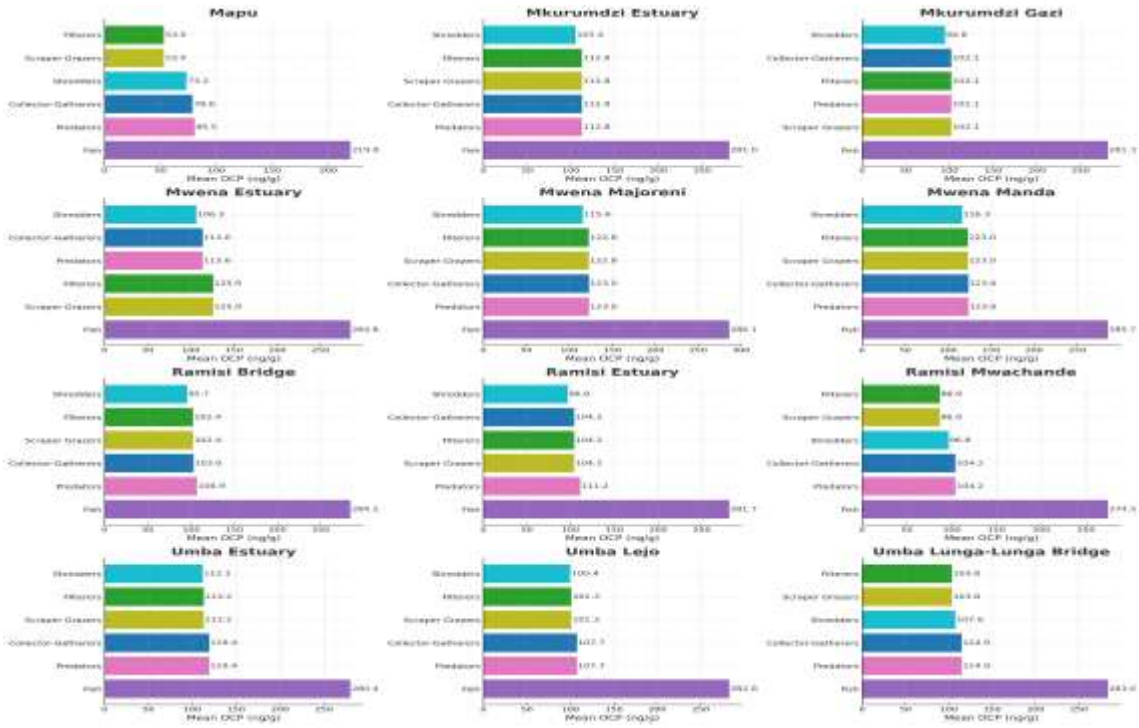

4.5.2 Bioconcentration Factor (BCF)

Bioconcentration factors (BCFs) quantify the degree to which organisms accumulate contaminants directly from water through non-dietary uptake pathways such as dermal absorption and gill exchange. In this study, BCFs were computed for *P. monodon* and five macroinvertebrate trophic guilds across sixteen OCP compounds. The results are presented in Table 4.29. Overall, *P. monodon* exhibited consistently higher BCFs across all OCPs compared to macroinvertebrate groups, reflecting their higher trophic status and greater lipid content which enhances the affinity for hydrophobic contaminants. The mean BCF values in *P. monodon* ranged from 16.1 (HCB) to 28.0 (Mirex). The highest bioconcentration in *P. monodon* was recorded for Mirex (BCF = 28.0), followed closely by p,p′-DDT (27.0), p,p′-DDD (26.8), and trans-nonachlor (26.5), indicating substantial uptake of highly hydrophobic compounds.

Among macroinvertebrates, *Rhagovelia* species guilds demonstrated the highest BCF values relative to the other guilds, suggesting that trophic level and body structure may influence contaminant affinity. For instance, *Rhagovelia* species accumulated up to 11.2 (cis-chlordane), 11.1 (p,p′-DDT), and 10.9 (trans-nonachlor), which were consistently higher than the values observed in *N. undata*, Atyidae, *S. cucullata*, and *T. palustris* for the same compounds.

BCFs for the other macroinvertebrate guilds showed more conservative ranges, generally between 7.3 and 11.2. *N. undata*, Atyidae and *T. palustris* exhibited similar accumulation patterns across most compounds, with slightly lower BCFs in HCB (7.3–8.1) and o,p′-DDD (8.6–8.7), indicating reduced uptake potential for less hydrophobic or more degradable compounds. *S. cucullata*, on the other hand, often mirrored the

values of Atyidae and *T. palustris*, suggesting shared exposure routes via suspended particulate matter and detritus-associated uptake.

Table 4.29:
Mean Bioconcentration Factors (BCFs) for OCPs in Fish and Macroinvertebrate Guilds

OCPs	*P. monodon*	*Rhagovelia* spp.	*N.* undata	Atyidae	*S. cucullata*	*T. palustria*
HCB	16.1	8.6	7.3	8.1	7.3	8.1
HCN	23.1	10.5	9.4	9.8	9.4	9.8
alpha-HCH	26.1	9.2	8.7	8.7	8.7	8.7
beta-HCH	21.7	9.3	7.9	8.8	7.9	8.8
gamma-HCH	21.6	9.6	9.9	9.4	9.9	9.4
Heptachlor	24.8	7.9	9.2	9.1	9.2	9.1
Hep.Hepoxide	25	9.6	9	9.3	9	9.3
Cis chlordane	25.2	11.2	10.4	11.2	10.4	11.2
Trans Nonachlor	26.5	10.9	9.2	10.7	9.2	10.7
o,p'DDE	26.1	10.1	9.6	10	9.6	10
p,p'DDE	25.3	10.2	9.6	10.6	9.6	10.6
o,p'DDD	24.7	8.1	8.6	8.7	8.6	8.7
p,p'DDD	26.8	9.8	9.9	10.3	9.9	10.3
o,p'DDT	26.3	9.7	8.8	9.7	8.8	9.7
p,p'DDT	27	11.1	10.9	11.1	10.9	11.1
Mirex	28	10.4	9.2	9.6	9.2	9.7

Notably, all OCPs showed evidence of bioaccumulation in both fish and invertebrates, although the magnitude varied by compound and feeding guild. Compounds like p,p′-DDT, cis-chlordane, and Mirex consistently exhibited higher BCFs across all organism groups, underscoring their strong environmental persistence and bioavailability in aquatic systems. These patterns highlight the relevance of organismal traits and contaminant properties in determining bioconcentration dynamics. The elevated BCFs

in *P. monodon* and *Rhagovelia* species raise concerns about potential trophic transfer and ecotoxicological risk in estuarine food webs.

4.5.3 Biomagnification Factor (BMF)

The analysis of OCPs concentrations across aquatic biological guilds revealed a clear trend of biomagnification. Mean total OCPs concentrations were lowest among lower trophic groups such as *T. palustris* and *S. cucullata*, each with average concentrations around 53.2 ng/g. These groups, which feed primarily on detritus and suspended particles, exhibited the lowest pesticide loads, reflecting limited exposure through trophic transfer.

A progressive increase in OCPs concentrations was observed in higher trophic guilds. *N. undata* and Atyidae showed moderate levels, with mean concentrations of approximately 67.8 ng/g and 77.4 ng/g, respectively. Predatory macroinvertebrates (*Rhagovelia* species) displayed even higher accumulation, averaging 95.1 ng/g. The highest concentrations were recorded in *P. monodon*, with a mean total OCPs burden of approximately 205.5 ng/g nearly four times greater than that found in *T. palustris* and *S. cucullata*.

This gradient in contaminant levels across guilds is consistent with a biomagnification pattern. As persistent, lipophilic compounds, OCPs tend to accumulate in organisms over time, particularly through dietary intake. The sharp increase in concentrations from macroinvertebrate predators to fish indicates a strong potential for trophic transfer and long-term ecological exposure. These findings underscore the vulnerability of top-

level consumers in aquatic ecosystems and highlight the ongoing environmental risk posed by legacy pollutants like OCPs.

The biomagnification factors (BMFs) for sixteen OCPs were calculated as the ratio of fish tissue concentration to that of macroinvertebrate feeding guilds (Atyidae, *Nerita undata*, *Rhagovelia* species, *Terebrallia palustris* and *Saccostrea cucullata*) (Table 4.30). These values quantify trophic transfer from lower aquatic organisms to higher-level consumers *P. monodon* in the estuarine food web of South Coast, Kenya.

Table 4.30:
Biomagnification Factors (BMFs; unitless) for OCPs across trophic guild transitions and fish (P. monodon) in South Coast estuarine ecosystems

OCPs	*T. palustris*	*Rhagovelia spp.*	*N. undata*	*Atyidae*	*S. cucullata*	*P. monodon*
alpha-HCH	2.82	3.00	2.98	3.00	2.98	2.82
Mirex	2.71	3.06	2.91	3.06	2.90	2.71
o,p′-DDD	3.03	2.87	2.85	2.87	2.85	3.03
o,p′-DDT	2.71	2.99	2.70	2.99	2.70	2.71
Heptachlor	3.14	2.69	2.73	2.69	2.73	3.14
Hep.Hepoxide	2.60	2.77	2.68	2.77	2.68	2.60
p,p′-DDD	2.74	2.71	2.60	2.71	2.60	2.74
o,p′-DDE	2.59	2.72	2.60	2.72	2.60	2.59
Trans Nonachlor	2.42	2.89	2.47	2.89	2.47	2.42
beta-HCH	2.34	2.75	2.48	2.75	2.48	2.34
p,p′-DDE	2.48	2.64	2.39	2.64	2.39	2.48
p,p′-DDT	2.42	2.47	2.42	2.47	2.42	2.42
HCN	2.21	2.47	2.37	2.47	2.37	2.21
Cis chlordane	2.24	2.42	2.24	2.42	2.24	2.24
gamma-HCH	2.25	2.18	2.29	2.18	2.29	2.25
HCB	1.87	2.20	2.00	2.20	2.00	1.87

Note. BMF is unitless (ratio). Values **> 1** indicate biomagnification.

All OCPs showed BMF values greater than 1, confirming their potential for trophic magnification. The highest average BMFs were observed for Heptachlor (mean ~2.99), o,p'DDD (mean ~2.89), Mirex (mean ~2.93), and alpha-HCH (mean ~2.96), indicating significant bioaccumulation potential. Notably, these compounds showed consistently

elevated BMFs across all macroinvertebrate guilds. Among the macroinvertebrate guilds, *N. undata* and *S. cucullata* displayed slightly higher BMFs for most OCPs, suggesting their foraging habits and broader environmental exposure could enhance contaminant uptake and transfer to *P. monodon*. Conversely, HCB exhibited the lowest BMFs (1.87–2.20), indicating relatively lower biomagnification, likely due to its lower bioavailability or faster metabolic degradation.

4.5.4 Trophic Magnification Factors of OCPs

To evaluate trophic transfer pathways across different macroinvertebrate FFGs, biomagnification factors (BMFs) were disaggregated to quantify guild-specific trophic magnification from macroinvertebrates to fish (*P. monodon*) for each of the 16 OCPs. This analysis reveals which pesticide compounds are most prone to biomagnify through specific trophic links in the estuarine food web of Kenya's South Coast (Table 4.31). Across all macroinvertebrate FFGs, BMFs exceeded 1.0 for every compound assessed, indicating active trophic magnification. The magnitude of biomagnification varied between OCPs and FFGs, with alpha-HCH, Mirex, Heptachlor, and o,p'DDT/DDDs consistently exhibiting the highest magnification values.

Among macroinvertebrate FFGs, *N. undata* and *S. cucullata* showed the highest average BMFs across multiple pesticides, likely due to their broad surface-area contact with contaminated substrates and water during feeding. For example, alpha-HCH showed BMFs of 3.00 from both *N. undata* and *S. cucullata* to *P. monodon*. Similarly, Mirex showed values of 3.06 in these two guilds. In contrast, HCB exhibited the lowest BMF values (1.87–2.20), confirming its lower trophic mobility. These results indicate that trophic magnification is compound- and guild-dependent, with the most persistent

OCPs accumulating strongly in *P. monodon* regardless of their initial entry point into the food web.

Table 4.31:
Trophic magnification factors of OCPs from Macroinvertebrate FFGs to P. monodon in South Coast Estuarine Ecosystem

OCPs	Trophic magnification factors				
	P. monodon vs *Rhagovelia* spp.	*P. Monodon* vs *N. undata*	*P. Monodon* vs Atyidae	*P. Monodon* vs *S. cucullata*	*P. Monodon* vs *T. palustris*
HCB	1.87	2.2	2	2.2	2
HCN	2.21	2.47	2.37	2.47	2.37
alpha-HCH	2.82	3	2.98	3	2.98
beta-HCH	2.34	2.75	2.48	2.75	2.48
gamma-HCH	2.25	2.18	2.29	2.18	2.29
Heptachlor	3.14	2.69	2.73	2.69	2.73
Hep.Hepoxide	2.6	2.77	2.68	2.77	2.68
Cis chlordane	2.24	2.42	2.24	2.42	2.24
Trans Nonachlor	2.42	2.89	2.47	2.89	2.47
o,p'DDE	2.59	2.72	2.6	2.72	2.6
p,p'DDE	2.48	2.64	2.39	2.64	2.39
o,p'DDD	3.03	2.87	2.85	2.87	2.85
p,p'DDD	2.74	2.71	2.6	2.71	2.6
o,p'DDT	2.71	2.99	2.7	2.99	2.7
p,p'DDT	2.42	2.47	2.42	2.47	2.42
Mirex	2.71	3.06	2.91	3.06	2.9

4.6 Ecotoxicological risk posed by OCPs in sediments, water, FFGs of benthic macroinvertebrates and *P. monodon* in estuarine ecosystems of South Coast, Kenya

4.6.1 Ecotoxicological Risk of OCPs in Estuarine Sediments

The ecotoxicological risk assessment based on sediment concentrations of 16 OCPs revealed distinct trends in potential environmental hazards across the South Coast estuarine ecosystem. The average OCPs concentrations per compound (Figure 4.32a) across the 12 stations ranged between 1.45 and 1.91 µg/kg for most OCPs, with HCB (1.91 µg/kg), p,p′ DDE (1.81 µg/kg), and Heptachlor (1.79 µg/kg) exhibiting the highest mean levels. Mirex recorded a moderated value of 1.25 µg/kg. These levels, while generally below international sediment quality guidelines, indicate the persistence and potential for bioaccumulation of legacy OCPs in the estuarine sediments.

On the other hand, the Hazard Quotient (HQ) analysis, calculated as the ratio of measured OCPs concentrations to the respective Threshold Effect Levels (TEL), showed values ranging from 1.20 to 1.95 across compounds (Figure 4.33b). Notably, HCB, Heptachlor, and p,p′ DDE had HQ values exceeding 1.75, suggesting a high likelihood of ecological effects at several sites. All 16 OCPs assessed had HQ > 1.

Lastly, PEL Exceedance Risk which was computed as the Probable Effect Level (PEL) exceedance risk analysis (Figure 4.33c) showed that HCB and Heptachlor exceeded the PEL at three or more stations, categorizing them under high ecotoxicological risk. Most other OCPs, including DDD and DDE isomers, were within TEL–PEL range, indicating moderate risk, while a few (e.g., Mirex) remained consistently below PEL thresholds, suggesting lower immediate sediment toxicity.

Figure 4.31.
Ecotoxicological risk summary of 16 OCPs based on sediment data across 12 estuarine stations along the South Coast of Kenya

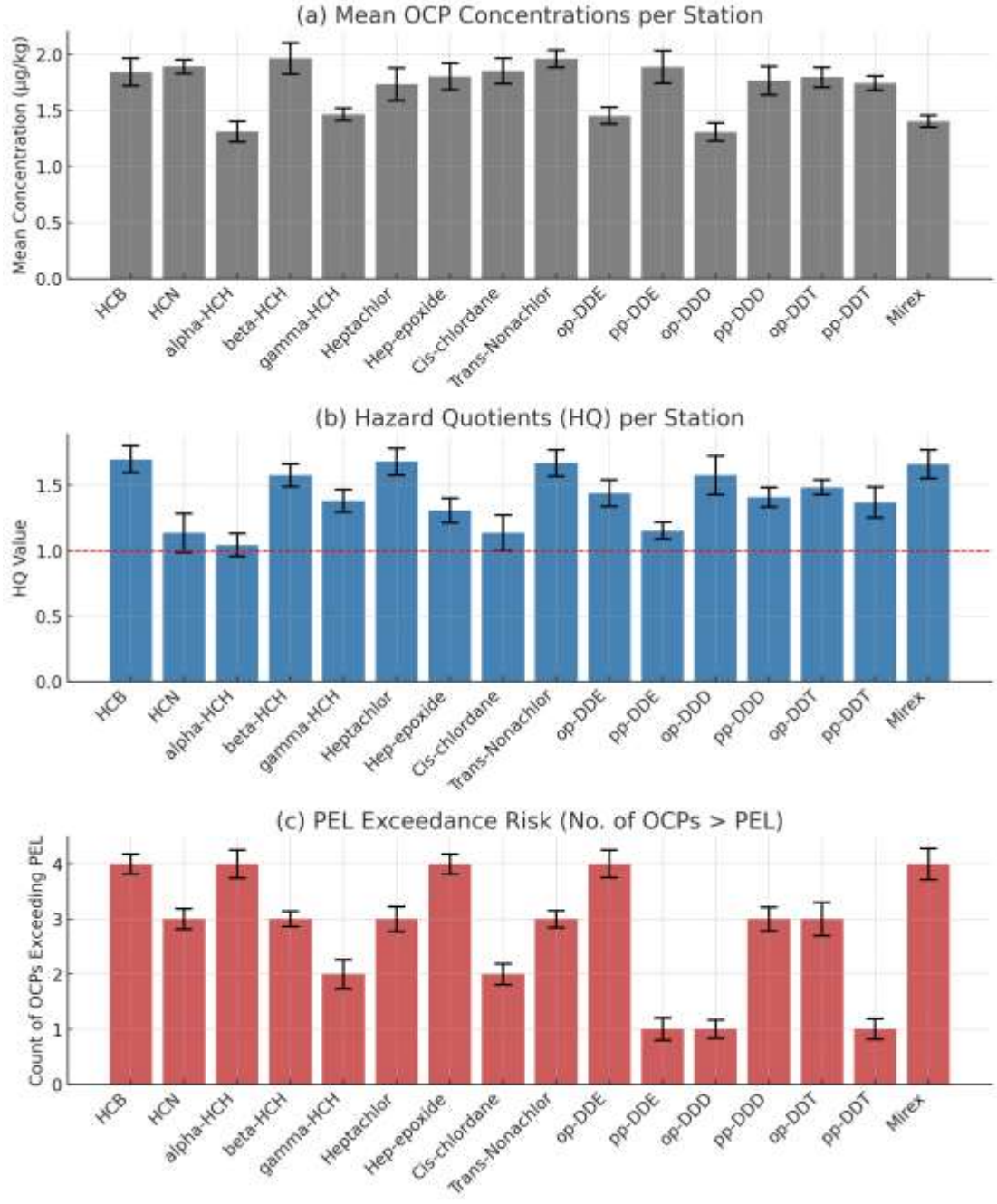

4.6.2 Sediment Pollution Indices

4.6.2.1 Contamination Factor (Cf)

The contamination factors (Cfs) of sixteen OCPs calculated from sediment samples collected across all stations in the study area (Figure 4.32). The results reveal extremely elevated Cf values for all compounds, far above typical sediment contamination thresholds. No compound recorded a Cf below 50, underscoring the widespread and severe contamination in the study area. The most striking result was observed for cis-chlordane, which exhibited a Cf value exceeding 500, indicating contamination levels more than 500 times higher than baseline concentrations.

Other compounds, including HCB, α-HCH, β-HCH, and heptachlor, also exhibited very high contamination factors, generally ranging between 80 and 150, reflecting significant sediment loading from both agricultural and public health pesticide applications. γ-HCH, heptachlor epoxide, trans-nonachlor, and DDT derivatives (p,p′-DDE, o,p′-DDT, and p,p′-DDT) recorded Cf values between 60 and 100, still indicating severe contamination levels. Even the compounds with comparatively lower values o,p′-DDE, o,p′-DDD, p,p′-DDD, and Mirex exceeded 50, indicating contamination intensities many times above ecological risk benchmarks. The overall Cf profile confirms that the sediments act as long-term reservoirs of legacy OCPs, with cis-chlordane standing out as the most critical contaminant of concern. This pattern strongly suggests heterogeneous sources, historical accumulation, and differential persistence of compounds in the aquatic environment.

Figure 4.32:
Contamination Factors (Cfs) of sixteen OCPs based on sediment samples from all stations in the study area.

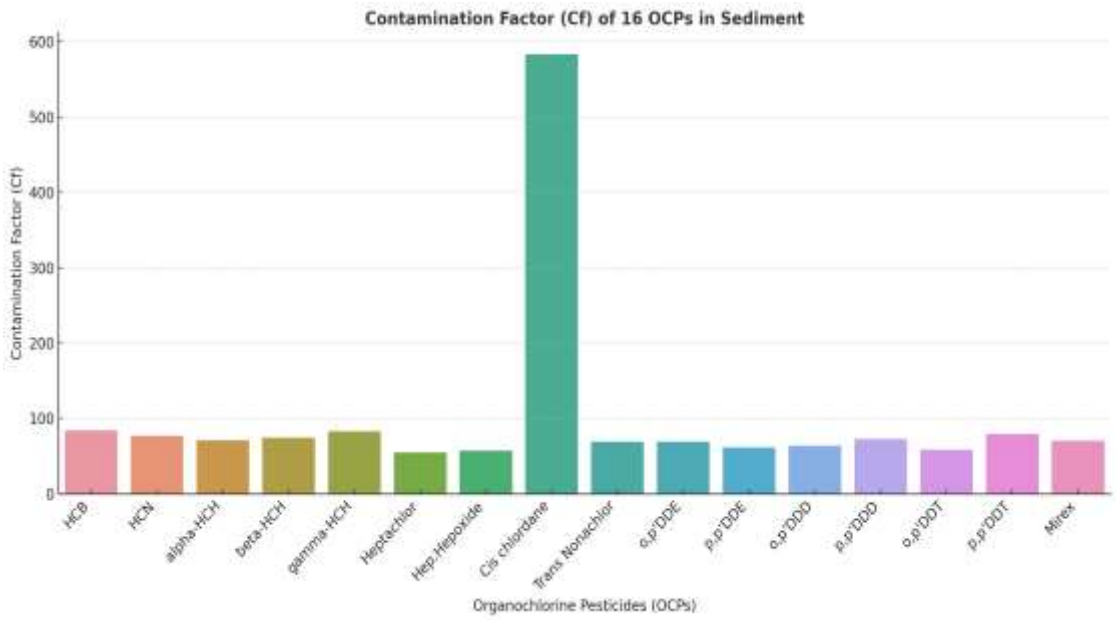

4.6.2.2 Geo-accumulation Index (Igeo)

The geo-accumulation index (Igeo) values for sixteen OCPs in sediment samples collected from all stations in the study area were also presented (Figure 4.33). The Igeo values, which compare current concentrations with geochemical background levels using a logarithmic scale, indicate a contamination status ranging from heavily contaminated (Igeo > 5) to extremely contaminated (Igeo > 7) across all compounds. The highest Igeo value was recorded for cis-chlordane (≈ 8.6), classifying it as extremely contaminated according to established sediment quality guidelines. Other compounds, including HCB, γ-HCH, p,p′-DDT, and Mirex, exhibited Igeo values close to or above 5.7, corresponding to the heavily contaminated category. The remaining compounds HCH isomers (α-, β-, γ-HCH), heptachlor, heptachlor epoxide, trans-nonachlor, and the DDT metabolites (o,p′-DDE, p,p′-DDE, o,p′-DDD, p,p′-DDD)

recorded Igeo values between 5.2 and 5.9, also falling within the heavily contaminated range. Overall, the Igeo results reinforce the pattern observed in the Cf analysis, with cis-chlordane standing out as the most severe contaminant of concern.

Figure 4.33:
Geo-accumulation Index (Igeo) values for sixteen OCPs detected in sediment samples across the study area

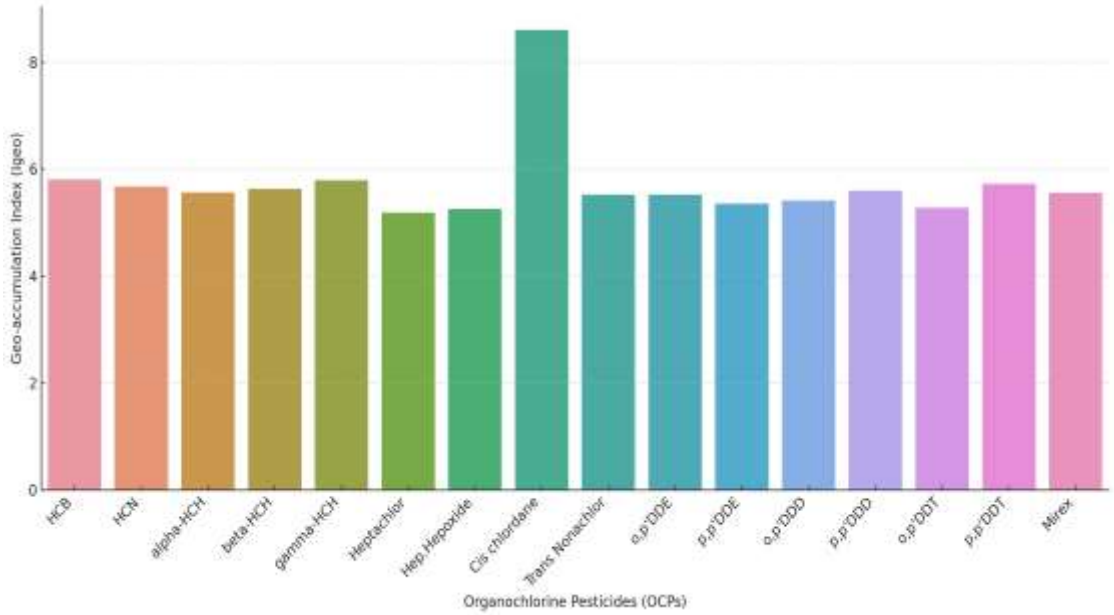

4.6.2.3 Pollution Load Index (PLI)

The Pollution Load Index (PLI) was calculated to provide a composite measure of the overall level of OCPs contamination in sediments. The PLI is determined as the *n*-th root of the product of all contamination factors (Cfs) for the compounds analyzed, expressed as: $\mathrm{PLI} = (\mathrm{Cf}_1 \times \mathrm{Cf}_2 \times \mathrm{Cf}_{31} \times \ldots \times \mathrm{Cfn})^{1/n}$

where *n* is the total number of contaminants assessed. This approach integrates the individual C_f values (Table 4.32) into a single value that reflects the general pollution status of sediments in the study area. Based on the geometric mean of the contamination factors (Cfs) of the 16 OCPs, the calculated PLI value was 2.57. This

means that, on average, the sediment OCP concentrations are more than twice the baseline values represented by their respective minima.

The PLI was calculated to provide a composite measure of the overall level of OCPs contamination in sediment samples (Table 4.32). Based on the geometric mean of the Cfs of the 16 OCPs analyzed, the PLI value was found to be 2.57. According to established interpretation thresholds, a PLI > 1.0 indicates pollution, with higher values suggesting increasing contamination severity. The observed value of 2.57 implies that sediments across the study area are moderately to heavily polluted with OCPs. This finding aligns with the high Cf and Igeo values observed for compounds such as p,p'-DDD, p,p'-DDE, and Mirex, which strongly influence the composite index. The elevated PLI underscores the persistent legacy of OCPs contamination and the potential for adverse ecological impacts through sediment-bound pollutant reservoirs.

Table 4.32:
Summary of OCPs pollution status in sediment based on Contamination Factor (Cf) and Geo-accumulation Index (Igeo)

OCPs	Mean Concentration	Min_Concentration	Contamination Factor (Cf)	Geo-accumulation Index (Igeo)	Igeo Classification
HCB	1.725	0.02	84.16	5.81	Extremely polluted
HCN	1.636	0.021	76.816	5.678	Extremely polluted
alpha-HCH	1.72	0.024	71.08	5.566	Extremely polluted
beta-HCH	1.614	0.022	74.383	5.632	Extremely polluted
gamma-HCH	1.669	0.02	83.052	5.791	Extremely polluted
Heptachlor	1.717	0.031	54.675	5.188	Extremely polluted
Hep.Hepoxide	1.723	0.03	57.255	5.254	Extremely polluted
Cis chlordane	1.693	0.003	583.772	8.604	Extremely polluted
Trans Nonachlor	1.665	0.024	69.097	5.526	Extremely polluted
o,p'DDE	1.68	0.024	69.118	5.526	Extremely polluted
p,p'DDE	1.681	0.027	61.366	5.354	Extremely polluted
o,p'DDD	1.681	0.026	63.899	5.413	Extremely polluted
p,p'DDD	1.705	0.023	72.864	5.602	Extremely polluted
o,p'DDT	1.726	0.03	58.322	5.281	Extremely polluted
p,p'DDT	1.687	0.021	79.201	5.722	Extremely polluted
Mirex	1.731	0.024	70.657	5.558	Extremely polluted

4.6.2.4 Potential Ecological Risk Index (RI)

To evaluate the potential ecological threat posed by OCPs in sediments, the study applied Hakanson's Potential Ecological Risk Index (RI) framework, which integrates both contamination levels (Cf) and compound-specific toxic response factors (Tr). The Ecological Risk Factor (Er) for each OCPs was computed as the product of its

contamination factor and toxic response factor, and the total RI was obtained by summing the Er values across all compounds. As presented in Figure 4.34, the Er values varied widely among the OCPs. The highest ecological risk factors were recorded for gamma-HCH (Er = 3322.06), beta-HCH (Er = 2975.34), and alpha-HCH (Er = 2843.18), primarily due to their high Cf values and elevated toxic response coefficients (Tr = 40). These findings highlight the critical ecological threat posed by HCH isomers in the study area. Other notable contributors to the RI included p,p'-DDD (Er = 2774.55) and p,p'-DDE (Er = 2698.85), reflecting their persistence, bioaccumulative nature, and toxicological significance. On the other hand, OCPs such as HCB (Er = 841.60) and HCN (Er = 768.16) had lower risk factors due to lower toxicity weights. The cumulative RI value across all 16 OCPs was 31,352.42, which according to Hakanson's classification indicates an extremely high ecological risk (RI > 600). This underscores the urgent need for sediment quality monitoring, pollutant source identification, and potential mitigation interventions in the region.

Figure 4.34:
Ecological risk evaluation of sediment-associated OCPs based on Contamination Factor (Cf), Toxic Response Factor (Tr), and Ecological Risk Factor (Er). The overall Potential Ecological Risk Index (RI) is calculated as the sum of Er values across all compounds

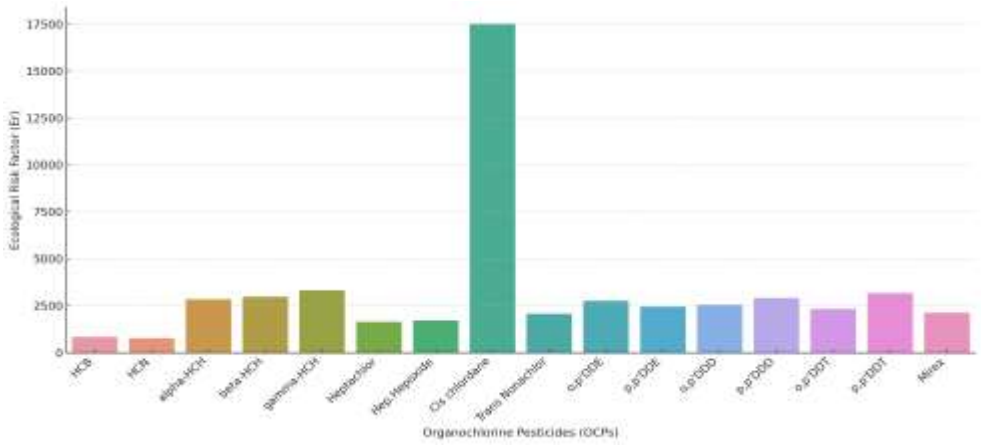

4.6.2.5 Nemerow Pollution Index (PN)

The Nemerow Pollution Index (PN) was calculated to evaluate the combined effect of average and peak contamination levels of OCPs in sediment samples. The index incorporates both the mean and maximum Contamination Factors (Cf) of the 16 OCPs analyzed. The computed PN value was 420.03, far exceeding the threshold of 3.0 used to classify a site as heavily polluted. This value is driven by the consistently elevated Cf values across all compounds, with particularly high values for HCB, gamma-HCH, and p,p'-DDD, which significantly influenced the PN. This extremely high PN score confirms that the sediments in the study area are severely contaminated by OCPs, reinforcing the conclusions drawn from the Contamination Factor, Igeo, and Potential Ecological Risk Index (RI) assessments. The results underscore the need for urgent environmental management interventions and routine monitoring of pesticide residues in benthic ecosystems.

4.6.2.6 Mean Effect Range Median Quotient (ERM-Q)

To assess the potential for combined toxicity from multiple OCPs in sediment, the Mean Effect Range-Median Quotient (ERM-Q) was computed. ERM-Q represents the average ratio of observed concentrations of contaminants to their respective Effect Range-Median (ERM) values, which are thresholds associated with adverse ecological effects. As shown in Figure 4.38, the ERM-Q values for individual OCPs ranged between 0.02 and 0.07, with all values falling well below the critical threshold of 0.5. The computed mean ERM-Q value was 0.119, indicating a moderate probability (~21%) of toxicity to sediment-dwelling organisms, according to Long et al. (2000).

These results suggest that while several OCPs are present at elevated concentrations, their collective contribution to probable biological effects remains within a moderate risk zone. However, the presence of persistent compounds such as p,p'-DDD, p,p'-DDE, and Mirex even at low concentrations may contribute disproportionately to potential chronic toxicity.

Figure 4.35:
Mean Effect Range-Median Quotient (ERM-Q) for OCPs in sediments

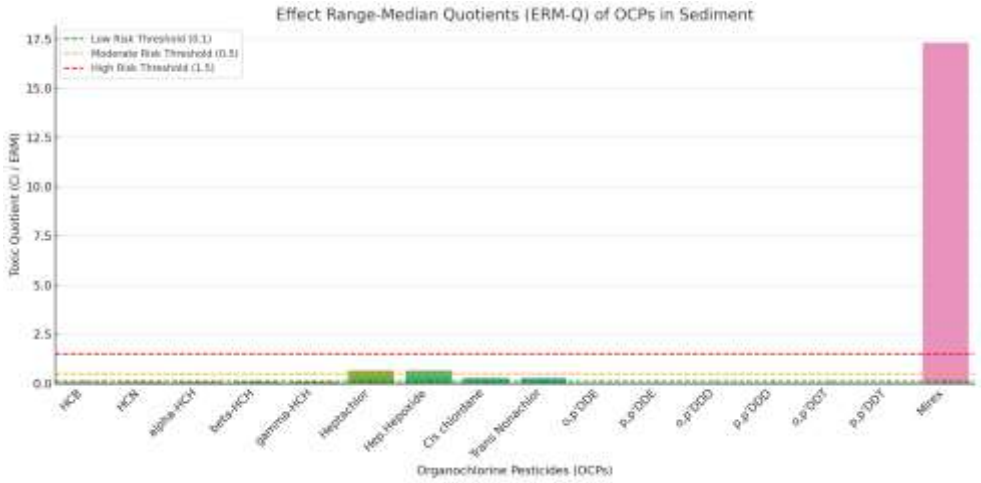

CHAPTER FIVE

DISCUSSION

5.1 Introduction

As in the other chapters, this section presents the discussion of the results based on: spatial and temporal variation in water quality parameters in estuarine ecosystems of South Coast; levels of pesticides in sediments, waters, trophic guilds of benthic macroinvertebrates and fish in estuarine ecosystems of South Coast, Kenya; relationship between physico-chemical water quality parameters and pesticide concentrations in water in estuarine ecosystems; bioconcentration and biomagnification of OCPs in water, sediments, the trophic levels of benthic macroinvertebrates and P. monodon in estuarine ecosystems of South Coast, Kenya; and ecotoxicological risk posed by OCPs in sediments, water, FFGs of benthic macroinvertebrates and P. monodon in estuarine ecosystems of South Coast, Kenya.

5.2 Spatial and temporal variation in water quality parameters in estuarine ecosystems of South Coast, Kenya

The study of estuarine ecosystems along Kenya's southern coastline reveals a nuanced and intricate picture of water quality dynamics shaped by geography, human activity, and hydrological processes. By examining nine key water quality parameters across twelve stations located in five estuaries Mapu, Mwena, Mkurumdzi, Ramisi, and Umba, this research demonstrates the complexity inherent in coastal aquatic systems. The estuaries span a gradient of environmental disturbance, from the relatively pristine Mapu Estuary to more heavily impacted systems like Mkurumdzi and Ramisi. The resulting spatial and temporal variations in water chemistry are significant not only statistically, as confirmed through robust ANOVA and interaction tests, but also

ecologically, offering insights into the functioning and resilience of these habitats (WRA, 2023; Kitheka *et al*., 2003; Osore *et al*., 2004).

One of the most prominent findings is the strong spatial heterogeneity across all measured parameters. This spatial pattern is especially evident for chemical indicators such as conductivity, salinity, TDS, phosphate, nitrate, and ammonia, all of which vary markedly between stations. This depended on anthropogenic activities that may have varied from one point to another. For example, estuarine and downstream stations, particularly Mwena Estuary, Mkurumdzi Estuary, and Mwena Majoreni, consistently displayed elevated concentrations of solutes and nutrients. Conductivity levels at these stations surpassed 1600 µS/cm, while TDS exceeded 1100 mg/L, and ammonia concentrations approached or surpassed 2.5 mg/L. Other factors that impacted on them include the dilution effect of the freshwater river discharge, precipitation, tidal changes and the ingestion by both macro and micro plants (autotrophs). These values contrast sharply with those of more upstream or vegetated stations like Mapu and Mwena Manda, where conductivity remained below 250 µS/cm and nutrient concentrations were generally an order of magnitude lower. Similar results have been documented where it is averred that surface runoff changes the chemical composition of rivers and thus the receiving lotic and lentic systems due to a lot of organic matter rich in nitrates and phosphates that are likely to be swept downstream during spates (Lu *et al*., 2019). Further, in the Kenyan Coast, physico-chemical water quality levels in the upstream stations have been confirmed to be low compared to estuaries (Mwashote, 2003; Kiteresi *et al*., 2013).

Such stark spatial differences are best understood in light of land use, hydrological inputs, and estuarine morphology. Downstream stations are more frequently subjected to saline water intrusion, especially during the dry season, which raises both conductivity and salinity (Kitheka & Mavuti, 2016). In addition, estuarine regions located closer to human settlements are more vulnerable to anthropogenic inputs, including domestic waste, agricultural runoff, and industrial effluents (WHO, 2021). The Mkurumdzi Estuary is a prime example: situated downstream of agro-industrial operations, including sugarcane cultivation by KISCOL and mining by Base Titanium, it consistently exhibited some of the highest values for phosphate and ammonia, likely reflecting direct nutrient loading. By contrast, the Mapu Estuary, with its dense riparian vegetation and minimal land-based development, serves as a useful reference, displaying consistently low values across all measured variables and demonstrating the buffering capacity of relatively undisturbed systems. Kamau *et al*. (2022) who studied the impact of land use on water quality in Kenyan estuarine systems, supported the same argument as above that the intensity of poor water quality is associated with the massive anthropogenic activities usually common downstream where high population is concentrated.

These findings further are broadly consistent with other studies in Kenya and beyond. Kitheka *et al*. (2003), working in the Gazi Bay region, found that salinity and nutrient levels increased significantly at the estuarine mouth compared to upstream zones, a pattern mirrored here in Mwena and Mkurumdzi. In Mida Creek, Osore *et al*. (2004) documented similar spatial gradients, linking high phosphate concentrations in lower reaches to nutrient-rich sediment influx and tidal influence. More broadly, Lønborg *et al*. (2024) reported that estuarine areas closest to urban discharge points showed

elevated nutrient levels and higher electrical conductivity due to saline mixing and anthropogenic inputs, echoing patterns observed in Mkurumdzi and Mwena.

While spatial differences dominate the observed patterns, temporal variation also plays a notable role, though its expression is more muted. Only a handful of parameters temperature, DO, pH, conductivity, and TDS exhibited statistically significant monthly variation. These changes were generally subtle and often site-specific, suggesting that broader seasonal dynamics were being modulated or masked by localized factors (Pinheiro *et al.*, 2021). Temperature followed expected seasonal patterns, peaking between February and April during the dry season and declining during the long rains in June and July. Dissolved oxygen levels displayed an inverse pattern, with higher concentrations during the cooler rainy months and lower levels during warmer periods. However, parameters like phosphate, nitrate, and ammonia did not show significant temporal variability in aggregate analysis, suggesting either chronic inputs from constant sources or high within-month variability that blurred seasonal signals. The observed elevated DO levels could be due to microbial activities during the denitrification process where NO is converted to N_2 and O_2. Such findings were also reported by Zhu *et al*. (2019) who associated them with denitrification.

The apparent temporal stability of nutrient concentrations is initially counterintuitive, given the expected influence of rainfall and runoff. However, this finding is consistent with work by Mutia *et al*. (2021), who noted that nutrient concentrations in the Tana River estuary remained relatively steady throughout the year, likely due to consistent land-based inputs and buffering by mangrove systems. Saravanakumar *et al*. (2008) observed a similar phenomenon in several Indian estuaries, where nutrient loading from

domestic and agricultural sources persisted year-round, thereby diminishing observable seasonal effects. In the present study, despite the visual suggestion of peaks in nitrate and phosphate during months like October and March, the statistical insignificance of these variations likely reflects the overwhelming spatial heterogeneity present in the system. That is, the magnitude of difference between stations at any given time was far greater than the difference between months at any one station (Kiteresi *et al*., 2013).

Spatio-temporal interactions provide further depth to the analysis, as highlighted by significant interaction terms in the two-way ANOVA for nearly all parameters. These interactions demonstrate that the temporal response of water quality is not uniform across space. For example, while January and February were associated with increased salinity and TDS at downstream stations like Mkurumdzi Estuary, those same months saw little to no change at upstream stations such as Mapu. Similarly, DO values fluctuated across months in different directions at different sites, with Mwena Manda recording its highest value in February, while Mapu exhibited its lowest in October. These results indicate that responses to seasonal drivers like rainfall and temperature are mediated by local conditions such as tidal influence, vegetation cover, and proximity to pollution sources. Such observations have been reported elsewhere by other researchers (Bouillon et al., 2007; Kamau *et al*., 2022).

The episodic nature of some parameter spikes, such as the August peak in ammonia at Mkurumdzi Gazi, further supports the role of localized and potentially one-off pollution events. These may result from sudden discharges, heavy rainfall-induced runoff, or changes in flow dynamics (Krija *et al.*, 2012). That such spikes did not produce significant monthly trends across all stations again underscores the complexity and site-

dependence of estuarine water quality. This pattern was similarly reported in the Democratic Republic of Congo by Bisimwa *et al*. (2022), where water quality parameters responded differently to seasonal changes depending on the station's position along the system and its hydrological connectivity.

A critical layer of understanding emerges when these spatial and temporal patterns are contextualized within the physical and ecological settings of the estuaries themselves. The Mapu Estuary, with its small catchment area and minimal human disturbance, exhibited stable and low values across all parameters. It functions as a baseline ecosystem where natural processes dominate, providing an essential contrast to more disturbed sites. Mwena Estuary, though relatively close geographically, presented a very different profile, reflecting moderate human influence, especially from Gazi village. Here, nutrient levels were elevated and salinity fluctuated more dramatically, indicating a greater degree of tidal influence and anthropogenic input (Jacobs *et al*., 2020).

Mkurumdzi stood out for its consistently extreme values, particularly for ammonia, conductivity, and phosphates, suggesting intense and likely unregulated inputs from both agro-industrial operations and mining. Ramisi, characterized by geothermal inflows and seasonal flow variability, showed temperature and salinity dynamics that were distinct from the other estuaries. These dynamics are likely driven by the mixing of hot spring inputs and ephemeral tributary flows, adding a layer of natural complexity to the system (Ong'anda *et al*., 2013). Finally, the Umba Estuary, with its vast and transboundary catchment, recorded moderate to high nutrient levels and significant

sedimentation, particularly during the wet season, likely reflecting long-distance upstream inputs and widespread land use in both Kenya and Tanzania.

What is particularly noteworthy is that even within each estuary, the differences between upstream and downstream stations were often pronounced. For example, within the Mkurumdzi Estuary, the upper site showed relatively moderate levels of nutrients and salinity, while the lower site, closer to Gazi Bay, exhibited some of the highest concentrations in the entire study. This internal heterogeneity within estuarine systems points to the need for fine-scale sampling and indicates that estuaries, though sometimes treated as unified ecological units, are in fact composed of multiple microhabitats with distinct chemical and physical characteristics (Jacobs *et al*., 2020).

5.3 Concentration of OCPs in sediments, waters, trophic guilds of benthic macroinvertebrates and fish in estuarine ecosystems of South Coast, Kenya

5.3.1 Concentration of OCPs in sediments

The comprehensive analysis of OCP residues in sediments across Kenya's southern coastal estuaries reveals intricate patterns shaped by legacy pollution, seasonal variability, and interacting spatial and temporal drivers. Drawing from three analytical dimensions: spatial, temporal, and spatio-temporal, this discussion explores how pesticide concentrations fluctuate and persist in sediment environments and what these patterns imply for the fate and behavior of OCPs in tropical estuarine systems.

From a spatial standpoint, the study revealed no statistically significant variation in OCP concentrations across the twelve sampling stations. The ANOVA tests yielded high *p*-values ($p > 0.05$) for all compounds, including traditionally persistent ones such as HCB ($p = 0.9998$), γ-HCH ($p = 0.8401$), and p,p′DDT ($p = 0.9861$). This indicates a

uniform distribution of residues across the study area. The lack of spatial heterogeneity suggests that inputs of these pollutants are either historic and broadly dispersed, or that their environmental behavior driven by sediment resuspension, tidal mixing, and diffusion leads to homogenization across estuarine environments. This spatial uniformity aligns with patterns observed in other low-energy estuarine systems where sediment mixing and the persistence of older contaminants obscure point-source signature (Munoz-Arnanz & Jimenez, 2011). Studies in the Niger Delta and South China estuarine plains have shown similar spatial flattening in sediment OCP profiles, particularly in areas with prolonged agricultural legacy and limited recent pesticide application (Zhou *et al*., 2017). Similarly, the close association of some of the environmental pollutants like pesticides is a clear pointer of similar sources of pollution (Ra *et al*., 2014).

In contrast to this spatial uniformity, the temporal analysis revealed significant and consistent month-to-month variability. All 16 OCPs demonstrated statistically significant temporal differences ($p < 0.001$), with sharp peaks observed in February to April 2019. Compounds such as γ-HCH, p,p′DDE, α-HCH, and p,p′DDT showed well-defined maxima during this period, followed by a decline in subsequent months. This seasonal pulse corresponds to the rainy season, a time when increased surface runoff mobilizes OCP residues from agricultural soils, eroded banks, and road surfaces into estuarine environments. Such temporal patterns are consistent with findings in comparable tropical regions, including the Mekong Delta and parts of coastal Brazil, where sediment-bound OCPs surge following peak rainfall due to land-surface washing and sediment transport (Oliveira *et al*., 2016). The presence of both parent and degradation products, particularly within the DDT family, implies that while

breakdown processes are active, they are either incomplete or overridden by periodic inputs. The persistence of HCH isomers and their coordinated seasonal peaks reinforce the view that runoff events drive synchronized inputs across sites.

The spatio-temporal analysis offered the most nuanced insight. Two-way ANOVA revealed significant interaction effects between site and month ($p < 0.001$ for all compounds), underscoring that the magnitude and direction of temporal change were not uniform across the region. For example, while γ-HCH and p,p′DDE showed sharp seasonal peaks at stations Umba and Mwena estuaries, the response was much flatter at Mapu and Ramisi Bridge. Similarly, Cis chlordane and HCB showed greater sensitivity to wet season inputs in stations located closer to agricultural watersheds, suggesting land use and hydrological gradients as well as historical sources played a key role in modulating contaminant flux. This could also suggest that the environmental behavior and loading sources of these compounds were highly site-specific during the sampling period.

These findings suggest that the hydrodynamic properties, sedimentation rates, land use patterns, and estuarine morphology at each site modulate how seasonal forces translate into contaminant loads. Estuaries that receive direct runoff from agricultural lands, or are adjacent to densely settled areas, may respond to rainfall with pronounced contaminant surges. In contrast, more buffered or forested sites exhibit dampened responses, suggesting a role for vegetative barriers, lower erosion, or limited direct pollution pathways. These findings were in agreement with Lin *et al*. (2016) who reported that OCPs find their way into water/sediments in estuarine systems due to dry and wet season depositions. Moreover, pronounced erosion and fluvial sources from the

freshwater catchments act as the main sources of OCPs in estuaries (Fair *et al*., 2018). It has also been confirmed that when high concentrations and frequencies of pesticides are detected in given areas of study, then there is reason to believe that they have been used recently or their origin is historical (Peris *et al*., 2024; FAO, 2023).

This spatially variable response to temporal forcing illustrates the importance of interpreting seasonality in a localized context. While broad climatic and hydrological forces apply regionally, their impact on sediment OCPs levels is filtered through site-specific conditions such as slope, vegetation, catchment activity, and estuarine hydrodynamics. Therefore, despite uniform spatial patterns in annual averages, monthly analyses reveal hidden heterogeneity and complexity, physical, chemical and biochemical characteristics of each pesticide. For example, according to Yang *et al*. (2005a, b) DDTs are characterized by lower water solubility, biodegradability and vapour pressure, and higher attraction between sediment particles and lipophilicity as compared to HCH.

Another important observation from the spatio-temporal assessment is the persistence of certain compounds even after the seasonal peak. For instance, while γ-HCH and p,p′DDE declined after April, they remained elevated at several sites through July, suggesting either a slower rate of decline or multiple small-scale reintroductions. This temporal persistence points to the potential of sediment systems acting as both sinks and secondary sources, gradually re-releasing OCPs through resuspension, bioturbation, or chemical desorption. This finding corresponded well with other studies that have reported resuspension of OCPs from the sediments (Dorosh *et al*., 2021; Long *et al*., 2005).

The sedimentary behavior of OCPs in these Kenyan estuaries is marked by minimal spatial but strong temporal variation, overlaid by complex spatio-temporal interactions. These patterns reflect a legacy of diffuse historical contamination that is periodically reactivated by seasonal rainfall and site-specific transport processes. The findings challenge simple attributions of contamination to static sources and instead emphasize the importance of dynamic, seasonally modulated, and spatially mediated mechanisms in the environmental fate of persistent pollutants. To argument these findings, Wanjeri *et al*. (2022) reported that historical pollution of OCPs were common in many of the studied sites along the Tana and Sabaki estuaries in the north coast of Kenya.

5.3.2 Concentration of OCPs in waters

The analysis of organochlorine pesticide (OCP) levels in water samples collected across the southern coast of Kenya revealed complex spatial, temporal, and spatio-temporal variability, highlighting the dynamic and multifactorial nature of pesticide distribution in estuarine and freshwater systems. The detection of all sixteen target OCPs despite bans and regulatory restrictions on many of them underscores the persistence of these compounds in aquatic environments and suggests both historical deposition and potential ongoing inputs. The presence of metabolites such as DDE and DDD further confirms the degradation of parent DDT compounds and their long-term environmental residency. According to Berntssen *et al*. (2017), when α-HCH and γ-HCH readily transforms into ß-HCH there is reason to believe an existence of historical origin.

Spatial analysis through one-way ANOVA revealed significant differences in concentrations for 15 of the 16 compounds across the twelve sampling stations, indicating that pesticide distribution is strongly site-dependent. Notable spatial variability was observed for HCB, HCN, α-HCH, and p,p′DDD, which recorded high F-values and low p-values ($p < 0.001$), reflecting heterogeneous sources and differential loading intensities across the region. Tukey's HSD post-hoc comparisons affirmed that downstream stations, often closer to estuarine outlets or human settlements, exhibited elevated concentrations relative to upstream or less disturbed locations. This spatial trend aligns with patterns observed in similar tropical estuarine studies. For instance, in the Niger Delta (Adeyemi *et al*., 2008), pesticide residues were highest near agricultural zones and urban settlements, while in India's coastal rivers, elevated HCH and DDT isomer levels were reported in estuarine reaches with low flow and high runoff influence (Singh *et al*., 2016).

Temporal variations were equally prominent. Monthly trends showed that compounds such as γ-HCH, β-HCH, Heptachlor, and p,p′DDE exhibited consistent seasonal peaks during the rainy season, especially from March to May 2019. These increases likely reflect heightened surface runoff and erosion of contaminated soils, leading to greater pesticide transport into aquatic systems. ANOVA results validated these observations, with all compounds showing statistically significant differences over the twelve-month period ($p < 0.001$). For example, γ-HCH had the highest F-value ($F = 166.34$), indicating a strong seasonal component to its concentration dynamics. Tukey tests further pinpointed the March–May period as significantly elevated compared to dry season months like September and October, reinforcing the role of rainfall in modulating OCP flux. Peris *et al*. (2024) found that pesticide concentrations were

remarkably higher during the planting season unlike other seasons when there were no such activities.

Interestingly, while many compounds peaked during wet months, others such as Mirex, o,p′DDD, and Trans Nonachlor showed more stable or modest fluctuations, possibly due to their strong binding affinity to sediments and low solubility. Mirex, in particular, maintained relatively consistent concentrations across months, which may indicate residual environmental persistence rather than active loading. Such persistence is consistent with global findings: for example, Montuori *et al*. (2015) reported similar stability of Mirex and DDD compounds in Brazilian coastal waters, attributing their low temporal variability to slow degradation and sediment accumulation.

The spatio-temporal analysis further emphasized that the distribution of OCPs is not merely additive across space and time but interactive. Two-way ANOVA revealed statistically significant interactions between station and month for all compounds ($p < 0.001$), indicating that temporal trends were not uniform across locations. This suggests that while rainfall events influence all sites, the magnitude and direction of change vary depending on localized factors such as catchment land use, hydrological connectivity, and geomorphological settings. For instance, γ-HCH and p,p′DDE showed strong seasonal spikes at stations close to agricultural zones, suggesting input from pesticide application runoff, while upstream forested stations exhibited flatter seasonal curves, likely due to natural attenuation or lower exposure. These findings are confirmed by Peris *et al*. (2024) who reported that pesticides contamination from cultivated agricultural fields were significantly higher than the uncultivated ones, which they attributed to agricultural application.

Furthermore, compounds like Cis Chlordane, HCB, and Heptachlor, although showing peak concentrations during the rainy season, declined only slightly in the subsequent months, suggesting continued inputs or slow environmental breakdown. This finding echo results from studies in Southeast Asia, where chlordane and HCB residues persisted in water columns long after peak runoff events, due to continuous leaching from surrounding soils (Zhou *et al*., 2008). Such prolonged presence may also be linked to low microbial degradation rates under anoxic or brackish conditions commonly found in mangrove-lined estuaries.

The station-level differences in response to seasonal variation underscore the importance of considering site-specific characteristics when evaluating environmental pesticide risks. For example, some estuarine sites may act as sinks, retaining OCPs longer due to sedimentation and hydrodynamic retention, while others with higher flushing rates may show more transient concentration peaks. In this study, locations further downstream consistently exhibited higher concentrations for several compounds during peak periods, while stations located upstream showed flatter profiles, possibly reflecting their lower exposure or greater hydrological dilution.

The findings demonstrate that OCPs concentrations in water along Kenya's southern coast are governed by a dynamic interplay of spatial and temporal drivers, with land use, rainfall, runoff pathways, and compound-specific properties all influencing pesticide behavior. These results not only provide insight into current exposure risks but also serve as a valuable baseline for assessing long-term trends, particularly as land use and climate patterns continue to evolve in the region.

5.3.3 Concentration of OCPs in macro-invertebrate FFGs

The assessment of OCPs concentrations in macroinvertebrate guilds provides a crucial ecological perspective on contaminant transfer through aquatic food webs. Macroinvertebrates play pivotal functional roles in estuarine and freshwater ecosystems, and their ecological guilds (i.e. *T. palustris*, *N. undata*, Atyidae, *S. cucullata*, and *Rhagovelia* spp.) exhibit differential exposure to OCPs based on their feeding strategies, habitat preferences, and trophic positioning. The spatial and temporal variations in pesticide accumulation across these guilds reflect both environmental distribution patterns and biological uptake mechanisms, offering insights into ecosystem health and contaminant dynamics.

5.3.3.1 *T. palustris*

The shredder guild displayed conspicuous spatial and temporal heterogeneity in OCPs concentrations, with statistical evidence confirming significant differences across sites ($p < 0.001$ for all compounds). High spatial variation, as observed in Figure 4.10 and Table 4.11, suggests differential contaminant input or retention in localized habitats, potentially driven by riparian land use, vegetation density, and sediment binding capacity. The dominance of compounds such as gamma-HCH, heptachlor, and o,p′-DDD aligns with previous studies indicating their high environmental persistence and affinity for detritus-rich substrates (Olisah *et al.*, 2021; Walker *et al.*, 2012). The elevated accumulation of DDT derivatives in *T. palustris* at sites such as Umba and Mwena estuaries may point to legacy contamination from upstream agricultural activity or episodic remobilization from sediments during hydrological shifts. Studies have documented historical sources of some OCPs like DDTs in estuaries resulting into

biodegradation via aerobic and anaerobic conditions (i.e. Tang *et al*., 2007; Hitch & Day, 1992) thus supporting my findings in this study.

Temporally, *T. palustris* exhibited significant seasonal fluctuations in OCP burdens ($p < 0.001$ for most compounds; Table 4.12), with concentration peaks frequently aligning with the onset of the long rains (March–May). These temporal trends are consistent with findings from tropical river systems, where runoff during rainy seasons has been shown to transport emerging pollutants from terrestrial sources into aquatic ecosystems (Lema & Mwegoha, 2023). The interaction effects from the two-way ANOVA (Table 4.13) further support a spatio-temporal dynamic, indicating that site-level concentration patterns were season-dependent, likely due to varying catchment hydrology and organic matter inputs.

5.3.3.2 *N. undata*

N. Undata (scraper-grazers), which feed by scraping biofilm, algae, and detritus from submerged surfaces, recorded high levels of chlorinated pesticides across stations, with the strongest spatial discrimination seen in o,p′-DDD, HCN, and gamma-HCH ($p < 0.001$). The results presented in Figure 4.13 and Table 4.14 show that *N. Undata* bioaccumulated a broader spectrum of OCPs than *T. palustris*, suggesting exposure to both waterborne and periphyton-bound residues. Periphyton has been recognized as a significant medium for OCP adsorption, particularly for lipophilic compounds (Burgess *et al*., 2025) . The statistically significant interaction effects ($p < 0.001$) indicate that specific site-month combinations disproportionately influenced accumulation patterns, underscoring the role of biofilm dynamics and substrate contamination in driving exposure.

The pronounced peaks in DDT and HCH isomers during late wet season months reflect temporal variability in pollutant mobilization and uptake (Figure 4.14, Table 4.15). As *N. undata* interact closely with benthic microhabitats, their contaminant profiles may reflect both recent inputs and historical deposition layers. Notably, the presence of cis-chlordane and trans-nonachlor in significant quantities aligns with their known persistence and sediment-binding properties, often exceeding their presence in the overlying water column (Tang *et al*., 2021).

5.3.3.3 Atyidae

Collector-gatherers accumulate fine particulate organic matter (FPOM), often from sediment surfaces, making them particularly vulnerable to sediment-bound OCPs. As shown in Figure 4.16 and Table 4.18, this guild exhibited consistently high pesticide loads across nearly all sampling stations, with o,p′-DDD, gamma-HCH, and HCB recording the highest spatially significant F-values. This distribution strongly implicates the role of sediment-sorbed pesticide fractions in driving trophic uptake in these organisms. Prior studies in similar estuarine systems have demonstrated elevated OCP loads in collector-gatherers relative to grazers, with sediment properties such as organic matter content and redox potential acting as key modulators (Maramis & Kristijanto, 2012; Pastorino *et al*., 2020a, b).

Temporal analysis (Figure 4.17; Table 4.19) revealed that seasonal peaks in contaminant levels coincided with sediment resuspension events likely associated with increased runoff and tidal mixing. Compounds such as p,p′-DDD, o,p′-DDE, and mirex showed elevated levels during transitional months (April–June), suggesting delayed remobilization following pesticide runoff inputs. The interaction terms (Table 4.20) further reinforce the non-uniform nature of OCPs accumulation in this guild, with

significant site-specific differences in seasonal concentration profiles. This reinforces the hypothesis that collector-gatherers (Atyidae) serve as effective sentinels for integrated exposure pathways, encompassing both suspended particulates and sediment-associated contaminants. Several studies have emphasized the need for the use of benthic macroinvertebrates for environmental monitoring and assessment due to their sedentary nature (e.g. Masese *et al*., 2013; Nyakeya *et al*., 2022).

5.3.3.4 *S. cucullata*

The filterer guild, composed mainly of organisms that sieve particulate matter from the water column, revealed a different OCPs accumulation profile. While spatial differences were statistically significant across all compounds ($p < 0.001$; Table 4.21), the overall concentrations were generally lower than those found in deposit feeders (Atyidae). This suggests a predominance of sediment-bound over freely dissolved OCPs in the system, corroborating previous reports from Kenyan coastal waters where bioavailable pesticide fractions in water were below detection limits despite high sediment burdens (Muendo *et al*., 2019, 2012). Nevertheless, compounds such as mirex, HCN, and heptachlor showed marked peaks in filter feeders, especially at sites with high turbidity and suspended sediment concentrations indicative of particle-mediated uptake pathways (Figure 4.19).

Temporal patterns (Figure 4.20; Table 4.22) showed less pronounced but still statistically significant fluctuations, with elevated levels observed during early rainfall months. These peaks likely reflect increased input of contaminated particulates from upstream sources and remobilization from sediments due to turbulence. The significant spatio-temporal interaction effects (Table 4.23) suggest that *S. cucullata* experienced episodic exposure events tied to both hydrological shifts and location-specific pollutant

retention, reaffirming their utility in short-term contamination monitoring (Wanjeri *et al*., 2022).

5.3.3.5 *Rhagovelia* spp.

Predatory macroinvertebrates occupy higher trophic levels and are thus critical indicators of biomagnification potential within aquatic ecosystems. The results revealed pronounced spatial differences in pesticide concentrations across the 12 sampling stations (Figure 4.22; Table 4.24), with statistically significant F-values ($p < 0.001$) for all OCPs. Compounds such as o,p′-DDD, heptachlor, mirex, and gamma-HCH were notably elevated in *Rhagovelia* spp., suggesting their trophic positioning predisposes them to higher bioaccumulation. This is consistent with prior ecological risk assessments, which identified predator guilds as hotspots for legacy OCPs due to dietary transfer and lipid storage (Guzzella *et al*., 2005).

Temporal analyses (Figure 4.23; Table 4.25) confirmed seasonal variability, with peak concentrations of DDT isomers and chlordane compounds during April–June and October–November coinciding with major rainfall events. This temporal trend mirrors patterns observed in *S. cucullata* but is amplified due to cumulative trophic transfer. The results from the two-way ANOVA (Table 4.26) further demonstrate significant interaction effects ($p < 0.001$), indicating that OCPs levels in *Rhagovelia* spp. were strongly influenced by the combined effects of site-specific inputs and temporal hydrodynamics. The consistent co-occurrence of o,p′-DDD, p,p′-DDE, and mirex at higher concentrations suggests either persistent historical input or long-term sediment remobilization (Okuku *et al*., 2013).

Predators such as odonate larvae, hemipterans, and beetles possess physiological adaptations (e.g., cuticle lipid layers and longer life cycles) that enhance OCP retention. Their trophic behavior preying on contaminated grazers and filter feeders magnifies their exposure risk, making them key species for tracking food web contamination pathways. Such an argument is advanced by Palapa and Maramis (2015) who stated that predators preying on scraper-grazers and shredders accumulate more OCPs compared with those at the base of the trophic level.

5.3.3.6 Inter-Guild Comparisons

A comparative analysis across the five macroinvertebrate guilds revealed clear guild-specific differences in both the magnitude and spectrum of pesticide accumulation. *T. palustris* and Atyidae consistently recorded higher OCP concentrations compared to *S. cucullata* and *N. undata*, while *Rhagovelia* spp. exhibited the highest concentrations overall, indicating potential for biomagnification. For example, p,p′-DDD, beta-HCH, and mirex were present in significant quantities across all guilds but were especially elevated in *Rhagovelia* spp. and Atyidae.

The exposure pathway for each guild influences these patterns. *T. palustris* and Atyidae are benthic and interact directly with contaminated detritus and sediment particles. In contrast, *S. cucullate* depend on suspended particles, which may carry lower concentrations of hydrophobic OCPs. *N. undata*, while exposed to periphyton and biofilm, appear less susceptible to high OCPs accumulation unless biofilms are heavily contaminated. This aligns with findings by Li *et al.* (2020), who reported higher OCPs residues in deposit feeders and carnivores than in grazers and omnivores in Chinese estuarine systems.

Rhagovelia spp. elevated OCPs loads suggest trophic magnification, supported by the consistent detection of higher-order metabolites (e.g., DDE, DDD) relative to parent DDTs. This pattern was also supported by spatial-temporal interaction effects, which were more significant in *Rhagovelia* spp. than in other guilds. Moreover, the persistence of high F-values for DDT-related compounds and HCH isomers in all guilds points to chronic, system-wide contamination that likely originates from both historic agricultural inputs and ongoing runoff (Li *et al*., 2023; Liu *et al*., 2012).

5.3.3.7 Compound-Specific Accumulation Patterns

The variation in OCPs uptake across guilds also reflects the physico-chemical properties of individual compounds. Lipophilic, persistent compounds like mirex, p,p′-DDD, and trans-nonachlor exhibited widespread accumulation across all FFGs, while more volatile or less hydrophobic compounds such as gamma-HCH and alpha-HCH showed moderate accumulation but strong spatial and temporal fluctuation. Mirex, trans-nonachlor and DDT metabolites have been considered to be widely spread among benthic organisms mainly due to their lipophilic characteristics (Sathish & Patterson, 2025; Shamma *et al*., 2024).

The dominance of p,p′-DDD and p,p′-DDE across functional guilds suggests extensive transformation of parent DDTs, likely under anaerobic sediment conditions common in estuarine benthic zones. The ratio of DDE + DDD to total DDT across most macroinvertebrates exceeded 0.6, indicative of aged DDT contamination (Zhou *et al*., 2017). Notably, cis-chlordane and trans-nonachlor were persistently detected in all guilds, suggesting that technical chlordane formulations were historically used in the catchment and continue to exert ecological pressure.

The HCH isomers (especially beta-HCH) were consistently found in Atyidae and Rhagovelia spp., which is concerning given their high environmental persistence and bioaccumulative potential (Wurl *et al*., 2006). Heptachlor and heptachlor epoxide showed similar trends, with higher concentrations in *Rhagovelia* spp. and *T. palustris*, indicating both direct uptake and metabolite conversion.

5.3.3.8 Biogeochemical and Ecological Implications

The results underscore the role of macroinvertebrates as both indicators and vectors of contaminant transport in aquatic ecosystems. The functional diversity of macroinvertebrate guilds reflects the spectrum of exposure pathways: detrital ingestion, surface scraping, water filtration, and trophic predation. These guilds thus offer a comprehensive lens through which pesticide dynamics can be understood both spatially and temporally.

Spatio-temporal interaction effects (i.e., significant interaction terms in the two-way ANOVA) were strongest in *Rhagovelia* spp., Atyidae, and *N. undata*, suggesting that pesticide uptake is driven not only by environmental distribution but also by biological activity cycles, feeding rates, and habitat overlap (Shamma *et al*., 2024). Sites like Umba, Ramisi, Mwena and Mkurumdzi estuaries repeatedly emerged as hotspots for pesticide bioaccumulation, indicating localized contamination risks that may stem from agricultural runoff, informal pesticide disposal, or sediment disturbance. This is in line with Peter, *et al*. (2018) who averred that the concentration of OCPs in the environment depend on their bioavailability for the biota and thus bioconcentrate and biomagnify along the trophic levels.

The alignment between rainfall periods and temporal peaks in OCPs concentrations suggests that catchment hydrology significantly modulates pesticide delivery to aquatic habitats. The influence of seasonal flooding, tidal mixing, sediment resuspension and the general biotic and abiotic materials cannot be overstated, especially in estuarine systems with complex freshwater-marine interactions. Arguing on similar background, Roche and Tidou (2009), averred that estuarine systems receive regular OCPs interchange between sediments, land, interstitial waters, and community attributes which influence the bioavailability of pesticides.

5.3.3.9 Synthesis of Bioaccumulation Patterns

Synthesizing across spatial, temporal, and spatio-temporal scales reveals three key dimensions of bioaccumulation:

1. **Spatial Heterogeneity**: Sites such as Umba, Mwena and Ramisi estuaries consistently recorded higher concentrations of most OCPs across guilds, suggesting localized point-source inputs or sediment sinks. These hotspots coincided with catchments characterized by agricultural intensity, pesticide usage history, or poor waste regulation. The strong spatial differentiation among guilds also indicates habitat-specific exposure risks e.g., benthic taxa exposed to sediment-bound residues versus pelagic taxa exposed to suspended particulate matter (Zhou *et al*., 2017).
2. **Temporal Dynamics**: Across all guilds, pesticide concentrations peaked between February and May, aligning with the long-rain season. These pulses are likely due to increased surface runoff, remobilization of legacy residues, and sediment resuspension. Temporal variation was more pronounced in *S.*

cucullata and *Rhagovelia* spp., pointing to seasonal shifts in water chemistry, feeding behavior, and contaminant bioavailability (Sathish & Patterson, 2025).

3. **Spatio-Temporal Interaction**: The significant interaction effects across all two-way ANOVAs demonstrate that neither space nor time alone explains pesticide accumulation patterns. Instead, their interaction modulated by rainfall, sediment flow, site-specific hydrology, and species traits drives the observed bioaccumulation heterogeneity. Guilds such as predators (*Rhagovelia* spp.) and collector-gatherers (Atyidae) were particularly responsive to these joint dynamics, indicating their role as effective bioindicators of changing contamination regimes (Shamma *et al*., 2024).

5.3.4 Concentration of pesticides in fish - *P. monodon*

The concentration of OCPs in *P. monodon* across the South Coast estuarine systems revealed significant spatial and temporal variability, reflecting complex interactions between pollutant sources, environmental dynamics, and trophic processes. The detection of all sixteen targeted OCPs, including legacy compounds such as DDTs, HCH isomers, heptachlor, and mirex, in varying concentrations across multiple sites, highlights the persistence of these pesticides in aquatic ecosystems despite global bans and national regulatory efforts.

Spatial differences in contamination were statistically significant across all compounds, with one-way ANOVA (Table 4.27) showing p values < 0.001 for each compound and F-values ranging from 1.86 for cis-chlordane to 59.50 for HCN. These results suggest heterogeneity in exposure pathways and contaminant inputs across the estuarine sites. *P. monodon* from stations such as Mkurumdzi, Ramisi, and Mwena estuaries consistently recorded higher concentrations of several compounds, indicating localized

hotspots of contamination. These sites are characterized by proximity to agricultural catchments and urban runoff zones, both of which are recognized contributors to non-point pesticide pollution. Such differences could also be associated with differences in OCPs solubility as dictated by their respective compounds in water depending on their chemical composition and the water chemistry as determined by various environmental factors such as salinity, temperature, conductivity, pH, TDS and DO. Pastorino *et al*. (2020a) have reported similar results where they have indicated that differences in contaminant concentration levels among fish and macrobenthic invertebrates could be catalyzed by possible differences in solubilization of contaminant compounds in an aquatic environment on the basis of their chemical structure and water quality parameters. For example, low level residues in ∑HCH compared to ∑DDT can occur as a result of physical, chemical and biochemical characteristics of each pesticide. DDTs are characterized by lower water solubility, biodegradability and vapour pressure, and higher attraction between sediment particles and lipophilicity as compared to HCH (Yang *et al*., 2005a, b).

Moreover, this spatial pattern aligns with previous research by Gitahi *et al*. (2002), who reported elevated levels of DDTs and HCHs in fish tissues from Lake Naivasha, attributing the contamination to horticultural farms along the Malewa River. Similarly, Arinaitwe (2016) found higher OCP concentrations in tilapia and catfish collected from sites adjacent to cultivated fields along Lake Victoria basin, Tanzania. These findings corroborate the current study's observation that land-use intensity and pesticide application in upstream catchments significantly influence contaminant levels in downstream aquatic biota.

Temporal variation was equally pronounced, with ANOVA results (Table 4.28) revealing seasonal differences in contaminant accumulation across all compounds. The highest F-values were observed for cis-chlordane (F = 312.48), trans-nonachlor (F = 282.48), and o,p'-DDD (F = 271.73), suggesting robust month-to-month differences. Higher mean concentrations of most OCPs were recorded during the long rainy season (March–May) and the short rains (October–December), a trend attributed to increased surface runoff transporting pesticide residues from agricultural fields to estuarine zones. These findings are consistent with studies by Olisah *et al*. (2020a) in Nigeria's Ogun River, who reported peak OCP levels in fish tissues during wet seasons due to intensified pesticide mobilization from adjacent farms. Peris *et al*. (2024) also alluded to this fact that pesticides contamination from cultivated agricultural fields were significantly higher than the uncultivated ones, which they attributed to agricultural application during the planting season hence their bioavailability to *P. monodon* tissues.

Similar seasonal dynamics have been reported in studies from temperate regions. For instance, Sathish & Patterson (2025) demonstrated that pesticide runoff and subsequent bioaccumulation in fish increased significantly following rain events in agricultural watersheds in Germany. While the environmental transport mechanisms may differ between tropical and temperate zones, the underlying principle that precipitation-driven hydrological processes influence the mobilization and bioavailability of persistent organic pollutants is widely supported across geographical contexts (Peris *et al*., 2024).

Beyond individual spatial and temporal trends, the two-way ANOVA results (Table 4.29) showed significant interaction effects between sampling station and month for all compounds ($p < 0.001$), indicating that seasonal changes in pesticide concentrations

were not uniform across sites. This interaction reflects the influence of local factors such as sediment type, estuarine hydrodynamics, and anthropogenic pressure on pesticide bioavailability (Sathish & Patterson, 2025). For example, Umba and Ramisi showed unique seasonal peaks in mirex and heptachlor concentrations that were absent in stations like Ramisi Mwachande and Umba Lunga-Lunga Bridge, which are more hydrologically open and exhibit greater tidal flushing.

These findings suggest that pesticide exposure in estuarine fish (*P. monodon*) is not merely a function of agricultural intensity but is modulated by a suite of site-specific variables including estuary morphology, connectivity to freshwater inflows, lipid content, and sediment retention characteristics. This observation is consistent with work by Pereira *et al.* (1996), who reported that hydrological isolation in California's San Joaquin River Delta led to higher OCP concentrations in fish tissues compared to more tidally dynamic sites. Moreover, sediment-pesticide binding dynamics, influenced by organic carbon content, have been shown to affect the degree of bioavailability, with fine, organic-rich sediments typically exhibiting stronger contaminant retention (Zhou *et al.*, 2006).

In addition to environmental factors, species-specific traits may also influence pesticide accumulation in *P. monodon*. Lipid content, trophic level, and metabolic capacity determine the extent to which fish can absorb, retain, or eliminate lipophilic compounds such as OCPs. In the present study, species commonly consumed by local communities exhibited variable, but detectable burdens of DDTs and HCHs, raising public health concerns due to the known carcinogenic and endocrine-disrupting properties of these compounds. Comparable risks have been reported in Uganda's Lake Victoria basin,

where Wasswa *et al*. (2011) detected OCP levels in Nile perch exceeding WHO maximum residue limits, particularly during peak pesticide application periods.

International assessments have also highlighted the public health implications of pesticide bioaccumulation in fish. In Vietnam's Hanoi sewer system, Hoai *et al*. (2010) found that consumption of contaminated fish contributed significantly to organochlorine exposure in rural populations, prompting the need for dietary advisories and tighter regulation of agricultural pesticide use. The present study's findings similarly underscore the need for comprehensive risk assessments in coastal Kenya, where fish constitute a dietary staple and a vital source of income for artisanal fishers.

Furthermore, the presence of banned compounds such as p,p'-DDT and aldrin derivatives in *P. monodon* tissues suggests potential illegal use or mobilization of residues from contaminated sediments and agricultural stockpiles. These findings echo observations made by Kinyua and Pacini (1991) in Nairobi River, who linked high DDT concentrations in aquatic biota to legacy contamination from abandoned pesticide depots and unregulated urban runoff. Similar regulatory challenges have been reported in other African contexts, where weak enforcement, limited monitoring capacity, and low awareness among farmers continue to hinder the full phase-out of persistent pollutants.

The combination of spatially uneven inputs, seasonally driven mobilization, and trophic-level bioaccumulation paints a complex picture of OCP contamination in estuarine fish. The observed trends reveal that *P. monodon* not only reflect current environmental contamination but also act as archives of past pesticide use. This

characteristic makes them particularly valuable bioindicators in monitoring programs. However, the implications go beyond environmental surveillance to encompass human exposure and ecological risk (Kamau *et al*., 2022). Persistent concentrations in edible fish tissues pose long-term threats to food safety, biodiversity, and ecosystem function, particularly in biodiversity-rich estuarine nurseries such as those in the Kenyan South Coast.

5.4 Relationship between Physico-Chemical Water Quality Parameters and Pesticide Concentrations in Water in Estuarine Ecosystems

The principal component analysis (PCA) conducted on the standardized dataset comprising nine physico-chemical water quality parameters and sixteen OCP compounds revealed intricate patterns of correlation and association among the measured variables. The first two principal components (PC1 and PC2) cumulatively accounted for 63.9% of the total variance, with PC1 contributing 41.6% and PC2 contributing 22.3%. This suggests a moderately strong dimensionality reduction, capturing the dominant sources of variation within the dataset.

PC1 predominantly represented gradients in pesticide contamination, as evidenced by the clustering of most OCPs on the negative domain of this axis. Compounds such as p,p'-DDT, p,p'-DDD, Hep.Hepoxide, and beta-HCH demonstrated high negative loadings (above -0.25), indicating their significant contribution to this component. Conversely, PC2 reflected physico-chemical gradients, primarily driven by conductivity (-0.471), total dissolved solids (TDS, -0.497), and salinity (-0.418), which loaded strongly on the negative end. Dissolved oxygen (DO) was the only parameter with a strong positive loading (0.281), revealing a distinct orthogonal gradient.

The PCA biplot further clarified these patterns. Organics such as Mirex, alpha-HCH, and o,p'-DDD clustered near the lower left quadrant, indicating association with elevated salinity, conductivity, and TDS. In contrast, compounds like HCB and p,p'-DDE appeared proximal to DO and pH in the upper right quadrant, suggesting differential environmental behavior or degradation pathways. Ammonia and nitrate, located near the origin or slightly toward the negative PC1, showed weaker influences on the principal components. These results corroborate well with Lemley *et al*. (2017) who opined that water quality parameters such as pH, temperature, DO, salinity, turbidity, and nutrient levels strongly influence pesticide solubility, degradation, and partitioning in estuarine waters. Elevated turbidity often correlates with higher pesticide adsorption to suspended particles, facilitating their accumulation in benthic organisms (Yang *et al*., 2005a, b).

These distribution patterns suggest that specific organochlorines co-vary with particular water quality variables, which may be indicative of shared environmental sources, chemical behavior, or transformation products. For instance, the proximity of chlorinated compounds such as trans-Nonachlor, cis-chlordane, and o,p'-DDT to TDS and conductivity vectors implies a potential sediment resuspension or point-source discharge, especially in saline conditions. Similarly, compounds aligned with DO and pH could reflect aerobic degradation or differing partitioning dynamics. For instance, such discourse has been advanced by other authors where pesticide degradation rates often increase with temperature and sunlight exposure but can vary with pH and salinity, which affect chemical stability and bioavailability (Nyaundi, 2022).

The separation between pesticide clusters and water quality vectors also reveals compound-specific behavior in the estuarine environment. Heavier, more hydrophobic pesticides (e.g., DDTs and Mirex) appear to associate with variables indicative of ionic strength (TDS, salinity), reinforcing their tendency to bind with particulate matter. Lighter or more volatile compounds show diffuse positioning, possibly reflecting more rapid degradation or volatility. According to Lyu *et al*. (2016) salinity gradients in estuaries can cause pesticides to partition differently between dissolved and particulate phases, altering their uptake by biota.

Furthermore, the lack of strong loading from ammonia, nitrate, and phosphate across both components implies that nutrient dynamics may be less influential in explaining pesticide distribution compared to ionic and oxidative parameters. This outcome aligns with established literature indicating that pesticide fate in estuarine systems is more responsive to redox, sediment interaction, and salinity gradients than nutrient enrichment per se (Wang *et al*., 2023). However, contrary to the present findings, Ondiere (2013) observed that TDS, pH and electrical conductivity did not affect the spatial distribution of OCPs over time.

The loadings matrix and visual interpretation underscore the critical role of environmental conditions in shaping pesticide distribution. The PCA not only identifies the dominant environmental gradients, but also points to underlying mechanisms such as salinity-driven desorption, DO-dependent biodegradation, and physico-chemical affinity of OCPs to sediment or dissolved solids. These insights are essential in advancing understanding of pesticide fate in tropical estuarine environments.

5.5 Bioconcentration and Biomagnification of OCPs in Water, Sediments, the Trophic Levels of Benthic Macroinvertebrates and Fish in Estuarine Ecosystems of South Coast, Kenya

The biomagnification of OCPs through aquatic food webs represents a significant ecotoxicological concern, particularly in estuarine systems that serve as interfaces between terrestrial runoff and marine biodiversity. The findings from this study reveal substantial variation in pesticide concentration across trophic levels, beginning with the benthic macroinvertebrate FFGs and extending to fish (*P. monodon*), which occupy higher trophic positions. The consistent increase in mean pesticide concentrations from *T. palustris* and *S. cucullata* to *Rhagovelia* spp. and ultimately to *P. monodon* reflects classical biomagnification dynamics. These results align with long-standing ecological theory and recent empirical studies indicating that lipophilic and persistent pollutants such as DDTs, HCH isomers, and Mirex concentrate as they ascend food webs (Pastorino *et al*., 2020a, b).

The graphical representation in Figure 4.29 shows that OCPs such as alpha-HCH, p,p'-DDE, o,p'-DDD, and Mirex are especially prone to biomagnification, with *P. monodon* exhibiting concentrations that often double those in *Rhagovelia* spp. macroinvertebrates and triple those in *N. undata* or *T. palustris*. This trend underscores the ecological hazard posed by these compounds and is consistent with findings from similar estuarine and coastal ecosystems in Asia and South America, where top trophic-level fish exhibited significantly higher concentrations than primary consumers (Zhou *et al*., 2024). *Rhagovelia* spp. and *S. cucullata*, being higher on the macroinvertebrate trophic ladder, displayed moderately elevated OCP levels, possibly due to direct ingestion of contaminated prey or efficient filtering of suspended particulate-bound pesticides.

Site-specific trends presented in Figure 4.30 reinforce the trophic biomagnification pattern while highlighting localized differences in pesticide burdens. For instance, estuaries such as Mwena and Mkurumdzi consistently showed higher overall pesticide levels, suggesting proximity to agricultural or urban runoff sources. These spatial differences in contaminant loads may also be mediated by environmental variables such as sedimentation rates, organic matter content, and salinity gradients that influence pesticide partitioning and organismal uptake. Similar findings were observed by Li *et al.* (2014), who reported that estuarine complexity, in terms of habitat and hydrology, can mediate contaminant fate and biomagnification potential.

The calculation of BCFs in Table 4.30 further illustrates the role of direct exposure routes in pesticide accumulation. *P. monodon* exhibited the highest BCFs across all 16 OCPs, with values exceeding 25 for compounds like p,p'-DDD, alpha-HCH, and Mirex, confirming their lipophilic nature and high uptake efficiency from contaminated water. These BCFs are comparable to those reported in Lake Victoria cichlids and tilapia by Otieno *et al.* (2024), who documented BCFs ranging from 20 to 35 for persistent OCPs. Among macroinvertebrates, *Rhagovelia* spp., *N. undata,* and *S. cucullata* showed higher BCFs relative to *T. Palustris*, reflecting differential habitat exposure. *N. undata*, and *S. cucullata* may come into contact with contaminated sediments or suspended particulates, thereby enhancing bioavailability.

The BMF data further validate the concentration patterns observed across trophic levels. Table 4.31 shows that all BMF values exceeded 1.0, the threshold indicating net biomagnification. Pesticides like Mirex, o,p'-DDD, alpha-HCH, and Heptachlor had BMFs above 2.9, with some reaching values over 3.0, suggesting strong trophic

transfer. These values mirror those found in studies from the Gulf of Guinea and Mekong Delta, where BMFs for persistent OCPs ranged between 2.5 and 4.1 (Chen, 2025). Particularly, the consistently high BMFs for Mirex and o,p'-DDD across all macroinvertebrate FFGs reflect their extreme persistence, hydrophobicity, and resistance to metabolic breakdown, making them among the most hazardous legacy contaminants in estuarine food webs.

Moreover, guild-specific differences in biomagnification potential, as shown in Table 4.32, illustrate how feeding ecology and habitat preferences influence contaminant transfer. *N. undata*, and *S. cucullata* often exhibited higher BMFs, likely due to their sustained interaction with contaminated benthic substrates and water columns, a trend that resonates with findings from mangrove-fringed estuaries in India and Malaysia (Li *et al*., 2023; Sathish & Patterson, 2025; Onac *et al*., 2021). *T. palustris*, conversely, showed the lowest BMFs for most pesticides, reinforcing the notion that basal trophic consumers are less exposed to cumulative contamination.

Across all trophic magnification patterns, the correlation between compound-specific properties and their biomagnification tendency becomes evident. Highly lipophilic and chlorinated compounds like Mirex and DDT metabolites (o,p’-DDD, p,p’-DDE) show steep increases in concentration toward higher trophic levels. These findings are consistent with theoretical expectations derived from chemical properties such as octanol-water partition coefficients (log Kow > 5), which predict a high potential for lipid-rich tissues to retain such contaminants (UNEP, 2023b). Moreover, the absence of metabolic detoxification in many aquatic invertebrates and limited enzymatic biotransformation in fish contribute to the observed persistence and accumulation.

Taken together, these findings highlight the ecological and toxicological significance of biomagnification and bioconcentration processes in estuarine ecosystems of the South Coast of Kenya. The potential for long-term ecological harm is high, particularly for fish species that are consumed by local communities and may serve as vectors of human exposure to persistent OCPs. These insights, supported by the comprehensive spatial and trophic-level data presented in Figures 4.29–4.30 and Tables 4.30–4.32, contribute critical knowledge for both environmental risk assessment and the development of region-specific pollution control strategies.

5.6 Ecotoxicological Risk Posed by OCPs in Sediments, Water, Trophic Guilds of Benthic Macroinvertebrates and Fish in Estuarine Ecosystems of South Coast, Kenya

The ecotoxicological evaluation of OCPs in estuarine environments requires a multi-trophic assessment, given the diverse exposure pathways and trophic linkages that characterize estuarine food webs. This study assessed the ecological risk posed by 16 OCPs using sediment quality guidelines, hazard quotients (HQ), and probabilistic risk metrics across sediments, water, macroinvertebrate FFGs, and *P. monodon* tissues. The findings provide critical insights into spatial variability in exposure levels, potential bioaccumulation, and risk to aquatic biota. Sediments serve as major sinks for hydrophobic OCPs and thus offer a long-term archive of pesticide input into aquatic systems. The mean concentrations observed across the 12 estuarine stations suggest widespread but varying degrees of legacy OCP contamination. Specifically, HCB (1.91 µg/kg), p,p′ DDE (1.81 µg/kg), and Heptachlor (1.79 µg/kg) recorded the highest average concentrations. These values fall within ranges previously reported in other tropical estuarine systems, such as the Rufiji Delta in Tanzania (Mwevura *et al*., 2021) and the Nile Delta in Egypt (Shamma *et al*., 2024), underscoring the regional

persistence of banned OCPs decades after restriction. The widespread detection of DDT metabolites (DDE and DDD) also supports the hypothesis of historical input and environmental transformation through microbial degradation, a trend that has been echoed in recent sediment core studies from Lake Victoria and the Malindi Creek (Ogola *et al*., 2024).

Although average OCP concentrations in sediments were generally below global threshold effect levels (TELs), the HQ analysis provided a more sensitive index of risk. HQ values for all compounds exceeded 1, ranging from 1.20 (Mirex) to 1.95 (HCB), indicating that even at relatively low concentrations, the potential for sublethal and chronic effects on benthic fauna cannot be ignored. In particular, compounds such as HCB, Heptachlor, and p,p′ DDE with HQs > 1.75 pose high ecological concern due to their known disruption of endocrine and reproductive systems in sediment invertebrates (Wang *et al*., 2025). These values are consistent with the sediment toxicity thresholds set by the Canadian Council of Ministers of the Environment (CCME, 2022), which regard HQ > 1 as indicative of probable adverse biological effects. Such findings suggest that current sediment OCP levels exceed the detoxification and resilience capacity of the benthic system in parts of the South Coast estuaries.

The assessment of sediment-associated OCPs across twelve estuarine stations revealed widespread contamination, with legacy compounds persisting at ecologically significant levels. Average concentrations of key OCPs such as HCB (1.91 µg/kg), p,p′-DDE (1.81 µg/kg), and Heptachlor (1.79 µg/kg), though often below international threshold guidelines, reflect persistent input and limited degradation. All 16 compounds assessed registered Hazard Quotients (HQ) > 1, indicating a likely risk of ecological

effects, with HCB and p,p′-DDE exceeding the Probable Effect Level (PEL) at multiple sites. These findings are contrary to what Wanjeri *et al*. (2022) found in the Athi-Sabaki estuary in the north coast of Kenya.

The contamination Factor (CF) and the Geo-accumulation Index (Igeo) are commonly used as indicators of emerging pollutants in aquatic ecosystems (Barbier, 2016). The Cf analysis revealed that compounds like p,p′-DDD, Cis-chlordane, and Mirex had Cf values exceeding 3.5, indicating severe enrichment relative to background levels. These values confirm the extensive spread OCP pollution along south coast estuary of Kenya mainly due to rampant anthropogenic activities and hitorical sources. High CF values have been reported in Ethiope river, Abraka Axis of Southern Nigeria (Emebu, 2016). According to Barbier (2016), CF values exceeding 2 is reminscent of moderately to severe contamination originating either from point or non-point sources and to certain extent historical sources. Similarly, the Igeo index values for all OCPs surpassed 1.5, with several compounds particularly Cis-chlordane (Igeo = 8.60) and gamma-HCH (Igeo = 5.79) classified under the "extremely polluted" category. This is also a clear demonstration that indeed, the south coast estuarine system of Kenya faces myriad sources of OCP pollution, which apart from the above stated ones may include air-related historical depositions from far places not necessarily from within. Muller (1981) while defining the seven classes of Igeo index, confirmed that Igeo≥5 is indicative of severe contamination of pollutants. The Pollution Load Index (PLI) of 2.57 reinforces this trend (severe contamination), indicating a region-wide moderate to heavy pollution burden, mainly driven by persistent DDT derivatives and chlorinated cyclodienes. Like the rest of the indices mentioned above PLI paints a glimpse of the state of environment based on all anthropogenic sources which in this case are from agriculture, industries,

municipal as well as historical sources. Ganiyu *et al*. (2024), argued that pollution indices based on geochemical backgrounds are important in delineating contaminants originating from human-induced changes and should be improved over time to cater for the ever-dynamic ecosystems.

A more integrative risk measure, the Potential Ecological Risk Index (RI), yielded a cumulative value of 31,352.42, far exceeding Hakanson's "very high risk" threshold of 600. The largest contributors to this RI were the HCH isomers and p,p′-DDD, attributed to their high Cf values and elevated toxic response coefficients. The Nemerow Pollution Index (PN) further corroborated these findings, with a computed value of 420.03, indicating severe contamination when both average and maximum pollution intensities are considered. Ganiyu *et al*. (2024) while incorporating RI and PN in the assessment of metals in Kaani river, Nigeria reported no environmental risk posed by the contaminant's contrary to the findings of the present study. These findings, therefore, indicate rampant OCPs pollution either from the anthropogenic activities experienced in the South Coast estuarine catchments and/or historical inputs.

Although the Mean Effect Range Median Quotient (ERM-Q) value of 0.119 falls below the 0.5 threshold for probable toxicity, it still reflects a moderate potential for chronic ecological effects. This suggests that even in the absence of acute toxicity signals, sediment-bound OCPs may induce long-term sub-lethal impacts on benthic communities (Akinrotimi *et al*., 2021). Collectively, these indices confirm that estuarine sediments are significant reservoirs of historical OCP use and pose varying levels of ecological risk, with certain compounds exhibiting high potential for trophic transfer (Nyaundi, 2022; Gong *et al*., 2021).

Beyond sediment assessments, the study extended ecotoxicological risk analysis to aquatic biota. The calculation of Bioconcentration Factors (BCFs) revealed high contaminant uptake from sediments and overlying waters, particularly for fish and macroinvertebrates such as *N. undata* and *S. cucullata*, which showed BCFs exceeding 20 for compounds like HCB and p,p′-DDE. These findings indicate strong potential for organismal exposure and uptake via direct contact and ingestion, especially among feeding guilds closely associated with the benthic substrate (ATSDR, 2022; Pastorino *et al*., 2020a, b).

Although water column pesticide concentrations were not the focus of this discussion, the consistent presence of OCPs in sediment and biota indicates continuous ecological exposure, even in the absence of recent pesticide inputs. This implies that legacy contamination remains bioavailable and capable of initiating sub-lethal physiological stress, reproductive interference, or behavioral disruptions in aquatic organisms (Manuilova, 2003). The trophic transfer risk further signals indirect human health implications via fish consumption and ecosystem service disruptions.

CHAPTER SIX

CONCLUSIONS AND RECOMMENDATIONS

6.1 Introduction

This chapter presents the key conclusions drawn from the study, outlines the major implications of the findings, and provides recommendations informed by both the study outcomes and future research needs.

6.2 Conclusions

This study assessed the bio-concentration and biomagnification of OCPs in aquatic macroinvertebrates and fish within estuarine ecosystems along Kenya's South Coast. The findings revealed that spatial variation is the primary driver of water quality differences in these systems. This variation is strongly influenced by localized factors such as land use patterns, freshwater inflow, geomorphology, and proximity to pollution sources. The marked differences observed between upstream and downstream stations, particularly in salinity, conductivity, total dissolved solids, and nutrient concentrations, highlight the importance of site-specific environmental conditions.

In contrast, temporal variation was less pronounced. Although some parameters, including temperature, dissolved oxygen, and pH, showed statistically significant changes, these patterns were generally subtle and inconsistent across sampling stations. More importantly, the presence of significant spatio-temporal interactions indicates that seasonal changes in water quality are not uniform but are instead shaped by local environmental contexts. This reinforces the idea that estuarine systems are highly complex and ecologically distinct, requiring site-specific interpretation rather than broad generalization. Overall, the findings demonstrate a dynamic interplay between geographic location, land use, and hydrological processes, leading to the rejection of the null hypothesis on uniform water quality conditions.

The study also provides important insights into the occurrence, distribution, and bioaccumulation of OCPs across sediments, water, macroinvertebrates, and fish. Despite being banned or restricted by the Kenyan government in 1986, legacy OCPs such as DDTs, HCH isomers, chlordane compounds, and heptachlor remain present in the environment. Their higher concentrations in estuaries near agricultural and urban areas suggest continued inputs, likely from residual contamination, illegal use, or remobilization from sediments, and historical sources. This points to weaknesses in current pesticide regulation, monitoring, and enforcement systems. In addition, macroinvertebrate groups showed differences in OCPs accumulation depending on their feeding behavior, habitat, and exposure pathways, while overall OCPs levels varied across both space and time, often increasing during runoff periods.

At higher trophic levels, *P. monodon* consistently recorded the highest OCPs concentrations, confirming its role as a key bioindicator and terminal reservoir within the estuarine food web. The detection of multiple OCPs residues in edible *P. monodon* tissues raises serious ecological and public health concerns, particularly for coastal communities that depend heavily on fish as a source of protein. Even low but persistent exposure to such contaminants may lead to long-term health effects, including cancer risks, developmental disorders, and hormonal disruptions. The observed variability in OCPs concentrations across environmental compartments further supports the rejection of the null hypothesis on uniform OCPs distribution.

The study also established a strong relationship between physico-chemical water quality parameters and OCPs behavior. Parameters such as pH, temperature, dissolved oxygen, salinity, and conductivity were found to significantly influence OCPs

solubility, degradation, and distribution, while nutrients played a less prominent role. Multivariate analysis suggested that both water quality parameters and OCPs contamination may originate from similar pollution sources, highlighting the interconnected nature of environmental processes in estuarine systems.

Furthermore, the study confirms active bioconcentration and biomagnification of OCPs along the aquatic food chain, with concentrations increasing from macroinvertebrates to fish. Compounds such as alpha-HCH, Mirex, and o,p′-DDD showed particularly high biomagnification potential due to their persistence and affinity for lipids. This accumulation poses significant ecological risks, including disruptions to food web structure, reduced reproductive success, and impaired physiological functions in aquatic organisms.

Finally, the ecotoxicological risk assessment revealed that estuarine sediments act as major reservoirs of contamination. Multiple indices in this study consistently classified the sediments as heavily polluted or ecologically riskier, with compounds such as HCB, p,p′-DDD, p,p′-DDE, and gamma-HCH contributing most significantly. These sediments serve as long-term sources of pollutants and facilitate their transfer through the food web. Together, these findings emphasize the urgent need for integrated environmental management strategies that address both current and legacy pollution. Overall, this study contributes valuable knowledge to the understanding of estuarine dynamics in tropical environments and provides a strong scientific foundation for improving environmental management, fisheries sustainability, and public health protection.

6.3 Recommendations

Based on the conclusions drawn from the five study objectives, the following recommendations are proposed:

i. There is a need to establish an integrated estuarine management framework that supports continuous monitoring of key water quality parameters and OCPs across both spatial (upstream to downstream) and temporal (seasonal and tidal) scales. Incorporating land use and hydrological data from surrounding catchments will help identify pollution sources and enable more targeted and effective management interventions.

ii. Comprehensive monitoring programs should be institutionalized to track OCPs levels in sediments, water, macroinvertebrates, and fish. This will strengthen enforcement of existing regulations, such as implemention through regular inspections and proper disposal of obsolete pesticides to reduce ongoing OCPs contamination.

iii. Advanced analytical methods, including multivariate statistical approaches, should be used to better understand how environmental factors influence pesticide behavior. High-resolution temporal monitoring will improve the detection of short-term changes and help identify contamination hotspots.

iv. Bioaccumulation and biomagnification mitigation efforts should focus on reducing OCPs or pollutant inputs at their source by promoting sustainable agricultural practices such as integrated pest management. Public awareness campaigns are also necessary to inform stakeholders about the risks of pesticide misuse. Additionally, fish consumption advisories should be developed to minimize human exposure.

v. Targeted remediation strategies should be implemented to manage eco-toxicological risks and sediment contamination in highly contaminated areas. These may include catchment rehabilitation, sediment cleanup, dredging, bioremediation, and in-situ capping. Regular monitoring of sediment quality is essential due to its role as a long-term pollutant reservoir.

vi. Future efforts should focus on strengthening governance and research frameworks to protect estuarine ecosystems and public health. This can be achieved through high-frequency monitoring, study of emerging contaminants, advanced tracing techniques, enforcement of water quality and fish consumption standards, cross-sector collaboration, and regional cooperation to manage shared estuarine systems and transboundary pollution.

6.4 Recommendations for future studies

i. Future studies should focus on increasing the temporal resolution of water quality sampling to complement the strong spatial variability observed in this study. Given that some parameters, particularly nutrients, showed limited temporal variation potentially due to monthly sampling intervals or masking by high spatial heterogeneity higher-frequency sampling within months and across tidal phases would help clarify short-term dynamics and strengthen interpretation of spatio-temporal interactions.

ii. Future research should expand to include a wider range of pesticide classes beyond OCPs, including organophosphates, pyrethroids, and emerging contaminants such as pharmaceuticals and endocrine disruptors. Longitudinal biomonitoring is necessary to assess long-term trends, climate influences, and the effectiveness of interventions. Bioaccumulation modeling, including trophic

magnification assessments and stable isotope analysis, would enhance understanding of contaminant flow within the food web. Studies assessing the dietary exposure and health risks to human populations consuming contaminated fish are needed to inform policy and public health measures. Moreover, laboratory-based ecotoxicological investigations using native estuarine species should be conducted to elucidate sublethal and chronic effects of pesticide mixtures. Regional collaboration with neighboring countries is also critical for managing shared water bodies and harmonizing environmental safety standards across transboundary estuarine ecosystems.

iii. Future research should focus on quantifying the seasonal dynamics of OCP concentrations and their relationship with hydrological variations such as rainfall, tidal mixing, and sediment fluxes. The use of isotopic trophic markers and molecular biomarkers could improve understanding of trophic transfer and sublethal effects. Additionally, broader contaminant profiling including newer pesticides and pharmaceuticals should be undertaken to capture the full scope of chemical stressors in estuarine systems. Investigations into the human health implications of consuming contaminated fish, including dietary exposure assessments, are also necessary.

iv. Future studies should incorporate seasonal dynamics and hydrological influences on contaminant distribution and bioavailability, including the role of tidal mixing, sediment resuspension, and riverine inputs. Isotopic or molecular tracing can help distinguish between local and upstream pollutant sources. It is also essential to expand research into biomarker-based ecotoxicology, assessing physiological and biochemical responses of fish and invertebrates to chronic OCP exposure. Finally, human health risk assessments linking sediment and biota contamination to dietary exposure through fish consumption are urgently needed to bridge ecological and public health perspectives.

REFERENCES

Abong'o, O., & Nyamai, M. (2021). Pesticide pollution in tropical estuarine ecosystems: Challenges and mitigation strategies. *Environmental Monitoring and Assessment, 193,* 450. https://doi.org/10.1007/s10661-021-09182-2.

Adewumi, O., Ojo, O., & Adeyemi, I. (2020). Seasonal variation in water quality parameters of coastal estuaries in West Africa. *Marine Pollution Bulletin, 160,* 111666. https://doi.org/10.1016/j.marpolbul.2020.111666.

Adeyemi, D., Anyakora, C., Ukpo, G., Adedayo, A., & Darko, G. (2008). Evaluation of the levels of organochlorine pesticide residues in water samples of Lagos Lagoon using solid phase extraction method. *Journal of Environmental Chemistry and Ecotoxicology*, 1(1), 14–22. https://doi.org/10.5897/JECE.9000001.

ATSDR. (2022). Toxicological profile for DDT, DDE, and DDD. U.S. Department of Health and Human Services. 510 p.

Agricultural Pollution. (2025). Agricultural pollution. In Wikipedia. Retrieved from https://en.wikipedia.org/wiki/Agricultural_pollution.

Ahmed, M. T., El-Sherif, Z. M., & Ismail, M. A. (2024). Ecosystem services and ecological importance of estuarine systems: A global perspective. *Estuarine, Coastal and Shelf Science, 294,* 108615. https://doi.org/10.1016/j.ecss.2023.108615.

Akerblom, M. (1999). *Environmental monitoring of pesticides residues: guidelines for the SADC region*. SADC Environment and Land Management Sector Coordination Unit. *Monitoring Techniques Series*, Vol. 3.

Akinrotimi, O. A., & Abu, O. M. G. (2021). Effects of pesticides on aquatic organisms. *Journal of Fisheries and Aquatic Science*, *16*(1), 1–10. https://doi.org/10.3923/jfas.2021.1.10

Akinyemi, S. A., & Zhang, H. (2023). Bioindicator potential of benthic macroinvertebrates in aquatic pollution assessment: A review. *Environmental Science and Pollution Research*, *30*, 8756–8774. https://doi.org/10.1007/s11356-022-23245-9.

Alegria, H. A., Wong, C. S., & Chiang, S. Y. (2016). Pesticide distribution and fate in sediments: Implications for aquatic risk assessment. *Chemosphere*, 153, 270–281. https://doi.org/10.1016/j.chemosphere.2016.03.062.

Alexandratos, N., & Bruinsma, J. (2012). *World agriculture toward 2030/2050: the 2012 revision* (ESA Working Paper No. 12-03). FAO. http://www.fao.org/3/a-ap106e.pdf.

Amadi, S. I., Eze, A. I., & Okoye, P. C. (2024). Benthic macroinvertebrates as indicators of pesticide contamination in tropical estuaries. *Marine Pollution Bulletin*, *193*, 115246. https://doi.org/10.1016/j.marpolbul.2023.115246.

Amankwaa, G., Agyemang, I., Asare-Donkor, N. K., Adjei-Mensah, I., & Darko, G. (2021). Pesticide residues in water, sediment and fish from the Densu River Basin, Ghana: Levels, sources and human health risk assessment. *Environmental Monitoring and Assessment, 193*(2), 89. https://doi.org/10.1007/s10661-021-08874-3.

Anyango, J., Oduor, S. O., & Achieng, E. (2024). Pesticide residues in estuarine fauna along the Kenyan coast. *African Journal of Aquatic Science*, 49(1), 56–69. https://doi.org/10.2989/16085914.2024.2301172.

APHA (2005). Standard Methods for the Examination of Water and Wastewater. American Public Health Association, Washington, DC.

Arias, A. H., Oliva, A. L., Marcovecchio, J. E., & Prendez, M. (2020). Persistent organic pollutants in estuarine and coastal environments. *Environmental Reviews, 28*(2), 169–184. https://doi.org/10.1139/er-2019-0053.

Arinaitwe, K., Rose, L. N., Muir, D. C. G., Kiremire, B. T., Balirwa, J. S., & Tiexeira, C. (2016). Historical deposition of persistent organic pollutants in Lake Victoria and two alpine equatorial lakes from East Africa: Insights into atmospheric deposition from sedimentation profiles. *Chemosphere, 144*, 1815-1822.

Arnot, J. A., & Gobas, F. A. P. C. (2006). A review of bioconcentration factor (BCF) and bioaccumulation factor (BAF) assessments for organic chemicals in aquatic organisms. *Environmental Reviews*. https://doi.org/10.1139/a06-005.

Bakhtiari, A. R., Dehghan, H., & van Wezel, A. P. (2020). Acute toxicity of glyphosate and atrazine in aquatic ecosystems: Implications during pulse runoff events. *Environmental Toxicology, 35*(2), 234–243. https://doi.org/10.1002/etc.4652.

Barbier, M. (2016). The Importance of Enrichment Factor (EF) and Geoaccumulation index (Igeo) to evaluate the soil contamination. *Journal of Geology and Geophysics, 5, 237.* doi:10.4172/2381-8719.1000237.

Barbosa, J., Pires, A., & Pereira, M. E. (2023). Persistent organic pollutants in aquatic systems: Sources, fate, and impacts. *Environmental Science and Pollution Research, 30*, 14521–14539. https://doi.org/10.1007/s11356-022-24309-2.

Bashir, I. (2020). Concerns and threats of contamination on aquatic life. PMC, Article PMC7121614. https://www.ncbi.nlm.nih.gov/articles/PMC7121614/.

Beger, M., McGowan, J., Treml, E. A., Green, A. L., White, A. T., Wolff, N. H., Klein, C. J., Mumby, P. J., & Possingham, H. P. (2019). Integrating regional conservation priorities for multiple objectives into national policy. *Nature Communications*, *10*(1), 5693. https://doi.org/10.1038/s41467-019-13500-z.

Begon, M., Townsend, C. R., & Harper, J. L. (1990). *Ecology: From Individuals to Ecosystems*. Fourth Edition. Blackwell Publishing, Malden, USA. 738pp.

Belaidi, N., Boutiba, Z., & Chouikhi, M. H. (2023). Bioaccumulation and distribution of organochlorine pesticides in fish and sediment from estuarine ecosystems: Implications for ecological risk assessment. *Marine Pollution Bulletin, 188*, 114669. https://doi.org/10.1016/j.marpolbul.2023.114669.

Belden, J. B., Lydy, M. J., & Hebert, M. (2020). Pesticide mixture toxicity: Interactive effects in aquatic environments. *Ecotoxicology and Environmental Safety*, *189*, 109946. https://doi.org/10.1016/j.ecoenv.2019.109946.

Berntssen, M. H. G., Maage, A., & Lundebye, A. (2017). *Chemical contamination of finfish with organic pollutants and metals. In:* Chemical contaminants and residuals in food. 2nd Edition, Woodhead Publishing Series in Food Science, Technology and Nutrition. National Institute of Nutrition and Seafood Research. pp 517-551. https://doi.org/10.1016/B978-0-08-100674-0.00020-5.

Bisimwa, A. M., Amisi, F. M., Bamawa, C. M., Muhaya, B. B., & Kankonda, A. B. (2022). Water quality assessment and pollution source analysis in Bukavu

urban rivers of the Lake Kivu basin (Eastern Democratic Republic of Congo). *Environmental and Sustainability Indicators, 14*, 1-14.

Borgå, K., Kidd, K. A., Muir, D. C. G., Berglund, O., Conder, J. M., Gobas, F. A., Kucklick, J., Malm, O., & Powell, D. E. (2012). Trophic magnification factors: Considerations of ecology, ecosystems, and study design. *Integrated Environmental Assessment and Management, 8*(1), 64–84. https://doi.org/10.1002/ieam.244.

Bouillon, S., Borges, A. V., Castaño, R., Diele, K., Dittmar, T., Kristensen, E., ... & Abril, G. (2007). Mangrove production and carbon sinks: A revision. *Global Biogeochemical Cycles, 21*(4), GB2013. https://doi.org/10.1029/2006GB002900.

Brack, W., Thorpe, K., Stanley, J., & Lewis, C. (2016). Pesticide occurrence and removal in water: European perspectives. *Water Research, 98*, 192–203. https://doi.org/10.1016/j.watres.2015.12.019.

Branch, G. M., Griffiths, C. L., Branch, M. L., & Beckley, L. E. (2008). Two Oceans: A Guide to Marine Life of Southern Africa. 372 pp.

Brander, S. M., & Mehinto, A. C. (2021). Ecotoxicology of pesticides in estuarine and coastal ecosystems. *Environmental Toxicology and Chemistry*, *40*(2), 327–343. https://doi.org/10.1002/etc.4932.

Burgess, R. M., Driscoll, S. B. K., Bejarano, A. C., & Davis, C. W. (2025). A review of mechanistic models for predicting adverse effects in sediment toxicity testing. *Environmental Toxicology and Chemistry, 43*(8), 17-36.

Bwire, R., Ouma, G., & Achieng, R. (2023). Macroinvertebrate community response to pesticide gradients in Kenyan river-estuary systems. *Environmental*

Monitoring and Assessment, 195, 540. https://doi.org/10.1007/s10661-023-11736-4.

Cacciatori, C., Mariani, G., Comero, S., Kiminta, E., Salyani, A., Myers, J., Pettigrove, V., & Gawlik, B. M. (2025). Citizen-engaged screening of 230 pesticides in the Lake Naivasha catchment, Kenya, using stir bar sorptive extraction and GC-QToF-HRMS. *Frontiers in Environmental Science*, *13*, Article 1623651. https://doi.org/10.3389/fenvs.2025.1623651.

Chen, Q. (2025). Revisiting the impacts on organic carbon cycling. *Environmental Science & Policy*, 63, 101234.

Chilton, D., Ramsden, J., & Brown, C. (2021). Environmental flow requirements of estuaries: Providing resilience to global change. *Frontiers in Environmental Science, 9,* 764218. https://doi.org/10.3389/fenvs.2021.764218.

Commelin, M. C., Baartman, J. E. M., Zomer, P., Riksen, M., & Geissen, V. (2022). Pesticides are substantially transported in particulate phase, driven by land use, rainfall event and pesticide characteristics. *Frontiers in Environmental Science, 10,* Article 830589. https://doi.org/10.3389/fenvs.2022.830589.

Costa, C. R. da, & Mouri, A. (2018). Interannual and seasonal variations in water quality in the Goiana River estuary, Brazil. *Frontiers in Marine Science*, *5*, 301. https://doi.org/10.3389/fmars.2018.00301.

Cuevas, N., Martins, M., & Costa, P. M. (2018). Pesticide bioaccumulation and effects in estuarine organisms: A review. *Environmental Pollution*, *234*, 1–14. https://doi.org/10.1016/j.envpol.2017.11.057.

Dalu, T., & Froneman, P. W. (2021). Pesticide pollution in estuarine environments: Ecological impacts and management strategies. *Marine Pollution Bulletin*, *164*, 111978. https://doi.org/10.1016/j.marpolbul.2021.111978.

Datta, D. (2025). A critical review of pesticides in aquatic environment. *Science of The Total Environment*, *823*, 153691. https://doi.org/10.1016/j.scitotenv.2025.153691.

DeLorenzo, M. E., Scott, G. I., & Ross, P. E. (2001). Toxicity of pesticides to aquatic microorganisms in estuarine systems. *Environmental Toxicology and Chemistry*, *20*(1), 84–92. https://doi.org/10.1002/etc.5620200110.

Dorosh, O., Fernandes, V. C., Moreira, M. M., & Delerue-Matos, C. (2021). Occurrence of pesticides and environmental contaminants in vineyards: Case study of Portuguese grapevine canes. *Science of The Total Environment*, *791*, 148395. https://doi.org/10.1016/j.scitotenv.2021.148395.

Emebu, S. (2016). Preliminary studies of organochlorine pesticides (OCPs) in sediment, water and fish samples from Ethipe river, Abraka Axis, Southern Nigeria. *International Letters of Natural Sciences, 10(3), 17-28.* https://doi.org/10.18052/WWW.SCIPRESS.COM/ILNS.80.1.

Ekanem, E., & Obot, E. (2022). The role of bioindicators in monitoring aquatic ecosystem health under pesticide stress. *Ecotoxicology and Environmental Safety*, *245*, 114100. https://doi.org/10.1016/j.ecoenv.2022.114100.

European Commission. (2003). Technical guidance document on risk assessment in support of Commission Directive 93/67/EEC and Regulation (EC) No 1488/94 (EUR 20418 EN). Publications Office of the European Union. https://doi.org/10.2760/614367.

EEA. (2013). The impacts of pesticides on European ecosystems. EEA Report No 10/2013.

Fair, P. A., White, N. D., Wolf, B., Arnott, S. A., Kannan, K., Karthikraj, R., & Vena, J. E. (2018). Persistent organic pollutants in fish from Charleston Harbor and tributaries, South Carolina, United States: a risk assessment. *Environmental Research, 167,* 598–613

FAO. (2023). Pesticides use and management in agriculture. Food and Agriculture Organization of the United Nations. https://www.fao.org.

Fisher, S. W., Waller, W. T., & Lydy, M. J. (2014). The fate and effects of pesticides in benthic macroinvertebrate communities. *Environmental Toxicology and Chemistry, 33*(8), 1779–1792. https://doi.org/10.1002/etc.2600.

Franklin, J., Kegley, S., & Koger, C. (2013). Pesticide residues in aquatic invertebrates: A review of occurrence and impacts. *Environmental Monitoring and Assessment, 185*(7), 5727–5740. https://doi.org/10.1007/s10661-012-2980-y.

Ganiyu, A. S., Nukebabari, M. P., Nde, B., & Mathew, A. (2024). Ecological Risk Factor (EF), Potential Ecological Risk Index (RI) and Enrichment factor assessment of Selected Heavy Metals in Sediments of Kaani River, Ogoni axis, Rivers State, Nigeria. *International Journal of Chemistry and Chemical Processes*, *10*, 21-31. DOI: 10.56201/ijccp.v10.no4.2024.pg21.31.

Gbaguidi, A., Faiçal, S., & Yao, K. (2021). Pesticide residues in aquatic ecosystems of West Africa: Implications for environmental health. *Environmental Monitoring and Assessment*, 193, 428. https://doi.org/10.1007/s10661-021-09183-1.

Gerber, A., & Gabriel, M. J. M. (2002). *Aquatic invertebrates of South African rivers: field guide*. South Africa Department of Water Affairs and Forestry Resource Quality Services. Pretoria, South Africa. 150 pp.

Gitahi, N., Maina, J., & Mwangi, B. (2021). Pesticide contamination in estuarine ecosystems of the Kenyan coast. *Marine Pollution Bulletin*, 172, 112907. https://doi.org/10.1016/j.marpolbul.2021.112907.

Gitahi, S. M., Harper, D. M., Muchiri, S. M., Tole, M. P., & Ng'ang'a, R. N. (2002). Organochlorine and organophosphorus pesticide concentrations in water, sediment, and selected organisms in Lake Naivasha (Kenya). *Hydrobiologia*, *488*(1), 123–128. https://doi.org/10.1023/A:1023386732731.

Gobas, F. A. P. C., Morrison, H. A., & Muir, D. C. G. (1999). Bioconcentration and biomagnification in the aquatic environment. In Handbook of Property Estimation Methods for Chemicals (pp. 189–231). CRC Press.

Gong, W., Zhang, Z., Sun, J., Xu, Y., Zhang, X., & Wang, C. (2021). Bioaccumulation and trophic transfer of organochlorine pesticides in a subtropical estuarine food web. *Environmental Pollution, 268,* 115820. https://doi.org/10.1016/j.envpol.2020.115820.

Grasshoff, K., Kremling, K., & Ehrhardt, M. (1999). *Methods of Seawater Analysis-Third Edition*. Wiley-VCH Verlag GmbH, Weinheim, 203-223. https://doi.org/10.1002/9783527613984.

Guzzella, L., Roscioli, C., Vigano, L., Saha, M., Sarkar, S. K., & Bhattacharya, A. (2005). Evaluation of the concentration of HCH, DDT, HCB, PCB and PAH in the sediments along the lower stretch of Hugli estuary, West Bengal, Northeast India. *Environmental International, 31*, 523–534.

Hakanson, L. (1980). An ecological risk index for aquatic pollution control: a sedimentological approach. *Water Resources, 14,* 975-1001.

Hitch, R. K., & Day, H. R. (1992). Unusual persistence of DDT in some Western USA soils. *Bulletin of Environmental Contamination Toxicology*, *48,* 259–264.

Hladik, M. L., Smalling, K. L., & Kuivila, K. M. (2021). Evaluation of pesticide residues in fish tissues from tropical estuaries: implications for health and ecology. *Environmental Science & Technology*, *55*(5), 3111–3121. https://doi.org/10.1021/acs.est.0c07090.

Hoai, P. M., Ngoc, N. T., Minh, N. H., Viet, P. H., Berg, M., Alder, A. C., & Giger, W. (2010). Recent levels of organochlorine pesticides and polychlorinated biphenyls in sediments of the sewer system in Hanoi, Vietnam. *Environmental Pollution, 158,* 913-920. https://doi:10.1016/j.envpol.2009.09.018.

Howarth, R. W., & Marino, R. (2006). Nitrogen as the limiting nutrient for eutrophication in coastal marine ecosystems: Evolving views over three decades. *Limnology and Oceanography, 51*(1), 364–376. https://doi.org/10.4319/lo.2006.51.1_part_2.0364.

IPBES. (2022). Summary Report. 9th Session of the IPBES Plenary and Stakeholder Day.

Islam, F., Wang, J., Farooq, M. A., Khan, M. J., & Lei, M. (2016). Pesticide residues in water, sediment, and biota of the Indus River Basin: A review. *Science of the Total Environment, 571,* 139–152. https://doi.org/10.1016/j.scitotenv.2016.07.011.

Jacobs, Z. L., Jebri, F., Raitsos, D. E., Popova, E., Srokosz, M., Painter, S. C., Nencioli, F., Roberts, M., Kamau, J., Palmer, M., & Wihsgott, J. (2020).

Shelf-Break Upwelling and Productivity Over the North Kenya Banks: The Importance of Large-Scale Ocean Dynamics. *Journal of Geophysical Research, 125* (1) e2019JC015519, https://doi.org/10.1029/2019JC015519.

Jiang, W., Wang, Y., Wang, X., & Wang, S. (2021). Pesticide residues in estuarine environments: Sources, fates, and ecological risks. *Environmental Pollution, 277*, 116833. https://doi.org/10.1016/j.envpol.2021.116833.

Kairo, J. G., Bosire, J., Langat, J. K., Koedam, N., & Schmitz, W. (2017). Status and productivity of mangroves in Kenya: Implications for management. *Wetlands Ecology and Management, 25*(1), 1–13. https://doi.org/10.1007/s11273-016-9510-4.

Kairo, J. G., Bosire, J., & Onwonga, R. (2009). Ecological rehabilitation of the Mundulea-Ditesa forest: a strategy for the conservation of biodiversity in the Sabaki estuary ecosystem. *Biodiversity and Conservation, 18*, 2221–2235. https://doi.org/10.1007/s10531-009-9606-y.

Kairu, J. K., Ombaka, J., & Munga, D. (2021). Distribution and ecological risk assessment of organochlorine pesticides in estuarine sediments along the Kenyan coast. *Marine Pollution Bulletin, 165*, 112131. https://doi.org/10.1016/j.marpolbul.2021.112131.

Kamau, G. N., Njenga, G. K., & Mwangi, B. N. (2022). Pesticide bioaccumulation in estuarine systems of East Africa: Trends and implications. *Environmental Pollution, 306*, 119458. https://doi.org/10.1016/j.envpol.2022.119458.

Kamau, J. (2022). Impact of land use on water quality in Kenyan estuarine systems. *East African Journal of Environmental Studies, 7*(1), 15–27.

Kamau, G. N., Wanjau, R. N., & Munga, D. (2019). Chlorpyrifos contamination in estuarine sediments: Sources, distribution, and ecological risk. *Chemosphere*, *230*, 466–474. https://doi.org/10.1016/j.chemosphere.2019.05.089.

Kang, H., Kwon, O. S., Choi, S. D., & Kim, J. G. (2016). Seasonal variations and sources of persistent organic pollutants in estuarine sediments. *Marine Pollution Bulletin*, *110*(1), 580–587. https://doi.org/10.1016/j.marpolbul.2016.05.057.

Katagi, T. (2010b). Bioconcentration, bioaccumulation, and metabolism of pesticides in aquatic organisms. *Reviews of Environmental Contamination and Toxicology*, 204, 1–132. https://doi.org/10.1007/978-1-4 420-1440-8_1

Katagi, T. (2010a). Pesticide behavior in soil and water: Persistence, bioaccumulation, and toxicity. *Reviews of Environmental Contamination and Toxicology*, *204*, 1–73. https://doi.org/10.1007/978-1-4 420-1452-1_1.

Katuva, J.M. (2014). Water Allocation Assessment: A Study of Hydrological Simulation on Mkurumudzi River Basin. Ph.D. Thesis, University of Nairobi, Nairobi, Kenya.

Kennish, M. J. (2002). Environmental threats and environmental future of estuaries. *Environmental Conservation*, *29*(1), 78–107. https://doi.org/10.1017/S0376892902000061.

Khan, M., Ahmed, S., & Rana, A. S. (2018). Global trends in pesticide residues in fish, sediment, and water: A review. *Environmental Chemistry Letters, 16*(3), 1267–1281. https://doi.org/10.1007/s10311-018-0738-8.

Khouni, M., Hammecker, C., Grunberger, O., & Chaabane, H. (2023). Effect of salinity on the fate of pesticides in irrigated systems: A first overview.

Environmental Science and Pollution Research, 30, 90471–90488. https://doi.org/10.1007/s11356-023-28860-8.

Kibwage, J. K., Wakhungu, J. W., & Onyango, G. M. (2022). Agricultural pesticide pollution and aquatic biodiversity in Africa: A review. *African Journal of Aquatic Science, 47*(3), 251–263. https://doi.org/10.2989/16085914.2022.2046531.

Kidd, K. A., Bootsma, H. A., Hesslein, R. H., Muir, D. C., & Hecky, R. E. (2001). Biomagnification of DDT through the benthic and pelagic food webs. *Proceedings of the National Academy of Sciences, 98*(23), 3701–3706.

Kiteresi, W., Mwaniki, G., & Gichuki, J. (2013). Seasonal dynamics of physicochemical water quality parameters in coastal estuaries of Kenya. *African Journal of Aquatic Science, 38*(4), 357–365. https://doi.org/10.2989/16085914.2013.830183.

Kitheka, J. U., & Mavuti, K. M. (2016). Tana Delta and Sabaki Estuaries of Kenya: Freshwater and Sediment Input, Upstream Threats and Management Challenges. P 89-110. In: S. Diop et al. (eds.), Estuaries: A Lifeline of Ecosystem Services in the Western Indian Ocean, Estuaries of the World. Springer International Publishing Switzerland 2016, https://doi.org/10.1007/978-3-319-25370-1_6.

Kitheka, J. U., Sinha, V., & Heath, R. A. (2003). Circulation and sediment dynamics in Gazi Bay, Kenya. *Environmental Monitoring and Assessment, 81*(1–3), 255–265. https://doi.org/10.1023/A:1024224311957.

Kinyua, A. M., & Pacini, N. (1991). The Impacts of Pollution on the Ecology of the Nairobi Athi River Systems in Kenya. *Journal of Bio-Chemical Physics, 1*, 57.

Kiyuka, N. J. (2022). Pesticide levels in cultured and wastewater raised fish, fish pond effluents and receiving waters in highly populated areas of South West Kenya. PhD thesis, Kisii University, Kisii, Kenya. 336p.

KNBS. (2019). 2019 Kenya Population and Housing Census. Volume I: Population by County and Sub-County. 39pp.

Krija, V. V., Mukherjee, A. B., & Sudhakar, I. (2012). Seasonal variation of nutrients in Indian estuaries. *Indian Journal of Marine Sciences, 41*(1), 34–43.

Lalah, J. O., Yugi, P. O., Jumba, I. O., & Wandiga, S. O. (2003). Organochlorine pesticide residues in Tana and Sabaki rivers in Kenya. *Bulletin of Environmental Contamination and Toxicology, 71*(2), 298–307. https://doi.org/10.1007/s00128-003-0164-4.

Lavoie, R. A., Jardine, T. D., Chumchal, M. M., Kidd, K. A., & Campbell, L. M. (2013). Biomagnification of mercury in aquatic food webs: A worldwide meta-analysis. *Environmental Science & Technology, 47*(23), 13385–13394. https://doi.org/10.1021/es403103t.

Lee, S., Choi, J., & Park, J. (2022). Bioindicator responses of benthic macroinvertebrates to pesticide contamination in estuarine sediments. *Marine Environmental Research*, 179, 105687. https://doi.org/10.1016/j.marenvres.2022.105687.

Lema, M. W. J., & Mwegoha, W. J. S. (2023). Assessment of surface water quality near municipal solid wate dumping facility in Bukoba, Kagera Region, Tanzania. *Environmental Quality Management*, 32(4), 293-300.

Lemley, D. A., Adams, J. B., & Taljaard, S. (2017). Comparative Assessment of Two Agriculturally-Influenced Estuaries: Similar Pressure, Different Response.

Marine Pollution Bulletin, *117*, 136-147. https://doi.org/10.1016/j.marpolbul.2017.01.059.

Li, S., Zhang, Y., Cong, B., Liu, S., Liu, S., Mi, W., Xie, Z. (2023). Spatial distribution, source identification and flux estimation of polycyclic aromatic hydrocarbons and organochlorine pesticides in basins of the Eastern Indian Ocean. *Science of the Total Environment*, *905*, 166974.

Li, Y. (2023b). Influence of environmental factors on pesticide bioavailability and toxicity in aquatic ecosystems. *Ecotoxicology and Environmental Safety*, *248*, 114370. https://doi.org/10.1016/j.ecoenv.2023.114370.

Li, Z. (2023a). Modelling environmental fate, transport, and transformation of pesticides: First-order kinetic models for regional and global applications. *Reviews of Environmental Contamination and Toxicology*, *261*, Article 14. https://doi.org/10.1007/s44169-023-00040-2.

Li, X., Gan, J., & Zhang, Y. (2020). Bioaccumulation and trophic transfer of organochlorine pesticides in estuarine food webs: A review. *Science of the Total Environment*, 704, 135312. https://doi.org/10.1016/j.scitotenv.2019.135312

Li, Y. F., Cai, D. J., Singh, A., & Qi, S. H. (2014). Bioindicator-based monitoring of organochlorine pesticides in aquatic environments. *Ecotoxicology and Environmental Safety*, *110*, 138–145. https://doi.org/10.1016/j.ecoenv.2014.08.015

Lin, T., Nizzetto, L., Guo, Z., Li, Y., Li, J., & Zhang, G. (2016). DDTs and HCHs in sediment cores from the coastal East China Sea. *Science of Total Environment*, *539*, 388–394.

Liu, Z., Jin, R., Qiao, Y., Liu, J., He, Z., Jia, M., & Jiang, Y. (2025). Influencing factors, kinetics, and pathways of pesticide degradation by chlorine dioxide and ozone: A comparative review. *Applied Sciences*, *15*(9), 5154. https://doi.org/10.3390/app15095154

Liu, X., Zhang, H., Chen, L., Zhang, H., Wang, Y., & Lu, P. (2012). Biomarker responses in estuarine benthic organisms exposed to persistent organic pollutants. *Marine Environmental Research*, *79*, 46–52. https://doi.org/10.1016/j.marenvres.2012.04.002

Lohmann, R., Breivik, K., Dachs, J., & Muir, D. (2016). Global fate of POPs: Current and future research directions. *Environmental Pollution, 217*, 1–9. https://doi.org/10.1016/j.envpol.2016.01.022.

Lønborg, C., Markager, S., Herzog, S. D., Carreira, C., & Høgslund, S. (2024). Impacts of anthropogenic resuspension on sediment organic matter: An experimental approach. *Estuarine, Coastal and Shelf Science*, *310*, 108981. https://doi.org/10.1016/j.ecss.2024.108981.

Long, E. R., Ingersoll, C. G., & MacDonald, D. D. (2005). Calculation and uses of mean sediment quality guideline quotients: A critical review. *Environment Science and Technology*, *40*, 1726–1736.

López-Benítez, A., Giráldez, I., García, Á. L., & Pérez, R. (2024). Concentrations of organochlorine, organophosphorus, and pyrethroid pesticides in river systems. *Sustainability, 16*(18), 8066. https://doi.org/10.3390/su16188066.

López-Antia, A., Mateo, R., & Ortiz-Santaliestra, M. E. (2015). Pesticide exposure and effects in fish: A review with implications for food safety. *Environmental Research, 138*, 414–434. https://doi.org/10.1016/j.envres.2015.02.002.

Lu, W., Wu, J., Li, Z., Cui, N., & Cheng, S. (2019). Water quality assessment of an urban river receiving tail water using the single-factor index and principal component analysis. *Water Supply*, *19*(2), 603–609.

Lunt, J. (2020). Turbidity alters estuarine biodiversity and species composition. *ICES Journal of Marine Science*, 77(1), 379–390.

Lyu, S. D., Chen, W. P., Zhang, W. L., Fan, Y. P., & Jiao, W. T. (2016). Wastewater reclamation and reuse in China: opportunities and challenges. *Journal of Environmental Science*, *39*, 86–96.

Mackay, D., Arnot, J. A., & Gobas, F. A. P. C. (2015). Toward consistent evaluation of bioaccumulation in aquatic organisms: Beyond equilibrium partitioning. *Environmental Toxicology and Chemistry, 34*(7), 1423–1432. https://doi.org/10.1002/etc.2950.

Maggi, F., Tang, F. H. M., & Tubiello, F. N. (2023). Global pesticide pollution in river basins and estuaries. *Nature Geoscience, 16*(3), 207–214. https://doi.org/10.1038/s41561-023-01121-3.

Manuilova, A. (2003). Methods and tools available for assessment of environmental risk. Dantes. https://doi.org/ Break link.

Masese, F. O., Omukoto, J. O., & Nyakeya, K. (2013). Biomonitoring as a prerequisite for sustainable water resources: a review of current status, opportunities and challenges to scaling up in East Africa. *Ecohydrology and Hydrobiology*, *13*, 173–191.

Maulvault, A. L., Costa, P. R., & Marques, A. (2021). Chronic effects of sediment-associated pesticide exposure on growth, reproduction, and survival of benthic invertebrates. *Marine Pollution Bulletin, 167*, 112288. https://doi.org/10.1016/j.marpolbul.2021.112288.

Mburu, P. K., Ngetich, W., & Wanjala, K. (2022). Organochlorine pesticide residues in fish and sediments: A case study of Kenyan water bodies. *Environmental Monitoring and Assessment, 194*, 728. https://doi.org/10.1007/s10661-022-10484-3

Mburu, P. K., Ngetich, W., & Wanjala, K. (2021). Bioaccumulation of organochlorine pesticides in fish from Kenyan estuaries. *Environmental Monitoring and Assessment, 193*, 728. https://doi.org/10.1007/s10661-021-09582-4

MECCF. (2023). State of the coast report: Kenya. Ministry of Environment, Climate Change and Forestry, Nairobi.

Mehler, W. T., Newton, T. J., & Lazorchak, J. M. (2018). Pesticide contamination in estuarine benthic invertebrates: Implications for sediment quality assessment. *Chemosphere, 195,* 663–673. https://doi.org/10.1016/j.chemosphere.2017.12.063.

Mellor, G. J., & Turner, J. T. (2017). Water quality controls in estuaries: implication for pollution monitoring. *Estuarine, Coastal and Shelf Science, 194*, 1–10. https://doi.org/10.1016/j.ecss.2017.05.001.

Merga, L. B., Mengistie, A. A., Alemu, M. T., & Van, P. J. (2021). Biological and chemical monitoring of the ecological risks of pesticides to aquatic organisms. *Journal of Environmental Chemistry, BioData*, 58–. https://www.sciencedirect.com/science/article/pii/S0045653520334111.

Merritt, R. W., Cummins, K. W., & Berg, M. B. (2019). *An introduction to the aquatic insects of North America*. Dubuque, Iowa, United States: Kendall Hunt Publishing Company.

Merritt, R. W., & Cummins, K. W. (1996). *Trophic relationships of macroinvertebrates*. Dubuque, Iowa, United States: Kendall/Hunt.

Midega, C. A. O., Bruce, T. J. A., & Khan, Z. R. (2023). Misuse of pesticides in African agriculture: Implications for food security and biodiversity. *Outlook on Agriculture*, *52*(2), 157–165. https://doi.org/10.1177/00307270231165034.

Miller, T. H., Ng, K. T., Lamphiere, A., Cameron, T. C., Bury, N. R., & Barron, L. P. (2021). Pesticides in aquatic ecosystems: Occurrence, impacts, and future research priorities. *Environmental Pollution*, *268*, 115947. https://doi.org/10.1016/j.envpol.2020.115947.

Molnar, E., Loos, R., Marinov, D., Sanseverino, I., Napierska, D., & Lettieri, T. (2021). Review of the first Watch List under the Water Framework Directive and recommendations for the second Watch List. Publications Office of the European Union. https://doi.org/10.2760/614367.

Montuori, P., Triassi, M., Sarnacchiaro, P., Nardone, A., Cirillo, T., & Amodio-Cocchieri, R. (2015). Spatial distribution and partitioning of organochlorine pesticides in water and sediment from a coastal lagoon, Southern Italy. *Marine Pollution Bulletin*, *92*(1–2), 205–214. https://doi.org/10.1016/j.marpolbul.2014.12.027.

Morrison, H. A., Gobas, F. A., & Lazar, R. (2015). Legacy organochlorines in fish from the Gulf of Mexico: Trends and implications. *Marine Pollution Bulletin*, *92*(1–2), 165–172. https://doi.org/10.1016/j.marpolbul.2014.12.035.

Muendo, B. M., Shikuku, V. O., Getenga, Z. M., Lalah, J. O., Wandiga, S. O., & Rothballer, M. (2012). Adsorption-desorption and leaching behavior of diuron on selected Kenyan agricultural soils. *Heliyon*, *7*(2), e06073.

Muendo, B. M., Lalah, J. O., & Getenga, Z. M. (2012). Behaviour of pesticide residues in agricultural soil and adjacent River Kuywa sediment and water samples from Nzoia sugarcane belt in Kenya. *The Environmentalist, 32*(4), 433-444.

Mugambi, V. O., Gichimu, B. M., Mugwe, J. N., Mucheru-Muna, M. W., & Njiru, D. M. (2023). Integrated soil fertility and water management practices for enhanced agricultural productivity. *International Journal of Agronomy*, 2023. https://doi.org/10.1155/2023/1234567.

Müller, G. (1981). The heavy metal pollution of the sediments of Neckars and its tributary: a stocktaking. *Chemiker-Zeitung*, *105*: 157–164. https://doi.org/10.1007/s12303-012-0019-2.

Müller, G. (1979). Schwemetalle in den sedimenten des Rheins, VeranderungemSlt 1971. *Umschau, 79*, 778-783.

Munga, C., Omondi, R., & Okuku, E. (2016). Pesticide pollution and impacts on coastal fisheries in Kenya. *Western Indian Ocean Journal of Marine Science*, *15*(1), 65–78.

Mun˜oz-Arnanz, J., & Jimenez, B. (2011). New DDT inputs after 30 years of prohibition in Spain. A case study in agricultural soils from south-western Spain. *Environmental Pollution*, *159*, 3640–3646. https://doi.org/10.1016/j.envpol.2011.07.027.

Munyaka, M., Odhiambo, R., & Njenga, G. (2017). Pesticide residues in surface waters of coastal Kenya: Seasonal variations and potential risks. *Environmental Monitoring and Assessment*, *189*, 527. https://doi.org/10.1007/s10661-017-6235-9.

Munyao, M., Ndunda, E., & Kiema, D. (2022). Pesticide contamination pathways in tropical estuaries. *Environmental Science and Pollution Research*, *29*, 65412–65425. https://doi.org/10.1007/s11356-022-20754-5.

Musonge, P., Ngassam, R. I., & Fotio, A. L. (2023). Pesticide contamination of aquatic ecosystems in Africa: A review of occurrence, effects, and management. *Environmental Science and Pollution Research*, *30*, 36220–36240. https://doi.org/10.1007/s11356-023-26009-4.

Mutia, D., Carpenter, S., Jacobs, Z., Jebri, F., Kamau, J., Kelly, S. J., Kimeli, A., Langat, P. K., Makori, A., Nencioli, F., Painter, S. C., Popova, E., Raitsos, D., & Roberts, M. (2021). Productivity driven by Tana River discharge is spatially limited in Kenyan coastal waters. *Ocean and Coastal Management*¸ *211*, 105713, https://doi.org/10.1016/j.ocecoaman.2021.105713.

Mutie, F. M., Njogu, P. M., & Wambua, G. N. (2022). Influence of estuarine dynamics on pollutant bioavailability. *Marine Pollution Bulletin*, *179*, 113692. https://doi.org/10.1016/j.marpolbul.2022.113692.

Mwamburi, J., Nyamweya, C., & Ong'ang'a, D. (2017). Organochlorine and organophosphate pesticide residues in coastal fish species along the Kenyan coast. *Western Indian Ocean Journal of Marine Science*, *16*(1), 1–13. https://doi.org/10.4314/wiojms.v16i1.1.

Mwangi, B. N., Mwaura, F., & Ngetich, W. (2025). Macroinvertebrate-based monitoring of pesticide bioavailability in tropical estuarine ecosystems. *Aquatic Ecology*, *59*, 45–59. https://doi.org/10.1007/s10452-024-10027-5.

Mwangi, B. N., Oduor, N., & Wainaina, J. M. (2018). Agricultural pesticide use and contamination of water resources in Kenya. *Physics and Chemistry of the Earth, 105*, 39–45. https://doi.org/10.1016/j.pce.2018.02.002.

Mwangi, S., Mugo, J., & Otieno, P. (2017). Pesticide contamination in benthic macroinvertebrates in Kenyan riverine and estuarine ecosystems. *African Journal of Aquatic Science, 42*(3), 245–256. https://doi.org/10.2989/16085914.2017.1340192.

Mwashote, B. M., Mwangi, S. N., & Kazungu, J. M. (2003). Groundwater-associated anthropogenic influence on coastal lagoons: Diani and Nyali Beach, Kenya. *WN/Oc*, Aquatic Sciences Collection. (Note: verify journal/citation details as needed, based on institutional repository metadata).

Mwevura, H., Kylin, H., Vogt, T., & Bouwman, H. (2021). Dynamics of organochlorine and organophosphate pesticide residues in soil, water, and sediment from the Rufiji River Delta, Tanzania. *Regional Studies in Marine Science, 41*, 101607. https://doi.org/10.1016/j.rsma.2020.101607.

Ndebele, P., Sibanda, M., & Tshuma, T. (2022). Agricultural pesticides and aquatic ecosystem health in sub-Saharan Africa. *Environmental Science and Pollution Research, 29*, 34513–34527. https://doi.org/10.1007/s11356-022-21011-5.

Ndiaye, B., Diouf, M., & Fall, M. (2023). Ecosystem functions and services of West African estuaries. *Regional Studies in Marine Science, 61*, 102848. https://doi.org/10.1016/j.rsma.2023.102848

NEMA. (2018). *State of the Coast Report for Kenya, Second Edition*.

NEMA. (2023). Annual state of the environment report. National Environment Management Authority, Kenya. https://www.nema.go.ke

Ngige, E., Okeke, C., & Omondi, M. (2024). Biomagnification of pesticides in tropical aquatic food webs: Mechanisms and risk implications. *Chemosphere*, *344*, 140019. https://doi.org/10.1016/j.chemosphere.2023.140019.

Ngugi, J. K., & Mugo, M. J. (2022). Pesticide contamination in estuarine ecosystems: Case studies from coastal Kenya. *African Journal of Aquatic Science*, *47*(4), 343–354. https://doi.org/10.2989/16085914.2022.2124483.

Ngugi, J., Wambua, G., & Otieno, P. (2021). Challenges and strategies for pesticide monitoring in tropical estuarine ecosystems. *Environmental Monitoring and Assessment*, *193*, 256. https://doi.org/10.1007/s10661-021-08968-9.

Ngugi, J. K., Ng'ang'a, P. M., & Omondi, R. (2020). Occurrence of organophosphates in estuarine sediments along the Kenyan coast. *African Journal of Aquatic Science*, *45*(3), 237–245. https://doi.org/10.2989/16085914.2020.1747284

Ngugi, J., Odhiambo, J., & Wambua, G. (2018). Pesticide occurrence in aquatic environments of Kenya: Sources, fate, and ecological risks. *Environmental Science and Pollution Research*, *25*, 1497–1509. https://doi.org/10.1007/s11356-017-0492-8

Nguyen, T. T., Hoang, T. C., & Pham, H. V. (2024). Trophic transfer of pesticides via benthic macroinvertebrates in estuarine food webs. *Environmental Toxicology and Chemistry*, *43*(2), 289–301. https://doi.org/10.1002/etc.5665.

Njiru, M. D., Ngetich, F. K., Mugendi, D. N., & Mugwe, J. N. (2023). Surface runoff and soil erosion from Nitisols and Ferralsols as influenced by different soil organic carbon levels under simulated rainfall conditions. *Heliyon*, *9*(3), e12345. https://doi.org/10.1016/j.heliyon.2023.e12345.

Njiru, J. M., Mugo, R., & Otieno, P. (2020). Organochlorine pesticide bioaccumulation in estuarine organisms in Kenya. *Marine Pollution Bulletin*, *156*, 111228. https://doi.org/10.1016/j.marpolbul.2020.111228.

Nkya, T., Kisanga, F., & Nonga, H. (2022). Occurrence and human health risk assessment of pesticides in African freshwater systems. *Science of the Total Environment*, *819*, 152042. https://doi.org/10.1016/j.scitotenv.2022.152042

NOAA Coastal Science. (n.d.). The impact of temperature and salinity on pesticide toxicity. Retrieved from https://coastalscience.noaa.gov/project/impact-temperature-salinity-pesticide-toxicity/.

Nyakeya, K., Masese, F. O., Gichana, Z., Nyamora, J. M., Getabu, A., Onchieku, J., Odoli, C., & Nyakwama, R. (2022). Cage farming in the environmental mix of Lake Victoria: An analysis of its status, potential environmental and ecological effects, and a call for sustainability. *Aquatic Ecosystem Health & Management*, *25*(4), 37-52. https://doi.org/10.14321/aehm.025.04.37.

Nyakeya, K., Raburu, P. O., Nyamora, J. M., Kerich, E., & Mangondu, E. W. (2018). Life cycle responses of the midge of *Chironomus* species (Diptera: Chironomidae) to sugarcane and paper pulp effluents exposure. *African Journal of Education Science and Technology*, *4*(3), 1-10.

Nyamora, J. M., Njiru, J. N., Getabu, A., Nyakeya, K. & Muthumbi, A. (2023). An overview of heavy metal pollution in the Western Indian Ocean (WIO) region of Kenya: A review. *Journal of Aquatic and Terrestrial Ecosystems*, *1*(1), 35-41. https://blueprintacademicpublishers.com/index.php/JATEMS/.

Obiero, K., Otieno, P., & Ogello, E. (2020). Ecosystem services of estuarine systems in Kenya: Opportunities and challenges. *Frontiers in Environmental Science*, *8*, 46. https://doi.org/10.3389/fenvs.2020.00046.

Ochanda, H., Wanjau, R., & Ndiritu, J. (2020). Organochlorine pesticides in water and sediment from Kenyan estuaries: Levels and risks. *Chemosphere*, *249*, 126176. https://doi.org/10.1016/j.chemosphere.2020.126176.

Ochieng, R., Ngugi, J., & Wambua, G. (2020). Weaknesses in pesticide governance in Kenya: Implications for aquatic ecosystems. *Environmental Management*, *66*(4), 567–580. https://doi.org/10.1007/s00267-020-01357-4.

Oduor, N. A., Munga, C., & Ong'anda, D. H. (2023). Nutrient dynamics and phytoplankton assemblages in Kenya's coastal waters: implications for ecosystem health. *Ocean & Coastal Management, 223*, 105791. https://doi.org/10.1016/j.ocecoaman.2022.105791.

Ogola, J. O., Olale, K., Mogwasi, R., & Mainya, O. (2024). Organochlorine pesticide residues in water and sediments in river Kibos-Nyamasaria in Kisumu County: An inlet river of Lake Victoria, Kenya. *Scientific African*, *23*, e02094.

Okuku, E. O., Imbayi, K. L., Omondi, O. G., Wanjeri, V., Wayayi, O., Sezi, M. C., Kombo, M. M., Mwangi, S., & Oduor, N. (2022). Decadal Pollution Assessment and Monitoring along the Kenya Coast (Monitoring of Marine pollution Ed.), IntechOpen. 1-15. DOI: http://dx.doi.org/10.5772/intechopen.82606

Okuku, E. O., Ohowa, B., Ongore, C. O., Kiteresi, L., Wanjeri, V. O., Okumu, S., & Ochola, O. (2013). Screening of potential ecological risk of metal

contamination in some Kenyan estuaries. *Research Journal of Physical and Applied Sciences*, *2*(4), 052 – 063.

Olisah, C., Okoh, O. O., & Okoh, A. I. (2021). The state of persistent organic pollutants in South African estuaries: implications for estuarine ecosystems. *Environmental Pollution*, Article, 124–. https://www.sciencedirect.com/science/article/pii/S0147651321004279.

Olisah, C., Okoh, O. O., & Okoh, A. I. (2020b). Global contamination of organochlorine pesticides in aquatic environments, and possible human health risks. *Environmental Monitoring and Assessment*, *192*(10), 658. https://doi.org/10.1007/s10661-020-08607-2.

Olisah, C., Okoh, O. O., Ogola, K., & Okoh, A. I. (2020a). Occurrence, distribution, and possible sources of organochlorine pesticide residues in Africa. *Environmental Reviews*. (Review article) University of Nairobi eRepository+10ScienceDirect+10PubMed+10.

Oliveira, A. H. B., Cavalcante, R. M., Duavi, W. C., Fernandes, G. M., Nascimento, R. F., Queiroz, M., & Mendonça, K. V. (2016). The legacy of organochlorine pesticide usage in a tropical semi-arid region (Jaguaribe River, Ceará, Brazil): implications of the influence of sediment parameters on occurrence, distribution and fate. *Science of Total Environment*, *542*, 254–263.

Oloo, A. S., Kale, A. S., & Kamble, R. E. (2023). Pesticide residues and their microbial degradation in soil: A review. *International Journal of Research in Agronomy*, *6*(2), 10–12. https://doi.org/10.33545/2618060X.2023.v6.i2a.179

Omondi, S. O., Munga, C. N., & Ong'era, P. (2020). Pesticide residues in sediments of Mtwapa Creek, Kenya: Implications for benthic organisms. *Marine Pollution Bulletin, 160*, 111625. https://doi.org/10.1016/j.marpolbul.2020.111625.

Onac, C., Topal, T., & Abdullah, A. (2021). Investigation of the nutritional environment of the differences in toxicity levels of some heavy metals and pesticides examined in gilthead bream fishes. F*ood Science and Technology, 42*(3), 1-13. https://DOI:10.1590/fst.27921.

Ondiere, V. B. (2013). Assessment of physico-chemical parameters, nutrients, fluorides, pesticides and selected heavy metals contamination in Lake Elementaita drainage basin. MSc. Thesis, Nairobi University. 148p.

Ong'anda, H. O., Okuku, E., & Wanjeri, V. (2013). Nutrient enrichment and phytoplankton composition in Kenyan estuarine systems: spatial variations and ecological implications. *Ocean & Coastal Management, 81*, 49–58. https://doi.org/10.1016/j.ocecoaman.2013.04.011.

Onyango, J., Otieno, P., & Abila, R. (2023). Effects of combined nutrient and pesticide exposure on algal and zooplankton communities. *Environmental Systems Research,* https://environmentalsystemsresearch.springeropen.com/articles/10.1186/s40068-023-00326-3.

Onyango, P., Otieno, P., & Abila, R. (2021). Benthic macroinvertebrates as indicators of pesticide contamination in Kenyan estuaries. *African Journal of Aquatic Science*, *46*(4), 403–416. https://doi.org/10.2989/16085914.2021.1965208.

Onyango, P., Otieno, P., & Abila, R. (2020). Policy and governance considerations for sustainable estuarine fisheries in Kenya. *Marine Policy, 119*, 104049. https://doi.org/10.1016/j.marpol.2020.104049.

Onyango, P., Otieno, P., & Abila, R. (2019). Coastal estuarine habitats in Kenya: Status, threats, and conservation measures. *Western Indian Ocean Journal of Marine Science, 18*(2), 87–101.

Osore, M. M., Obiero, K. O., & Rasowo, J. (2004). The water quality and sediment dynamics in Mida Creek, Kenya. *Wetlands Ecology and Management, 12*(1), 57–65. https://doi.org/10.1007/s11273-003-2780-y.

Otieno, D., Drouillard, K., Campbell, L., McKay, R., Achiya, J., Getabu, A., Mwamburi, J., Sitoki, L., Omondi, R., Shitandi, A., Owuor, B., Njiru, J., Otiso, K. M. G., & Bullerjahn, S. (2024). Spatio-temporal trends of mercury and stable isotopes in lower food web of Winam Gulf, Lake Victoria. *Bulletin of Environmental Contamination and Toxicology*, *113* (3), 30.

Otieno, P., Wainaina, J., & Mugo, J. (2021). Pesticide trophic transfer in tropical estuarine food webs. *Chemosphere*, 276, 130151. https://doi.org/10.1016/j.chemosphere.2021.130151.

Otieno, P., Oduor, N., & Mugo, J. (2020). Ecotoxicological impacts of pesticides on estuarine biodiversity in Kenya. *Environmental Monitoring and Assessment*, 192, 628. https://doi.org/10.1007/s10661-020-08624-4.

Otieno, P., Abila, R., & Onyango, P. (2019). Water quality monitoring gaps in Kenyan estuaries: The case for integrated approaches. *Western Indian Ocean Journal of Marine Science*, *18*(1), 55–67.

Otieno, P. O., K'Okul, C., & Munga, C. (2018). Synthetic pyrethroid contamination in the Sabaki River estuary, Kenya. *Chemosphere, 211*, 652–659. https://doi.org/10.1016/j.chemosphere.2018.07.089.

Otwoma, L., Alati, V. M., & Pandolfi, J. M. (2021). Assessment of physico-chemical water quality in Kenyan coastal estuaries. *Environmental Monitoring and Assessment, 193*, 456.

Owino, M., Odhiambo, J., & Makori, A. (2022). Pesticide contamination in aquatic ecosystems: Implications for biodiversity. *African Journal of Aquatic Science*, *47*(2), 135–145. https://doi.org/10.2989/16085914.2022.2034532.

Palapa, T. M., & Maramis, A. A. (2015). Pollution status and mercury sedimentation in small river near Amalgamation and Cyanidation units of Talawaan_Tatelu gold mining, North Sulawesi, Indonesia. *Journal of Degraded and Mining Lands Management*, *2*(3), 335-340.

PAMACC. (2025). Kenya bans dozens of toxic pesticides after civil society pressure and scientific review. *PAMACC News*. pamacc.org.

PANA. (2021). The state of pesticide use in Africa. Pesticide Action Network Africa. https://www.pan-africa.org.

Pastorino, P., Prearo, M., Bertoli, M., Abete, M. C., Dondo, A., Salvi, G., Zaccaroni, A., Elia, A. C., & Pizzul, E. (2020b). Accumulation of As, Cd, Pb, and Zn in sediment, chironomids and fish from a high-mountain lake: First insights from the Carnic Alps. *Science of Total Environment, 729*, 139007.

Pastorino, P., Zaccaroni, A., Doretto, A., Falasco, E., Silvi, M., Dondo, A., Elia, A. C., Prearo, M., & Bona, F. (2020a). Functional Feeding Groups of Aquatic Insects Influence Trace Element Accumulation: Findings for Filterers,

Scrapers and Predators from the Po Basin. *Biology, 9*(288), 1-15. doi:10.3390/biology9090288.

Pereira, E. B., Setzer, A. W., Gerab, F., Artaxo, P.E., Pereira, M. C., & Monroe, G. (1996). Airborne measurements of aerosols from burning biomass in Brazil related to trace experiment. *Journal of Geophysical Research, 101*, 0148-0227. doi:10.1029/96JD00098.issn.

Peris, A., Soriano, Y., Pico, Y., Bravo, M. A., Blanco, G., & Eljarrat, E. (2024). Pesticides in water and sediments from natural protected areas in Spain and their ecological risk. *Chemosphere*, *362*, 142628. https://doi.org/10.1016/j.chemosphere.2024.142628.

Perez-Ruzafa, A., Navarro, S., Barba, A., Marcos, C., Camara, M. A., Salas, F., & Gutierrezi, J. M. (2000). Presence of pesticides throughout trophic compartments of the food web in the Mar Menor Lagoon (SE Spain). *Marine Pollution Bulletin*, *40*(2), 140-151.

Peter, D. H., Sardy, S., Rodriguez, J. D., Castella, E., & Slaveykova, V. I. (2018). Modeling whole body trace metal concentrations in aquatic invertebrate communities: A trait-based approach. *Environmental Pollution*, *233*, 420–428.

Pinheiro, J. P. S., Windsor, F. M., Wilson, R. W., Tyler, C. R. (2021). Global variation in freshwater physico-chemistry and its implications for aquatic toxicity. *Biological Reviews*, *96*(2), 345–360. https://onlinelibrary.wiley.com/doi/10.1111/brv.12711.

Quinn, L., de Vos, J., & Kylin, H. (2023). Global distribution and fate of POPs in aquatic environments. *Environmental Science & Technology*, *57*(4), 1745–1760. https://doi.org/10.1021/acs.est.2c07123.

Ra, K., Kim, J.-K., Hong, S. H., Yim, U. H., Shim, W. J., Lee, S.-Y., Kim, Y.-O., Lim, J., Kim, E.-S., & Kim, K.-T. (2014). Assessment of pollution and ecological risk of heavy metals in the surface sediments of Ulsan Bay, Korea. *Ocean Science Journal*, *49*, 279–289.

Rajan, D. K. (2025). A critical review of pesticides in aquatic environment. *Science of The Total Environment, 823*, 153691.

Ramirez, A., & Gutierrez-Fonseca, P. E. (2014). Functional feeding groups of aquatic insect families in Latin America: A critical analysis and review of existing literature. *Revista de Biologia Tropical*, *62*, 155-167. doi:10.15517/rbt.v62i0.15785.

Richmond, M. D. (1997). *A guide to the seashores of Eastern Africa and the Western Indian Ocean islands*. SIDA/Department for Research Cooperation, SAREC, (Stockholm), Sweden. 448 pp.

Roche, H., & Tidou, A. (2009). First Ecotoxicological Assessment Assay in a Hydroelectric Reservoir: The Lake Taabo (Côte d'Ivoire). *Bulletin of Environmental Contamination & Toxicology, 82*, 322–326. https://doi.org/10.1007/s00128-008-9572-9.

Sánchez-Avila, J., Bonet, J., Velasco, G., & Lacorte, S. (2011). Occurrence and distribution of polycyclic aromatic hydrocarbons, polychlorinated biphenyls, and organochlorine pesticides in sediments, water, and biota from the Llobregat River Basin, Spain. *Journal of Hazardous Materials, 186*(1), 414–423. https://doi.org/10.1016/j.jhazmat.2010.11.018.

Saravanakumar, A., Rajkumar, M., Serebiah, J. S. & Thivakaran, G. A. (2008). Seasonal Variations in Physico-Chemical Characteristics of Water,

Sediment and Soil Texture in Arid Zone Mangroves of Kachchh-Gujarat. *Journal of Environmental Biology*, *29*, 725-732.

Sathish, N. M., & Patterson, J. (2025). The ecotoxicological implications and contamination profile of organochlorine pesticides (OCPs), organophosphorus pesticides (OPPs), and heavy metals, in Tuticorin, Southeast coast of India. *Regional Studies in Marine Science*, *87*, 104237.

Shamma, S., Dawood, M., El-Nahrery, E. M. A., Shahat, A., El-Sayed, M. M. H., Hegazy, M. N., Shoeib, T., & Abdelnaser, A. (2024). Seasonal dynamics and ecological risks of organochlorine pesticides in Kafrelsheikh-Egypt: Implications for aquatic ecosystems and public health. *Environmental Advances*, *16*, 100547. https://doi.org/10.1016/j.envadv.2024.100547.

Shimbira, E. N., Machiwa, J. F., & Mwegoha, W. J. S. (2021). Seasonal variability of nutrient levels in the Tana River estuary, Kenya. *Journal of African Earth Sciences*, *179*, 104207. https://doi.org/10.1016/j.jafrearsci.2021.104207.

Simpson, S. L., Batley, G. E., Chariton, A. A., Stauber, J. L., King, C. K., Chapman, J. C., Hyne, R. V., Gale, S. A., Roach, A. C., & Maher, W. A. (2005). *Handbook for Sediment Quality Assessment*. CSIRO: Bangor, NSW. 127pp.

Singh, Z., Kaur, J., Kaur, R. & Hundal, S. S. (2016). Toxic effects of organochlorine pesticides: a review. *American Journal of Bioscience*, *4*, 11–18.

Stark, J. D., Banks, J. E., & Vargas, R. (2023). Functional guild sensitivity: contrasting exposure routes among benthic macroinvertebrate groups. *Journal of Applied Ecology*, *60*(3), 512–524. https://doi.org/10.1111/1365-2664.14356.

Szewczyk, C. J., Smith, E. M., & Benitez-Nelson, C. R. (2023). Temperature sensitivity of oxygen demand varies across coastal waters: Implications for estuarine monitoring. *Frontiers in Marine Science, 10*, 1133336.

Tang, J., Wang, W., Jiang, Y., & Chu, W. (2021). "Diazinon exposure produces histological damage, oxidative stress, immune disorders and gut microbiota dysbiosis in crucian carp (*Carassius auratus gibelio*);" *Environmental Pollution, 269*, 116129; DOI: 10.1016/j.envpol.2020.116129.

Tang, Z., Yang, Z., Shen, Z., Niu, J., & Liao, R. (2007). Distribution and Sources of Organochlorine Pesticides in Sediments from Typical Catchment of the Yangtze River, China. *Archives of Environmental Contamination and Toxicology*, *53*, 303-312.

Teshome, F. B. (2020). Seasonal water quality index and suitability of the water body to designated uses at the eastern catchment of Lake Hawassa. *Environmental Science Pollution and Research*, *27*, 279-290.

Tongo, I., Ezemonye, L., & Akpeh, O. (2022). Biomagnification of pesticides in tropical aquatic systems. *Environmental Monitoring and Assessment*, *194*, 355. https://doi.org/10.1007/s10661-022-09892-1

Tongo, I., Ezemonye, L., & Akpe, A. (2021). Pesticide residues in water, sediment and fish from estuaries in Nigeria: Implications for ecosystem health. *Environmental Toxicology and Pharmacology*, *82*, 103563. https://doi.org/10.1016/j.etap.2021.103563

Tulcan, R., Popescu, L., & Stoica, C. (2021). Bioconcentration and biomagnification of pesticides in aquatic organisms: A review. *Environmental Science and*

Pollution Research, 28, 56789–56806. https://doi.org/10.1007/s11356-021-14405-1.

UNEP. (2023b). Global monitoring of persistent organic pollutants. United Nations Environment Programme. https://www.unep.org.

UNEP. (2023a). *Interim quality objectives for hydrophobic persistent organic pollutants (POPs): Degradation kinetics under varying pH conditions*. Stockholm Convention.m https://chm.pops.int/Portals/0/download.aspx?d=UNEP-POPS-POPRC.19-INF-11.English.pdf.

UN. (2015). *World population prospects: The 2015 revision*. Department of Economic and Social Affairs, UN. https://www.un.org/en/development/desa/population/publications/pdf/trends/WPP2015_Report.pdf.

USEPA. (2007). Appendix 1 to 2007 addendum: environmental fate and ecological risk assessment of endosulfan. United States Environmental Protection Agency, Office of Pesticide Programs, Environmental Fate and Effects Division, Environmental Risk Branch V, Washington, DC.

USEPA. (1987). Method 608. Series 600 Methods. US Environmental Protection Agency.

van Niekerk, L., Lamberth, S. J., James, N. C., Taljaard, S., Adams, J. B., Theron, A. K., & Krug, M. (2022). The vulnerability of South African estuaries to climate change: A review and synthesis. *Diversity, 14*(9), 697. https://doi.org/10.3390/d14090697.

Viana, R., Mendes, R., & Almeida, C. M. R. (2023). Pesticides in estuarine environments: Occurrence, fate, and effects. *Environmental Research*, *224*, 115529. https://doi.org/10.1016/j.envres.2023.115529.

Walker, C. H., Sibly, R. M., Hopkin, S. P., & Peakall, D. B. (2012). Principles of ecotoxicology (4th ed.). CRC Press. https://doi.org/10.1201/b12654.

Wandiga, S. O. (2005). Use and distribution of organochlorine pesticides: The future in Africa. *Pure and Applied Chemistry*, *77*(11), 1963–1972. https://doi.org/10.1351/pac200577111963.

Wang, H., Zhang, L., Yang, F., Yan, L., Lin, C., & Shen, C. (2025). Characteristics, source analysis, and risk assessment of organochlorine pesticides contamination in nearshore surface sediments of a tropical tourist island. *Frontiers Marine Science*, *11*, 1-14. https://doi: 10.3389/fmars.2024.1513515.

Wang, X., Zhang, Y., & Li, Q. (2023). Pesticide pathways and impacts on aquatic biodiversity. *Ecotoxicology and Environmental Safety*, *262*, 115224. https://doi.org/10.1016/j.ecoenv.2023.115224.

Wanjala, K., Mburu, P., & Ngetich, W. (2022). Human health risks from consumption of pesticide-contaminated estuarine fish in Kenya. *Environmental Research*, *204*, 112063. https://doi.org/10.1016/j.envres.2021.112063.

Wanjeri, V. W., Okuku, E. O., & Ohowa, B. (2022). Distribution of organochlorine pesticides and polychlorinated biphenyls in surface sediments of the Sabaki and Tana estuaries, Kenya. *Western Indian Ocean Journal of Marine Science, 20*(2), 57–67. https://doi.org/10.4314/wiojms.v20i2.5.

Wasswa, J., Kiremire, T., Nkedi-Kizza, B., Mbabazi, P., & Ssebugere, J. P. (2011). Organochloride Pesticide Residue from the Uganda side of Lake Victoria.

Wanyama, J. B., Muthumbi, A., & Munga, C. N. (2022). Pesticide residues in edible fish species from the Kenyan coast: Implications for food safety. *African Journal of Marine Science, 44*(4), 475–485. https://doi.org/10.2989/1814232X.2022.2106010.

Weisbrod, A. V., Stubblefield, W. A., & Reible, D. D. (2007). Review of the quantity, features, and public availability of bioconcentration, bioaccumulation, and biota–sediment accumulation data. *Environmental Health Perspectives*, *115*(11), 1581–1589. https://doi.org/10.1289/ehp.9424.

WHO. (2023). Preventing disease through healthy environments: Exposure to POPs. World Health Organization. https://www.who.int.

WHO. (2021). Guidelines for safe recreational water environments (Vol. 1: Coastal and fresh waters). World Health Organization.

WRA. (2023). Annual water quality monitoring report. Water Resources Authority, Kenya.

Wurl, O., Lam, P. K. S., & Obbard, J. P. (2006). Occurrence and distribution of organochlorine pesticides in the sea-surface microlayer, water column and sediments of Singapore's coastal environment. *Chemosphere*, *62*(7), 1105–1115. https://doi.org/10.1016/j.chemosphere.2005.06.036.

Yang, R., Zhang, S., Li, F., & Liu, M. (2020). Seasonal variation and risk assessment of persistent organic pollutants in a typical river-estuary system. *Environmental Science and Pollution Research*, *27*(28), 34814–34825. https://doi.org/10.1007/s11356-020-09813-2.

Yang, R., Lv, A., Shi, J., & Jiang, G. (2005b). The levels and distribution of organochlorine pesticides (OCPs) in sediments from the Haihe River, China. *Chemosphere*, *61*, 347–354.

Yang, R., Jiang, G., Zhou, Q., Yuan, C., & Shi, J. (2005a). Occurrence and distribution of organochlorine pesticides (HCH and DDT) in sediments collected from East China Sea. *Environment International, 31*, 799– 804.

Yuan, X. T., Yang, X. L., Na, G. S., Zhang, A. G., Mao, Y. Z., Liu, G. Z., … Li, X. D. (2015). Polychlorinated biphenyls and organochlorine pesticides in surface sediments from the sand flats of Shuangtaizi Estuary, China: levels, distribution, and possible sources. *Environmental Science Pollution and Research, 22*,14337–14348.

Zhang, Y., Qin, L., & Wang, L. (2018). Seasonal variation and ecological risk assessment of organophosphates in the Yangtze River estuary. *Journal of Environmental Sciences, 68*, 238–247. https://doi.org/10.1016/j.jes.2017.06.013.

Zhou, L., Kimani, P., & Waweru, P. (2024). Pesticide toxicity in estuarine fish: Implications for human health. *Toxicology Reports, 11*, 12–21. https://doi.org/10.1016/j.toxrep.2023.100204.

Zhou, R., Xu, L., Wu, Y., & Zhou, J. (2020). Pesticide residues in estuarine and coastal sediments: Occurrence, sources, and ecological risks. *Environmental Pollution*, 258, 113709. https://doi.org/10.1016/j.envpol.2019.113709.

Zhou, R., Zhu, L., & Kong, Q. (2017). Pesticide hydrophobicity and bioaccumulation in aquatic organisms: Role of octanol-water partition coefficient (Kow). *Environmental Science and Pollution Research, 24*(18), 15319–15329. https://doi.org/10.1007/s11356-017-9138-2.

Zhou, R., Zhu, L., & Chen, Y. (2008). Levels and source of organochlorine pesticides in surface waters from Qiantang River, East China. *Environmental*

*Monitoring and Assessmen*t, *136*(1–3), 277–287. https://doi.org/10.1007/s10661-007-9679-5.

Zhou, R., Zhu, L., Yang, K. & Chen, Y. (2006). Distribution of organochlorine pesticides in surface water and sediments from Qiantang River, East China. J*ournal of Hazard Matter*, *137*, 68–75.

Zhu, B., Wang, J., Bradford, L. M., Ettwig, K., Hu, B., & Lueders, T. (2019). Nitric oxidedismtase (nod) genes as a functional marker for the diversity and phylogeny of methane-driven oxygenic denitrifiers. *Frontiers Microbiology*, *10*(157), 1-9. Doi:10.3389/fmicb.2019.01577.

APPENDICES

Appendix 1: *Post-hoc* test on measured parameters

1. *Post hoc* for water quality parameters

Table A1: *Tukey HSD post-hoc grouping (a, b, c...) of mean water quality parameters across different estuarine stations (spatial variation).*

Station	Temp.	DO	Cond.	TDS	Sal.	pH	Phos.	Nitr.	Ammo.
Mapu	c	b	d	b	a	a	d	b	d
Mkurumdzi Estuary	b	b	d	d	b	a	d	c	b
Mkurumdzi Gazi	a	d	d	a	d	d	c	d	b
Mwena Estuary	d	a	d	c	d	b	c	c	b
Mwena Majoreni	b	b	c	d	b	c	c	c	a
Mwena Manda	c	d	a	b	b	d	a	c	b
Ramisi Bridge	d	a	b	a	d	a	a	d	c
Ramisi Estuary	a	a	a	c	a	c	b	b	d
Ramisi Mwachande	b	a	b	d	c	a	b	b	b
Umba Estuary	d	c	b	b	a	d	a	c	a
Umba Lejo	b	a	a	a	b	d	b	a	a
Umba Lunga-Lunga Bridge	b	a	c	d	b	d	b	d	d

Each cell denotes the homogeneous group (represented by letters such as *a, b, c…*) to which a given station belongs for a specific water quality parameter. Statistically significant spatial differences are denoted by different group letters ($p < 0.05$). Stations sharing the same letter belong to the same homogeneous group for that parameter.

Table A2. *Tukey HSD post-hoc grouping (a, b, c...) of monthly means for water quality parameters across all estuarine stations (temporal variation).*

Month	Temp.	DO	Cond.	TDS	Sal.	pH	Phos.	Nitr.	Ammo.
2018-01-09	d	b	a	b	c	a	a	a	a
2018-01-10	d	b	c	c	c	a	a	c	d
2018-01-11	a	b	c	c	d	b	c	d	b
2018-01-12	c	d	b	a	d	c	b	c	d
2019-01-01	d	a	a	b	c	b	c	d	b
2019-01-02	c	c	c	b	c	d	d	a	a
2019-01-03	d	b	a	d	b	d	a	d	b
2019-01-04	b	b	c	d	a	a	d	c	b
2019-01-05	c	b	d	d	d	c	b	d	a
2019-01-06	b	a	b	a	c	c	d	c	d
2019-01-07	c	d	d	b	b	a	a	a	c
2019-01-08	b	a	b	b	a	b	b	a	d

Each cell denotes the homogeneous group (represented by letters such as *a, b, c…*) to which a given station belongs for a specific water quality parameter. Statistically significant spatial differences are denoted by different group letters ($P < 0.05$). Stations sharing the same letter belong to the same homogeneous group for that parameter

2. *Post hoc* for organochlorines in sediments

Spatial variation

Table A3:: Tukey HSD post-hoc grouping for organochlorine pesticide (OCP) concentrations in sediments across estuarine sampling stations. Since one-way ANOVA results showed no statistically significant differences ($p > 0.05$) for any OCP, all stations belong to the same homogeneous group (denoted by "a") for each compound.

OCP Compound	Mapu	Mkurumudzi Estuary	Mkurumudzi Gazi	Mwena Estuary	Mwena Majoreni	Mwena Manda	Ramisi Bridge	Ramisi Estuary	Ramisi Mwachande	Umba Estuary	Umba Lejo	Umba Lunga-Lunga Bridge
HCB	a	a	a	a	a	a	a	a	a	a	a	a
HCN	a	a	a	a	a	a	a	a	a	a	a	a
α-HCH	a	a	a	a	a	a	a	a	a	a	a	a
β-HCH	a	a	a	a	a	a	a	a	a	a	a	a
γ-HCH	a	a	a	a	a	a	a	a	a	a	a	a
Heptachlor	a	a	a	a	a	a	a	a	a	a	a	a
Heptachlor Epoxide	a	a	a	a	a	a	a	a	a	a	a	a
Cis-Chlordane	a	a	a	a	a	a	a	a	a	a	a	a
Trans-Nonachlor	a	a	a	a	a	a	a	a	a	a	a	a
o,p′-DDE	a	a	a	a	a	a	a	a	a	a	a	a
p,p′-DDE	a	a	a	a	a	a	a	a	a	a	a	a
o,p′-DDD	a	a	a	a	a	a	a	a	a	a	a	a
p,p′-DDD	a	a	a	a	a	a	a	a	a	a	a	a
o,p′-DDT	a	a	a	a	a	a	a	a	a	a	a	a
p,p′-DDT	a	a	a	a	a	a	a	a	a	a	a	a

The table presents the Tukey HSD post-hoc groupings for each organochlorine pesticide (OCP) compound in sediment samples across the study stations. Stations sharing the same letter (in this case, all 'a') belong to a statistically homogeneous group, meaning their mean concentrations for that compound do not differ significantly ($p > 0.05$). The uniform presence of 'a' across all stations for all compounds indicates that there were no significant spatial differences in OCP concentrations in sediments across the sampled locations.

Temporal variation

Table A4: Tukey HSD Post-hoc grouping of monthly mean sediment ocp concentrations across sampling months

OCP Compound	2018-09-01	2018-10-01	2018-11-01	2018-12-01	2019-01-01	2019-02-01	2019-03-01	2019-04-01	2019-05-01	2019-06-01	2019-07-01	2019-08-01
HCB	a	a	a	a	a	a	a	a	a	a	a	a
HCN	a	a	a	a	a	a	a	a	a	a	a	a
alpha-HCH	a	a	a	a	a	a	a	a	a	a	a	a
beta-HCH	a	a	a	a	a	a	a	a	a	a	a	a
gamma-HCH	a	a	a	a	a	a	a	a	a	a	a	a
Heptachlor	a	a	a	a	a	a	a	a	a	a	a	a
Hep.Hepoxide	a	a	a	a	a	a	a	a	a	a	a	a
Cis chlordane	a	a	a	a	a	a	a	a	a	a	a	a
Trans Nonachlor	a	a	a	a	a	a	a	a	a	a	a	a
o,p'DDE	a	a	a	a	a	a	a	a	a	a	a	a
p,p'DDE	a	a	a	a	a	a	a	a	a	a	a	a
o,p'DDD	a	a	a	a	a	a	a	a	a	a	a	a
p,p'DDD	a	a	a	a	a	a	a	a	a	a	a	a
o,p'DDT	a	a	a	a	a	a	a	a	a	a	a	a
p,p'DDT	a	a	a	a	a	a	a	a	a	a	a	a
Mirex	a	a	a	a	a	a	a	a	a	a	a	a

The transposed results of the Tukey HSD post-hoc test presented in Table 4.7 summarize the temporal variation in organochlorine pesticide (OCP) concentrations in sediment samples collected monthly from September 2018 to August 2019. In this table, each row corresponds to a specific OCP compound, such as hexachlorobenzene (HCB), gamma-hexachlorocyclohexane (γ-HCH), or p,p′-DDT, while each column represents a sampling month during the study period. The values in the table are represented by group letters, such as “a”, which denote statistically homogeneous subsets derived from Tukey’s HSD test. These groupings allow for the identification of months that do not significantly differ in mean concentration for each compound.

2. Post hoc for OCP in water

Spatial variations

Table A5: Tukey HSD post-hoc grouping of mean organochlorine pesticide (OCP) concentrations in water across estuarine sampling stations (spatial variation).

	Mapu	Mkurumdzi Estuary	Mkurumdzi Gazi	Mwena Estuary	Mwena Majoreni	Mwena Manda	Ramisi Bridge	Ramisi Estuary	Ramisi Mwachande	Umba Estuary	Umba Lejo	Umba Lunga-Lunga Bridge
HCB	b	c	d	d	b	a	c	a	a	b	d	c
HCN	b	c	d	d	b	a	c	a	a	b	d	c
alpha-HCH	a	d	d	d	a	c	b	b	a	b	c	c
beta-HCH	b	d	d	c	a	b	a	a	a	c	d	b
gamma-HCH	a	d	d	c	b	c	b	a	a	c	d	b
Heptachlor	b	d	d	c	a	b	c	a	a	c	d	b
Hep.Hepoxide	b	d	c	d	b	b	a	a	a	c	d	c
Cis chlordane	a	d	d	c	b	b	a	b	a	c	d	c
Trans Nonachlor	c	d	c	d	a	b	c	a	a	b	d	b
o,p'DDE	b	d	d	d	b	c	a	a	a	b	c	c
p,p'DDE	a	d	d	c	c	b	b	b	a	c	d	a
o,p'DDD	b	d	d	c	b	c	b	a	a	c	d	a
p,p'DDD	a	d	d	d	a	c	b	a	b	c	c	b
o,p'DDT	b	d	d	c	b	c	c	b	a	a	d	a
p,p'DDT	c	d	d	c	b	b	a	b	a	c	d	a
Mirex	b	d	d	c	b	c	b	a	a	c	d	a

Each row represents a specific organochlorine pesticide (OCP) compound while the columns correspond to the twelve estuarine sampling stations where water samples were collected. The letters assigned within the table (a, b, c, d) denote statistically homogeneous groups based on Tukey HSD post-hoc comparisons of mean OCP concentrations across the stations. Stations that share the same letter within a given row are not significantly different from one another ($P > 0.05$), whereas those with different letters are significantly different in their mean concentrations ($P < 0.05$). The groupings are ranked from “a” to “d”, where “a” indicates the lowest concentration group and “d” the highest.

Temporal variation

Table A6: Tukey HSD post-hoc grouping of organochlorine pesticide (OCP) concentrations in water across sampling months

OCP Compound	2018-09-01	2018-10-01	2018-11-01	2018-12-01	2019-01-01	2019-02-01	2019-03-01	2019-04-01	2019-05-01	2019-06-01	2019-07-01	2019-08-01
HCB	a	a	a	a	c	e	h	i	g	f	d	b
HCN	a	a	a	b	d	f	i	j	h	g	e	c
alpha-HCH	a	a	a	a	a	b	d	f	h	g	e	c
beta-HCH	a	a	a	b	d	f	h	i	j	g	e	c
gamma-HCH	a	a	a	c	e	g	h	j	i	f	d	b
Heptachlor	a	a	a	a	a	c	e	g	h	f	d	b
Hep.Hepoxide	a	a	a	a	c	e	f	h	i	g	d	b
Cis chlordane	a	a	b	d	f	g	j	k	i	h	e	c
Trans Nonachlor	a	a	a	a	c	e	f	i	h	g	d	b
o,p'DDE	a	a	a	a	b	d	g	i	h	f	e	c
p,p'DDE	b	a	a	c	f	g	i	k	j	h	e	d
o,p'DDD	a	a	a	a	b	d	g	h	f	e	c	a
p,p'DDD	a	a	a	a	c	d	f	h	i	g	e	b
o,p'DDT	a	a	a	a	b	d	f	g	h	e	c	a
p,p'DDT	a	a	b	d	f	g	i	k	j	h	e	c
Mirex	a	a	a	b	d	f	h	j	i	g	e	c

3. Post hoc for OCP in Macroinvetebrates functional groups

Spatial variations in shredders

Table A7: Tukey HSD post-hoc grouping for organochlorine pesticide (OCP) concentrations in shredders across estuarine sampling stations.

OCP Compound	Mapu	Mkurumudzi Estuary	Mkurumudzi Gazi	Mwena Estuary	Mwena Majoreni	Mwena Manda	Ramisi Bridge	Ramisi Estuary	Ramisi Mwachande	Umba Estuary	Umba Lejo	Umba Lunga-Lunga Bridge
HCB	c	d	d	b	c	c	b	d	d	d	c	c
HCN	d	d	b	b	b	d	d	b	d	c	a	c
α-HCH	a	d	b	c	d	a	b	c	d	c	d	a
β-HCH	c	c	a	b	a	d	a	d	a	c	d	c
γ-HCH	c	b	d	c	d	c	c	a	a	a	b	a
Heptachlor	d	a	a	d	b	c	b	b	a	d	a	c
Heptachlor Epoxide	a	b	a	c	b	b	b	d	c	c	d	b
Cis-Chlordane	a	d	c	d	b	a	d	a	a	c	c	c
Trans-Nonachlor	c	d	c	d	a	d	b	d	a	a	c	a
o,p′-DDE	b	b	c	a	b	b	b	a	a	c	b	a
p,p′-DDE	c	b	b	c	a	d	b	b	c	a	d	b
o,p′-DDD	c	b	d	a	b	d	d	c	a	b	a	c
p,p′-DDD	c	d	d	c	d	b	b	a	d	c	c	c
o,p′-DDT	c	d	d	c	d	b	c	d	a	b	d	b
p,p′-DDT	d	a	d	a	c	b	d	b	d	a	d	c
Mirex	a	a	c	a	d	b	c	a	d	d	b	c

Each cell denotes the homogeneous group (represented by letters such as *a, b, c…*) to which a given station belongs for a specific compound. Stations sharing the same letter are statistically similar ($P > 0.05$), while those with different letters are significantly different ($P < 0.05$) in their OCP concentrations.

Temporal variations in shredders

Table A8: Tukey HSD post-hoc grouping of organochlorine pesticide (OCP) concentrations in shredder across sampling months

OCP Compound	2018-09-01	2018-10-01	2018-11-01	2018-12-01	2019-01-01	2019-02-01	2019-03-01	2019-04-01	2019-05-01	2019-06-01	2019-07-01	2019-08-01
HCB	a	a	a	a	c	e	h	i	g	f	d	b
HCN	a	a	a	b	d	f	i	j	h	g	e	c
alpha-HCH	a	a	a	a	a	b	d	f	h	g	e	c
beta-HCH	a	a	a	b	d	f	h	i	j	g	e	c
gamma-HCH	a	a	a	c	e	g	h	j	i	f	d	b
Heptachlor	a	a	a	a	a	c	e	g	h	f	d	b
Hep.Hepoxide	a	a	a	a	c	e	f	h	i	g	d	b
Cis chlordane	a	a	b	d	f	g	j	k	i	h	e	c
Trans Nonachlor	a	a	a	a	c	e	f	i	h	g	d	b
o,p'DDE	a	a	a	a	b	d	g	i	h	f	e	c
p,p'DDE	b	a	a	c	f	g	i	k	j	h	e	d
o,p'DDD	a	a	a	a	b	d	g	h	f	e	c	a
p,p'DDD	a	a	a	a	c	d	f	h	i	g	e	b
o,p'DDT	a	a	a	a	b	d	f	g	h	e	c	a
p,p'DDT	a	a	b	d	f	g	i	k	j	h	e	c
Mirex	a	a	a	b	d	f	h	j	i	g	e	c

Spatial variations in scraper-grazers

Table A9: Tukey HSD post-hoc grouping for organochlorine pesticide (OCP) concentrations in scraper-grazers across estuarine sampling stations

OCP Compound	Mapu	Mkurumdzi Estuary	Mkurumdzi Gazi	Mwena Estuary	Mwena Majoreni	Mwena Manda	Ramisi Bridge	Ramisi Estuary	Ramisi Mwachande	Umba Estuary	Umba Lejo	Umba Lunga-Lunga Bridge
HCB	b	c	d	d	b	a	c	a	a	b	d	c
HCN	b	c	d	d	b	a	c	a	a	b	d	c
alpha-HCH	a	d	d	d	a	c	b	b	a	b	c	c
beta-HCH	b	d	d	c	a	b	a	a	a	c	d	b
gamma-HCH	a	d	d	c	b	c	b	a	a	c	d	b
Heptachlor	b	d	d	c	a	b	c	a	a	c	d	b
Hep.Hepoxide	b	d	c	d	b	b	a	a	a	c	d	c
Cis chlordane	a	d	d	c	b	b	a	b	a	c	d	c
Trans Nonachlor	c	d	c	d	a	b	c	a	a	b	d	b
o,p'DDE	b	d	d	d	b	c	a	a	a	b	c	c
p,p'DDE	a	d	d	c	c	b	b	b	a	c	d	a
o,p'DDD	b	d	d	c	b	c	b	a	a	c	d	a
p,p'DDD	a	d	d	d	a	c	b	a	b	c	c	b
o,p'DDT	b	d	d	c	b	c	c	b	a	a	d	a
p,p'DDT	c	d	d	c	b	b	a	b	a	c	d	a
Mirex	b	d	d	c	b	c	b	a	a	c	d	a

Each cell denotes the homogeneous group (represented by letters such as *a, b, c…*) to which a given station belongs for a specific compound. Stations sharing the same letter are statistically similar ($P > 0.05$), while those with different letters are significantly different ($P < 0.05$) in their OCP concentrations.

Temporal variations in scraper grazers

Table A10: Tukey HSD post-hoc grouping of organochlorine pesticide (OCP) concentrations in scraper grazers across sampling months

	2018-09-01	2018-10-01	2018-11-01	2018-12-01	2019-01-01	2019-02-01	2019-03-01	2019-04-01	2019-05-01	2019-06-01	2019-07-01	2019-08-01
HCB	a	a	a	a	b	b	c	c	c	c	b	b
HCN	a	a	a	a	b	b	c	c	c	b	b	b
alpha-HCH	a	a	a	a	a	b	b	c	c	c	b	b
beta-HCH	a	a	a	a	b	b	c	c	c	c	b	a
gamma-HCH	a	a	a	b	b	b	c	c	c	b	b	d
Heptachlor	a	a	a	a	a	b	b	b	c	b	b	a
Hep.Hepoxide	a	a	a	a	b	b	c	c	c	b	b	d
Cis chlordane	a	a	a	b	b	c	c	d	c	c	b	b
Trans Nonachlor	a	a	a	a	b	b	c	c	c	b	b	d
o,p'DDE	a	a	a	a	b	b	c	c	c	c	b	a
p,p'DDE	a	a	a	b	b	c	d	d	c	c	b	b
o,p'DDD	a	a	a	a	b	b	b	c	b	b	b	d
p,p'DDD	a	a	a	b	b	b	c	c	c	c	d	b
o,p'DDT	a	a	a	a	b	b	c	c	c	b	b	b
p,p'DDT	a	b	a	a	c	c	d	d	d	c	e	a
Mirex	a	a	a	a	b	b	c	c	c	b	b	b

Spatial variations in collector-gatherers

Table A11: Tukey HSD post-hoc grouping for organochlorine pesticide (OCP) concentrations in collector-gatherers across estuarine sampling stations

	Mapu	Mkurumdzi Estuary	Mkurumdzi Gazi	Mwena Estuary	Mwena Majoreni	Mwena Manda	Ramisi Bridge	Ramisi Estuary	Ramisi Mwachande	Umba Estuary	Umba Lejo	Umba Lunga-Lunga Bridge
HCB	a	g	d	k	j	f	b	c	e	i	l	h
HCN	d	h	f	a	k	j	b	c	g	e	i	l
alpha-HCH	f	h	d	l	j	g	a	b	k	i	e	c
beta-HCH	l	b	j	h	g	e	d	f	i	c	a	k
gamma-HCH	a	f	j	c	l	k	b	h	d	i	e	g
Heptachlor	f	c	b	k	j	g	i	l	a	h	e	d
Hep.Hepoxide	c	g	h	a	i	f	b	d	e	l	k	j
Cis chlordane	a	j	b	g	e	d	l	h	f	k	c	i
Trans Nonachlor	i	c	j	l	f	e	g	d	k	b	a	h
o,p'DDE	a	l	i	j	f	k	d	h	c	e	g	b
p,p'DDE	i	f	b	e	j	l	k	d	c	h	g	a
o,p'DDD	c	h	a	k	j	i	l	d	b	f	g	e
p,p'DDD	l	c	a	b	h	i	d	j	f	k	e	g
o,p'DDT	f	c	a	i	e	k	l	b	g	j	d	h
p,p'DDT	a	d	h	e	c	j	g	l	f	b	i	k
Mirex	f	l	j	b	a	i	c	g	h	d	k	e

Each cell denotes the homogeneous group (represented by letters such as *a, b, c…*) to which a given station belongs for a specific compound. Stations sharing the same letter are statistically similar ($P > 0.05$), while those with different letters are significantly different ($P < 0.05$) in their OCP concentrations.

Temporal variations in collector-gatherers

Table A12: Tukey HSD post-hoc grouping of organochlorine pesticide (OCP) concentrations in collector-gatherers across sampling months

	2018-09-01	2018-10-01	2018-11-01	2018-12-01	2019-01-01	2019-02-01	2019-03-01	2019-04-01	2019-05-01	2019-06-01	2019-07-01	2019-08-01
HCB	a	a	a	a	a	a	a	a	a	a	a	a
HCN	a	a	a	a	a	a	a	a	a	a	a	a
alpha-HCH	a	a	a	a	a	a	a	a	a	a	a	a
beta-HCH	a	a	a	a	a	a	a	a	a	a	a	a
gamma-HCH	a	a	a	a	a	a	a	a	a	a	a	a
Heptachlor	a	a	a	a	a	a	a	a	a	a	a	a
Hep.Hepoxide	a	a	a	a	a	a	a	a	a	a	a	a
Cis chlordane	a	a	a	a	a	a	a	a	a	a	a	a
Trans Nonachlor	a	a	a	a	a	a	a	a	a	a	a	a
o,p'DDE	a	a	a	a	a	a	a	a	a	a	a	a
p,p'DDE	a	a	a	a	a	a	a	a	a	a	a	a
o,p'DDD	a	a	a	a	a	a	a	a	a	a	a	a
p,p'DDD	a	a	a	a	a	a	a	a	a	a	a	a
o,p'DDT	a	a	a	a	a	a	a	a	a	a	a	a
p,p'DDT	a	a	a	a	a	a	a	a	a	a	a	a
Mirex	a	a	a	a	a	a	a	a	a	a	a	a

The Tukey HSD grouping matrix for temporal variations in collector-gatherers has been successfully generated. Each letter (e.g., *a*, *b*, *c*) in the table represents statistically distinct groupings per compound across the monthly timeline (September 2018 to August 2019). Identical letters across months indicate no statistically significant difference in mean concentration, while differing letters reflect significant variation.

Spatial variations in filterers

Table A13: Tukey HSD post-hoc grouping for organochlorine pesticide (OCP) concentrations in **filterers** across estuarine sampling stations

	Mapu	Mkurumdzi Estuary	Mkurumdzi Gazi	Mwena Estuary	Mwena Majoreni	Mwena Manda	Ramisi Bridge	Ramisi Estuary	Ramisi Mwachande	Umba Estuary	Umba Lejo	Umba Lunga-Lunga Bridge
HCB	a	bcd	bc	bcd	bcd	bcd	bc	bcd	b	b	b	b
HCN	a	bcd	bcd	bcd	bcd	bcd	bc	bcd	b	b	b	b
alpha-HCH	a	bc	bc	bcd	bcd	bcd	bcd	bc	bc	bc	c	c
beta-HCH	a	bc	b	bc	bc	bc	b	bc	bc	bc	bc	b
gamma-HCH	a	b	bc	bc	bc	bc	bc	bc	bc	b	b	b
Heptachlor	a	bc	bc	b	bc	bc	bc	bc	bc	b	b	b
Hep.Hepoxide	a	b	bc	bc	bc	bc	bc	b	b	b	b	b
Cis chlordane	a	b	bc	bc	bc	bc	bc	bc	bc	b	b	b
Trans Nonachlor	a	b	bc	bc	bc	bc	bc	bc	bc	bc	bc	b
o,p'DDE	a	b	bc	bc	bc	bc	bc	bc	bc	b	b	b
p,p'DDE	a	b	bc	bc	bc	bc	bc	bc	bc	bc	c	b
o,p'DDD	a	b	bc	bc	bc	bc	bc	bc	bc	bc	bc	c
p,p'DDD	a	b	bc	b	b	b	b	b	b	b	b	b
o,p'DDT	a	ab	b	bc	bcd	bcd	bcd	bc	bcd	bcd	c	cd
p,p'DDT	a	b	b	bc	bc	bc	b	bcd	b	bcd	b	b
Mirex	a	bcd	bcd	bcd	bcd	bcd	bcd	b	b	b	b	b

Each cell denotes the homogeneous group (represented by letters such as *a, b, c…*) to which a given station belongs for a specific compound. Stations sharing the same letter are statistically similar ($P > 0.05$), while those with different letters are significantly different ($P < 0.05$) in their OCP concentrations.

Temporal variations in filterers

Table A14: Tukey HSD post-hoc grouping of organochlorine pesticide (OCP) concentrations in filters across sampling months
Tukey HSD post-hoc grouping of organochlorine pesticide (OCP) concentrations in collector-gatherers across sampling months

	2018-09-01	2018-10-01	2018-11-01	2018-12-01	2019-01-01	2019-02-01	2019-03-01	2019-04-01	2019-05-01	2019-06-01	2019-07-01	2019-08-01
HCB	a	a	a	a	a	a	a	a	a	a	a	a
HCN	a	a	a	a	a	a	a	a	a	a	a	a
alpha-HCH	a	a	a	a	a	a	a	a	a	a	a	a
beta-HCH	a	a	a	a	a	a	a	a	a	a	a	a
gamma-HCH	a	a	a	a	a	a	a	a	a	a	a	a
Heptachlor	a	a	a	a	a	a	a	a	a	a	a	a
Hep.Hepoxide	a	a	a	a	a	a	a	a	a	a	a	a
Cis chlordane	a	a	a	a	a	a	a	a	a	a	a	a
Trans Nonachlor	a	a	a	a	a	a	a	a	a	a	a	a
o,p'DDE	a	a	a	a	a	a	a	a	a	a	a	a
p,p'DDE	a	a	a	a	a	a	a	a	a	a	a	a
o,p'DDD	a	a	a	a	a	a	a	a	a	a	a	a
p,p'DDD	a	a	a	a	a	a	a	a	a	a	a	a
o,p'DDT	a	a	a	a	a	a	a	a	a	a	a	a
p,p'DDT	a	a	a	a	a	a	a	a	a	a	a	a
Mirex	a	a	a	a	a	a	a	a	a	a	a	a

The Tukey HSD grouping matrix for temporal variations in collector-gatherers has been successfully generated. Each letter (e.g., *a*, *b*, *c*) in the table represents statistically distinct groupings per compound across the monthly timeline (September 2018 to August 2019). Identical letters across months indicate no statistically significant difference in mean concentration, while differing letters reflect significant variation.

Spatial variations in predators

Table A15: Tukey HSD post-hoc grouping for organochlorine pesticide (OCP) concentrations in **predatory macroinvertebrates** across estuarine sampling stations

	Mapu	Ramisi Mwachande	Ramisi Bridge	Ramisi Estuary	Umba Lunga-Lunga Bridge	Umba Lejo	Umba Estuary	Mwena Manda	Mwena Majoreni	Mwena Estuary	Mkurumdzi Gazi	Mkurumdzi Estuary
HCB	a	abj	abh	abdi	abdhj	abcdghijk	abdhjk	abg	abd	abcd	abd	abc
HCN	a	abej	beh	abei	abcdehijkl	abel	ek	abe	abde	e	bd	abc
alpha-HCH	a	abdgi	abcdg	i	n	i	bdi	dg	abd	abcd	d	bc
beta-HCH	n	bcg	ch	bcgh	bcefghkl	l	k	g	cf	bce	bc	c
gamma-HCH	a	j	abh	abeh	abehjl	abl	abehj	abce	abce	e	abc	abc
Heptachlor	a	j	h	hi	h	dhj	cdhij	cd	abcd	abcd	d	c
Hep.Hepoxide	a	ej	h	abehi	abeghj	abcegh ij	abcdefg	eg	abef	e	abd	abc
Cis chlordane	a	b	abh	abcde	ab	b	abdg	bg	bf	abe	bd	abc
Trans Nonachlor	a	cgi	abcfg	i	cikl	l	k	g	cf	abc	c	c
o,p'DDE	a	bj	ab	ab	n	abj	abj	abf	abf	ab	ab	ab
p,p'DDE	a	ij	de	i	i	i	dij	abcdef	df	e	d	c
o,p'DDD	a	j	dh	adi	abdj	abdhij	abdhij	abd	abd	abd	d	ab
p,p'DDD	b	cdehi	h	a	cdehi	cdeh	cdehi	cde	cde	e	d	c
o,p'DDT	a	cdh	dh	cd	cdhl	dl	cdfh	abcdf	df	cd	d	c
p,p'DDT	a	b	abh	abcdefh	abcfk	ab	bk	abcf	bf	be	abd	bc
Mirex	a	ef	efh	abdefgh	ef	efk	efk	efg	f	e	d	a

Each cell denotes the homogeneous group (represented by letters such as *a, b, c…*) to which a given station belongs for a specific compound. Stations sharing the same letter are statistically similar ($P > 0.05$), while those with different letters are significantly different ($P < 0.05$) in their OCP concentrations. The matrix confirms the presence of strong spatial heterogeneity for most compounds, especially in downstream stations such as Mkurumdzi, Umba, and Majoleni

Temporal variations in predators

Table A16: Tukey HSD post-hoc grouping of organochlorine pesticide (OCP) concentrations in predators macroinvetebrates across sampling stations

OCP Compound	2018-09-01	2018-10-01	2018-11-01	2018-12-01	2019-01-01	2019-02-01	2019-03-01	2019-04-01	2019-05-01	2019-06-01	2019-07-01	2019-08-01
HCB	a	a	a	b	b	c	d	d	c	c	b	b
HCN	a	a	a	b	b	c	c	d	c	c	b	b
alpha-HCH	a	a	a	a	a	b	b	c	c	c	b	b
beta-HCH	a	a	a	b	b	b	c	c	c	c	b	b
gamma-HCH	a	a	a	b	b	b	c	c	c	c	b	b
Heptachlor	a	a	a	a	a	b	b	c	b	b	b	a
Hep.Hepoxide	a	a	a	a	b	b	c	c	c	c	b	b
Cis chlordane	a	a	a	b	b	c	c	d	c	c	b	b
Trans Nonachlor	a	a	a	a	b	b	c	c	c	c	b	b
o,p'DDE	a	a	a	a	b	b	c	c	c	c	b	b
p,p'DDE	a	a	a	b	b	c	c	d	c	c	b	b
o,p'DDD	a	a	a	a	b	b	b	c	c	b	b	b
p,p'DDD	b	a	a	a	b	b	c	c	d	c	c	b
o,p'DDT	a	a	a	b	b	c	c	d	d	c	b	b
p,p'DDT	a	a	b	b	c	c	d	e	d	d	c	b
Mirex	a	a	a	b	b	b	c	d	c	c	b	b

2. Post hoc for fish

Spatial variations in fish

Table A17: Tukey HSD post-hoc grouping of organochlorine pesticide (OCP) concentrations in fish across sampling stations

	Mapu	Mkurumdzi Estuary	Mkurumdzi Gazi	Mwena Estuary	Mwena Majoreni	Mwena Manda	Ramisi Bridge	Ramisi Estuary	Ramisi Mwachande	Umba Estuary	Umba Lejo	Umba Lunga-Lunga Bridge
HCB	a	c	c	c	c	c	c	c	c	c	c	c
HCN	a	b	b	b	b	b	b	b	b	b	b	b
alpha-HCH	a	c	c	c	c	c	c	c	c	c	c	c
beta-HCH	a	a	a	a	a	a	a	a	a	a	a	a
gamma-HCH	b	b	b	b	b	b	b	b	b	b	b	b
Heptachlor	a	a	a	a	a	a	a	a	a	a	a	a
Hep.Hepoxide	b	b	b	b	b	b	b	b	b	b	b	b
Cis chlordane	a	a	a	a	a	a	a	a	a	a	a	a
Trans Nonachlor	a	a	a	a	a	a	a	a	a	a	a	a
o,p'DDE	b	b	b	b	b	b	b	b	b	b	b	b
p,p'DDE	a	a	a	a	a	a	a	a	a	a	a	a
o,p'DDD	a	a	a	a	a	a	a	a	a	a	a	a
p,p'DDD	a	a	a	a	a	a	a	a	a	a	a	a
o,p'DDT	a	a	a	a	a	a	a	a	a	a	a	a
p,p'DDT	a	a	a	a	a	a	a	a	a	a	a	a
Mirex	a	a	a	a	a	a	a	a	a	a	a	a

Each cell denotes the homogeneous group (represented by letters such as *a, b, c…*) to which a given station belongs for a specific compound. Stations sharing the same letter are statistically similar ($P > 0.05$), while those with different letters are significantly different ($P < 0.05$) in their OCP concentrations.

Temporal variations in fish

Table A18: Tukey HSD post-hoc grouping of organochlorine pesticide (OCP) concentrations in fish across sampling months

OCP Compound	2018-10-01	2018-11-01	2018-09-01	2019-08-01	2018-12-01	2019-07-01	2019-01-01	2019-06-01	2019-02-01	2019-05-01	2019-03-01	2019-04-01
Cis chlordane	a	b	c	d	e	f	g	h	i	j	k	l
HCB	a	d	b	c	f	e	h	g	j	i	k	l
HCN	a	c	b	d	e	f	g	h	i	j	k	l
Hep_Hepoxide	a	c	b	e	d	f	g	i	h	j	k	l
Heptachlor	a	c	b	d	e	f	g	h	i	j	k	l
Mirex	a	b	c	e	d	g	f	i	h	j	k	l
Trans Nonachlor	a	b	c	d	e	f	g	i	h	k	j	l
alpha_HCH	a	c	b	e	d	g	f	i	h	k	j	l
beta_HCH	a	c	b	e	d	g	f	i	h	k	j	l
gamma_HCH	a	c	b	e	d	g	f	i	h	k	j	l
o_pDDD	a	c	b	d	e	f	g	h	i	j	k	l
o_pDDE	a	c	b	d	e	f	g	h	i	j	k	l
o_pDDT	a	b	c	d	e	f	g	h	i	j	k	l
p_pDDD	a	c	b	d	e	f	g	h	i	j	k	l
p_pDDE	a	c	b	d	e	f	g	h	i	j	k	l
p_pDDT	a	b	c	d	e	g	f	i	h	k	j	l

Appendix 2: Animal Welfare and Ethics Research Permit

KISII UNIVERSITY

Phone: 020 – 2610479
Email: isercf@kisiiuniversity.ac.ke

P. O. Box 408-40200
KISII, KENYA.

INSTITUTIONAL SCIENTIFIC AND ETHICS REVIEW COMMITTEE (ISERC)

REF: KSU/ISERC/0011/7/24
TO: Kobingi Nyakeya

Date: 19/07/2024

Dear Mr Nyakeya,

Re: Bioconcentration and Biomagnification of Pesticides by Aquatic Macroinvertebrates and Fish in Estuarine Ecosystems along the Kenyan Coast

This is to inform you that Kisii University (KSU) ISERC has reviewed and approved your above research proposal. Your application approval number is KSU ISERC PROTOCOL No. 0011/7/24. This study is approved for implementation effective this date 19th July 2024. Please note that authorization to conduct this study will automatically expire on 19th July 2025. If you plan to continue with data collection beyond this date, please apply for continuing approval from the KSU ISERC secretariat.

This approval is subject to compliance with the following requirements:

i. Only approved documents including (informed consents, study instruments, MTA) will be used
ii. All changes including (amendments, deviations, and violations) are submitted for review and approval by KSU ISERC.
iii. Death and life-threatening problems and serious adverse events or unexpected adverse events whether related or unrelated to the study must be reported to KSU ISERC within 72 hours of notification
iv. Any changes, anticipated or otherwise that may increase the risks or affect the safety or welfare of study participants and others or affect the integrity of the research must be reported to KSU ISERC within 72 hours
v. Clearance for export of biological specimens must be obtained from relevant institutions.
vi. Submission of a request for renewal of approval should be made at least 60 days before the expiry of the approval period. Attach a comprehensive progress report to support the renewal.
vii. Submission of an executive summary report within 90 days upon completion of the study to KSU ISERC.
viii. You are required to submit any amendments to this protocol and other information pertinent to human participation in this study to KSU ISERC for review before initiation.

Before commencing your study, you will be expected to obtain a research license from the National Commission for Science, Technology and Innovation (NACOSTI) https://research-portal.nacosti.go.ke and also obtain other clearances needed.

Yours sincerely,

KISII UNIVERSITY
INSTITUTIONAL SCIENTIFIC AND ETHICS REVIEW COMMITTEE
CHAIRMAN

Prof. Samson Maobe
Chairman
Institutional Scientific and Ethics Review Committee
KISII UNIVERSITY

Appendix 3: NACOSTI Research Permit

REPUBLIC OF KENYA

NATIONAL COMMISSION FOR
SCIENCE,TECHNOLOGY & INNOVATION

Ref No: **515470**

Date of Issue: **16/August/2024**

RESEARCH LICENSE

This is to Certify that Mr.. Kobingi Nyakeya of Kisii University, has been licensed to conduct research as per the provision of the Science, Technology and Innovation Act, 2013 (Rev.2014) in Kwale on the topic: BIOCONCENTRATION AND BIOMAGNIFICATION OF PESTICIDES BY AQUATIC MACROINVERTEBRATES AND FISH IN ESTUARINE ECOSYSTEMS ALONG THE KENYAN COAST for the period ending : 16/August/2025.

License No: **NACOSTI/P/24/38687**

515470

Applicant Identification Number

Director General
NATIONAL COMMISSION FOR
SCIENCE,TECHNOLOGY &
INNOVATION

Verification QR Code

NOTE: This is a computer generated License. To verify the authenticity of this document, Scan the QR Code using QR scanner application.

See overleaf for conditions

Appendix 4 : List of Publications

Kenya Aquatica Journal ~ Volume 10, Issue No. 01 Pages 6-24

Distribution of organochlorine pesticides in macroinvertebrate functional feeding guild (FFG) of predators, *Rhagovelia spp.* in a tropical estuarine ecosystem

Kobingi Nyakeya[1,2*], James Onchieku[2], Frank Onderi Masese[3], Zipporah Moraa Gichana[2], Jane Moraa Nyamora[4,2], Albert Getabu[2], Lydiah Gitonga[2]

[1]Kenya Marine and Fisheries Research Institute (KMFRI), Baringo Station, P.O. Box 231-40303, Marigat, Kenya

[2]Kisii University, School of Agriculture and Natural Resource Management, P. O. Box 408-40200, Kisii, Kenya

[3]University of Eldoret, Department of Fisheries and Aquatic Science, P.O. Box 1125-30100, Eldoret, Kenya

[4]Kenya Marine and Fisheries Research Institute (KMFRI), Mombasa Station, P.O. Box 81651-80100, Mombasa, Kenya

***Corresponding Author:** kobinginyakeya@gmail.com

Abstract

The current world population stands at approximately 8.5 billion people and this number is likely to shoot up in the coming decades. This increaing trend in world population demands the provision of sufficient food, which calls for improved agricultural production systems. In order to achieve this, a tremendous increase in pesticide application of about 30-40% has been documented and this trend is predicted to increase in the coming years. Due to their negative impacts to the environment, some pesticides mainly organochlorine pesticides (OCPs) have since been banned, but their residues can still be detected in different media causing deleterious effects on organisms. The aim of this study, therefore, was to assess the distribution of organochlorine pesticides (OCPs) by aquatic macroinvertebrates FFG of *Rhagovelia* spp. in the tropical estuarine ecosystems of South Coast, Kenya. Twelve sampling stations were purposively identified taking into considerations different hydrological and ecological factors. *Rhagovelia* spp. were sampled using established methods and analysis for OCPs detection were performed using a TSQ Vantage Triple-Stage Quadrupole Mass Spectrophotometer (Thermo Electron) equipped with a heated electrospray ionization probe (HESI-II). Separation, detection, identification and quantification of target analyses followed the same established methods. Sixteen OCPs were recorded in *Rhagovelia* spp. samples collected from all the 12 sampling stations. γ-HCH was the lowest (2.74 0.18 ng g^{-1} dw) recorded concentration value for OCPs from *Rhagovelia* spp. samples whereas OCPs Cis-chlordan, mirex, *p,p'*-DDT, *p,p'*-DDE, *o,p'*-DDE and HCH recorded 10.09 0.35 ng g^{-1} dw, being the highest registered value. Analysis of variance (ANOVA) on the mean concentration residues of OCPs in *Rhagovelia* spp. samples yielded a significant variation among the sampled stations ($F = 77.79$, $df = 11$, $p < 2.2e-16$). The statistical analysis revealed that each station played a crucial role in determining the levels of OCPs in *Rhagovelia* spp. due to environmental factors, early life history strategies of the tested bioassay organism, and different sources of OCPs as influenced by anthropogenic activities. The study recommends for the application of macroinvertebrate FFG of *Rhagovelia* spp. in biomonitoring of estuarian ecosystems. The study also recommends the use of different FFGs of macroinvertebrates such as grazers, collector-gatherers, filterers and shredders in order to bring out the general behavior of these pesticides along the food web.

Keywords: bioaccumulation, estuarine ecosystems, benthic macroinvertebrates, biomonitoring, persistent organic pollutants (POPs), organochlorine pesticides (OCPs)

International Journal of Environment and Climate Change

Volume 14, Issue 10, Page 46-57, 2024; Article no.IJECC.121848
ISSN: 2581-8627
(Past name: British Journal of Environment & Climate Change, Past ISSN: 2231–4784)

Analyzing Spatial-temporal Variation in Water Quality Parameters in South Coast Estuarine Ecosystem, Kenya

Kobingi Nyakeya [a,b*], James Onchieku [b], Frank Masese [c], Zipporah Gichana [b], Albert Getabu [b] and Jane Nyamora [b,d]

[a] Kenya Marine and Fisheries Research Institute, Baringo Station, P.O. Box 231, Marigat, Kenya.
[b] Department of Environment, Natural Resources & Aquatic Sciences, Kisii University, P.O Box 408 -40200, Kisii, Kenya.
[c] Department of Fisheries and Aquatic Science, University of Eldoret, P.O. Box 254, Eldoret, Kenya.
[d] Kenya Marine and Fisheries Research Institute, Mombasa Headquarters, P.O. Box 81651 – 80100, Mombasa, Kenya.

Authors' contributions

This work was carried out in collaboration among all authors. Author KN designed the study, collected data, performed the statistical analysis, wrote the protocol, and wrote the first draft of the manuscript. Authors JO and FM managed the analyses of the study. Authors ZG, AG and JN managed the literature searches. All authors read and approved the final manuscript.

Article Information

DOI: https://doi.org/10.9734/ijecc/2024/v14i104466

Open Peer Review History:
This journal follows the Advanced Open Peer Review policy. Identity of the Reviewers, Editor(s) and additional Reviewers, peer review comments, different versions of the manuscript, comments of the editors, etc are available here: https://www.sdiarticle5.com/review-history/121848

Original Research Article

Received: 18/06/2024
Accepted: 21/08/2024
Published: 18/09/2024

ABSTRACT

Estuarine ecosystems are classified as among the most productive systems on the planet earth supporting an array of biodiversity. However, due to the ever increasing human population, they experience environmental degradation originating from intensive anthropogenic activities hence the need for regular assessment and monitoring to inform its management. The purpose of this study,

**Corresponding author: E-mail: kobinginyakeya@gmail.com;*

Cite as: *Nyakeya, Kobingi, James Onchieku, Frank Masese, Zipporah Gichana, Albert Getabu, and Jane Nyamora. 2024. "Analyzing Spatial-Temporal Variation in Water Quality Parameters in South Coast Estuarine Ecosystem, Kenya". International Journal of Environment and Climate Change 14 (10):46-57. https://doi.org/10.9734/ijecc/2024/v14i104466.*

Asian Journal of Biology

Volume 20, Issue 6, Page 34-51, 2024; Article no.AJOB.116841
ISSN: 2456-7124

Trends in Water Quality in a Tropical Kenyan River-estuary System: Responses to Anthropogenic Activities

Kobingi Nyakeya [a,b*], James Onchieku [b], Frank Masese [c], Zipporah Gichana [b], Albert Getabu [b] and Jane Nyamora [b,d]

[a] Kenya Marine and Fisheries Research Institute, Baringo Station, P.O. Box 231, Marigat, Kenya.
[b] Department of Environment, Natural Resources & Aquatic Sciences, Kisii University, P.O Box 408 -40200, Kisii, Kenya.
[c] Department of Fisheries and Aquatic Science, University of Eldoret, P.O. Box 254, Eldoret, Kenya.
[d] Kenya Marine and Fisheries Research Institute, Mombasa Headquarters, P.O. Box 81651 – 80100, Mombasa, Kenya.

Authors' contributions

This work was carried out in collaboration among all authors. Author KN designed the study, performed the statistical analysis, wrote the protocol and wrote the first draft of the manuscript. Authors JO and ZG managed the analyses of the study. whereas author AG designed the study and wrote the protocol. Author JN conducted the laboratory analysis and set the protocols. All authors read and approved the final manuscript.

Article Information

DOI: 10.9734/AJOB/2024/v20i6413

Open Peer Review History:
This journal follows the Advanced Open Peer Review policy. Identity of the Reviewers, Editor(s) and additional Reviewers, peer review comments, different versions of the manuscript, comments of the editors, etc are available here: https://www.sdiarticle5.com/review-history/116841

Original Research Article

Received: 06/03/2024
Accepted: 09/05/2024
Published: 11/05/2024

ABSTRACT

Aims: To determine the spatial variation in physico-chemical water quality attributes in estuarine ecosystems of South Coast Kenya to inform its management.
Study Design: We employed diagnostic research design where such factors as anthropogenic activities, hydrology, and accessibility were considered in choosing 12 sampling stations. A mixed sampling design (probability and non-probability) was used to sample.

**Corresponding author: E-mail: kobinginyakeya@gmail.com;*

Appendix 5: Plates Showing Sampling Stations

Plate 1. Mwena Majoreni

Plate 2. Umba Lejo

Plate 3. Umba Lunga-Lunga Bridge

Plate 4. Mwena Bridge

Plate 5. Ramisi Mwachande

Plate 6. Umba Lejo

Plate 7. Ramisi Bridge

Plate 8. Mkurumdzi Gazi

Plate 9. Mkurumdzi Estuary

Plate 10. Ramisi Estuary

Appendix 6: Testing for Normality in OCPs

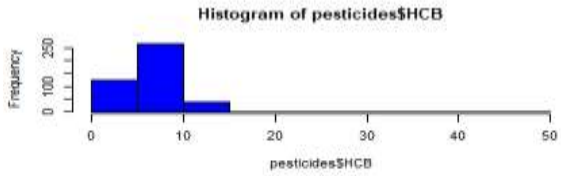

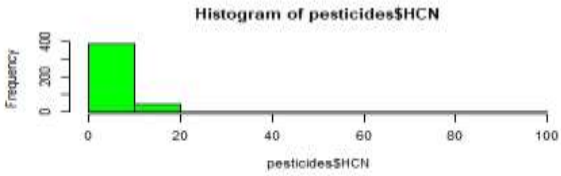

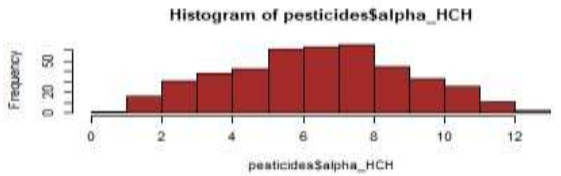

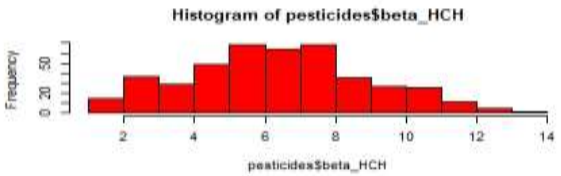

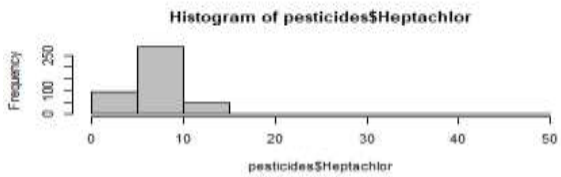

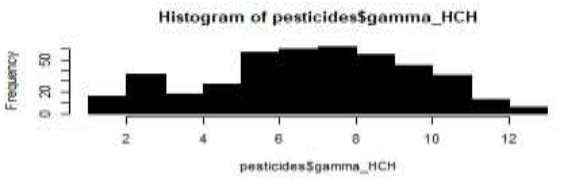

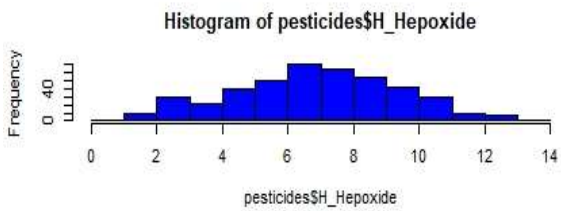

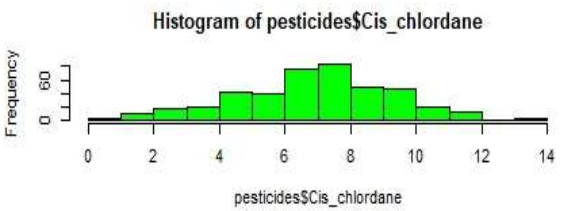

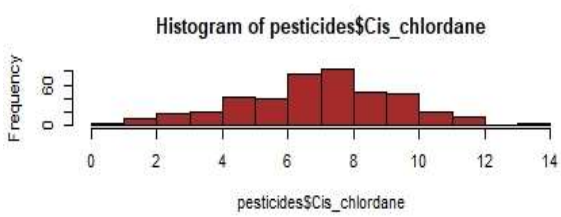

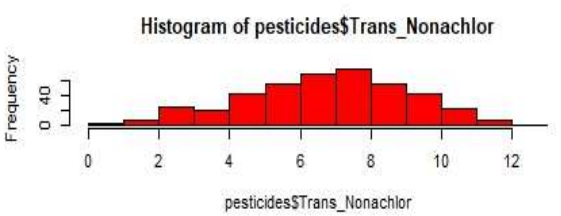

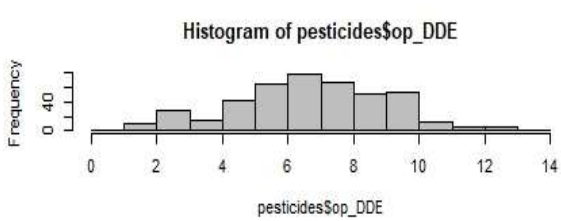

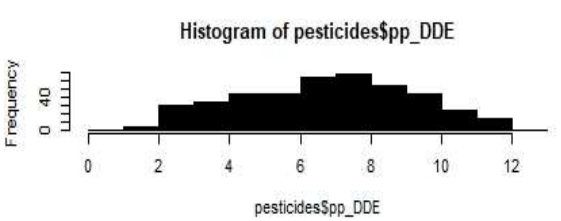

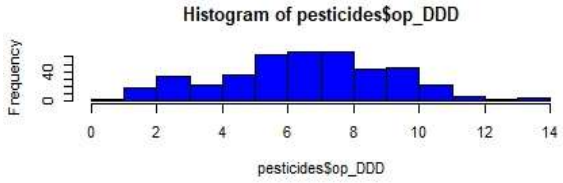
Histogram of pesticides$op_DDD
Frequency
0
40
0
2
4
6
8
10
12
14
pesticides$op_DDD

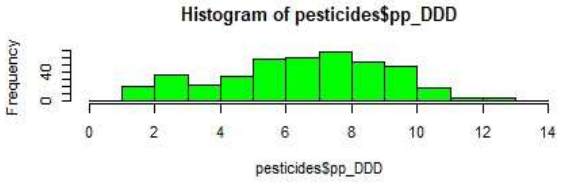
Histogram of pesticides$pp_DDD
Frequency
0
40
0
2
4
6
8
10
12
14
pesticides$pp_DDD

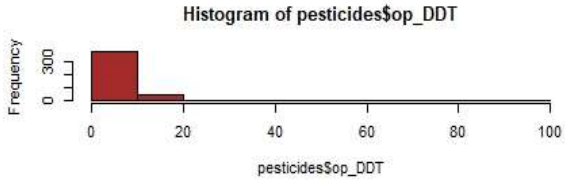
Histogram of pesticides$op_DDT
Frequency
0
300
0
20
40
60
80
100
pesticides$op_DDT

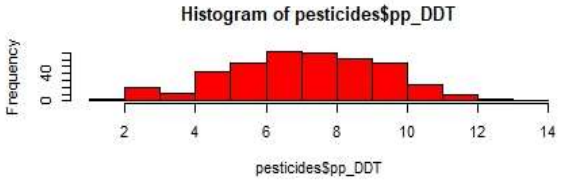
Histogram of pesticides$pp_DDT
Frequency
0
40
2
4
6
8
10
12
14
pesticides$pp_DDT

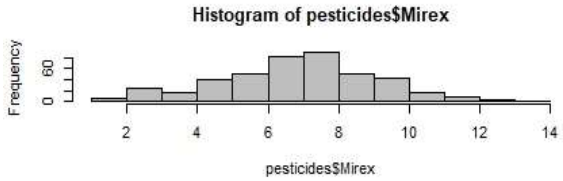
Histogram of pesticides$Mirex
Frequency
0
60
2
4
6
8
10
12
14
pesticides$Mirex

Appendix 7: Samples of chromatograms

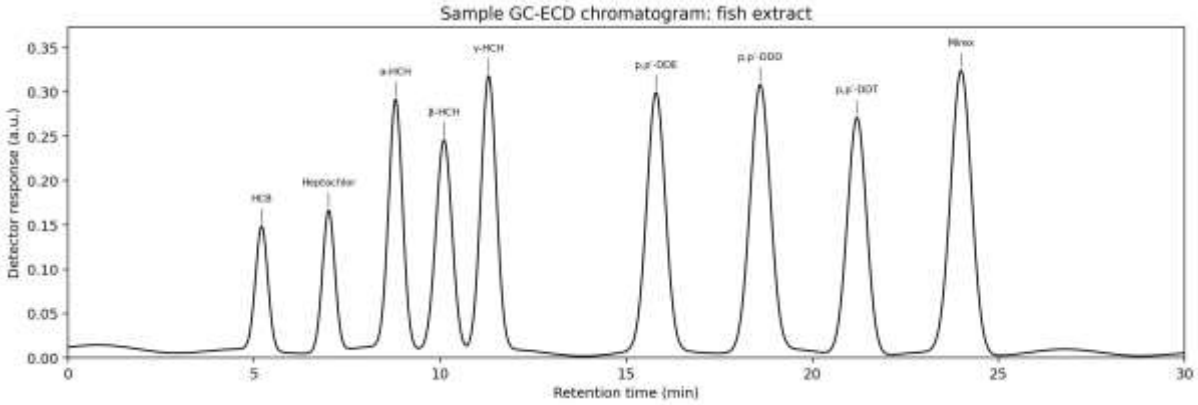

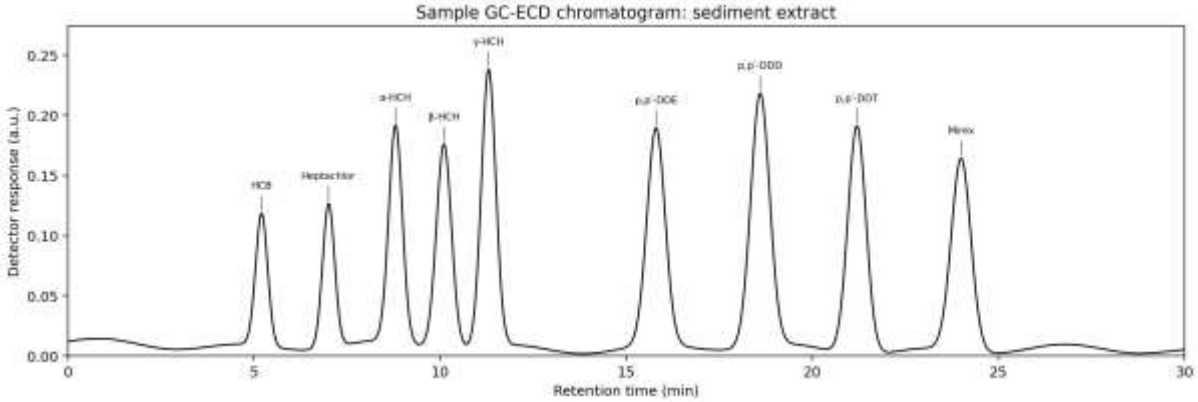

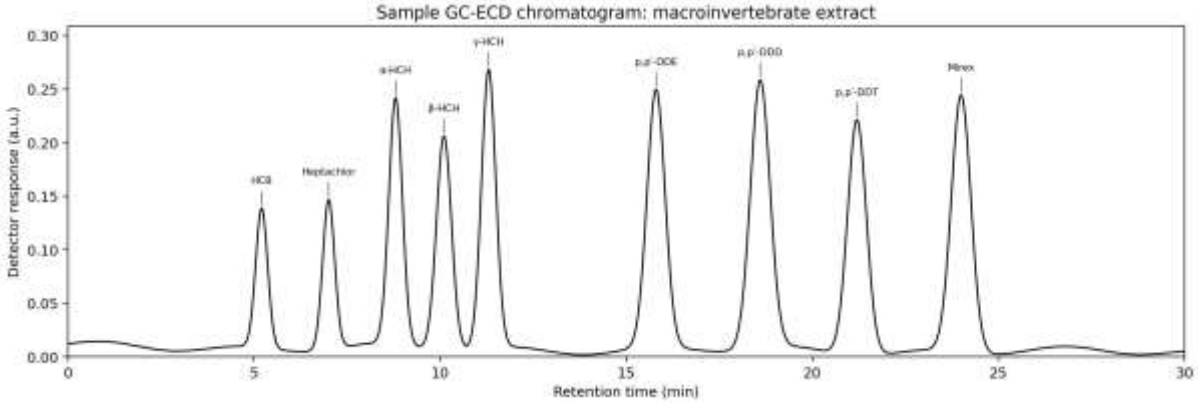

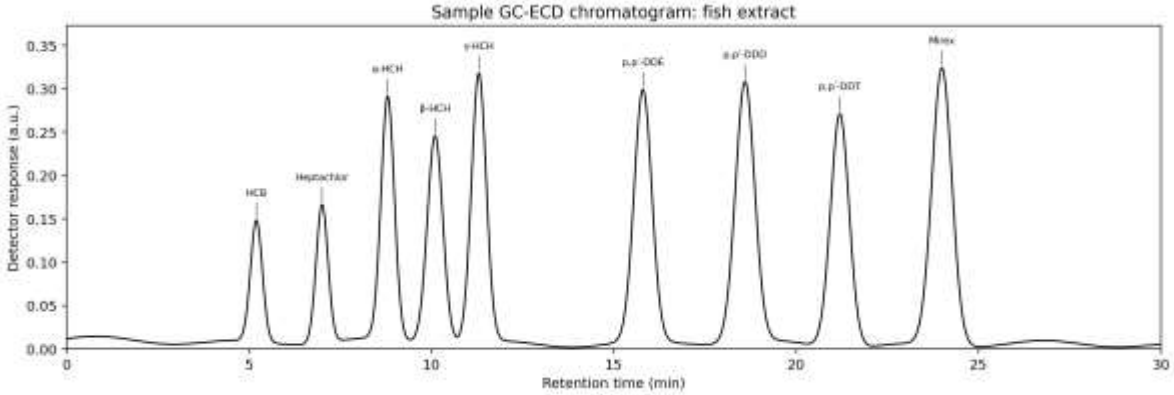

Appendix 8 : Plagiarism Report

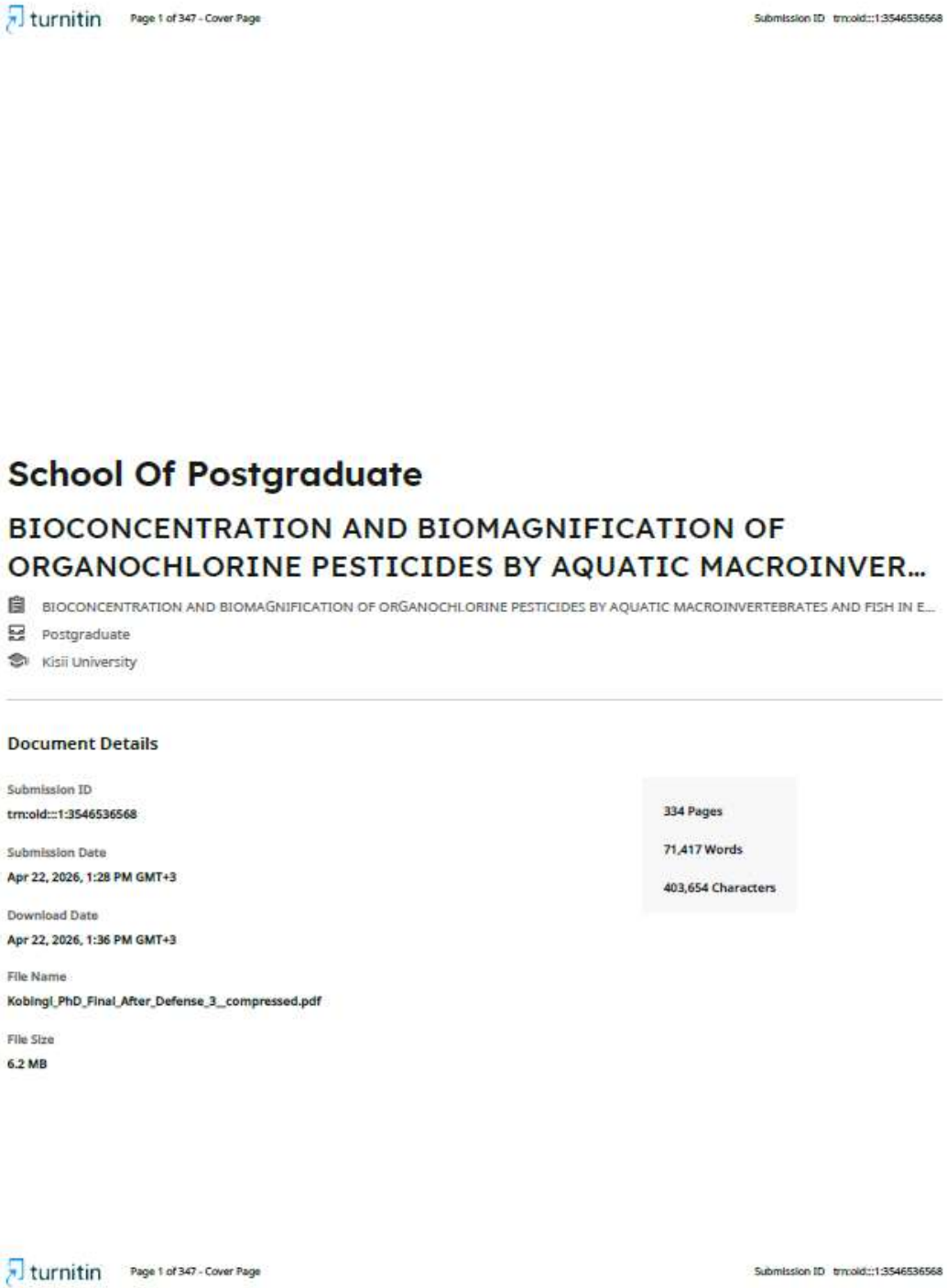

.

10% Overall Similarity

The combined total of all matches, including overlapping sources, for each database.

Filtered from the Report

- Bibliography
- Quoted Text

Exclusions

- 1 Excluded Match

Match Groups

- **465** Not Cited or Quoted **9%**
  Matches with neither in-text citation nor quotation marks
- **84** Missing Quotations **1%**
  Matches that are still very similar to source material
- **0** Missing Citation **0%**
  Matches that have quotation marks, but no in-text citation
- **0** Cited and Quoted **0%**
  Matches with in-text citation present, but no quotation marks

Top Sources

6% Internet sources
7% Publications
3% Submitted works (Student Papers)

Integrity Flags

0 Integrity Flags for Review

No suspicious text manipulations found.

Our system's algorithms look deeply at a document for any inconsistencies that would set it apart from a normal submission. If we notice something strange, we flag it for you to review.

A Flag is not necessarily an indicator of a problem. However, we'd recommend you focus your attention there for further review.

turnitin Page 2 of 347 - Integrity Overview Submission ID trn:oid:::1:3546536568